Advances in High Energy Physics

Quantum Information and Holography

Lead Guest Editor: Juan F. Pedraza
Guest Editors: Elena Caceres, Cynthia Keeler, Sandipan Kundu, and Esperanza Lopez

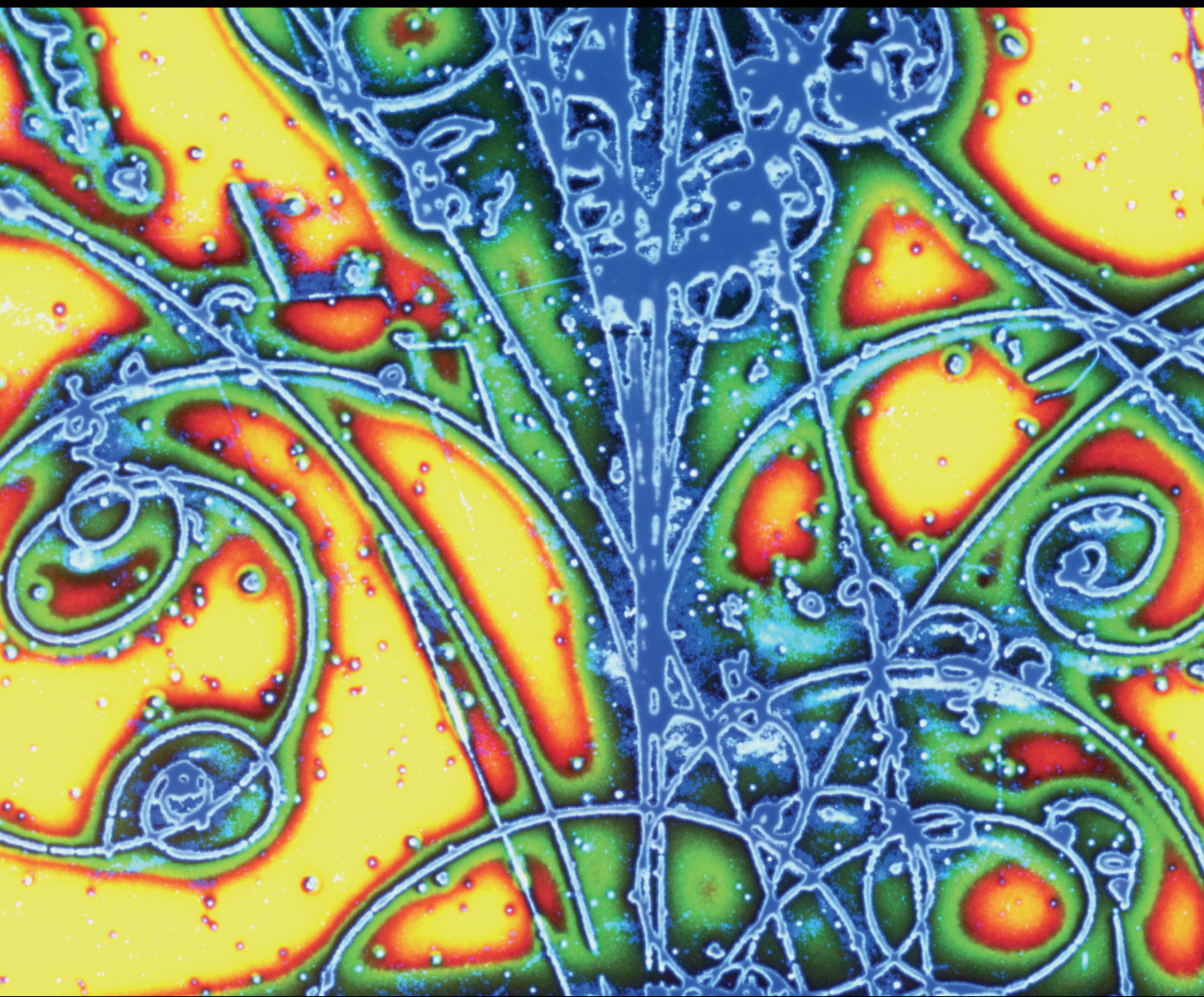

Quantum Information and Holography

Advances in High Energy Physics

Quantum Information and Holography

Lead Guest Editor: Juan F. Pedraza
Guest Editors: Elena Caceres, Cynthia Keeler, Sandipan Kundu, and Esperanza Lopez

Editorial Board

Contents

Hindawi
Advances in High Energy Physics
Volume 2019, Article ID 3436254, 2 pages
https://doi.org/10.1155/2019/3436254

Editorial
Quantum Information and Holography

Juan F. Pedraza,[1] **Elena Caceres**,[2] **Cynthia Keeler**,[3] **Sandipan Kundu**,[4] **and Esperanza Lopez**[5]

[1]*Institute for Theoretical Physics, University of Amsterdam, Amsterdam, Netherlands*
[2]*Theory Group, The University of Texas at Austin, Austin, USA*
[3]*Department of Physics, Arizona State University, Tempe, USA*
[4]*Department of Physics and Astronomy, Johns Hopkins University, Baltimore, USA*
[5]*Instituto de Física Teórica UAM/CSIC, Madrid, Spain*

Correspondence should be addressed to Juan F. Pedraza; jpedraza@uva.nl

Received 18 April 2019; Accepted 21 April 2019; Published 12 May 2019

The discovery of AdS/CFT and, more generally, the gauge/gravity correspondence has led to many new insights in quantum gravity and quantum field theory. Its relevance in theoretical physics is with no doubt exceptional, since it provides one of the few nonperturbative definitions of string theory, a quantum theory of gravity.

In recent years, the AdS/CFT community has borrowed various tools of quantum information theory. Quantities such as complexity and entanglement in its various guises have been extremely useful to understand the emergence of bulk spacetime from quantum field theory degrees of freedom. The chaotic and fast scrambling properties of black holes and their dual field theories have provided a fresh look into the thermodynamic nature of gravity, providing new hints on various long-standing problems, puzzles, and paradoxes.

This special issue focusses on the interplay between different aspects of quantum information theory and holography, with applications to both, quantum aspects of gravity and strongly coupled gauge theories.

In the paper by S. F. Lokhande entitled "Spread of Entanglement in Non-Relativistic Theories" the author studies a simple holographic toy model that describes a global quench in strongly coupled non-relativistic theories and uses entanglement entropy to characterize the post-quench evolution. The author shows that the quantum entanglement of small subsystems follows a simple linear response relation that can be thought of as a time-dependent generalization of the first law of entanglement entropy. Via holography, this result can be extrapolated to a wide class of non-relativistic critical theories and some condensed matter systems.

In the paper by J.-C. Ding et al. entitled "Apparent Horizon and Gravitational Thermodynamics of Universe in the Eddington-Born-Infeld Theory" the authors investigate the thermodynamics of the Universe in the Eddington-Born-Infeld using holographic gravitational equations. Various properties of the apparent horizon are discussed including cases where the surface is timelike, spacelike, or null, depending on the parameter of state in the EBI Universe. The unified first law and second law of gravitational thermodynamics for the open system inside the apparent horizon are obtained.

In the paper by M. Gogberashvili entitled "Cosmological Constant from the Entropy Balance Condition" the author argues that the entanglement between degrees of freedom inside and outside the apparent horizon should be taken into account in the thermodynamic description of cosmological backgrounds. This is due to the fact that the variations of quantum fields should be extended up to the event horizon, instead of the apparent horizon. The author identifies this missing term with the dark energy density and expresses it as the critical density multiplied by the ratio of the apparent and event horizons radii.

In the paper by J. A. Zapata entitled "Gauge from Holography and Holographic Gravitational Observables" the author investigates the holographic imprints of a spacetime

divided into two regions by a hypersurface. A nontrivial perturbation of a bulk field leaving a holographic imprint on the dividing hypersurface which does not affect perturbations on the other side should be considered physically irrelevant. For a large class of theories including vacuum general relativity, it is shown that all local observables are holographic in the sense that they can be written as integrals of over the dividing surface. However, non-holographic observables are needed to distinguish between gauge inequivalent solutions.

In the review paper by A. Kundu entitled "Steady States, Thermal Physics, and Holography" the author revisits the main features of a large class of holographic systems in a steady-state that admit an effective thermodynamic description. This idea has arisen in various setups, including in the dynamics of fundamental matter coupled to adjoint degrees of freedom. In this article, the author discusses some features of this physics, ranging from the basic description of such configurations in terms of strings and branes to observable effects of this effective thermal description.

In the review paper by V. Jahnke entitled "Recent Developments in the Holographic Description of Quantum Chaos" the author gives an overview of the connection between quantum chaos and black holes in holographic theories. Particular attention is given to the characterization of quantum chaos based on the time evolution of out-of-time-order correlators and its realization in the dual gravitational description. Other topics that are covered in the review include the connections between chaos and the spread of quantum entanglement and diffusion phenomena.

Conflicts of Interest

The guest editors declare that they do not have any conflicts of interest.

Juan F. Pedraza
Elena Caceres
Cynthia Keeler
Sandipan Kundu
Esperanza Lopez

Hindawi
Advances in High Energy Physics
Volume 2019, Article ID 9632708, 18 pages
https://doi.org/10.1155/2019/9632708

Review Article

Recent Developments in the Holographic Description of Quantum Chaos

Viktor Jahnke [1,2]

[1] *Departamento de Física de Altas Energias, Instituto de Ciencias Nucleares, Universidad Nacional Autónoma de México, Apartado Postal 70-543, CDMX 04510, Mexico*
[2] *School of Physics and Chemistry, Gwangju Institute of Science and Technology, Gwangju 61005, Republic of Korea*

Correspondence should be addressed to Viktor Jahnke; viktor.jahnke@correo.nucleares.unam.mx

Received 16 November 2018; Accepted 31 January 2019; Published 26 March 2019

Guest Editor: Elena Caceres

We review recent developments encompassing the description of quantum chaos in holography. We discuss the characterization of quantum chaos based on the late time vanishing of out-of-time-order correlators and explain how this is realized in the dual gravitational description. We also review the connections of chaos with the spreading of quantum entanglement and diffusion phenomena.

1. Introduction

The characterization of quantum chaos is fairly complicated. Possible approaches range from semiclassical methods to random matrix theory: in the first case one studies the semiclassical limit of a system whose classical dynamics is chaotic; in the later approach the characterization of quantum chaos is made by comparing the spectrum of energies of the system in question to the spectrum of random matrices [1]. Despite the insights provided by the above-mentioned approaches, a complete and more satisfactory understanding of quantum chaos remains elusive.

Surprisingly, new insights into quantum chaos have come from black holes physics! In the context of so-called gauge-gravity duality [2–4], black holes in asymptotically AdS spaces are dual to strongly coupled many-body quantum systems. It was recently shown that the chaotic nature of many-body quantum systems can be diagnosed with certain out-of-time-order correlation (OTOC) functions which, in the gravitational description, are related to the collision of shock waves close to the black hole horizon [5–9]. In addition to being useful for diagnosing chaos in holographic systems and providing a deeper understanding for the inner-working mechanisms of gauge-gravity duality, OTOCs have also proved useful in characterizing chaos in more general nonholographic systems, including some simple models like the kicked-rotor [10], the stadium billiard [11], and the Dicke model [12].

In this paper we review the recent developments in the holographic description of quantum chaos. We discuss the characterization of quantum chaos based on the late time vanishing of OTOCs and explain how this is realized in the dual gravitational description. We also review the connections of chaos with spreading of quantum entanglement and diffusion phenomena. We focus on the case of $d-$dimensional gravitational systems with $d \geqslant 3$, which excludes the case of gravity in AdS_2 and SYK-like models [13–16]. (Another interesting perspective on the characterization of chaos in the context of (regularized) AdS_2/CFT_1 is provided by [17–19].) Also, due the lack of the author's expertise, we did not cover the recent developments in the direct field theory calculations of OTOCs. This includes calculations for CFTs [20], weakly coupled systems [21, 22], random unitary models [23–25], and spin chains [26–30].

2. A Bird Eye's View on Classical Chaos

In this section we briefly review some basic aspects of classical chaos. For definiteness we consider the case of a

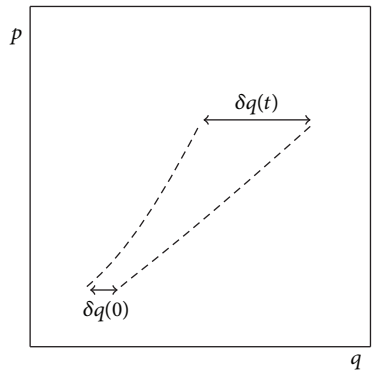

Figure 1: Variation of a trajectory in the phase space under small modifications of the initial condition. For a chaotic system the distance between two initially nearby trajectories increases exponentially with time, i.e., $|\delta q(t)| = |\delta q(0)| e^{\lambda t}$.

classical thermal system with phase space denoted as $\mathbf{X} = (\mathbf{q}, \mathbf{p})$, where $\mathbf{q}$ and $\mathbf{p}$ are multidimensional vectors denoting the coordinates and momenta of the phase space. We can quantify whether the system is chaotic or not by measuring the stability of a trajectory in phase space under small changes of the initial condition. Let us consider a reference trajectory in phase space, $\mathbf{X}(t)$, with some initial condition $\mathbf{X}(0) = \mathbf{X}_0$. A small change in the initial condition $\mathbf{X}_0 \longrightarrow \mathbf{X}_0 + \delta\mathbf{X}_0$ leads to a new trajectory $\mathbf{X}(t) \longrightarrow \mathbf{X}(t) + \delta\mathbf{X}(t)$. This is illustrated in Figure 1. For a chaotic system, the distance between the new trajectory and the reference one increases exponentially with time

$$\begin{aligned} |\delta\mathbf{X}(t)| &\sim |\delta\mathbf{X}_0| e^{\lambda t} \\ \text{or } \frac{\partial\mathbf{X}(t)}{\partial\mathbf{X}_0} &\sim e^{\lambda t}, \end{aligned} \tag{1}$$

where λ is the so-called Lyapunov exponent. This should be contrasted with the behavior of nonchaotic systems, in which $\delta\mathbf{X}(t)$ remains bounded or increases algebraically [31].

The exponential increase depends on the orientation of $\delta\mathbf{X}_0$ and this leads to a spectrum of Lyapunov exponents, $\{\lambda_1, \lambda_2, \ldots, \lambda_K\}$, where K is the dimensionality of the phase space. A useful parameter characterizing the trajectory instability is

$$\lambda_{\max} = \lim_{t\longrightarrow\infty} \lim_{\delta\mathbf{X}_0\longrightarrow 0} \frac{1}{t} \log\left(\frac{\delta\mathbf{X}(t)}{\delta\mathbf{X}_0}\right), \tag{2}$$

which is called the maximum Lyapunov exponent. When the above limits exist and $\lambda_{\max} > 0$, the trajectory shows sensitivity to initial conditions and the system is said to be chaotic [31].

The chaotic behavior can be a consequence of either a complicated Hamiltonian or simply the contact with a thermal heat bath. This is because chaos is a common property of thermal systems. For the latter to make contact with black holes physics, we consider the case of a classical thermal system with inverse temperature β. If $F(\mathbf{X})$ is some function of the phase space coordinates, we define its classical expectation value as

$$\langle F\rangle_\beta = \frac{\int d\mathbf{X} e^{-\beta H(\mathbf{X})} F(\mathbf{X})}{\int d\mathbf{X} e^{-\beta H(\mathbf{X})}} \tag{3}$$

where $H(\mathbf{X})$ is the system's Hamiltonian.

Classical thermal systems have two exponential behaviors that have analogues in terms of black holes physics: the Lyapunov behavior, characterizing the sensitive dependence on initial conditions, and the Ruelle behavior, characterizing the approach to thermal equilibrium [32, 33].

To quantify the sensitivity to initial conditions in a thermal system we need to consider thermal expectation values. Note that (1) can have either signs. To avoid cancellations in a thermal expectation values, we consider the square of this derivative

$$F(t) = \left\langle \left(\frac{\partial\mathbf{X}(t)}{\partial\mathbf{X}(0)}\right)^2 \right\rangle_\beta. \tag{4}$$

The expected behavior of this quantity is the following [34]

$$F(t) \sim \sum_k c_k e^{2\lambda_k t}, \tag{5}$$

where c_k are constants and λ_k are the Lyapunov exponents. At later times the behavior is controlled by the maximum Lyapunov exponent $F \sim e^{2\lambda_{\max} t}$.

The approach to thermal equilibrium or, in other words, how fast the system forgets its initial condition can be quantified by two-point functions of the form

$$G(t) = \langle \mathbf{X}(t)\mathbf{X}(0)\rangle_\beta - \langle\mathbf{X}\rangle_\beta^2, \tag{6}$$

whose expected behavior is [34]

$$G(t) \sim \sum_j b_j e^{-\mu_j t}, \tag{7}$$

where b_j are constants and μ_j are complex parameters called Ruelle resonances. The late time behavior is controlled by the smallest Ruelle resonance $G \sim e^{-\mu_{\min} t}$.

3. Some Aspects of Quantum Chaos

In this section we review some aspects of quantum chaos. For a long time, the characterization of quantum chaos was made by comparing the spectrum of energies of the system in question to the spectrum of random matrices or using semiclassical methods [1]. Here we follow a different approach, which was first proposed by Larkin and Ovchinnikov [35] in the context of semiclassical systems, and it was recently developed by Shenker and Stanford [6–8] and by Kitaev [9].

For simplicity, let us consider the case of a one-dimensional system, with phase space variables (q, p). Classically, we know that $\partial q(t)/\partial q(0)$ grows exponentially with time for a chaotic system. The quantum version of this quantity can be obtained by noting that

$$\frac{\partial q(t)}{\partial q(0)} = \{q(t), p(0)\}_{\text{P.B.}}, \tag{8}$$

where $\{q(t), p(0)\}_{\text{P.B.}}$ denotes the Poisson bracket between the coordinate $q(t)$ and the momentum $p(0)$. The quantum version of $\partial q(t)/\partial q(0)$ can then be obtained by promoting the Poisson bracket to a commutator

$$\{q(t), p(0)\}_{\text{P.B.}} \longrightarrow \frac{1}{i\hbar}\left[\widehat{q}(t), \widehat{p}(0)\right] \tag{9}$$

where now $\widehat{q}(t)$ and $\widehat{p}(0)$ are Heisenberg operators.

We will be interested in thermal systems, so we would like to calculate the expectation value of $[\widehat{q}(t), \widehat{p}(0)]$ in a thermal state. However, this commutator might have either signs in a thermal expectation value and this might lead to cancellations. To overcome this problem, we consider the expectation value of the square of this commutator

$$C(t) = \left\langle -\left[\widehat{q}(t), \widehat{p}(0)\right]^2 \right\rangle_\beta, \tag{10}$$

where β is the system's inverse temperature and the overall sign is introduced to make $C(t)$ positive. More generally, one might replace $\widehat{q}(t)$ and $\widehat{p}(0)$ by two generic Hermitian operators V and W and quantify chaos with the *double commutator*

$$C(t) = \left\langle -[W(t), V(0)]^2 \right\rangle_\beta. \tag{11}$$

This quantity measures how much an early perturbation V affects the later measurement of W. As chaos means sensitive dependence on initial conditions, we expect $C(t)$ to be 'small' in nonchaotic system and 'large' if the dynamics is chaotic. In the following we give a precise meaning for the adjectives 'small' and 'large'.

For some class of systems the quantum behavior of $C(t)$ has a lot of similarities with the classical behavior of $\langle(\partial q(t)/\partial q(0))\rangle_\beta$. However, the analogy between the classical and quantum quantities is not perfect because there is not always a good notion of a small perturbation in the quantum case (remember that classical chaos is characterized by the fact that a small perturbation in the past has important consequences in the future). If we start with some reference state and then perturb it, we easily produce a state that is orthogonal to the original state, even when we change just a few quantum numbers. Because of that it seems unnatural to quantify the perturbation as small. Fortunately, there are some quantum systems in which the notion of a small perturbation makes perfect sense. An example is provided by systems with a large number of degrees of freedom. In this case a perturbation involving just a few degrees of freedom is naturally a small perturbation.

For some class of chaotic systems, which include holographic systems, $C(t)$ is expected to behave as (see [30, 36] for a discussion of different possible OTOC growth forms)

$$C(t) \sim \begin{cases} N_{\text{dof}}^{-1} & \text{for } t < t_d, \\ N_{\text{dof}}^{-1} \exp(\lambda_L t) & \text{for } t_d \ll t \ll t_* \\ \mathcal{O}(1) & \text{for } t > t_*, \end{cases} \tag{12}$$

where N_{dof} is the number of degrees of freedom of the system. Here, we have assumed V and W to be unitary and Hermitian operators, so that $VV = WW = 1$. The exponential growth of $C(t)$ is characterized by the Lyapunov exponent (this is actually the quantum analogue of the classical Lyapunov exponent; the two quantities are not necessarily the same in the classical limit [21]; here we stick to the physicists long standing tradition of using misnomers and just refer to λ_L as the Lyapunov exponent) λ_L and takes place at intermediate time scales bounded by the dissipation time t_d and the scrambling time t_*. The dissipation time is related to the classical Ruelle resonances ($t_d \sim \mu^{-1}$) and it characterizes the exponential decay of two-point correlators, e.g., $\langle V(0)V(t)\rangle \sim e^{-t/t_d}$. The dissipation time also controls the late time behavior of $C(t)$. The scrambling time $t_* \sim \lambda_L^{-1} \log N_{\text{dof}}$ is defined as the time at which $C(t)$ becomes of order $\mathcal{O}(1)$. See Figure 2. The scrambling time controls how fast the chaotic system scrambles information. If we perturb the system with an operator that involves only a few degrees of freedom, the information about this operator will spread among the other degrees of freedom of the system. After a scrambling time, the information will be scrambled among all the degrees of freedom and the operator will have a large commutator with almost any other operator.

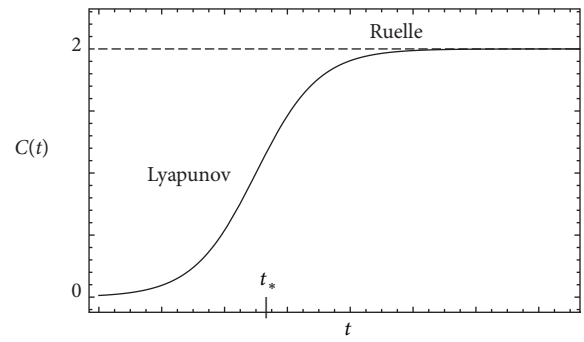

Figure 2: Schematic form of $C(t)$. We indicated the regions of Lyapunov and Ruelle behavior. $C(t) \sim \mathcal{O}(1)$ at $t \sim t_*$.

To understand how the above behavior relates to chaos, we write the double commutator as

$$C(t) = \left\langle -[W(t), V(0)]^2 \right\rangle_\beta \tag{13}$$

$$= 2 - 2\langle W(t) V(0) W(t) V(0)\rangle_\beta, \tag{14}$$

where we made the assumption that W and V are Hermitian and unitary operators. Note that all the relevant information about $C(t)$ is contained in the OTOC:

$$\text{OTO}(t) = \langle W(t) V(0) W(t) V(0)\rangle. \tag{15}$$

The fact that $C(t)$ approaches 2 at later times implies that the OTO(t) should vanish in that limit. To understand why this is related to chaos we think of OTO(t) as an inner-product of two states

$$\text{OTO}(t) = \langle \psi_2 \mid \psi_1 \rangle, \tag{16}$$

where

$$\begin{aligned} |\psi_1\rangle &= W(-t) V(0) |\beta\rangle, \\ |\psi_2\rangle &= V(0) W(-t) |\beta\rangle \end{aligned} \tag{17}$$

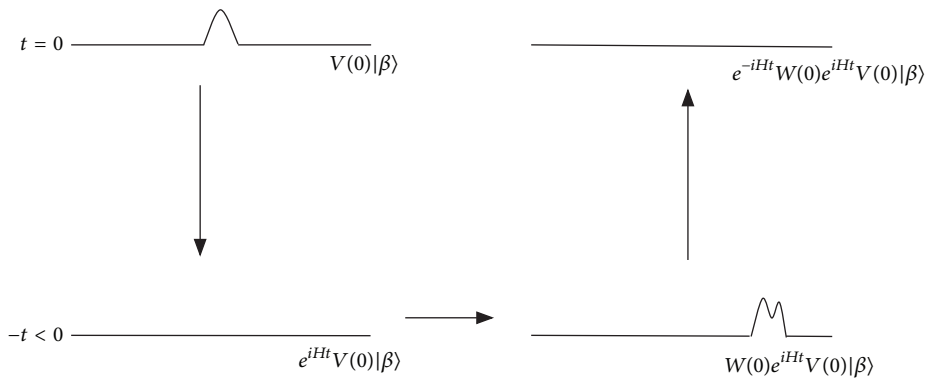

Figure 3: Construction of the state $W(-t)V(0)|\beta\rangle$. For a chaotic system the perturbation V fails to rematerialize at $t = 0$. In a nonchaotic system we expect the perturbation V to rematerialize at $t = 0$.

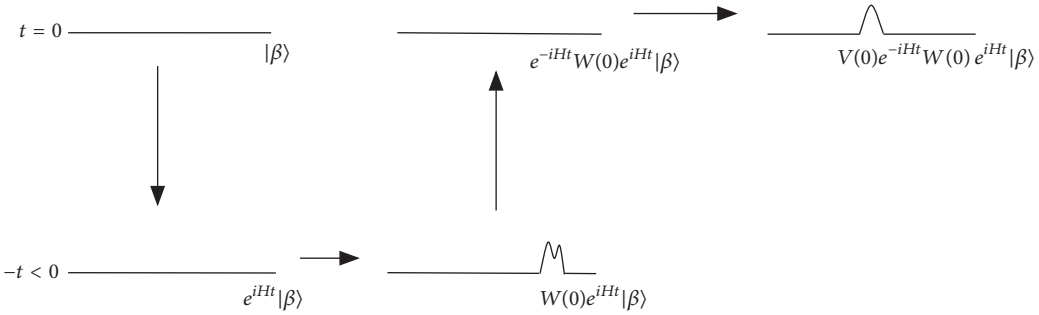

Figure 4: Construction of the state $V(0)W(-t)|\beta\rangle$. By construction, this state displays the perturbation V at $t = 0$.

where $|\beta\rangle$ is some thermal state and we replace $t \longrightarrow -t$ to make easier the comparison with black holes physics.

If $[V(0), W(t)] \approx 0$ for any value of t, the two states are approximately the same, and $\langle\psi_1 \mid \psi_2\rangle \approx 1$, implying $C(t) \approx 0$. That means the system displays no chaos—the early measurement of V has no effect on the later measurement of W. If, on the other hand, $[V(0), W(t)] \neq 0$, the states $|\psi_1\rangle$ and $|\psi_2\rangle$ will have a small superposition $\langle\psi_1 \mid \psi_2\rangle \approx 0$, implying $C(t) \approx 2$. That means that V has a large effect on the later measurement of W.

In Figure 3 we construct the states $|\psi_1\rangle$ and $|\psi_2\rangle$ and explain why $\langle\psi_1 \mid \psi_2\rangle \approx 0$ for large t means chaos. Let us start by constructing the state $|\psi_1\rangle = W(-t)V(0)|\beta\rangle = e^{-iHt}W(0)e^{iHt}V(0)|\beta\rangle$. The unperturbed thermal state is represented by a horizontal line. We initially consider the state $V(0)|\beta\rangle$, which is the thermal state perturbed by V. If we evolve the system backwards in time (applying the operator e^{iHt}) for some time which is larger than the dissipation time, the system will thermalize and it will no longer display the perturbation V. After that, we apply the operator W, which should be thought of as a small perturbation, and then we evolve the system forwards in time (applying the operator e^{-iHt}). The final results of this set of operations depend on the nature of the system. If the system is chaotic, the perturbation W will have a large effect after a scrambling time, and the perturbation that was present at $t = 0$ will no longer rematerialize. This is illustrated in Figure 3. In contrast, for a nonchaotic system, the perturbation W will have little effect on the system at later times, and the perturbation V will (at least partially) rematerialize at $t = 0$.

We now construct the state $|\psi_2\rangle = V(0)W(-t)|\beta\rangle = V(0)e^{-iHt}W(0)e^{iHt}|\beta\rangle$. This is illustrated in Figure 4. We start with the thermal state $|\beta\rangle$ and then we evolve this state backwards in time $e^{iHt}|\beta\rangle$. After that, we apply the operator W and then we evolve the system forwards in time, obtaining the state $e^{-iHt}W(0)e^{iHt}|\beta\rangle$. Finally, we apply the operator V, obtaining the state $V(0)W(-t)|\beta\rangle$. Note that, by construction, this state displays the perturbation V at $t = 0$, while the state $W(-t)V(0)|\beta\rangle$ does not. As a consequence, the two states are expected to have a small superposition $\langle W(-t)V(0) \mid W(-t)V(0)\rangle_\beta \approx 0$. This should be contrasted to the case where the system is not chaotic. In this case the perturbation V rematerializes at $t = 0$, and the states $|\psi_1\rangle$ and $|\psi_2\rangle$ have a large superposition, i.e., $\langle W(-t)V(0) \mid W(-t)V(0)\rangle_\beta \approx 1$.

In this construction we assumed the operators $V(0)$ and $W(-t)$ to be separated by a scrambling time, i.e., $|t| > t_*$. This is important because, at earlier times, the two operators, which in general involve different degrees of freedom of the system, generically commute. The operators manage to have a nonzero commutator at later times because of the phenomenon of operation growth that we will describe in the next section.

3.1. Operator Growth and Scrambling. The operators V and W act generically at different parts of the physical system, yet they can have a nonzero commutator at later times. This

is possible because in chaotic systems the time evolution of an operator makes it more and more complicated, involving and increasing number of degrees of freedom. As a result, an operator that initially involves just a few degrees of freedom becomes delocalized over a region that grows with time. The growth of the operator $W(t)$ is maybe more evident from the point of view of the Baker-Campbell-Hausdorff (BCH) formula, in terms of which we can write

$$\begin{aligned} W(t) &= e^{iHt} W(0)\, e^{-iHt} \\ &= \sum_{k=0}^{\infty} \frac{(-it)^k}{k!} \left[H\left[H, \ldots [H, W(0)] \ldots\right]\right]. \end{aligned} \tag{18}$$

From the above formula it is clear that, at each order in t, there is a more complicated contribution to $W(t)$. In chaotic systems the operator becomes more and more delocalized as the time evolves, and it eventually becomes delocalized over the entire system. The time scale at which this occurs is the so-called scrambling time t_*. After the scrambling time the operator $W(t)$ manages to have a nonzero and large commutator with almost any other operator, even operators involving only a few degrees of freedom.

This can be clearly illustrated in the case of a spin chain. Let us follow [7] and consider an Ising-like model with Hamiltonian

$$H = -\sum_i \left(Z_i Z_{i+1} + g X_i + h Z_i\right), \tag{19}$$

where X_i, Y_i, and Z_i denote Pauli matrices acting on the ith site of the spin chain. The above system is integrable if we take $g = 1$ and $h = 0$, but it is strongly chaotic if we choose $g = -1.05$ and $h = 0.5$.

To illustrate the concept of scrambling, we consider the time evolution of the operator Z_1. Using the BCH formula we can write the following.

$$\begin{aligned} Z_1(t) = Z_1 - it\left[H, Z_1\right] - \frac{t^2}{2!}\left[H, \left[H, Z_1\right]\right] \\ + \frac{it^3}{3!}\left[H, \left[H, \left[H, Z_1\right]\right]\right] + \ldots \end{aligned} \tag{20}$$

Ignoring multiplicative constants and signs we can write the above terms (schematically) as follows.

$$\begin{aligned} \left[H, Z_1\right] &\sim Y_1 \\ \left[H, \left[H, Z_1\right]\right] &\sim Y_1 + X_1 Z_2 \\ \left[H, \left[H, \left[H, Z_1\right]\right]\right] &\sim Y_1 + Y_2 X_1 + Y_1 Z_2 \\ \left[H, \left[H, \left[H, \left[H, Z_1\right]\right]\right]\right] &\sim X_1 + Y_1 + Z_1 + X_1 X_2 + Y_1 Y_2 \\ &\quad + Z_1 Z_2 + X_1 Z_2 + Z_3 Y_1 \\ &\quad + Y_1 Z_2 Y_2 + Z_1 X_2 X_1 \\ &\quad + X_2 Z_3 X_1 \end{aligned} \tag{21}$$

As the time evolves, higher order terms become important in series (20), and the operator $Z_1(t)$ becomes more and more complicated, involving terms in an increasing number of sites. For large enough t the operator will involve all the sites of the spin chain and it will manage to have a nonzero commutator with a Pauli operator in any other site of the system. In this situation the information about Z_1 is essentially scramble among all the degrees of freedom of the system. As discussed before, this occurs after a scrambling time. Above this time the double commutator $C(t)$ saturates to a constant value. This should be contrasted to what happens for an integrable system. In this case the operator grows, but it also decreases at later times. In the chaotic case, the operator remains large at later times [7].

3.2. Probing Chaos with Local Operators. In quantum field theories we can upgrade (11) to the case where the operators are separated in space

$$C(t, x) = \left\langle -\left[V(0,0), W(t,x)\right]^2 \right\rangle_\beta. \tag{22}$$

Strictly speaking, the above expression is generically divergent, but it can be regularized by adding imaginary times to the time arguments of the operators V and W. For a large class of spin chains, higher-dimensional SYK-models, and CFTs, the above commutator is roughly given by

$$C(t, x) \sim \exp\left[\lambda_L\left(t - t_* - \frac{|x|}{v_B}\right)\right], \tag{23}$$

where v_B is the so-called butterfly velocity. (Actually, v_B represents the "velocity of the butterfly effect". Here we continue to follow the tradition of using misnomers.) This velocity describes the growth of the operator W in physical space and it acts as a low-energy Lieb-Robinson velocity [37], which sets a bound for the rate of transfer of quantum information. From the above formula, we can see that there is an additional delay in scrambling due to the physical separation between the operators. The butterfly velocity defines an effective light-cone for commutator (22). Inside the cone, for $t - t_* \geqslant |x|/v_B$, we have $C(t, x) \sim \mathcal{O}(1)$, whereas for outside the cone, for $t - t_* < |x|/v_B$, the commutator is small, $C(t, x) \sim 1/N_{\text{dof}} \ll 1$. Outside the light-cone the Lorentz invariance implies a zero commutator. The light-cone and the butterfly effect cone are illustrated in Figure 5.

4. Chaos and Holography

In this section we review how the chaotic properties of holographic theories can be described in terms of black holes physics. Black holes behave as thermal systems and thermal systems generically display chaos. This implies that black holes are somehow chaotic. This statement has a precise realization in the context of the gauge/gravity duality. According to this duality, some strongly coupled nongravitational systems are dual to higher-dimensional gravitational systems. In the most known and studied example of this duality the $\mathcal{N} = 4$ super Yang-Mills (SYM) theory living in $R^{3,1}$ is dual to type IIB supergravity in $AdS_5 \times S^5$. More generically, a $d-$dimensional nongravitational theory living in $R^{d-1,1}$ is dual to a gravity theory living in a higher-dimensional space

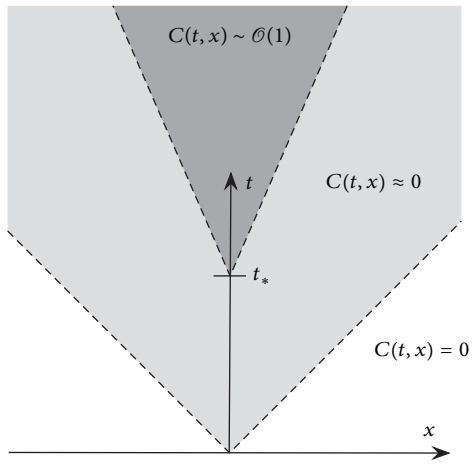

Figure 5: Light-cone (gray region) and butterfly effect cone (dark gray region). Inside the butterfly effect cone, for $t - t_* \geqslant |x|/v_B$, we have $C(t,x) \sim \mathcal{O}(1)$, whereas for outside the cone, for $t - t_* < |x|/v_B$, the commutator is small, $C(t,x) \sim 1/N_{\text{dof}} \ll 1$. Outside the light-cone the Lorentz invariance implies a zero commutator.

of the form $AdS_{d+1} \times \mathcal{M}$, where $\mathcal{M}$ is generically a compact manifold. The nongravitational theory can be thought of as living in the boundary of AdS_{d+1} and because of that is usually called the *boundary theory*. The gravitational theory is also called the *bulk theory*.

There is a dictionary relating physical quantities in the boundary and bulk description [3, 4]. An example is provided by the operators of the boundary theory, which are related to bulk fields. The boundary theory at finite temperature can be described by introducing a black hole in the bulk. The thermalization properties of the boundary theory have a nice visualization in terms of black holes physics. By applying a local operator in the boundary theory we produce some perturbation that describes a small deviation from the thermal equilibrium. The information about $V(x)$ is initially contained around the point x, but it gets delocalized over a region that increases with time, until it completely melts into the thermal bath. In the bulk theory, the application of the operator $V(x)$ produces a particle (field excitation) close to the boundary of the space, which then falls into the black hole. The return to the thermal equilibrium in the boundary theory corresponds to the absorption of the bulk particle by the black hole. Figure 6 illustrates the bulk description of thermalization.

The approach to thermal equilibrium is controlled by the black hole's quasinormal modes (QNMs). In holographic theories, the quasinormal modes control the decay of two-point functions of the boundary theory

$$\langle V(t)\, V(0)\rangle_\beta \sim e^{-t/t_d} \tag{24}$$

where the dissipation time t_d is related to the lowest quasinormal mode ($\text{Im}(\omega) \sim t_d^{-1}$). From the point of view of the bulk theory the QNMs describes how fast a perturbed black hole returns to equilibrium. Clearly, the black hole's quasinormal modes correspond to the classical Ruelle resonances. In holographic theories the dissipation time is roughly given by $t_d \sim \beta$.

Another important exponential behavior of black holes is provided by the blue-shift suffered by the in-falling quanta or, equivalently, the red shift suffered by the quanta escaping from the black hole. The blue-shift suffered by the in-falling quanta is determined by the black hole's temperature. If the quanta asymptotic energy is E_0, this energy increases exponentially with time

$$E = E_0 e^{(2\pi/\beta)t}, \tag{25}$$

where β is the Hawking's inverse temperature. Later we will see that this exponential increase in the energy of the in-falling quanta gives rise to the Lyapunov behavior of $C(t,x)$ of holographic theories.

4.1. Holographic Setup

The TFD State & Two-Sided Black Holes. In the study of chaos it is convenient to consider a thermofield double state made out of two identical copies of the boundary theory

$$|\text{TFD}\rangle = \frac{1}{Z^{1/2}} \sum_n e^{-\beta E_n/2} |n\rangle_{\text{L}} |n\rangle_{\text{R}}, \tag{26}$$

where L and R label the states of the two copies, which we call QFT_{L} and QFT_{R}, respectively. The two boundary theories do not interact and only know about each other through their entanglement. This state is dual to an eternal (two-sided) black hole, with two asymptotic boundaries, where the boundary theories live [38]. This is a wormhole geometry, with an Einstein-Rosen bridge connecting the two sides of the geometry. The wormhole is not traversable, which is consistent with the fact that the two boundary theories do not interact.

For definiteness we assume a metric of the form

$$ds^2 = -G_{tt}(r)\, dt^2 + G_{rr}(r)\, dr^2 + G_{ij}\left(r, x^k\right) dx^i dx^j, \tag{27}$$

where the boundary is located at $r = \infty$, where the above metric is assumed to asymptote AdS_{d+1}. We take the horizon as located at $r = r_{\text{H}}$, where G_{tt} vanishes and G_{rr} has a first order pole. For future purposes, let β be the Hawking's inverse temperature, and S_{BH} be the Bekenstein-Hawking entropy.

In the study of shock waves it is more convenient to work with Kruskal-Szekeres coordinates, since these coordinates cover smoothly the globally extended spacetime. We first define the tortoise coordinate

$$dr_* = \sqrt{\frac{G_{rr}}{G_{tt}}}\, dr, \tag{28}$$

and then we introduce the Kruskal-Szekeres coordinates U, V as follows.

$$U = +e^{(2\pi/\beta)(r_* - t)},$$

$$V = -e^{(2\pi/\beta)(r_* + t)}$$

(left exterior region)

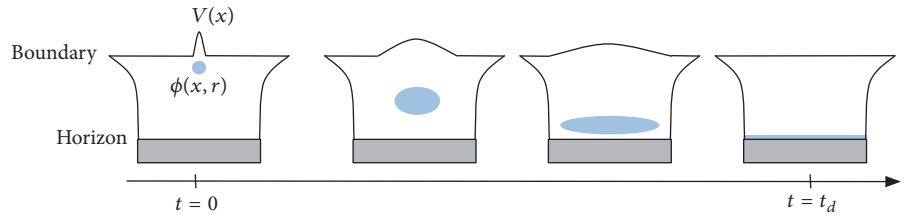

Figure 6: Bulk picture of thermalization. The figure represents an asymptotically *AdS* black hole geometry. The boundary is at the top edge, while the black hole horizon is at the bottom edge. The black hole's interior is shown in gray. The boundary operator V is dual to the bulk field ϕ. From the point of view of the boundary theory the perturbation produced by V is initially localized around the point x, but it gets delocalized over a region that increases with time. In the bulk description this is described by a particle (field excitation) that is initially close to the boundary and then falls into the black hole.

$$
\begin{aligned}
U &= -e^{(2\pi/\beta)(r_*-t)}, \\
V &= +e^{(2\pi/\beta)(r_*+t)} \\
&\qquad \text{(right exterior region)} \\
U &= +e^{(2\pi/\beta)(r_*-t)}, \\
V &= +e^{(2\pi/\beta)(r_*+t)} \\
&\qquad \text{(future interior region)} \\
U &= -e^{(2\pi/\beta)(r_*-t)}, \\
V &= -e^{(2\pi/\beta)(r_*+t)} \\
&\qquad \text{(past interior region)}
\end{aligned}
\tag{29}
$$

In terms of these coordinates the metric reads

$$
ds^2 = 2A(UV)\, dUdV + G_{ij}(UV)\, dx^i dx^j, \tag{30}
$$

where

$$
A(UV) = \frac{\beta^2}{8\pi^2} \frac{G_{tt}(UV)}{UV}. \tag{31}
$$

In these coordinates the horizon is located at $U = 0$ or at $V = 0$. The left and right boundaries are located at $UV = -1$ and the past and future singularities at $UV = 1$. The Penrose diagram for this metric is shown in Figure 7.

The global extended spacetime can also be described in terms of complexified coordinates [39]. In this case one defines the complexified Schwarzschild time

$$
t = t_{\mathrm{L}} + i t_{\mathrm{E}}, \tag{32}
$$

where t_{L} and t_{E} are the Lorentzian and Euclidean times, and then one describes the time in each of the four patches (left and right exterior regions, and the future and past interior regions) as having a constant imaginary part.

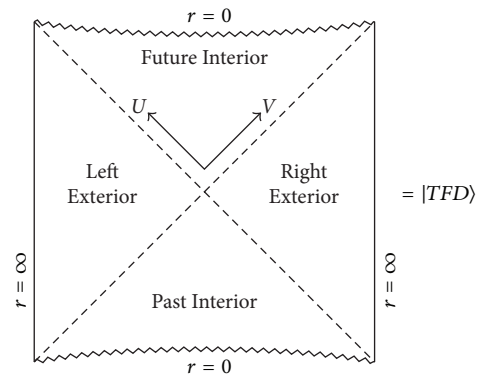

Figure 7: Penrose diagram for the two-sided black holes with two boundaries that asymptote *AdS*. This geometry is dual to a thermofield double state constructed out of two copies of the boundary theory.

$$
\begin{aligned}
t_{\mathrm{E}} &= 0 \quad \text{(right exterior region)} \\
t_{\mathrm{E}} &= -\frac{\beta}{4} \quad \text{(future interior region)} \\
t_{\mathrm{E}} &= -\frac{\beta}{2} \quad \text{(left exterior region)} \\
t_{\mathrm{E}} &= +\frac{\beta}{4} \quad \text{(past interior region)}
\end{aligned}
\tag{33}
$$

The Euclidean time has a period of β. The Lorentzian time increases upward (downward) in the right (left) exterior region, and to the right (left) in the future (past) interior.

Note that, with the complexified time, one can obtain an operator acting on the left boundary theory by adding (or subtracting) $i\beta/2$ to the time of an operator acting on the right boundary theory.

Perturbations of the TFD State & Shock Wave Geometries. We now turn to the description of states of the form

$$
W(t)\,|\mathrm{TFD}\rangle \tag{34}
$$

where W is a thermal scale operator that acts on the right boundary theory. This state can be describe by a 'particle'

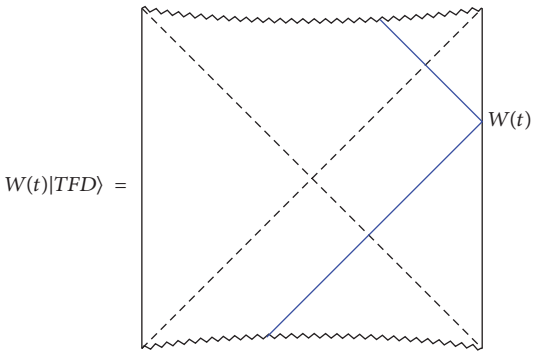

FIGURE 8: Bulk description of the state $W(t)|\text{TFD}\rangle$. In blue is shown the trajectory of a 'particle' that comes out of the past horizon, reaches the boundary at time t producing the perturbation W, and then falls into the future horizon. From now on, we will refer to this bulk excitation as the *W-particle*.

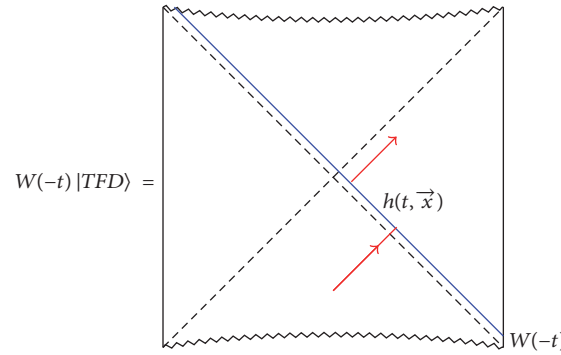

FIGURE 9: Bulk description of the state $W(-t)|\text{TFD}\rangle$. An early enough perturbation produces a shock wave geometry. The effect of the shock wave (shown in blue) is to produce a shift $U \longrightarrow U+h(t,\vec{x})$ in the trajectory of a probe particle (shown in red) crossing it.

(field excitation) in the bulk that comes out of the past horizon, reaches the right boundary at time t, and then falls into the future horizon, as illustrated in Figure 8.

If $|t|$ is not too large, the state $W(t)|\text{TFD}\rangle$ will represent just a small perturbation of the TFD state and the corresponding description in the bulk will be just an eternal two-sided black hole geometry slightly perturbed by the presence of a probe particle. This is no longer the case if $|t|$ is large. In this case there is a nontrivial modification of the geometry. A very early perturbation, for example, is described in the bulk in terms of a particle that falls towards the future horizon for a very long time and gets highly blue-shifted in the process. If the particle's energy is E_0 in the asymptotic past, this energy will be exponentially larger from the point of view of the $t = 0$ slice of the geometry, i.e., $E = E_0 e^{(2\pi/\beta)t}$. Therefore, for large enough $|t|$, the particle's energy will be very large and one needs to include the corresponding back-reaction.

The back-reaction of a very early (or very late) perturbation is actually very simple—it corresponds to a shock wave geometry [40, 41]. To understand that, we first need to notice that, under boundary time evolution, the stress energy of a generic perturbation W gets compressed in the $V-$direction and stretched in the $U-$direction. For large enough $|t|$ we can approximate the stress tensor of the W-particle as

$$T_{VV} \sim P^U \delta(V)\, a\left(\vec{x}\right), \tag{35}$$

where $P^U \sim \beta^{-1} e^{(2\pi/\beta)t}$ is the momentum of the W-particle in the $U-$direction and $a(\vec{x})$ is some generic function that specifies the location of the perturbation in the spatial directions of the right boundary. Note that T_{VV} is completely localized at $V = 0$ and homogeneous along the $U-$direction. Besides, even if the W-particle is massive, the exponential blue-shift will make it follow an almost null trajectory, as shown in Figure 9.

The shock wave geometry produced by the W-particle is described by the metric

$$\begin{aligned} ds^2 &= 2A(UV)\, dUdV + G_{ij}(UV)\, dx^i dx^j \\ &\quad - 2A(UV)\, h\left(t,\vec{x}\right)\delta(V)\, dV^2, \end{aligned} \tag{36}$$

which is completely specified by the shock wave transverse profile $h(t,\vec{x})$. This geometry can be seen as two pieces of an eternal black hole glued together along $V = 0$ with a shift of magnitude $h(t,\vec{x})$ in the $U-$direction. We find it useful to represent this geometry with the same Penrose diagram of the unperturbed geometry, but with the prescription that any trajectory crossing the shock wave gets shifted in the $U-$direction as $U \longrightarrow U + h(t,\vec{x})$. See Figure 9.

The precise form of $h(t,\vec{x})$ can be determined by solving the $VV-$component of Einstein's equation. For a local perturbation, i.e., $a(\vec{x}) = \delta^{d-1}(\vec{x})$, the solution reads

$$\begin{aligned} &h\left(t,\vec{x}\right) \sim G_{\text{N}} e^{(2\pi/\beta)t-\mu|\vec{x}|}, \\ &\text{with } \mu = \frac{2\pi}{\beta}\sqrt{\frac{(d-1)\, G'_{ii}(r_{\text{H}})}{G'_{tt}(r_{\text{H}})}}, \end{aligned} \tag{37}$$

where, for simplicity, G_{ij} has been assumed to be diagonal and isotropic.

Interestingly, the shock wave profile contains information about the parameters characterizing the chaotic behavior of the boundary theory. Indeed, the double commutator has a region of exponential growth at which $C(t,\vec{x}) \sim h(t,\vec{x})$. From this identification, we can write

$$h\left(t,\vec{x}\right) \sim e^{(2\pi/\beta)(t-t_*-|\vec{x}|/v_{\text{B}})} \tag{38}$$

where (the leading order contribution to) the scrambling time scales logarithmically with the Bekenstein-Hawking entropy

$$t_* \sim \frac{\beta}{2\pi}\log\frac{1}{G_{\text{N}}} \sim \frac{\beta}{2\pi}\log S_{\text{BH}}, \tag{39}$$

while the Lyapunov exponent is proportional to the Hawking's temperature.

$$\lambda_L = \frac{2\pi}{\beta}. \tag{40}$$

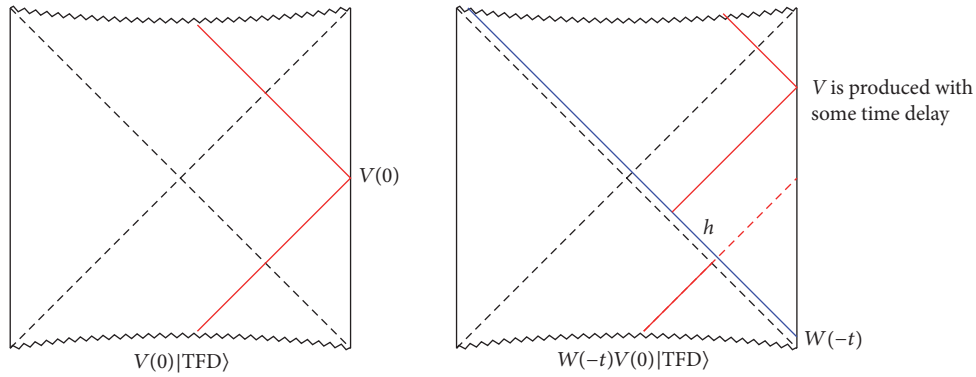

FIGURE 10: *Left panel*: bulk description of the state $V(0)|\text{TFD}\rangle$. The V-particle comes out of the past horizon, reaches the boundary at time $t = 0$ producing the perturbation V, and then falls into the future horizon. *Right panel*: bulk description of the 'in' state $|\psi_{\text{in}}\rangle = W(-t)V(0)|\text{TFD}\rangle$. The W-particle (shown in blue) produces a shock wave along $V = 0$. The trajectory of the V-particle (shown in red) suffers a shift and the perturbation V is produced at the boundary with some time delay.

The butterfly velocity is determined from the near-horizon geometry. (Here we are assuming isotropy. In the case of anisotropic metrics the formula for v_B is a little bit more complicated. See, for instance, Appendix A of [42] or Appendix B of [43].)

$$v_B^2 = \frac{G'_{tt}(r_{\text{H}})}{(d-1)\,G'_{ii}(r_{\text{H}})}. \tag{41}$$

4.2. Bulk Picture for the Behavior of OTOCs. In this section we present the bulk perspective for the vanishing of OTOCs at later times. In order to do that, we write the OTOC as a superposition of two states

$$\begin{aligned}\text{OTO}(t) &= \langle \text{TFD}|\, W(-t)\, V(0)\, W(-t)\, V(0)\, |\text{TFD}\rangle \\ &= \langle \psi_{\text{out}} \mid \psi_{\text{in}} \rangle,\end{aligned} \tag{42}$$

where the 'in' and 'out' states are given by the following.

$$\begin{aligned}|\psi_{\text{in}}\rangle &= W(-t)\, V(0)\, |\text{TFD}\rangle, \\ |\psi_{\text{out}}\rangle &= V^{\dagger}(0)\, W^{\dagger}(-t)\, |\text{TFD}\rangle\end{aligned} \tag{43}$$

The interpretation of a vanishing OTOC in terms of the bulk theory is actually very simple. Let us go step by step and construct first the state $V(0)|\beta\rangle$. This state is described by a particle that comes out of the past horizon, reaches the boundary at $t = 0$, and then falls back into the future horizon. See the left panel of Figure 10.

Now the 'in' state can be obtained as

$$\begin{aligned}|\psi_{\text{in}}\rangle &= W(-t)\, V(0)\, |\text{TFD}\rangle \\ &= e^{-iHt} W(0)\, e^{iHt} V(0)\, |\text{TFD}\rangle.\end{aligned} \tag{44}$$

This amounts to the following: evolving the state $V(0)|\text{TFD}\rangle$ backwards in time, applying the operator W, and then evolving the system forwards in time. The corresponding description in the bulk is shown in the right panel of Figure 10. From this picture we can see that the perturbation

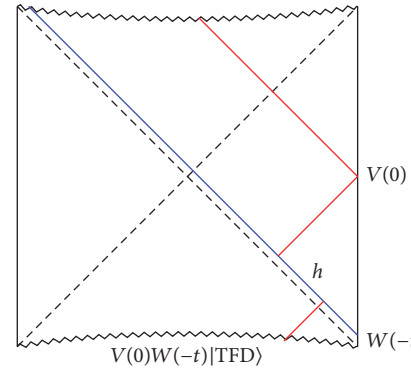

FIGURE 11: Bulk description of the 'out' state $|\psi_{\text{out}}\rangle = V(0)W(-t)|\text{TFD}\rangle$. The W-particle produces the shock wave geometry. The trajectory of the V-particle is such that, after suffering the shift $U \longrightarrow U + h(t, \vec{x})$, it reaches the boundary at time $t = 0$, producing the perturbation V.

W produces a shock wave that causes a shift in the trajectory of the V-particle, which no longer reaches the boundary at time $t = 0$, but rather with some time delay. The physical interpretation is that a small perturbation in the asymptotic past (represented by W) is amplified over time and destroys the initial configuration (represented by the state $V(0)|\text{TFD}\rangle$).

The bulk description of the 'out' state can be obtained in the same way. As this state displays the perturbation V at $t = 0$, the V-particle should be produced in the asymptotic past in such a way that, after its trajectory gets shifted as $U \longrightarrow U + h$, it reaches the boundary at the time $t = 0$ producing the perturbation V.

Comparing the bulk description of the state $|\psi_{\text{in}}\rangle$ (shown in the right panel of Figure 10) with the description of the state $|\psi_{\text{out}}\rangle$ (shown in Figure 11) we can see that these states are indistinguishable when $h(t, \vec{x})$ is zero, but they become more and more different for large values of $h(t, \vec{x})$. As a consequence, the overlap $C(t) = \langle \psi_{\text{out}} \mid \psi_{\text{in}} \rangle$ is equal to one when $h = 0$, but it decreases to zero as we increase the value of h.

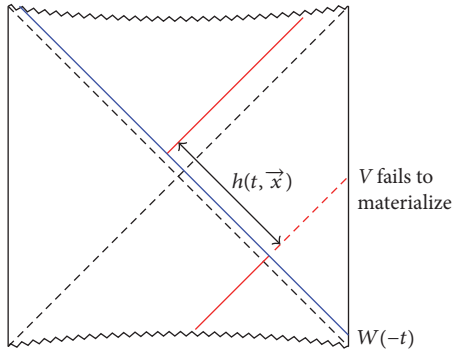

FIGURE 12: Bulk description of the state $W(-t)V(0)|\text{TFD}\rangle$ for the case where $|t| \geq t_*$. The V-particle's trajectory undergoes a shift, and it is captured by the black hole. The perturbation V never forms, and the corresponding state has no superposition with the 'out' state $V(0)W(-t)|\text{TFD}\rangle$, resulting in a vanishing OTOC.

The exponential behavior of $h(t, \vec{x})$ implies that an early enough perturbation can produce a very large shift in the V-particle's trajectory, causing it to be captured by the black hole and preventing the materialization of the V perturbation at the boundary. See Figure 12. This should be compared with the physical picture given in Figure 3.

The physical picture of the process described in Figure 12 is quite simple. The state $V(0)|\text{TFD}\rangle$ can be represented by a black hole geometry in which a particle (the V-particle) escapes from the black holes and reaches the boundary at time $t = 0$. The state $W(-t)V(0)|\text{TFD}\rangle$ is obtained by perturbing the state $V(0)|\text{TFD}\rangle$ in the asymptotic past. This corresponds to the addition of a W-particle to the system in the asymptotic past. This particle gets highly blue-shifted as it falls towards the black hole. The black hole captures the W-particle and becomes bigger. The V-particle fails to escape from the bigger black hole and never reaches the boundary to produce the V perturbation. This physical picture is illustrated in Figure 13.

The precise form of the above OTOC can be obtained by calculating the overlap $\langle \psi_{\text{out}} \mid \psi_{\text{in}} \rangle$ using the Eikonal approximation [8], in which the Eikonal phase δ is proportional to the shock wave profile $\delta \sim h(t, \vec{x})$. The OTOC can be written as an integral of the phase $e^{i\delta}$ weighted by kinematical factors which are basically Fourier transforms of bulk-to-boundary propagators for the V and W operators.

The result for Rindler AdS_3 reads (the below result assumes $\Delta_W \gg \Delta_V$)

$$\frac{\langle V(i\epsilon_1) W(t+i\epsilon_2) V(i\epsilon_3) W(t+i\epsilon_4)\rangle}{\langle V(i\epsilon_1) V(i\epsilon_3)\rangle \langle W(i\epsilon_2) W(i\epsilon_4)\rangle} = \left(\frac{1}{1-\left(8\pi i G_N \Delta_W/\epsilon_{13}\epsilon_{24}^*\right) e^{(2\pi/\beta)(t-|\vec{x}|/v_B)}}\right)^{\Delta_V} \quad (45)$$

where Δ_V and Δ_W are the scaling dimensions of the operators V and W, respectively, and $\epsilon_{ij} = i(e^{i\epsilon_i} - e^{i\epsilon_j})$. For this system $\beta = 2\pi$ and $v_B = 1$. This formula matches the direct CFT calculation (the CFT perspective for the onset of chaos has been widely discussed in [44]; other references in this direction include, for instance, [45–48].) obtained in [20]. It can also be derived using the geodesic approximation for two-sided correlators in a shock wave background [5, 20].

Expanding the above result for small values of $G_N e^{(2\pi/\beta)(t-|\vec{x}|/v_B)}$, we obtain

$$\text{OTO}(t) = 1 - 8\pi i G_N \frac{\Delta_V \Delta_W}{\epsilon_{13}\epsilon_{24}^*} e^{(2\pi/\beta)(t-|\vec{x}|/v_B)}, \quad (46)$$

and, since $h(t, \vec{x}) \sim G_N e^{(2\pi/\beta)(t-|\vec{x}|/v_B)}$, the above result implies

$$C\left(t, \vec{x}\right) \sim h\left(t, \vec{x}\right). \quad (47)$$

The above result is valid for small (in AdS/CFT the Newton constant is related to the rank of the gauge group of dual CFT as $G_N \sim 1/N^a$, where a is a positive number that depends on the dimensionality of the bulk space time (cf. section 7.2 of [49]); our classical gravity calculations are only valid in the large-N limit (that suppresses quantum corrections) so it is natural to consider G_N as a small parameter) values of G_N, or for any value of G_N, but for times in the range $t_d \ll t \ll t_*$, where $t_* = (\beta/2\pi)\log(1/G_N)$.

Despite being true in the Rindler AdS_3 case, the proportionality between the double commutator and the shock wave profile has not been demonstrated in more general cases. However, the authors of [8] argued that, in regions of moderate scattering between the V- and W-particle, the identification $C(t, \vec{x}) \sim h(t, \vec{x})$ is approximately valid.

At very late times, the behavior of the OTO(t) is expected to be controlled by the black hole quasinormal modes. Indeed, in the case of a compact space it is possible to show that

$$C(t) \sim e^{-2i\omega(t-t_*-R/v_B)}, \quad \text{with } \text{Im}(\omega) < 0, \quad (48)$$

where R is the diameter of the compact space and ω is the system lowest quasinormal frequency [8].

4.2.1. Stringy Corrections. In this section we briefly discuss the effects of stringy corrections to the Einstein gravity results for OTOCs. We start by reviewing the Einstein gravity results from the perspective of scattering amplitudes. In the framework of the Eikonal approximation, the phase shift suffered by the V-particle is given by

$$\delta = -P^V h\left(t, \vec{x}\right) \sim G_N s, \quad (49)$$

where we used the fact that $h(t, \vec{x}) \sim G_N P^U$ and introduced a Mandelstam-like variable $s = 2A(0)P^U P^V$. In a small-G_N expansion the double commutator $C(t)$ and the phase shift δ scale with s in the same way, namely,

$$C(t) \sim G_N s, \quad (50)$$

where $s \sim \beta^{-2} e^{(2\pi/\beta)t}$.

The string corrections can be incorporated using the standard Veneziano formula for the relativistic scattering

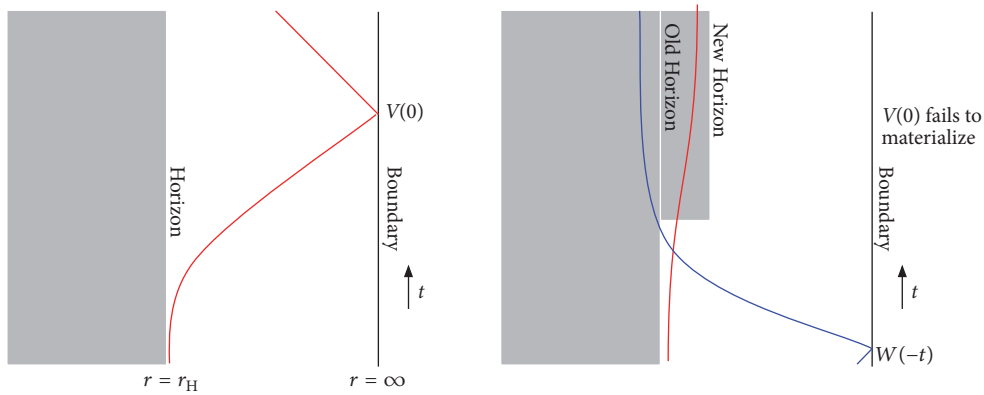

FIGURE 13: *Left panel*: bulk description of the state $V(0)|\text{TFD}\rangle$. The V-particle (whose trajectory is shown in red) escapes from the black hole (shown in gray), reaches the boundary at time $t = 0$, and then falls back towards the horizon. *Right panel*: bulk description of the state $W(-t)V(0)|\text{TFD}\rangle$ for the case where $|t| \gtrsim t_*$. The W-particle (whose trajectory is shown in blue) gets blue-shifted and increases the black hole size as it falls into it. The V-particle fails to escape from the larger black hole, and the perturbation V never forms at the boundary.

amplitude $\mathcal{A} \sim s\delta$. The phase shift can then be schematically written as an infinite sum

$$\delta \sim \sum_J G_N s^{J-1}, \tag{51}$$

where each term corresponds to the contribution due to the exchange of a spin-J field. In Einstein gravity the dominant contribution comes from the exchange of a spin-2 field, the graviton. In string theory, we have to include an infinite tower of higher spin fields. Naively, it looks like these higher spin contributions will increase the development of chaos. However, the resummation of the above sum actually leads to a decrease in the development of chaos. The string-corrected phase shift has a milder dependence with s, namely,

$$\delta \sim G_N s^{J_{\text{eff}}-1}, \tag{52}$$

with the effective spin given by [8]

$$J_{\text{eff}} = 2 - \frac{d\,(d-1)\,\ell_s^2}{4\ell_{AdS}^2} \tag{53}$$

where ℓ_s is the string length, ℓ_{AdS} is the AdS length scale, and d is the number of dimensions of the boundary theory. As a result, the string-corrected double commutator grows in time with an effective smaller Lyapunov exponent

$$C_{\text{string}}(t) \sim e^{(2\pi/\beta)(1-d(d-1)\ell_s^2/4\ell_{AdS}^2)t}, \tag{54}$$

and this leads to a larger scrambling time. (At small scales, the string-corrected shock wave has a Gaussian profile, and the concept of butterfly velocity is not meaningful. It was recently shown, however, that at larger scales is possible to define a string-corrected butterfly velocity. The result for $\mathcal{N} = 4$ SYM theory reads [50] $v_B = \sqrt{2/3}(1 + (23\zeta(3)/16)(1/\lambda^{3/2}))$, where λ is the 't Hooft coupling, which can be written in terms of string length scale as $\lambda = (\ell_{AdS}/\ell_s)^4$.)

$$t_*^{\text{string}} = t_* \left(1 + \frac{d\,(d-1)\,\ell_s^2}{4\ell_{AdS}^2}\right). \tag{55}$$

The above discussion implies that for a theory with a finite number of high-spin fields ($J > 2$) chaos would develop faster than in Einstein gravity. These theories, however, are known to violate causality [51]. It is then natural to speculate that the Lyapunov exponent obtained in Einstein gravity has the maximal possible value allowed by causality. This is indeed true and this is the topic of the next section.

4.2.2. Bounds on Chaos. One of the remarkable insights that came from the holographic description of quantum chaos is the fact that there is a bound on chaos—the quantum Lyapunov exponent is bounded from above, while the scrambling time is bounded from below. A distinct feature of holographic systems is that they saturate these two bounds.

Let us follow the historical order and start by discussing the lower bound on the scrambling time. In black holes physics the scrambling time defines how fast the information that has fallen into a black holes can be recovered from the emitted Hawking radiation. (This assumes that half of the black hole's initial entropy has been radiated [52].) In the context of the Hayden-Preskill thought experiment, the scrambling time is barely compatible with black hole complementarity [52], since a smaller scrambling time would lead to a violation of the no-cloning principle. This led Susskind and Sekino to conjecture that black holes are the fastest scramblers in nature; i.e., they have the smallest possible scrambling time [53]. The lower bound on the scrambling time of a generic many-body quantum system can be written as

$$t_* \geqslant C(\beta) \log N_{\text{dof}} \tag{56}$$

where $C(\beta)$ is some function of the inverse temperature. In the case of black holes this function is simply given by $C(\beta) = \beta/2\pi$.

The scrambling time defines a stronger notion of thermalization and should not be confused with the dissipation time. In fact, for black holes, one expects the dissipation time to be given by the black hole quasinormal modes (this is true in the case of low dimension operators) $t_d \sim \beta$, while the scrambling

time is parametrically larger $t_* \sim \beta \log N_{\text{dof}}$. This brings us to the second bound on chaos: for systems with such a large hierarchy between the scrambling and the dissipation, time is possible to derive an upper bound for the Lyapunov exponent [54]:

$$\lambda_L \leqslant \frac{2\pi}{\beta}. \tag{57}$$

One should emphasize that this bound does not depend on the existence of a holographic dual. It can be derived for generic many-body quantum systems under some very reasonable assumptions.

The fact that black hole always has a maximum Lyapunov exponent led to the speculation that the saturation of the chaos bound might be a sufficient condition for a system to have an Einstein gravity dual [9, 54]. In fact, there have been many attempts to use the saturation of the chaos bound as a criterion to discriminate holographic CFTs from the nonholographic ones [20, 44–48, 55, 56]. It was recently shown, however, that this criterion, though necessary, is insufficient to guarantee a dual description purely in terms of Einstein gravity [57, 58].

Since v_B defines the speed at which information propagates, it is natural to question whether this quantity is also bounded. From the perspective of the boundary theory, causality implies

$$v_B \leqslant 1, \tag{58}$$

meaning that information should not propagate faster than the speed of light. Indeed, the above bound can be derived in the context of Einstein gravity by using Null Energy Condition (NEC) and assuming an asymptotically AdS geometry (this derivation uses an alternative definition for v_B, which is based on entanglement wedge subregion duality [59]) [60]. This is consistent with the expectation that gravity theories in asymptotically AdS geometries are dual to relativistic theories. In contrast, for geometries which are not asymptotically AdS, the butterfly velocity can surpass the speed of light [42, 60], which is consistent with the non-Lorentz invariance of the corresponding boundary theories.

If we further assume isotropy, it is possible to derive a stronger bound for v_B [61]

$$v_B \leqslant v_B^{\text{Sch}} = \sqrt{\frac{d}{2(d-1)}}, \tag{59}$$

where v_B^{Sch} is the value of the butterfly velocity for an AdS-Schwarzschild black brane in $d+1$ dimensions. This is also the butterfly velocity for a d-dimensional thermal CFT.

The above formula shows that, for thermal CFTs, v_B does not depend on the temperature. However, if we deform the CFT, v_B acquires a temperature dependence as we move along the corresponding renormalization group (RG) flow. In fact, by considering deformations that break the rotational symmetry, it was noticed that the butterfly velocity violates the above bound, but remains bounded from above by its value at the infrared (IR) fixed point, never surpassing the speed of light [62–64]. The above bound can also be violated by higher curvature corrections, but v_B remains bounded by the speed of light as long as causality is respected. (For instance, in 4-dimensional Gauss-Bonnet (GB) gravity, the butterfly velocity surpasses the speed of light for $\lambda_{GB} < -3/4$, but causality requires $\lambda_{GB} > -0.19$ [65, 66]. Moreover, it was recently shown that, unless one adds an infinite tower of extra higher spin fields, GB gravity might be inconsistent with causality for any value of the GB coupling [51].) The violation of the bound given in (59) by anisotropy or higher curvature corrections is reminiscent of the well-known violation of the shear viscosity to entropy density ratio bound [67–72].

4.3. Chaos and Entanglement Spreading. The thermofield double state displays a very atypical left-right pattern of entanglement that results from nonzero correlations between subsystems of QFT_L and QFT_R at $t = 0$. The chaotic nature of the boundary theories is manifested by the fact that small perturbations added to the system in the asymptotic past destroy this delicate correlations [5].

The special pattern of entanglement can be efficiently diagnosed by considering the mutual information $I(A, B)$ between spatial subsystems $A \subset \text{QFT}_L$ and $B \subset \text{QFT}_R$, defined as

$$I(A, B) = S_A + S_B - S_{A\cup B}, \tag{60}$$

where S_A is the entanglement entropy of the subsystem A and so on. The mutual information is always positive and provides an upper bound for correlations between operators $\mathcal{O}_L$ and $\mathcal{O}_R$ defined on A and B, respectively [73],

$$I(A, B) \geqslant \frac{\left(\langle \mathcal{O}_L \mathcal{O}_R \rangle - \langle \mathcal{O}_L \rangle \langle \mathcal{O}_R \rangle\right)^2}{2\langle \mathcal{O}_L^2 \rangle \langle \mathcal{O}_R^2 \rangle}. \tag{61}$$

The thermofield double state has nonzero mutual information between large (for small subsystems, the mutual information is zero) subsystems of the left and right boundary, signaling the existence of left-right correlations. These correlations can be destroyed by small perturbations in the asymptotic past, meaning that initially positive mutual information drops to zero when we add a very early perturbation to the system.

Interestingly, the vanishing of the mutual information can be connected to the vanishing of the OTOCs discussed earlier. If, for simplicity, we assume that $\mathcal{O}_L$ and $\mathcal{O}_R$ have zero thermal one point function, then the disruption of the mutual information implies the vanishing of the following four-point function

$$\langle \mathcal{O}_L \mathcal{O}_R \rangle_W = \langle \text{TFD}| W_R^\dagger \mathcal{O}_L \mathcal{O}_R W_R |\text{TFD}\rangle = 0, \tag{62}$$

which is related by analytic continuation to the one-sided out-of-time-order correlator introduced earlier. (To obtain an OTOC with operators acting only on the right boundary theory, one just needs to add $i\beta/2$ to time argument of the operator $\mathcal{O}_L$ in the above formula.)

The disruption of the mutual information has very simple geometrical realization in the bulk. The entanglement entropies that appear in the definition of $I(A, B)$ can be

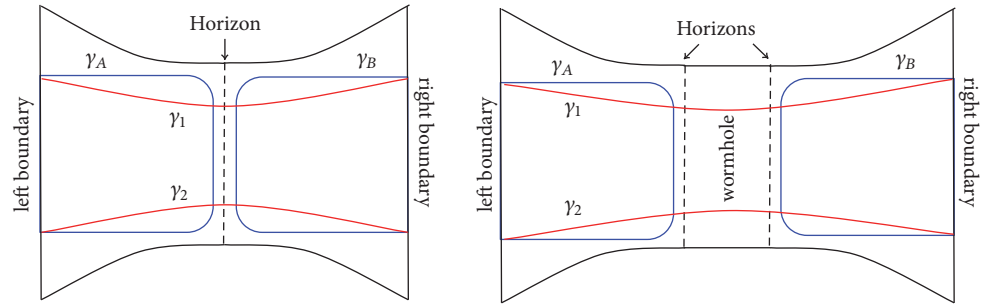

FIGURE 14: Illustration of the entangling surfaces in the $t = 0$ slice of a two-sided black brane geometry. The U-shaped surfaces (γ_A and γ_B) are represented by blue curves. The surface stretching through the wormhole is given by the union of the two red surfaces $\gamma_{\text{wormhole}} = \gamma_1 \cup \gamma_2$. In the *left panel* we represent the unperturbed geometry, in which the two horizons coincide. In the *right panel* we represent the geometry in the presence of a shock wave added at some time t_0 in the past. In this case the size of the wormhole is effectively larger, and the two horizons no longer coincide.

holographically calculated using the HRRT prescription [74, 75]

$$S_A = \frac{\text{Area}\,(\gamma_A)}{4G_N}, \tag{63}$$

where γ_A is an extremal surface whose boundary coincides with the boundary of the region A. There is an analogous formula for S_B. Both γ_A and γ_B are U-shaped surfaces lying outside of the event horizon, in the left and right side of the geometry, respectively. There are two candidates for the extremal surface that computes $S_{A\cup B}$: the surface $\gamma_A \cup \gamma_B$ or the surface γ_{wormhole} that connects the two asymptotic boundaries of the geometry. See Figure 14. According to the RT prescription, we should pick the surface with less area. If $\gamma_A \cup \gamma_B$ has less area than γ_{wormhole}, then $I(A, B) = 0$, because Area($\gamma_A \cup \gamma_B$)=Area(γ_A)+Area(γ_B). On the other hand, if γ_{wormhole} has less area than $\gamma_A \cup \gamma_B$, i.e., Area(γ_{wormhole}) < Area(γ_A)+Area(γ_B), then we have a positive mutual information

$$\begin{aligned} I\,(A, B) &= \frac{1}{4G_{\text{N}}}\left[\text{Area}\,(\gamma_A) + \text{Area}\,(\gamma_B) - \text{Area}\,(\gamma_{\text{wormhole}})\right] \\ &> 0. \end{aligned} \tag{64}$$

Now, an early perturbation of the thermofield double state gives rise to a shock wave geometry in which the wormhole becomes longer. As a consequence, the area of the surface γ_{wormhole} increases, resulting in a smaller mutual information. It is then clear that the mutual information will drop to zero if the wormhole is longer enough. The length of the wormhole depends on the strength of the shock wave, which, by its turn, depends on how early the perturbation is producing it. Therefore, an early enough perturbation will produce a very long wormhole in which the mutual information will be zero. The fact that the shock wave geometry produces a longer wormhole (along the $t = 0$ slice of the geometry) is clearly seen if we represent the shock wave geometry with a tilted Penrose diagram. See, for instance, Figure 3 of [76].

The mutual information $I(A, B)$ decreases as a function of the time t_0 at which we perturbed the system. For $t_0 \gtrsim t_*$, the mutual information decreases linearly with behavior controlled by the so-called entanglement velocity v_E [63]

$$\frac{dI\,(A, B)}{dt_0} = -\frac{dS_{A\cup B}}{dt_0} = -v_E s_{\text{th}} \text{Area}\,(A \cup B)\,, \tag{65}$$

where s_{th} is the thermal entropy density and Area($A \cup B$) is the area of $A \cup B$ (or the volume of the boundary of this region). The two-sided black hole geometry with a shock wave can be thought of as an additional example of a holographic quench protocol [63], and the time-dependence of entanglement entropy can be understood in terms of the so-called 'entanglement tsunami' picture. See [77] for field theory calculations and [78–82] for holographic calculations. However, it was recently shown that the entanglement tsunami picture is not very sharp. See [59] for further details. In [81, 82], the entanglement velocity was conjectured to be bounded as

$$v_E \leqslant v_E^{\text{Sch}} = \frac{\sqrt{d}\,(d-1)^{1/2-1/d}}{[2\,(d-1)]^{1-1/d}}, \tag{66}$$

where v_E^{Sch} is the entanglement velocity for a $(d + 1)$-dimensional Schwarzschild black brane or, equivalently, the value of v_E for a d-dimensional thermal CFT. This bound can be derived in the context of Einstein gravity assuming an asymptotically AdS geometry, isotropy, and NEC [61]. Just like in the case of v_B, the entanglement velocity in thermal CFTs does not depend on the temperature. But v_E acquires a temperature dependence if we deform the CFT and move along the corresponding RG flow [63, 64]. In these cases, v_E violates the above bound, but it remains bounded by its corresponding value at the IR fixed point, never surpassing the speed of light.

One can also prove that the entanglement velocity is also bounded by the speed of light. (See [83, 84] for a discussion about small subsystems.) This can be done by using positivity of the mutual information [85] or using inequalities involving the relative entropy [86]. More generally, the authors of [59] conjecture that $v_E \leqslant v_B$, which implies the bound $v_E < 1$ in the cases where v_B is bounded. However, both [85, 86] assumed that the theory is Lorentz invariant. In the case of

non-Lorentz invariant theories (e.g., noncommutative gauge theories) the entanglement velocity can surpass the speed of light. This has been verified both in holography calculations [42] and in field theory calculations [87].

Finally, we mention that other concepts from information theory can also be used to diagnose chaos in holography. It has been shown, for instance, that the relative entropy is also a useful tool to diagnose chaotic behavior [88]. For a connection between chaos and computational complexity, see, for instance [89, 90].

4.4. Chaos and Hydrodynamics. Recently, there has been a growing interest in the connection between chaos and hydrodynamics [91–99]. Here we briefly review some interesting connection between chaos and diffusion phenomena.

A longstanding goal of quantum condensed matter physics is to have a deeper understanding of the so-called 'strange metals'. These are strongly correlated materials that do not have a description in terms of quasiparticles excitations and whose transport properties display a remarkable degree of universality. In [100, 101] Sachdev and Damle proposed that such a universal behavior could be explained by a fundamental dissipative timescale

$$\tau_P \sim \frac{\hbar}{2\pi k_B T}, \tag{67}$$

which would govern the transport in such systems.

Interestingly, the Lyapunov exponent defines a time scale $\tau_L = 1/\lambda_L$, and the upper bound on λ_L translates into a lower bound for τ_L that precisely coincides with τ_P

$$\tau_L \geqslant \frac{\hbar\beta}{2\pi k_B}, \tag{68}$$

where we reintroduced $\hbar$ and the Boltzmann constant in the expression for the bound on the Lyapunov exponent. (In systems of units where $\hbar$ and k_B are not equal to one, the bound on the Lyapunov exponent reads $\lambda_L \leqslant 2\pi k_B/\hbar\beta$.) Holographic systems saturate the above bound, and this explains the universality observed in the transport properties of these systems.

A prototypical example of universality is the linear resistivity of strange metals. In [102], Hartnoll proposed that the linear resistivity could be explained by the existence of a universal lower bound on the diffusion constants related to the collective diffusion of charge and energy

$$D \gtrsim \frac{\hbar v^2}{(k_B T)}, \tag{69}$$

where v is some characteristic velocity of the system. As D is inversely proportional to the resistivity, systems saturating the above bound would display linear resistivity behavior. (See [103] for a recent successful holographic description of linear resistivity at high temperature.)

One should think of (69) as a reformulation of the Kovtun-Son-Starinets (KSS) bound [104]

$$\frac{\eta}{s} \geqslant \frac{1}{4\pi}\frac{\hbar}{k_B}, \tag{70}$$

which also relies on the idea of a fundamental dissipative timescale $\tau_L \sim \hbar/(k_B T)$ controlling transport in strongly interacting systems. Naively, the observed violations of the KSS bound would seem to indicate the existence of systems in which the bound (68) is violated. The bound (69) saves the idea of a fundamental dissipative timescale by introducing an additional parameter in the game, namely, the characteristic velocity v. The fact that η/s can be made arbitrarily small in some systems corresponds to the fact that the characteristic velocity is highly suppressed in those cases. See [91] for further details.

In [91, 92] Blake proposed that, at least for holographic systems with particle-hole symmetry, the characteristic velocity v should be replaced by the butterfly velocity. More precisely

$$D_c \geqslant C_c v_B^2 \tau_L, \tag{71}$$

where D_c is the electric diffusivity and C_c is a constant that depends on the universality class of theory. This proposal was motivated by the fact that both D_c and v_B are determined by the dynamics close to the black hole horizon in the aforementioned systems. Despite working well for systems where energy and charge diffuse independently, this proposal was shown to fail in more general cases [93, 105–108]. This is related to the fact that, in more general cases, the diffusion of energy and charge is coupled, and the corresponding transport coefficients are not given only in terms of the geometry close to the black hole horizon. Hence, there is no reason for these coefficients to be related to the butterfly velocity, which is always determined solely by the near-horizon geometry.

There is, however, a universal piece of the diffusivity matrix that can be related to the chaos parameters at infrared fixed points. This is the thermal diffusion constant [94]

$$D_T \geqslant C_T v_B^2 \tau_L, \tag{72}$$

where C_T is a universality constant (different from C_c). This proposal was shown to be valid even for systems with spatial anisotropy [109]. The above relation is not well defined when the system's dynamical critical exponent z is equal to one, but it can be extended in this case (we thank Hyun-Sik Jeong for calling our attention to this) [110].

Finally, we mention that there is an interesting relation between chaos and hydrodynamics that manifests itself in the so-called 'pole-skipping' phenomenon. See [95–97] for further details.

5. Closing Remarks

The holographic description of quantum chaos not only has provided new insights into the inner-workings of gauge-gravity duality, but also has given insights outside the scope of holography: some examples include the characterization of chaos with OTOCs, the definition of a quantum Lyapunov exponent, and the existence of a bound for chaos.

The success of this new approach to quantum chaos explains the growing experimental interest that OTOCs

have been received. Indeed, several protocols for measuring OTOCs have been proposed, and there are already a few experimental results. See [111] and references therein.

Finally, one of the remarkable features of quantum chaos is level statistics described by random matrices. The fact that this is present in the infrared limit of the SYK model [112–114] suggests that it should also be present in quantum black holes (we thank A. M. García-García for calling our attention to this), although this has not yet been verified [115].

Conflicts of Interest

The author declares that there are no conflicts of interest regarding the publication of this paper.

Acknowledgments

It is a pleasure to thank A. M. García-García, S. Nicolis, S. A. H. Mansoori, and N. Garcia-Mata for useful correspondence. I also would like to thank Hyun-Sik Jeong for useful discussions. This work was supported in part by Basic Science Research Program through the National Research Foundation of Korea (NRF) funded by the Ministry of Science, ICT & Future Planning (NRF2017R1A2B4004810) and GIST Research Institute (GRI) grant funded by the GIST in 2018.

References

[1] D. Ullmo and S. Tomsovic, *Introduction to quantum chaos*, 2014, http://www.lptms.u-psud.fr/membres/ullmo/Articles/eolss-ullmo-tomsovic.pdf.

[2] J. Maldacena, "The large N limit of superconformal field theories and supergravity," *Advances in Theoretical and Mathematical Physics*, vol. 2, no. 2, pp. 231–252, 1998, [International Journal of Theoretical Physics, vol. 38, article 1113, 1999].

[3] S. S. Gubser, I. R. Klebanov, and A. M. Polyakov, "Gauge theory correlators from non-critical string theory," *Physics Letters B*, vol. 428, no. 1-2, pp. 105–114, 1998.

[4] E. Witten, "Anti de Sitter space and holography," *Advances in Theoretical and Mathematical Physics*, vol. 2, no. 2, pp. 253–291, 1998.

[5] S. H. Shenker and D. Stanford, "Black holes and the butterfly effect," *Journal of High Energy Physics*, vol. 1403, no. 067, 2014.

[6] S. H. Shenker and D. Stanford, "Multiple shocks," *Journal of High Energy Physics*, vol. 1412, no. 046, 2014.

[7] D. A. Roberts, D. Stanford, and L. Susskind, "Localized shocks," *Journal of High Energy Physics*, vol. 1503, no. 51, 2015.

[8] S. H. Shenker and D. Stanford, "Stringy effects in scrambling," *Journal of High Energy Physics*, vol. 1505, no. 132, 2015.

[9] A. Kitaev, "Hidden correlations in the hawking radiation and thermal noise, talk given at Fundamental Physics Prize Symposium," in *Proceedings of the Stanford SITP seminars*, 2014.

[10] E. B. Rozenbaum, S. Ganeshan, and V. Galitski, "Lyapunov exponent and out-of-time-ordered correlator's growth rate in a chaotic system," *Physical Review Letters*, vol. 188, Article ID 086801, 2017.

[11] E. B. Rozenbaum, S. Ganeshan, and V. Galitski, "Universal level statistics of the out-of-time-ordered operator," https://arxiv.org/abs/1801.10591.

[12] J. Chávez-Carlos, B. López-Del-Carpio, M. A. Bastarrachea-Magnani et al., "Quantum and classical lyapunov exponents in atom-field interaction systems," *Physical Review Letters*, vol. 122, Article ID 024101, 2019.

[13] J. Polchinski and V. Rosenhaus, "The spectrum in the Sachdev-Ye-Kitaev model," *Journal of High Energy Physics*, vol. 1604, no. 1, 2016.

[14] J. Maldacena and D. Stanford, "Remarks on the Sachdev-Ye-Kitaev model," *Physical Review D: Particles, Fields, Gravitation and Cosmology*, vol. 94, no. 10, Article ID 106002, 2016.

[15] J. Maldacena, D. Stanford, and Z. Yang, "Conformal symmetry and its breaking in two-dimensional nearly anti-de Sitter space," *PTEP. Progress of Theoretical and Experimental Physics*, vol. 12C104, no. 12, 2016.

[16] A. Kitaev and S. J. Suh, "The soft mode in the Sachdev-Ye-Kitaev model and its gravity dual," *Journal of High Energy Physics*, vol. 1805, no. 183, 2018.

[17] M. Axenides, E. Floratos, and S. Nicolis, "Modular discretization of the AdS2/CFT1 holography," *Journal of High Energy Physics*, vol. 1402, no. 109, 2014.

[18] M. Axenides, E. Floratos, and S. Nicolis, "Chaotic information processing by extremal black holes," *International Journal of Modern Physics D: Gravitation, Astrophysics, Cosmology*, vol. 24, no. 9, Article ID 1542012, 2015.

[19] M. Axenides, E. Floratos, and S. Nicolis, "The quantum cat map on the modular discretization of extremal black hole horizons," *The European Physical Journal C*, vol. 78, no. 5, Article ID 412, 2018.

[20] D. A. Roberts and D. Stanford, "Two-dimensional conformal field theory and the butterfly effect," *Physical Review Letters*, vol. 115, no. 13, Article ID 131603, 2015.

[21] D. Stanford, "Many-body chaos at weak coupling," *Journal of High Energy Physics*, vol. 1610, no. 009, 2016.

[22] E. Plamadeala and E. Fradkin, "Scrambling in the quantum Lifshitz model," *Journal of Statistical Mechanics: Theory and Experiment*, vol. 1806, no. 6, Article ID 063102, 2018.

[23] A. Nahum, S. Vijay, and J. Haah, "Operator spreading in random unitary circuits," *Physical Review X*, vol. 8, no. 2, Article ID 021014, 2018.

[24] V. Khemani, A. Vishwanath, and D. A. Huse, "Operator spreading and the emergence of dissipative hydrodynamics under unitary evolution with conservation laws," *Physical Review X*, vol. 8, no. 3, Article ID 031057, 2018.

[25] T. Rakovszky, F. Pollmann, and C. von Keyserlingk, "Diffusive hydrodynamics of out-of-time-ordered correlators with charge conservation," *Physical Review X*, vol. 8, no. 3, Article ID 031058, 2018.

[26] D. J. Luitz and Y. Bar Lev, "Information propagation in isolated quantum systems," *Physical Review B: Condensed Matter and Materials Physics*, vol. 96, no. 2, Article ID 020406, 2017.

[27] A. Bohrdt, C. B. Mendl, M. Endres, and M. Knap, "Scrambling and thermalization in a diffusive quantum many-body system," *New Journal of Physics*, vol. 19, no. 6, Article ID 063001, 2017.

[28] M. Heyl, F. Pollmann, and B. Dóra, "Detecting equilibrium and dynamical quantum phase transitions in ising chains via out-of-time-ordered correlators," *Physical Review Letters*, vol. 121, no. 1, Article ID 016801, 2018.

[29] C. Lin and O. I. Motrunich, "Out-of-time-ordered correlators in a quantum Ising chain," *Physical Review B: Condensed Matter and Materials Physics*, vol. 97, Article ID 144304, 2018.

[30] S. Xu and B. Swingle, "Accessing scrambling using matrix product operators," https://arxiv.org/abs/1802.00801.

[31] M. Cencini, F. Cecconi, and A. Vulpiani, *Chaos-from Simple Models to Complex Systems*, World Scientific, Singapore, 2009.

[32] J. Polchinski, "Chaos in the black hole S-matrix," https://arxiv.org/abs/1505.08108.

[33] I. García-Mata, M. Saraceno, R. A. Jalabert, A. J. Roncaglia, and D. A. Wisniacki, "Chaos signatures in the short and long time behavior of the out-of-time ordered correlator," *Physical Review Letters*, vol. 121, no. 21, Article ID 210601, 2018.

[34] D. Stanford, "Many-body quantum chaos," in *Proceedings of the Seminar at the school, IAS PiTP 2018: From Qubtis to Spacetime*, 2018, https://video.ias.edu/PiTP/2018/0723-DouglasStanford.

[35] A. I. Larkin and Y. N. Ovchinnikov, "Quasiclassical method in the theory of superconductivity," *Journal of Experimental and Theoretical Physics*, vol. 28, no. 6, pp. 1200–1205, 1969.

[36] V. Khemani, D. A. Huse, and A. Nahum, "Velocity-dependent Lyapunov exponents in many-body quantum, semiclassical, and classical chaos," *Physical Review B: Condensed Matter and Materials Physics*, vol. 98, no. 14, Article ID 144304, 2018.

[37] D. A. Roberts and B. Swingle, "Lieb-robinson bound and the butterfly effect in quantum field theories," *Physical Review Letters*, vol. 117, no. 9, Article ID 091602, 2016.

[38] J. Maldacena, "Eternal black holes in anti-de Sitter," *Journal of High Energy Physics. A SISSA Journal*, vol. 0304, no. 021, 2003.

[39] L. Fidkowski, V. Hubeny, M. Kleban, and S. Shenker, "The black hole singularity in AdS/CFT," *Journal of High Energy Physics. A SISSA Journal*, vol. 0402, no. 014, 2004.

[40] T. Dray and G. 't Hooft, "The gravitational shock wave of a massless particle," *Nuclear Physics. B. Theoretical, Phenomenological, and Experimental High Energy Physics. Quantum Field Theory and Statistical Systems*, vol. 253, no. 1, pp. 173–188, 1985.

[41] K. Sfetsos, "On gravitational shock waves in curved spacetimes," *Nuclear Physics. B. Theoretical, Phenomenological, and Experimental High Energy Physics. Quantum Field Theory and Statistical Systems*, vol. 436, no. 3, pp. 721–745, 1995.

[42] W. Fischler, V. Jahnke, and J. F. Pedraza, "Chaos and entanglement spreading in a non-commutative gauge theory," *Journal of High Energy Physics*, vol. 1811, no. 072, 2018.

[43] M. Baggioli, B. Padhi, P. W. Phillips, and C. Setty, "Conjecture on the butterfly velocity across a quantum phase transition," *Journal of High Energy Physics*, vol. 1807, no. 049, 2018.

[44] E. Perlmutter, "Bounding the space of holographic CFTs with chaos," *Journal of High Energy Physics*, vol. 1610, no. 069, 2016.

[45] A. L. Fitzpatrick and J. Kaplan, "A quantum correction to chaos," *Journal of High Energy Physics*, vol. 1605, no. 070, 2016.

[46] P. Caputa, T. Numasawa, and A. Veliz-Osorio, "Out-of-time-ordered correlators and purity in rational conformal field theories," *PTEP. Progress of Theoretical and Experimental Physics*, vol. 2016, no. 11, Article ID 113B06, 2016.

[47] G. J. Turiaci and H. Verlinde, "On CFT and quantum chaos," *Journal of High Energy Physics*, vol. 1612, no. 110, 2016.

[48] P. Caputa, Y. Kusuki, T. Takayanagi, and K. Watanabe, "Out-of-time-ordered correlators in a $(T^2)^n/\mathbb{Z}_n$ CFT," *Physical Review D: Particles, Fields, Gravitation and Cosmology*, vol. 96, no. 4, Article ID 046020, 2017.

[49] M. Taylor, "Generalized conformal structure, dilation gravity and SYK," *Journal of High Energy Physics*, vol. 1801, no. 010, 2018.

[50] S. Grozdanov, "On the connection between hydrodynamics and quantum chaos in holographic theories with stringy corrections," *Journal of High Energy Physics*, vol. 2019, no. 1, 2019.

[51] X. O. Camanho, J. D. Edelstein, J. Maldacena, and A. Zhiboedov, "Causality constraints on corrections to the graviton three-point coupling," *Journal of High Energy Physics*, vol. 1602, no. 020, 2016.

[52] P. Hayden and J. Preskill, "Black holes as mirrors: quantum information in random subsystems," *Journal of High Energy Physics*, vol. 0709, no. 9, Article ID 120, 2007.

[53] Y. Sekino and L. Susskind, "Fast scramblers," *Journal of High Energy Physics*, vol. 0810, no. 10, pp. 065-065, 2008.

[54] J. Maldacena, S. H. Shenker, and D. Stanford, "A bound on chaos," *Journal of High Energy Physics*, vol. 1608, no. 106, 2016.

[55] B. Michel, J. Polchinski, V. Rosenhaus, and S. J. Suh, "Four-point function in the IOP matrix model," *Journal of High Energy Physics*, vol. 1605, no. 048, 2016.

[56] P. Padmanabhan, S.-J. Rey, D. Teixeira, and D. Trancanelli, "Supersymmetric many-body systems from partial symmetries—integrability, localization and scrambling," *Journal of High Energy Physics*, vol. 1705, no. 136, 2017.

[57] J. de Boer, E. Llabrés, J. F. Pedraza, and D. Vegh, "Chaotic strings in AdS/CFT," *Physical Review Letters*, vol. 120, no. 20, Article ID 201604, 2018.

[58] A. Banerjee, A. Kundu, and R. R. Poojary, "Strings, branes, schwarzian action and maximal chaos," https://arxiv.org/abs/1809.02090.

[59] M. Mezei and D. Stanford, "On entanglement spreading in chaotic systems," *Journal of High Energy Physics*, vol. 1705, no. 065, 2017.

[60] X. L. Qi and Z. Yang, "Butterfly velocity and bulk causal structure," https://arxiv.org/abs/1705.01728.

[61] M. Mezei, "On entanglement spreading from holography," *Journal of High Energy Physics*, vol. 1705, no. 046, 2017.

[62] D. Giataganas, U. Gürsoy, and J. F. Pedraza, "Strongly coupled anisotropic gauge theories and holography," *Physical Review Letters*, vol. 121, no. 12, 2018.

[63] V. Jahnke, "Delocalizing entanglement of anisotropic black branes," *Journal of High Energy Physics*, vol. 1801, no. 102, 2018.

[64] D. Ávila, V. Jahnke, and L. Patiño, "Chaos, diffusivity, and spreading of entanglement in magnetic branes, and the strengthening of the internal interaction," *Journal of High Energy Physics*, vol. 1809, no. 131, 2018.

[65] X. O. Camanho and J. D. Edelstein, "Causality constraints in AdS/CFT from conformal collider physics and Gauss-Bonnet gravity," *Journal of High Energy Physics*, vol. 1004, no. 007, 2010.

[66] A. Buchel, J. Escobedo, R. C. Myers, M. F. Paulos, A. Sinha, and M. Smolkin, "Holographic GB gravity in arbitrary dimensions," *Journal of High Energy Physics*, vol. 1003, no. 111, 2010.

[67] M. Brigante, H. Liu, R. C. Myers, S. Shenker, and S. Yaida, "Viscosity bound violation in higher derivative gravity," *Physical Review D: Particles, Fields, Gravitation and Cosmology*, vol. 77, no. 12, Article ID 126006, 2008.

[68] M. Brigante, H. Liu, R. C. Myers, S. Shenker, and S. Yaida, "Viscosity bound and causality violation," *Physical Review Letters*, vol. 100, Article ID 191601, 2008.

[69] X. O. Camanho, J. D. Edelstein, and M. F. Paulos, "Lovelock theories, holography and the fate of the viscosity bound," *Journal of High Energy Physics*, vol. 1105, no. 127, 2011.

[70] J. Erdmenger, P. Kerner, and H. Zeller, "Non-universal shear viscosity from Einstein gravity," *Physics Letters B*, vol. 699, no. 4, pp. 301–304, 2011.

[71] A. Rebhan and D. Steineder, "Violation of the holographic viscosity bound in a strongly coupled anisotropic plasma," *Physical Review Letters*, vol. 108, Article ID 021601, 2012.

[72] V. Jahnke, A. S. Misobuchi, and D. Trancanelli, "Holographic renormalization and anisotropic black branes in higher curvature gravity," *Journal of High Energy Physics*, vol. 1501, no. 122, 2015.

[73] M. M. Wolf, F. Verstraete, M. Hastings, and J. I. Cirac, "Area laws in quantum systems: mutual information and correlations," *Physical Review Letters*, vol. 100, Article ID 7070502, 2008.

[74] S. Ryu and T. Takayanagi, "Holographic derivation of entanglement entropy from AdS/CFT," *Physical Review Letters*, vol. 96, Article ID 181602, 2006.

[75] V. E. Hubeny, M. Rangamani, and T. Takayanagi, "A covariant holographic entanglement entropy proposal," *Journal of High Energy Physics*, vol. 0707, no. 062, 2007.

[76] S. Leichenauer, "Disrupting entanglement of black holes," *Physical Review D: Particles, Fields, Gravitation and Cosmology*, vol. 90, no. 4, Article ID 046009, 2014.

[77] P. Calabrese and J. Cardy, "Evolution of entanglement entropy in one-dimensional systems," *Journal of Statistical Mechanics: Theory and Experiment*, vol. 0504, Article ID P04010, 2005.

[78] J. Abajo-Arrastia, J. Aparício, and E. López, "Holographic evolution of entanglement entropy," *Journal of High Energy Physics*, vol. 1011, no. 149, 2010.

[79] T. Albash and C. V. Johnson, "Evolution of holographic entanglement entropy after thermal and electromagnetic quenches," *New Journal of Physics*, vol. 13, no. 4, Article ID 045017, 2011.

[80] T. Hartman and J. Maldacena, "Time evolution of entanglement entropy from black hole interiors," *Journal of High Energy Physics*, vol. 1305, no. 014, 2013.

[81] H. Liu and S. J. Suh, "Entanglement tsunami: Universal scaling in holographic thermalization," *Physical Review Letters*, vol. 112, Article ID 011601, 2014.

[82] H. Liu and S. J. Suh, "Entanglement growth during thermalization in holographic systems," *Physical Review D: Particles, Fields, Gravitation and Cosmology*, vol. 89, Article ID 066012, 2014.

[83] S. Kundu and J. F. Pedraza, "Spread of entanglement for small subsystems in holographic CFTs," *Physical Review D: Particles, Fields, Gravitation and Cosmology*, vol. 95, no. 8, Article ID 086008, 2017.

[84] S. F. Lokhande, G. W. J. Oling, and J. F. Pedraza, "Linear response of entanglement entropy from holography," *Journal of High Energy Physics*, vol. 1710, no. 104, 2017.

[85] H. Casini, H. Liu, and M. Mezei, "Spread of entanglement and causality," *Journal of High Energy Physics*, vol. 1607, no. 077, 2016.

[86] T. Hartman and N. Afkhami-Jeddi, "Speed limits for entanglement," https://arxiv.org/abs/1512.02695.

[87] P. Sabella-Garnier, "Time dependence of entanglement entropy on the fuzzy sphere," *Journal of High Energy Physics*, vol. 1708, no. 121, 2017.

[88] Y. O. Nakagawa, G. Sárosi, and T. Ugajin, "Chaos and relative entropy," *Journal of High Energy Physics*, vol. 1807, no. 002, 2018.

[89] J. M. Magán, "Black holes, complexity and quantum chaos," *Journal of High Energy Physics*, vol. 1809, no. 043, 2018.

[90] S. A. H. Mansoori and M. M. Qaemmaqami, "Complexity growth, butterfly velocity and black hole thermodynamics," https://arxiv.org/abs/1711.09749.

[91] M. Blake, "Universal charge diffusion and the butterfly effect in holographic theories," *Physical Review Letters*, vol. 117, no. 9, Article ID 091601, 2016.

[92] M. Blake, "Universal diffusion in incoherent black holes," *Physical Review D: Particles, Fields, Gravitation and Cosmology*, vol. 94, no. 8, Article ID 086014, 2016.

[93] R. A. Davison, W. Fu, A. Georges, Y. Gu, K. Jensen, and S. Sachdev, "Thermoelectric transport in disordered metals without quasiparticles: The Sachdev-Ye-Kitaev models and holography," *Physical Review B*, vol. 95, no. 15, Article ID 155131, 2017.

[94] M. Blake, R. A. Davison, and S. Sachdev, "Thermal diffusivity and chaos in metals without quasiparticles," *Physical Review D: Particles, Fields, Gravitation and Cosmology*, vol. 96, no. 10, Article ID 106008, 2017.

[95] S. Grozdanov, K. Schalm, and V. Scopelliti, "Black hole scrambling from hydrodynamics," *Physical Review Letters*, vol. 120, no. 23, Article ID 231601, 2018.

[96] M. Blake, H. Lee, and H. Liu, "A quantum hydrodynamical description for scrambling and many-body chaos," *Journal of High Energy Physics*, vol. 2018, no. 10, 2018.

[97] S. Grozdanov, K. Schalm, and V. Scopelliti, "Kinetic theory for classical and quantum many-body chaos," *Physical Review E: Statistical, Nonlinear, and Soft Matter Physics*, vol. 99, no. 1, 2019.

[98] M. Blake, R. A. Davison, S. Grozdanov, and H. Liu, "Many-body chaos and energy dynamics in holography," *Journal of High Energy Physics*, vol. 1810, no. 035, 2018.

[99] F. M. Haehl and M. Rozali, "Effective field theory for chaotic CFTs," *Journal of High Energy Physics*, vol. 1810, no. 118, 2018.

[100] K. Damle and S. Sachdev, "Nonzero-temperature transport near quantum critical points," *Physical Review B: Condensed Matter and Materials Physics*, vol. 56, no. 14, pp. 8714–8733, 1997.

[101] S. Sachdev, *Quantum Phase Transitions*, Cambridge University Press, Cambridge, UK, 1999.

[102] S. A. Hartnoll, "Theory of universal incoherent metallic transport," *Nature Physics*, vol. 11, no. 1, pp. 54–61, 2015.

[103] H. Jeong, C. Niu, and K. Kim, "Linear-T resistivity at high temperature," *Journal of High Energy Physics*, vol. 1810, no. 191, 2018.

[104] P. K. Kovtun, D. T. Son, and A. O. Starinets, "Viscosity in strongly interacting quantum field theories from black hole physics," *Physical Review Letters*, vol. 94, no. 11, Article ID 111601, 2005.

[105] A. Lucas and J. Steinberg, "Charge diffusion and the butterfly effect in striped holographic matter," *Journal of High Energy Physics*, vol. 1610, no. 143, 2016.

[106] M. Baggioli, B. Goutéraux, E. Kiritsis, and W.-J. Li, "Higher derivative corrections to incoherent metallic transport in holography," *Journal of High Energy Physics*, vol. 1703, no. 170, 2017.

[107] C. Niu and K.-Y. Kim, "Diffusion and butterfly velocity at finite density," *Journal of High Energy Physics*, vol. 1706, no. 030, 2017.

[108] A. Mokhtari, S. A. H. Mansoori, and K. B. Fadafan, "Diffusivities bounds in the presence of Weyl corrections," *Physics Letters B*, vol. 785, pp. 591–604, 2018.

[109] H.-S. Jeong, Y. Ahn, D. Ahn, C. Niu, W.-J. Li, and K.-Y. Kim, "Thermal diffusivity and butterfly velocity in anisotropic Q-lattice models," *Journal of High Energy Physics*, no. 1, 35 pages, 2018.

[110] R. A. Davison, S. A. Gentle, and B. Goutéraux, "mpact of irrelevant deformations on thermodynamics and transport in holographic quantum critical states," https://arxiv.org/abs/1812.11060.

[111] B. Swingle, "Unscrambling the physics of out-of-time-order correlators," *Nature Physics*, vol. 14, no. 10, pp. 988–990, 2018.

[112] J. S. Cotler, G. Gur-Ari, M. Hanada et al., "Black holes and random matrices," *Journal of High Energy Physics*, vol. 1705, no. 118, 2017, Erratum: [Journal of High Energy Physics, vol. 1809, article 002, 2018].

[113] A. M. García-García and J. J. M. Verbaarschot, "Spectral and thermodynamic properties of the Sachdev-Ye-Kitaev model," *Physical Review D*, vol. 94, no. 12, Article ID 126010, 2016.

[114] A. M. García-García and J. J. M. Verbaarschot, "Analytical spectral density of the Sachdev-Ye-Kitaev Model at finite N," *Physical Review D*, vol. 96, no. 6, Article ID 066012, 2017.

[115] P. Saad, S. H. Shenker, and D. Stanford, "A semiclassical ramp in SYK and in gravity," https://arxiv.org/abs/1806.06840.

Hindawi
Advances in High Energy Physics
Volume 2019, Article ID 2635917, 27 pages
https://doi.org/10.1155/2019/2635917

Review Article

Steady States, Thermal Physics, and Holography

Arnab Kundu

Theory Division, Saha Institute of Nuclear Physics, HBNI, 1/AF Bidhannagar, Kolkata 700064, India

Correspondence should be addressed to Arnab Kundu; arnab.kundu@gmail.com

Received 16 November 2018; Accepted 20 January 2019; Published 6 March 2019

Guest Editor: Cynthia Keeler

It is well known that a Rindler observer measures a nontrivial energy flux, resulting in a thermal description in an otherwise Minkowski vacuum. For systems consisting of large number of degrees of freedom, it is natural to isolate a small subset of them and engineer a steady state configuration in which these degrees of freedom act as Rindler observers. In Holography, this idea has been explored in various contexts, specifically in exploring the strongly coupled dynamics of a fundamental matter sector, in the background of adjoint matters. In this article, we briefly review some features of this physics, ranging from the basic description of such configurations in terms of strings and branes, to observable effects of this effective thermal description.

1. Introduction

Thermodynamics is ubiquitous. Typically, for a collection of large number of degrees of freedom, be it strongly interacting or weakly interacting, a thermodynamic description generally holds across various energy scales and irrespective of whether it is classical or quantum mechanical. The underlying assumption here is a notion of at least a *local thermal equilibrium*, for which such a formulation is possible. Intuitively, this is simple to define: a thermal equilibrium occurs when there is no net flow of energy. Typically this can be characterized by an intensive variable, temperature, with zero or very small time variation. The *smallness* needs to be established in terms of the smallest time-scale that is present in the corresponding system.

While thermodynamics has a remarkable reach of validity, equilibrium is still an approximate description of Nature, at best. Most natural events are dynamical in character. Of these, a particular class of phenomena can be easily factored out, that of systems at steady state. While steady state systems are not strictly in thermodynamic equilibrium, they can be described in terms of stationary macroscopic variables. For such systems, there is a nonvanishing expectation value of a flow, such as an energy flow or a current flow, which does not evolve with time. Typically, such states can be reached *asymptotically* starting from a generic initial state, or they appear as *transient* states before time evolution begins.

In this article, we will consider a similar situation. The prototype will consist of a *bath* degree of freedom, which is assumed to be infinitely large and will serve the purpose of a reservoir. In this *bath* background, we will consider the dynamics of a *probe* sector. In this sector, a stationary configuration can be easily constructed, by dumping all the excess energy into the reservoir. For example, consider a nonvanishing current flow in the probe sector. There will be work done to maintain the constant current flow; therefore it is expected that the actual description is dynamical. However, if we engineer the bath sector as a source of providing this energy, or a sink in which this energy is deposited, the resulting configuration remains stationary.

In the framework of quantum field theory (QFT), a similar construction was considered by Feynman-Vernon in [1], based on the Schwinger-Keldysh formalism of [2, 3]. For some review on this formalism, see, *e.g.,* [4–6]. In recent times, much work has gone into the reformulation of the Schwinger-Keldysh formalism; see, *e.g.,* [7–9]. While much of our subsequent discussion potentially has a leg deep inside this formalism, we will not make explicit use of the formalism, to keep a terse discourse. The basic idea is based on the so-called thermofield double construct, which has appeared

long time back in [10]. Subsequently, in [11], a connection of classical black holes with the thermofield double construct was also established. For us, these two ideas are sufficient.

Consider the basic idea behind the thermofield double. Consider a quantum mechanical system, with a Hamiltonian H and a complete set of eigenstates $|n\rangle$, such that

$$H\,|n\rangle = E_n\,|n\rangle\,, \tag{1}$$

where E_n is the energy of the corresponding eigenstate. Evidently, $\{|n\rangle\}$ constitute a basis of the Hilbert space. Let us now double the total degrees of freedom, by considering two copies of the same system. At the level of the dynamics, these two copies of degrees of freedom are noninteracting between them. (The total Hamiltonian of the doubled system can be defined as $(H_1 + H_2)$ or $(H_1 - H_2)$. With the latter choice, the thermofield double state does not evolve with time.) Therefore, the Hilbert space of the doubled quantum system is spanned by $\{|m\rangle_1|n\rangle_2\}$. Given this, the thermofield double state is defined as

$$|\mathrm{TFD}\rangle = \frac{1}{\sqrt{Z(\beta)}}\sum_n \exp\left(-\frac{\beta E_n}{2}\right)|n\rangle_1\,|n\rangle_2\,. \tag{2}$$

This is certainly a special state in the doubled quantum system. We can assign a density matrix corresponding to this state: $\rho_{\mathrm{TFD}} = |\mathrm{TFD}\rangle\langle\mathrm{TFD}|$. This is a pure density matrix, as can be explicitly checked by establishing $\rho^2_{\mathrm{TFD}} = \rho_{\mathrm{TFD}}$.

Given such a pure density matrix, let us compute the reduced density matrix while integrating out one copy of the system. Thus we obtain

$$\rho_{\mathrm{th}} = \mathrm{Tr}_2\rho_{\mathrm{TFD}} = \frac{1}{Z(\beta)}\sum_n \exp(-\beta E_n)\,|n\rangle_1\,\langle n|_1\,. \tag{3}$$

The reduced density matrix, denoted above by ρ_{th}, appears thermal in nature, with a temperature β^{-1}. Thus, given the thermofield double state, one can construct an equivalent thermal description. The process of integrating out one copy of the system may be conducted in various ways: this can be thought of as integrating out a subsystem to compute entanglement between the two. In the context of a black hole, similar to [11], or in the presence of a causal horizon, one can construct a Kruskal extension of the geometry. This maximal extension of the geometry can be thought of as the thermofield double and by integrating out one side, an effective thermal density matrix is obtained. It is also clear from the above discussion that, given any gauge invariant observable or a collection of such operators acting on the untraced system, denoted by $\mathcal{O}$, the expectation value is simply given by

$$\langle\mathrm{TFD}|\,\mathcal{O}\,|\mathrm{TFD}\rangle = \frac{1}{Z(\beta)}\sum_n \exp(-\beta E_n)\,\langle n|\,\mathcal{O}\,|n\rangle\,, \tag{4}$$

which is the thermal expectation value.

A similar picture holds true in the Holographic framework, which will be the primary premise in our subsequent discussions. In [12], eternal black holes in an asymptotically AdS geometry were proposed to be dual to two copies of the conformal field theory (CFT). Each CFT corresponds to the dual CFT that is defined on the conformal boundary of AdS. The basic picture is represented in Figure 1. In the Euclidean signature, the corresponding thermofield double state is created by the Euclidean path integral over an interval of $\beta/2$. The thermofield double state, defined in (2), is maximally entangled from the point of view of the doubled degrees of freedom. Tracing over one copy produces a thermal effective description and this seems to lie at the core of the construction. Motivated by this, one can surmise that a qualitative emergent description of a thermofield double state ensures an effective thermodynamics. For this to happen, the essential ingredient is a black hole like causal structure. An intriguing idea relating quantum entanglement and the existence of an Einstein-Rosen bridge has recently been proposed in [13].

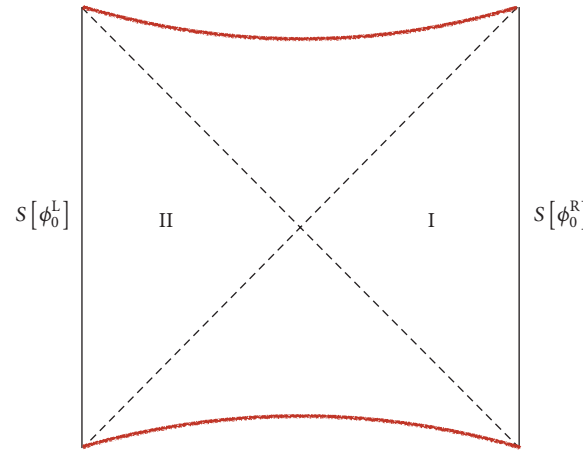

Figure 1: The Penrose diagram corresponding to an eternal black hole in AdS. The left and the right boundaries are where the dual CFT is defined, which are schematically denoted by $S[\phi^0_{\mathrm{L}}]$ and $[\phi^0_{\mathrm{R}}]$, respectively.

Let us now crystalize our discussion towards our specific goal. All of the above discussions are assumed to go through the framework of QFT. In general, of course, for weakly coupled QFT systems, explicit perturbative calculations are sometimes feasible, although those are certainly not simple for processes involving real-time dynamics. Furthermore, the existence of such a small coupling is far from guaranteed in Nature, *e.g.,* the quark-gluon plasma (QGP) at the Relativistic Heavy Ion Collider (RHIC) and the Large Hadron Collider (LHC) at TeV-scale (see, *e.g.,* [14]), or the cold atoms at unitarity at eV-scale (see, *e.g.,* [15]). In general, at strong coupling, powerful symmetry constraints in terms of Ward-Takahashi identities or nonperturbative Schwinger-Dyson equations can sometimes help. However, for many explicit cases, these approaches have limitations. One can certainly try to formulate such complicated issues on a computer, using lattice-methods and its modern generalizations, at the cost of analytical control over the physics.

An interesting avenue is to explore the Gauge-Gravity duality, or the Holographic principle, or the AdS/CFT correspondence [16–19]. While all these words, in a precise sense,

carry different meaning, we will not distinguish between them. The basic statement here is as follows: A large class of strongly coupled QFTs, such as the $\mathcal{N} = 4$ super Yang-Mills (SYM) theory with an SU(N_c) gauge group in the limit $N_c \longrightarrow \infty$, is dual to classical (super) gravity in an $AdS_5 \times S^5$ geometry. By this duality, one translates questions of strongly coupled large N_c gauge theories into questions of classical gravity. The latter is a more familiar and tractable framework for explicit calculations. Although this class of QFTs is not what one would like to understand for experimental processes in the RHIC or the LHC, they certainly can serve the purpose of instructive toy examples. Mathematically, the duality statement schematically takes the form:

$$\left\langle \exp\left(\int_{\partial \mathrm{AdS}} d^d x \phi_0 \mathcal{O}\right)\right\rangle \equiv \mathcal{Z}_{\mathrm{gravity}}\left[\phi_{\mathrm{AdS}} \mid \phi_{\partial \mathrm{AdS}} = \phi_0\right], \tag{5}$$

where the left hand side is an expression in the CFT and the right hand side is defined as the gravity partition function in AdS, subject to a specific boundary condition. Correspondingly, correlations in the CFT can be calculated by taking functional derivatives on the LHS, with respect to ϕ_0. The duality relates this correlation function to a similar calculation in the bulk gravity scenario on the RHS. For a detailed discussion on correlation functions in this framework, see [20] for Minkowski-space correlators, [21] for a Schwinger-Keldysh framework, [22] for a real-time analysis, and [23, 24] for a detailed account of the real-time correlation functions.

During the past couple of decades, a wide range of research has been carried out in this framework, in the context of quantum chromodynamics (QCD) as well as several condensed matter-type systems. Popularly, these efforts are sometimes dubbed as AdS/QCD or AdS/CMT literature. By no stretch of imagination, we will attempt to be extensive: for some recent reviews, see, *e.g.,* [25–27] for the former and [28, 29] for the latter.

The Holographic framework, which can also be viewed as the most rigorous definition of a theory of quantum gravity, is a promising avenue to explore complicated gauge theory dynamics, qualitatively. There already exists a large literature analyzing various dynamical features of thermalization, quench dynamics for strongly coupled systems. We will not attempt to enlist the references here, however, presenting one example of new results, such as scaling laws in quantum quench processes [30]. For a more general discourse on nonequilibrium aspects in Holography, see, *e.g.,* [31].

Even though remarkable progress has been made in understanding dynamical issues, they remain rather involved and, in general, far more complex than equilibrium physics. Thermal equilibrium is particularly simple since it can be macroscopically described in terms of a small number of intensive and extensive variables. Intriguingly, for steady state configurations, which are neither in precise thermal equilibrium nor fullly dynamical, an *effective* thermal description may hold. See, for example, [32–34], in systems at quantum criticality [35] or aging glass systems [36]. In this review, we will briefly summarize a similar construct for a wide class of strongly coupled gauge theories, within the Holographic framework.

As mentioned earlier, we have one *bath* sector and one *probe* sector. These are made of the adjoint matter of an SU(N_c) gauge theory and a fundamental matter sector, respectively. A canonical example of this is to consider an $\mathcal{N} = 2$ hypermultiplet matter as a probe introduced in the $\mathcal{N} = 4$ SYM system. We will work in the limit $N_c \ll N_f$, where N_f is the number of the fundamental matter. This limit ensures the suppression of backreaction by the matter sector and we can safely treat them as probes. In a more familiar language, this limit is similar to the *quenched* limit in the lattice literature, wherein one ignores loop effects of quark degrees of freedom (which are the fundamental sector here), but includes loop effects in the gluonic matter (which is the adjoint matter).

The adjoint matter sector in $(p + 1)$-dimension comes from the low energy limit of a stack of Dp-branes, from the open string description of the brane. Equivalently, the closed string low energy description of the same stack of branes is given by a classical supergravity background in ten-dimensions. Gauge-Gravity duality is an equivalence between the two descriptions. Now, in this picture, one can introduce an additional set of N_f Dq branes, in the limit $N_f \ll N_c$, which introduces an additional set of open string degrees of freedom. In the probe limit, the gravitational backreactions of the Dq-branes are ignored and therefore these only have an open string sector description. This open string sector, geometrically, can be studied by analyzing the embedding problem of Dq branes in the given supergravity background.

Within this framework, many interesting physics have been uncovered within the probe fundamental sector, specially the thermal physics; see, *e.g.,* [37–40]. There is a vast literature on this, and we will not attempt to provide a substantial reference here. For us, the steady state configuration will be engineered in this probe sector, by exciting a U(1)-flux on the probe D-brane worldvolume. This steady state will be maintained by working in the $N_f \ll N_c$ limit. Pictorially, this is demonstrated in Figure 2.

The nonlinear dynamics of the brane, along with the U(1)-flux, will induce an event horizon to which only the brane degrees of freedom are coupled, with an open string analogue of equivalence principle. Qualitatively, therefore, one inherits a black hole like causal structure and a corresponding thermofield double description. As we have discussed above, we are thus led to a thermal density matrix starting from a maximally entangled state. This construction lies at the core of our subsequent discussions. Interestingly, this description can be explicitly realized both on a string worldsheet, in which one studies a probe long open string in a supergravity background, by studying the dynamics of Nambu-Goto (NG) action, and on a probe D-brane by studying the Dirac-Born-Infeld (DBI) action. In the latter, although open strings are present, they may not appear explicit.

Based on these ideas, a lot of interesting physics has been explored over the years. Here we will merely present a few broad categories and some representative references, which

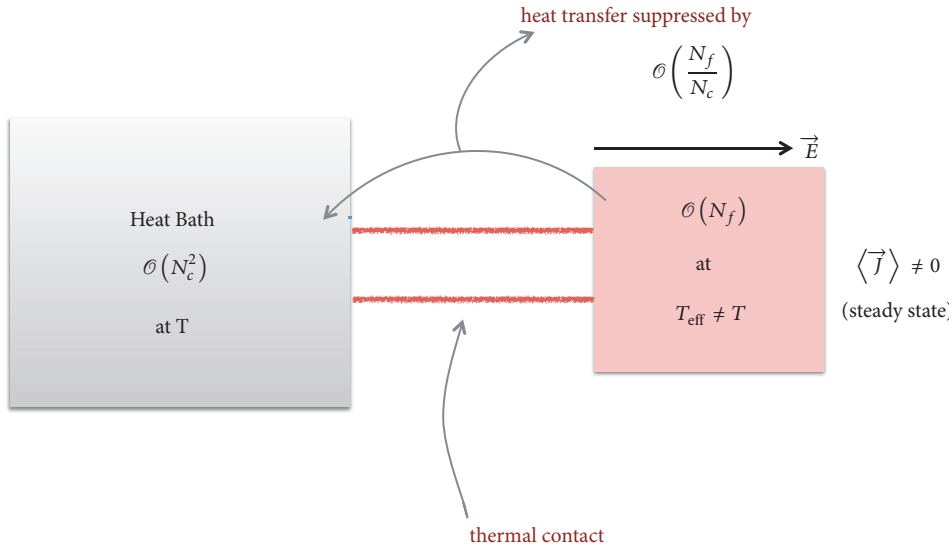

Figure 2: A schematic arrangement of the steady state. The $\mathcal{O}(N_f)$ fundamental degrees of freedom are in a steady-state, situated in a heat bath of $\mathcal{O}(N_c^2)$ degrees of freedom.

we will not explicitly discuss in this review. In [41, 42], the drag force on an external quark passing through the $\mathcal{N} = 4$ SYM was calculated, meson dissociation by acceleration was explored in [43], and the causal structure on the string worldsheet was discussed in detail in [44]. Stochasticity and Brownian motion associated with the worldsheet event horizon were explored in [45–48]. For a review on the hard probe dynamics, see, *e.g.,* [26, 27]; for a quark dynamics review, see, *e.g.,* [49], and for a general review, see, *e.g.,* [25]. The idea of ER=EPR has been explored on the string worldsheet in, *e.g.,* [50–53]. On the probe brane, a nonequilibrium description of phase transition and effective temperature is explored in, *e.g.,* [54–58]. Relatedly, thermalization on this probe sector is discussed in, *e.g.,* [59–61].

This article is divided into the following parts: In the next section, we begin with a brief description of how nonlinearity can result in a black hole like causal structure, and how this is currently being investigated to understand features of QCD. In Section 3, we introduce the Holographic framework. In the next three sections, we discuss some explicit and instructive features of the effective temperature on a string worldsheet as well as a D-brane worldvolume, based on analytically controllable examples. Section 7 is devoted to a generic discussion of the physics, without reference to any explicit example. Finally, we conclude in Section 8.

2. Temperature, Outside the Folklore

The standard folklore concept of temperature is certainly in describing equilibrium thermal systems, at least in a local sense. In physics, there are various ways to define the temperature of a system: In thermodynamics, temperature is defined as an intensive variable that encodes the change of entropy with respect to the internal energy of the system. In kinetic theory, the definition of temperature can be given in terms of the equipartition theorem for every microscopic degree of freedom. In linear response theory, temperature can also be defined in terms of the fluctuation-dissipation relation.

Outside the realm of equilibrium thermal description, the notion of a temperature can sometimes be generalized. This is a vast and evolving topic in itself and we will refer the interested to reader to, *e.g.,* [62]. One particular method, which is also relevant for our discussions, is to use the fluctuation-dissipation relation to define temperature in a nonequilibrium process with a slow dynamics; see, *e.g.,* [63]. In particular, these apply reasonably well within classical and quantum mechanical systems at steady state. However, it is unclear, even within such systems, whether these ideas hold at strong coupling.

Intriguingly though, strong coupling seems to suggest a much simpler scenario. Most of our review will concern with the standard strongly coupled systems (and toy models) within the framework of gauge-gravity duality, where a fluctuation-dissipation based temperature is already explored in [64]. However, in this section, let us briefly review some recent interests and activities in strongly coupled quantum chromodynamics (QCD) itself. The Schwarzschild radius of a typical hadron of mass 1 GeV turns out to be $\sim 10^{-39}$ fm. This estimate assumes gravitational interaction in determining the Schwarzschild. Instead, one replaces the gravitational interaction by the strong interaction, which amounts to multiplying the above estimate by a factor of α_s/G_N, where $\alpha_s \sim \mathcal{O}(1)$ is the strong coupling constant and G_N is Newton's constant. This yields a Schwarzschild radius ~ 1 fm [65]. Let us discuss further motivation, following [65].

As described in [66], the nonlinear effects of a medium for simple electrodynamics can lead to the trapping of photons.

This is described in terms of an effective Lagrangian, denoted by $\mathscr{L}(F)$, and an emergent metric of the form:

$$g_{\mu\nu} = \eta_{\mu\nu}\mathscr{L}' - 4F_{\alpha\mu}F^{\alpha}_{\nu}\mathscr{L}''. \tag{6}$$

The photon trapping surface is simply obtained by solving the equation $g_{00} = 0$. Thus, even with a simple U(1) theory, nonlinear effects lead to a black hole like configuration.

Now, QCD or any such non-Abelian gauge theory is inherently nonlinear and produces a nontrivial medium for itself. In this case, the effective action can be fixed to be (see the discussion in [65])

$$\mathscr{L}_{\mathrm{QCD}} = \frac{1}{4}F_{\mu\nu}F^{\mu\nu}\epsilon\left(g_{\mathrm{QCD}}F\right), \tag{7}$$

where $\epsilon(g_{\mathrm{QCD}}F)$ represents a dielectric variable of the medium and g_{QCD} is the bare QCD coupling. Perturbatively, this function can be evaluated and at one-loop we get

$$\epsilon\left(g_{\mathrm{QCD}}F\right) = 1 - \frac{11N_c - 2N_f}{48\pi^2}\left(\frac{g^2_{\mathrm{QCD}}}{4\pi}\right)\log\left(\frac{\Lambda^2}{g_{\mathrm{QCD}}F}\right), \tag{8}$$

where Λ is the cut-off scale. Setting $\epsilon = 0$ yields an algebraic solution for $g_{\mathrm{QCD}}F$, which is given by

$$g_{\mathrm{QCD}}F = \Lambda^2 \exp\left[-\frac{4\pi}{g^2_{\mathrm{QCD}}}\frac{48\pi^2}{11N_c - 2N_f}\right]. \tag{9}$$

This already indicates a possible event horizon structure, since this zero is the locus where the effective kinetic term in (7) changes sign. Note that this event horizon structure is already visible at the perturbative level with a nonlinearly interacting theory. However, this is not strictly rigorous, since the perturbative result for ϵ assumes a small g_{QCD}. Thus near the $\epsilon = 0$ locus, perturbative calculations are not valid.

Based on the hints above, the basic conjecture was made in [65]: due to confinement, the physical vacuum is equivalent to an event horizon for quarks and gluons. This event horizon can be penetrated only through quantum processes such as tunnelling. This constitutes a QCD analogue of the Hawking radiation, which is hence thermal. While the basic idea is essentially based on the thermofield double type construction, the above also makes certain predictions in terms of a universality in thermal hadron production in high energy collisions, in terms of an effective temperature that is defined in terms of the QCD confinement-scale. This is based primarily on two inputs: (i) a thermal description of high energy collision processes with an effective temperature determined in terms of the QCD string tension, or the gluon saturation momentum [67, 68]; (ii) the experimental data of hadron production across a large energy scale from GeV to TeV exhibiting a universal thermal behaviour, with an effective universal temperature $T_{\mathrm{eff}} \sim 150 - 200$ MeV [69–71].

The resulting essential consequences are as follows: color confinement and vacuum pair production leads to the event horizon. The only information that can escape this horizon is a color-neutral thermal description with an effective temperature. The resulting hadronization is essentially a result of such successive tunnelling processes. Also, there is no clear notion of "thermalization" through standard kinetic theoretic collision processes. A thermal description emerges as a consequence of the strongly coupled dynamics and the pair production. We will end our brief review here, since this is still an active field of research and is an evolving story.

3. The Holographic Framework

In this article, we will primarily review the progress made and important results obtained in the framework of holography, the AdS/CFT correspondence [16] to be precise. AdS/CFT correspondence can be viewed as a successful marriage between 't Hooft's early ideas on large N gauge theories as string theories [72] and, later, the idea of holography pioneered by 't Hooft and Susskind in [73, 74]. This correspondence arises from a more fundamental duality between open and closed strings, in string theory, and has become the cornerstone of quantum gravitational physics so much so that the modern understanding of the correspondence identifies it with the most rigorous definition of a quantum theory of gravity, in an asymptotically AdS-spacetime. For our purpose, we will only require the technical aspects of this correspondence.

To do so, we briefly review the standard understanding of how this correspondence (or, duality) emerges. Closed string theories describe a consistent theory, and in the low energy limit, this consistent description can be truncated to various supergravity theories, in general. On the other hand, open string theories naturally arise as boundary conditions which contain the information of the string end point. The canonical construction begins with a stack of N Dp branes and analyzing the corresponding low energy description of the system. Let us recap the best understood example of this, *i.e.,* when $p = 3$.

For a stack of N D3-branes, the massless spectrum arising from open strings can be readily obtained. Assuming that the open strings are oriented, the degrees of freedom at the open string end points can be shown to transform under the adjoint representation of U(N) group. Furthermore, global symmetry of this stack of D3-branes uniquely determines the interacting description in the massless sector of the open string spectrum: the $\mathcal{N} = 4$ super Yang-Mills (SYM) in (3+1)-dimension. Also, the U(N) gauge group splits naturally into a global U(1) and an SU(N). For the gauge theoretic description of the system, we can safely ignore the overall U(1) mode, since this corresponds to an overall excitation; see, *e.g.,* [19] for more details.

Alternatively, a stack of D3-branes will source gravity, which is captured by the closed string excitation of this system. In this case, such a stack of N D3-branes can be obtained explicitly by solving the low energy description of the corresponding closed strings, which is given by type IIB supergravity in ten dimensions. This solution is given by

$$ds^2 = H^{-1/2}\eta_{\mu\nu}dx^{\mu}dx^{\nu} + H^{1/2}\delta_{ij}dx^i dx^j, \tag{10}$$

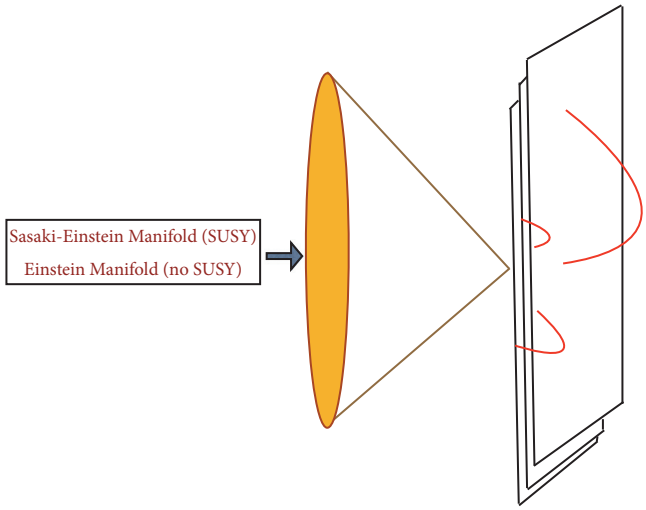

FIGURE 3: A schematic presentation of a generic D-brane construction. A certain N number of D3-branes are placed on the tip of a cone, whose base could be a Sasaki-Einstein manifold (susy preserving), or simply an Einstein manifold (susy breaking). This picture assumes the cone is a six-dimensional manifold. This condition is not required and can be relaxed easily for other dimensional cases, at least, in principle. The red curves are strings beginning and ending on the stack of the D-branes, whose low energy limit can be captured by a standard gauge theory, similar to the $\mathcal{N} = 4$ SYM.

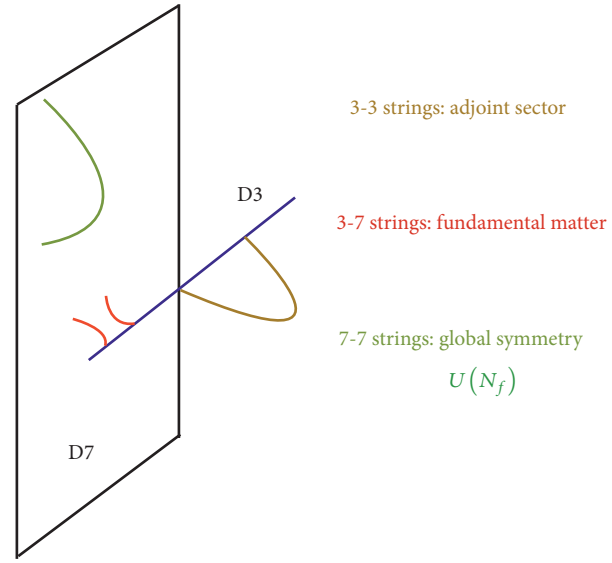

FIGURE 4: A schematic presentation of a generic D-brane construction. A certain N number of D3-branes, N_f number of D7-branes, before taking the decoupling limit. The low energy degrees of freedom can be simply obtained by considering string spectrum. The $3-3$ strings yield the matter content of $\mathcal{N} = 4$ SYM, the $3-7$ and $7-3$ strings yield the $\mathcal{N} = 2$ hypermultiplet, and the $7-7$ string sector is nondynamical; *i.e.,* it yields a global symmetry.

$$e^{\phi} = g_s, \tag{11}$$

$$C_{(4)} = H^{-1} g_s^{-1} dx^0 \wedge \ldots \wedge dx^3, \quad H = 1 + \frac{4\pi g_3 N \alpha'^2}{r^4}, \tag{12}$$

where $\mu, \nu = 0, \ldots, 3$; $i, j = 4, \ldots, 9$; α' yields the inverse string tension; g_s is the string coupling. The dilaton field, denoted by ϕ, sets the string coupling constant and the D3-brane sources the so-called Ramond-Ramond 4-form, denoted by $C_{(4)}$. Defining a new radial coordinate, $u = r/\alpha'$, and taking the $\alpha' \longrightarrow 0$ limit then decouples the near horizon physics of the geometry in (10) from the asymptotic flat infinity. The geometry becomes an $AdS_5 \times S^5$ and this corresponds to the low energy description of the D3 branes' physics. Thus, the correspondence reads: type IIB superstring theory in $AdS_5 \times S^5$ background is equivalent to $\mathcal{N} = 4$ SU(N) SYM theory in $(3 + 1)$-dimension. This $(3 + 1)$-dimensional geometry is simply the conformal boundary of the AdS_5-background. A similar construction can be obtained for a generic D3-brane, placed on the tip of a cone, as shown in Figure 3 and correspondingly obtain a similar duality. In fact, this can be further generalized for a stack of Dp-branes [75].

The construction above can now be generalized by introducing additional degrees of freedom. In the dual gauge theory, this corresponds to introducing additional matter sector transforming in different representations of the SU(N) gauge group; in the gravitational description, this corresponds to the inclusion of new gravitational degrees of freedom. A specially interesting case is to consider a matter sector that transforms in the fundamental representation of the gauge group. This can be done by adding a $\mathcal{N} = 2$ hypermultiplet to the $\mathcal{N} = 4$ SYM. Gravitationally, this can be realized by introducing a stack of N_f D7 branes in the near-horizon (*i.e.,* decoupled) $AdS_5 \times S^5$ geometry of (10). A particularly instructive limit to explore is to take $N_f \ll N$ such that gravitational backreaction of the additional D7 branes can be safely ignored. Pictorially, this is represented in Figure 4. Evidently, these constructions can be generalized for a wide class of examples, following the approach in [76]. We will elaborate more on these constructions in later sections.

The prototype model in our subsequent discussion is based on the dynamics of this additional set of branes, which capture the dynamics of open long strings. There is a "bath" with a large number of degrees of freedom which is provided by the stack of N D3-branes, in which N_f D7-branes are embedded, in the limit $N_f \ll N$. Generically, we intend to study the embedding of a probe Dq-brane in the background of a large number of Dp-branes. In this probe sector, a steady-state can be engineered by simply pumping energy into the system, which can be dissipated into the bath without causing any energy change of the bath. This is facilitated by the $N_f \ll N$ limit, and away from this limit the above approximation breaks down. We will concentrate only on this probe regime.

Before moving further, let us note the following: The fundamental matter sector, essentially, is described by long, open strings. It is not unreasonable to assume that there is a sensible limit in which the probe D-brane becomes irrelevant and the essential physics can be captured by the dynamics of explicit strings. Indeed, for specific models, this limit can be made precise: For example, if we introduce a mass of the $\mathcal{N} =$

2 hypermultiplet sector, in the large mass limit, the probe D7 brane is pushed far away at the UV, leaving a family of strings that connect between the UV D7-brane and the IR D3-brane. In this limit, one can simply consider the open string sector only. Motivated by this, we will review the physics of open strings in an AdS-background, in the next section.

4. The String Worldsheet Description

We begin with reviewing a general description of a string worldsheet which is embedded in an AdS-background, following closely the treatment of [77, 78]. The simplest case is to take an $AdS_5 \times S^5$ geometry, in which the AdS/CFT dictionary is very well known. The discussion below, however, is far more generic and applies to a more general supergravity background which can be bisected by an AdS_2. Let us begin with the Poincaré patch:

$$ds^2 = \frac{R^2}{z^2}\left(-dt^2 + d\vec{x}^2 + dz^2\right) + ds^2_{S^5}, \tag{13}$$

where R is the curvature scale of the AdS_5, $\{t, \vec{x}\}$ represent the $\mathbb{R}^{1,3}$ in which the dual $\mathcal{N} = 4$ SYM theory is defined, and z is the AdS-radial coordinate. The conformal boundary is located at $z \longrightarrow 0$ limit and the infra-red (IR) is located at $z \longrightarrow \infty$. In the presence of a bulk event horizon, the IR is cut off at some finite location, which we denote by z_h. Note that it is possible to select general radial foliations of the bulk AdS geometry such that the dual CFT (in this case, the $\mathcal{N} = 4$ SYM) is defined on the corresponding Lorentzian manifold $\mathcal{M}^{1,3}$, which is realized as the conformal boundary of the bulk spacetime. This is best expressed in the so-called Fefferman-Graham patch [79], which is suitable to describe any asymptotically AdS geometry:

$$ds^2 = \frac{R^2}{z^2}\left(dz^2 + g_{AB}dx^A dx^B\right), \tag{14}$$

where g_{AB} is a function of the radial coordinate z, as well as the x^A coordinates. The corresponding CFT is defined on the background whose metric is given by $ds^2_{CFT} = g_{AB}dx^A dx^B|_{z\longrightarrow 0}$, which defines the line-element on $\mathcal{M}^{1,3}$. The background in (14) is uniquely determined in terms of the boundary data $g_{AB}|_{z\longrightarrow 0}$ and a subleading mode of the function $g_{AB}(z)$, in a z-expansion around the conformal boundary. This subleading mode, essentially, contains the data of the CFT stress-tensor. The detailed procedure of extracting the resulting CFT stress-tensor, which is based on holographic renormalization, is discussed in, *e.g.,* [80–82]. The corresponding 't Hooft coupling is given by $\lambda \equiv g^2_{YM}N_c = R^4/\alpha'^2$, where g_{YM} is the gauge theory coupling and N_c determines the rank of the gauge group, while α' is the inverse tension of the string.

The dynamics of the string is governed by the Nambu-Goto action:

$$\begin{aligned} S_{NG} &= -\frac{1}{2\pi\alpha'}\int d\tau d\sigma \sqrt{-\det\gamma} + S_{\text{boundary}}, \\ \gamma_{ab} &= G_{\mu\nu}(X)\,\partial_a X^\mu \partial_b X^\nu, \end{aligned} \tag{15}$$

where $\{\tau, \sigma\}$ represent the worldsheet coordinates, $\alpha' = l_s^2$ sets the string tension (while l_s is the string length), and S_{boundary} is a generic boundary term. The background manifold is described by the metric $G_{\mu\nu}(X)$, while X represents the coordinate patch chosen to describe the manifold. The various indices are chosen to represent the following: $a, b, \ldots$ denote the worldsheet coordinates, $A, B, \ldots$ denote the coordinates on the manifold where the CFT is defined (in general, denoted by $\mathcal{M}^{1,3}$), and $\mu, \nu, \ldots$ denote the full ten-dimensional supergravity background. We will consider cases in which the string is extended along the radial direction, and therefore the boundary term can capture the coupling of the end-point with an applied external field:

$$S_{\text{boundary}} = \int d\tau A_B \partial_\tau X^B. \tag{16}$$

Before proceeding further, let us offer some comments regarding the boundary term. The physical picture is as follows: Given the ten-dimensional geometry, one considers such *long* strings which extend from the IR of the geometry all the way to the UV. Note that these open strings must have an end point on a D-brane and therefore it makes sense to think of the end point as a point on a D-brane at the UV. There are various ways to think about such configurations; for our purpose we can introduce a UV cut-off z_{UV} where the string ends. Such a string certainly carries an energy, as a function of $\{z_{IR}, z_{UV}\}$, where z_{IR} is the IR end of the geometry. Irrespective of the details, one can naturally assign a physical mass-scale, M, associated with the heavy string with a static and constant profile:

$$M = \frac{\lambda^{1/2}}{2\pi z_{UV}}. \tag{17}$$

The $\sqrt{\lambda}$ behaviour simply comes from the string tension, which is proportional to α'^{-1}. Thus, we simply introduce a fundamental degree of freedom (*i.e.,* like a quark) with a nonvanishing mass. In the context of $\mathcal{N} = 4$ SYM, this fundamental matter can sit inside an $\mathcal{N} = 2$ hypermultiplet, for example.

Given the above action in (15), one can solve the classical equations of motion. Instead of choosing a gauge and solving for the equations of motion, let us review the general solution of [83] in the embedding space formalism. We begin with a description of the AdS_5 geometry as an hyperbolic submanifold in $\mathbb{R}^{2,4}$, described by

$$\begin{aligned} Y^M Y_M = \eta_{MN}Y^M Y^N = -R^2, \\ \eta_{MN} = \text{diag}\,(-1,-1,1,1,1,1)\,. \end{aligned} \tag{18}$$

To describe a two-dimensional worldsheet, let us define a light-like vector $\ell^M(\tau)$ which obeys

$$\begin{aligned} \eta_{MN}\ell^M\ell^N = 0, \\ \eta_{MN}\partial_\tau\ell^M\partial_\tau\ell^N = -R^2. \end{aligned} \tag{19}$$

Using the relations above, it is easy to show that the general solution of (18) is given by

$$Y^M(\tau,\sigma) = \pm\partial_\tau\ell^M(\tau) + \sigma\ell^M(\tau)\,. \tag{20}$$

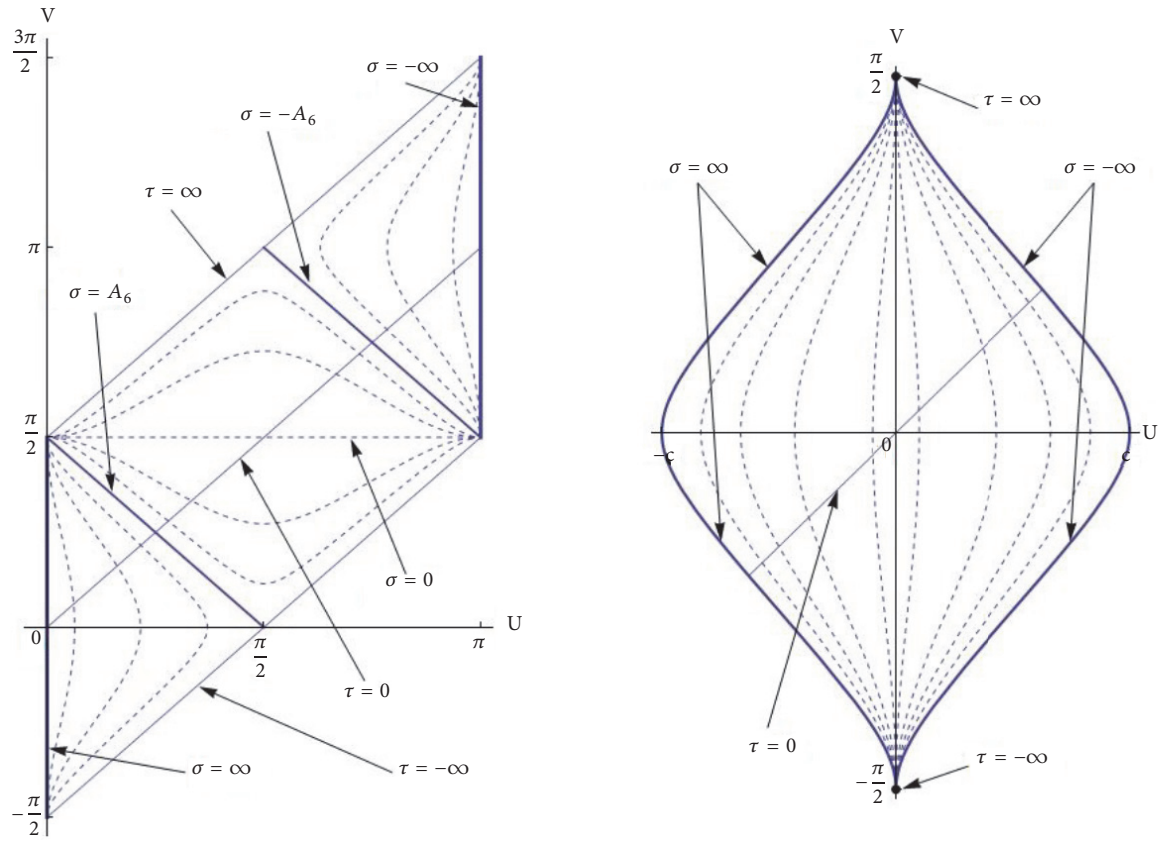

FIGURE 5: The left diagram corresponds to $A_6^2 > 0$, with a subsequent causal structure which is divided into two regions by the $\sigma = A_6$ curve. The end points of the worldsheet, denoted by $\sigma = \pm\infty$, corresponds to two fundamental degrees of freedom with opposite charges. The right Penrose diagram corresponds to $A_6^2 < 0$, and the resulting causal structure does not possess any event horizon. Dashed lines on both diagrams correspond to curves with constant σ. This diagram is taken from [77], with the authors' consent.

As demonstrated in [83], (20) is an extremal surface inside AdS_5. The overall sign in front of the first term in (20) corresponds to a purely ingoing and outgoing nonlinear wave solutions, with respect to the location of the source. The induced worldsheet metric is subsequently given by

$$ds_{ws}^2 = \left[\eta_{MN}\left(\partial_\tau^2 \ell^M\right)\left(\partial_\tau^2 \ell^N\right) + \sigma^2\right] d\tau^2 - 2d\tau d\sigma. \quad (21)$$

Following the discussion in [77], we introduce the following:

$$A_6^2 = -\eta_{MN}\left(\partial_\tau^2 \ell^M\right)\left(\partial_\tau^2 \ell^N\right),$$
$$d\tau = d\tilde{\tau} - \frac{d\sigma}{A_6^2 - \sigma^2}, \quad (22)$$

where A_6 represents the proper acceleration, defined on the embedding space $\mathbb{R}^{2,4}$. The resulting induced metric is given by

$$ds_{ws}^2 = -\left(\sigma^2 - A_6^2\right) d\tilde{\tau}^2 + \frac{d\sigma^2}{\left(\sigma^2 - A_6^2\right)}. \quad (23)$$

In general, A_6 is a τ-dependent function. However, for cases when A_6 is a constant, the worldsheet describes an AdS_2-black hole. The corresponding causal structure is best described in terms of the Penrose diagram, which is shown in Figure 5. The relevant change of coordinates is given in [77], which we also review below:

$$V = \frac{1}{2}\left[\tan^{-1}\left(\tau + \frac{1}{A_6}\log\left(\frac{\sigma + A_6}{\sigma - A_6}\right)\right) + \tan^{-1}\tau\right], \quad (24)$$

$$U = \frac{1}{2}\left[\tan^{-1}\left(\tau + \frac{1}{A_6}\log\left(\frac{\sigma + A_6}{\sigma - A_6}\right)\right) - \tan^{-1}\tau\right], \quad (25)$$

for $\sigma > A_6$. For $\sigma < -A_6$, the corresponding patches are obtained by adding a π-shift to (24) and (25). For the region $\mathrm{Abs}(\sigma) < A_6$, the relevant coordinate changes are given by

$$V = \frac{1}{2}\left[\pi - \tan^{-1}\left(\tau + \frac{2}{A_6}\tanh^{-1}\left(\frac{\sigma}{A_6}\right)\right) + \tan^{-1}\tau\right], \quad (26)$$

$$U = \frac{1}{2}\left[\pi - \tan^{-1}\left(\tau + \frac{2}{A_6}\tanh^{-1}\left(\frac{\sigma}{A_6}\right)\right) - \tan^{-1}\tau\right]. \quad (27)$$

Note that the worldsheet metric in the $\{V, U\}$ coordinate takes the form $ds^2 \propto (dU^2 - dV^2)$, where the proportionality factor

is a function of the U and V coordinates. For the case when $A_6^2 < 0$, the following coordinate change [77]

$$2V = \tan^{-1}\left(\tau - \frac{2}{\sqrt{-A_6^2}}\tan^{-1}\left(\frac{\sigma}{\sqrt{-A_6^2}}\right) + \tan^{-1}\tau\right), \quad (28)$$

$$2U = \tan^{-1}\left(\tau - \frac{2}{\sqrt{-A_6^2}}\tan^{-1}\left(\frac{\sigma}{\sqrt{-A_6^2}}\right) - \tan^{-1}\tau\right), \quad (29)$$

again brings the worldsheet metric back to the desired form. A detailed analysis of various trajectories is discussed in [77], which results in the Penrose diagram shown in Figure 5. The crucial point to note is the presence of a causal horizon in the case $A_6^2 > 0$ (the left Penrose diagram in Figure 5), which is absent for $A_6^2 < 0$ (the right Penrose diagram in Figure 5). We will now discuss a few simple and explicit examples.

The string with a single end point at the UV, which is what is described above, can be written in a particularly recognizable form [50]:

$$t\left(t_r, z\right) = t_r \pm \frac{z}{\sqrt{1 - \vec{v}\left(t_r\right)^2}}, \quad (30)$$

$$\vec{x}\left(t_r, z\right) = \vec{x}\left(t_r\right) \pm \frac{\vec{v}\left(t_r\right) z}{\sqrt{1 - \vec{v}\left(t_r\right)^2}}, \quad (31)$$

where the background is written in the standard Poincaré patch of (13). The positive sign corresponds to a retarded solution, in which energy flux propagates from the end point of the string to the Poincaré horizon and the negative sign corresponds to an advanced solution with a reverse energy flow. The time argument t_r denotes retarded or advanced time, correspondingly. The above solution corresponds to an infinitely massive fundamental matter; for a nonvanishing but finite mass, the corresponding solutions are discussed in [84–86].

4.1. Asymptotically Uniform Acceleration. We can describe the string profile in terms of the embedding space; however, in this case it is straightforward to adopt a Poincaré patch description of the profile. This can simply be done by using, *e.g.,* Poincaré slicing of the embedding space and subsequently choosing an appropriate vector ℓ^M. Evidently, various slicing of the embedding space yields various AdS-metrics and correspondingly the manifold on which the CFT is defined. For an explicit exposition of such slices, see, *e.g.,* [87].

Here we will discuss the particular case, in which an infinitely massive quark (*i.e.,* the string end point) undergoes a uniform acceleration. In the standard Poincaré patch, this worldsheet embedding is given by [88]

$$x\left(t, z\right)^2 = a^{-2} + t^2 - z^2. \quad (32)$$

Clearly, we have chosen a static gauge $\sigma = z$, $\tau = t$ to describe the above solution of the Nambu-Goto action in (15). The embedding function $x(t, z)$ is simply one of the Minkowski-direction coordinates of the CFT. There is a clear sign choice involved in the function $x(t, z)$; this corresponds to the overall charge of the string end point. For simplicity, we can easily think of them as quark and anti-quark degrees of freedom.

The causal structure induced from the embedding in (32) is similar to a black hole in AdS-background, in which the event horizon is located at $z_{\mathrm{h}} = a^{-1}$. Moreover, the embedding in (32) can be constructed by patching two sections of (30) and (31). Physically, because of the uniform acceleration, a given retarded string profile terminates at the worldsheet event horizon: $z_{\mathrm{h}} = a^{-1}$, where the local speed of propagation exceeds the speed of light. Therefore the rest of the profile needs to be completed accordingly. This can be done by smoothly patching the retarded solution with an advanced solution. This class of embeddings, along with various generalizations, were discussed in detail in [50, 51].

Patching a retarded solution and an advanced solution has been discussed extensively in [50]. The advanced and the retarded configurations cover nonsymmetric regions of the configuration space. This construction is perhaps best represented in terms of the figures in [50], which we include in Figure 6, with the authors' consent.

4.2. Uniform Circular Trajectory. A simple but instructive example is to consider the string end point moving in a circle of constant radius. Evidently, the end point does undergo an acceleration. Let us review this based on [77]. Let us begin with the Poincaré slicing of the embedding in (18), given by

$$Y^0 = \frac{R}{2z}\left(1 + x^2 + z^2\right),$$
$$Y^A = \frac{R}{z}x^A, \quad (33)$$
$$Y^1 = \frac{R}{2z}\left(1 - x^2 - z^2\right).$$

The induced AdS is given by the Poincaré disc and the dual field theory is defined on an $\mathbb{R}^{1,3}$. To describe a string embedding, further, we need to specify the vector ℓ^M, which is given by

$$\ell^0 = \frac{1}{2}\left[1 - \left(x\left(\tau\right)\right)^2\right],$$
$$\ell^1 = \frac{1}{2}\left[1 - \left(x\left(\tau\right)\right)^2\right], \quad (34)$$

$$\ell^\mu = x^\mu\left(\tau\right), \quad (35)$$

where x^2 is constructed by taking an inner product with a Minkowski metric $\eta_{\mu\nu}$ of the vector $x^\mu \in \mathbb{R}^{1,3}$. To satisfy (19), we further impose $(\partial_\tau x^\mu)(\partial_\tau x_\mu) = 1$. The parameter τ is physically identified with the proper time associated with

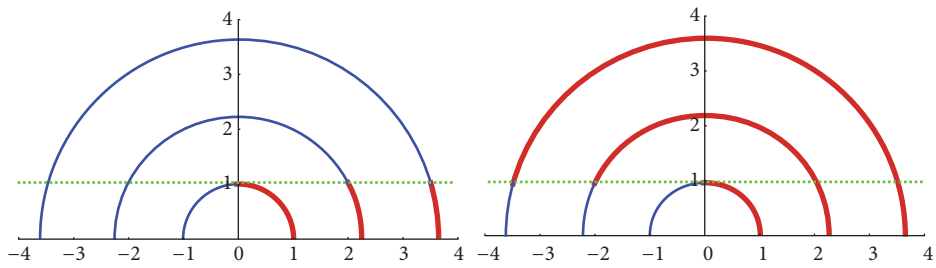

FIGURE 6: We have shown here various string profiles in $\{z, x\}$-plane. The vertical axis is the z-axis and the horizontal axis is the x-axis. The left diagram corresponds to $t < 0$ and the semicircular profiles shrink as time increases towards positive values. On the right, we have $t > 0$ and the semicircular profiles grow as time increases. In both, the advanced solution is denoted by the blue, thin curve and the retarded solution is represented by the red, thick curve. The green horizontal dashed line corresponds to the worldsheet event horizon, located at $z_h = a^{-1}$. We have taken these diagrams from [50], with the authors' consent.

the string end point. Fixing $\sigma^{-1} = z$, the embedding in (20) is given by

$$x(\tau, z) = z\left(\partial_\tau x^\mu(\tau)\right) + x^\mu(\tau). \tag{36}$$

Let us now describe the particular case, first discussed in [89]. In this case, the string end point is moving with a constant angular velocity ω, in a circle of radius r_0. The solution can be described by a collection of the functions $x^\mu(\tau)$. The nontrivial components are given by

$$\begin{aligned} x^1 &= r_0 \cos\left(\omega t_{\text{ret}}(\tau)\right), \\ x^2 &= r_0 \sin\left(\omega t_{\text{ret}}(\tau)\right), \end{aligned} \tag{37}$$

while (19) yields

$$\begin{aligned} \partial_\tau t_{\text{ret}} &= \frac{1}{\sqrt{1-\omega^2 r_0^2}} = \gamma = \frac{1}{\sqrt{1-v^2}}, \\ &\Longrightarrow t_{\text{ret}} = \gamma\tau. \end{aligned} \tag{38}$$

Thus, the full solution can be represented by

$$x^0 = z\gamma + t_{\text{ret}}, \tag{39}$$

$$\begin{aligned} x^1 &= r_0 \cos\left(\omega t_{\text{ret}}(\tau)\right), \\ x^2 &= r_0 \sin\left(\omega t_{\text{ret}}(\tau)\right). \end{aligned} \tag{40}$$

The induced geometry on the worldsheet inherits an event horizon at $z_h = 1/(\omega^2\gamma v)$. Propagating modes across this radial scale become causally disconnected and therefore yield an effective temperature:

$$T_{ws} = \frac{v\gamma^2\omega}{2\pi}. \tag{41}$$

On these simple examples, the general picture is already emerging and clear. We will not further explicitly discuss more possibilities, specially the ones that appear in the global patch of AdS. However, let us briefly summarize the physics.

In the global AdS patch, the boundary theory is kept at a finite volume and likewise develops a mass gap. Thus, a rotating string will not develop an event horizon on the worldsheet for any value of the frequency, unlike the Poincaré-slice result. In this case, for sufficiently large angular frequency $\omega L_{\text{typical}} > 1$, where L_{typical} is the typical length-scale associated with the finite volume, the worldsheet develops an event horizon and measures an effective thermal description on the worldsheet. For $\omega L_{\text{typical}} < 1$, there is no event horizon and thus no effective thermal description holds. As pointed out in [77], this is similar to the behaviour of an Unruh-DeWitt detector [90], undergoing a circular motion in a compact space. The corresponding Hawking radiation of the string worldsheet was analyzed in terms of a synchrotron radiation in the dual gauge theory in [89]. There certainly are numerous interesting such string configurations which demonstrate very interesting physics, driven by the worldsheet event horizon. We will not elaborate more on examples; instead we will briefly discuss some recent advances in understanding the same physics from a slightly different perspective, in the next section.

4.3. Chaos: A Recent Development. A thermal effective description ensures that the string end point will undergo a stochastic motion, because of the thermal fluctuations. This results in a Brownian motion for the string end point. In [45], this effect was explored in detail by considering fluctuations of the string around a classical saddle. The fluctuation degrees of freedom, effectively, propagate in a curved geometry with an event horizon and therefore exhibit random fluctuations due to the Hawking-Unruh radiation. In [46], a Schwinger-Keldysh description of the stochastic was discussed, which is based on a Kruskal-type extension of the worldsheet geometry. Such Brownian motions are expected to be dissipated in the medium, since the system is thermalized.

Given a thermal system, how fast a small perturbation relaxes to the thermal value sets the thermalization time scale for such small excitations. This is closely related to the scrambling time for the system, which determines the speed at which a quantum system spreads a localized information. In [91], it was conjectured that black holes are the fastest scramblers in Nature, for which the scrambling time scales as the logarithm of the number of degrees of freedom. In the context of Holography, therefore, a strongly coupled system in thermal equilibrium will also satisfy this bound.

The notion of ergodicity and thermalization are intimately related. In a semi-classical description, the physics of thermalization is further related to a particular notion of growth of n-point correlation functions, where $n \geq 4$. Also, the correlator must contain operators which are not time-ordered. Conventionally, these are known as the out-of-time order correlator, or OTOC in brief. The basic idea here is rather simple, which we quickly review below.

Given a classical system, a phase space description is provided in terms of canonical coordinates and momenta variables: $q(t)$ and $p(t)$, respectively. The notion of classical chaos is defined as a response of a classical trajectory at late times, in terms of the variation of its initial value. Typically, a chaotic system is characterized by exponentially diverging trajectories at sufficiently late times:

$$\{q(t), p\} \equiv \frac{\partial q(t)}{\partial q(0)} \sim \exp(\lambda_{\mathrm{L}} t), \tag{42}$$

where the real number λ_{L} is known as the Lyapunov exponent. The left most expression is the standard classical Poisson bracket. Within a semi-classical framework, the diagnostic of chaos, along with the notion of Lyapunov exponents, can be easily generalized for a quantum system, by replacing the Poisson bracket with a commutator, and finally, computing the square of this commutator to make sure that no accidental phase cancellation takes place. (Note that it is expected that, for higher powers of the commutator, one would observe a growing OTOC. For SYK-type models, this growth can be explicitly calculated in the form of a six-point OTOC; see, *e.g.,* [92].) Thus, a chaos diagnostic can be defined in terms of the following correlator:

$$C(t) = -\left\langle [W(t), V(0)]^2 \right\rangle, \tag{43}$$

where $W(t)$ and $V(0)$ are generic Hermitian operators. The function, $C(t)$, possesses both time-ordered and out-of-time ordered correlator, but the exponential growth is visible in the OTOC sector only. In terms of this diagnostic function $C(t)$, the scrambling time is also defined as the time scale when $C(t) \sim \mathcal{O}(1)$. The basic behaviour of the diagnostic function is pictorially demonstrated in Figure 7. The basic idea here is simple: Given a thermal state, one computes an OTOC based on a Schwinger-Keldysh construction. Now, in the limit $t \gg t_d$, where t_d is the dissipation time-scale, one observes a growth in the correlator. In case this is an exponential growth, it is simple to extract the corresponding Lyapunov exponent. This particular notion of the growth of an operator is intrinsic to a semi-classical description.

It is not simple to calculate higher point OTOCs, in general and there are currently a handful of tractable examples. Nevertheless, in [93], a bound for the Lyapunov exponent was derived $\lambda_{\mathrm{L}} \leq 2\pi T$, for a system with temperature T, and in natural units. It was further conjectured that the maximal chaos limit is saturated for holographic theories. For a black hole in AdS, this saturation is simply guaranteed by the near horizon dynamics, where a local Rindler description holds. This intuition is based on recasting the four-point OTOC in terms of a two-two high energy scattering amplitude in the thermofield double picture; see, *e.g.,* [94–96].

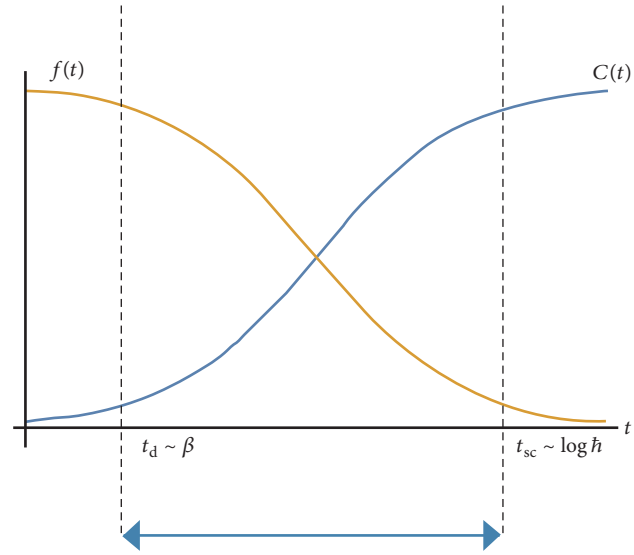

Figure 7: A schematic representation of the chaos diagnostic function(s). Here, qualitatively, $f(t) = 1 - C(t)$, while both $f(t)$ and $C(t)$ individually carry the information of an exponential decay (for $f(t)$) or growth (for $C(t)$) of the corresponding correlator. The exponential behaviour occurs in a regime between a $\mathcal{O}(1)$ time-scale, such as the dissipation time t_d, and a parametrically large time-scale, such as the scrambling time t_{sc}. This hierarchy of t_d and t_{sc} is ensured in the $\hbar \longrightarrow 0$ limit.

Given the black hole like causal structure on the string worldsheet, it is therefore expected that such a saturation will hold on the worldsheet horizon as well. Indeed, it was explicitly shown in [97, 98] that the maximal saturation occurs on the string worldsheet, with the effective temperature. Moreover, a corresponding soft sector effective action, which is a Schwarzian derivative action, was explicitly obtained in [99, 100], and its coupling with various heavy modes was explicitly determined. The soft sector action can be simply obtained by embedding the string worldsheet in an AdS_3-background and using the Brown-Henneaux large diffeomorphisms, projected on the worldsheet. This yields

$$S_{\mathrm{effective}} = \frac{\epsilon_{\mathrm{IR}}}{\alpha'} \int dx \{\varphi(x), x\}, \qquad \{\varphi(x), x\} \equiv \frac{3}{2}\frac{\varphi''^2}{\varphi'^2} - \frac{\varphi'\varphi'''}{\varphi'^2}, \tag{44}$$

where α' is the inverse string tension, ϵ_{IR} is a physical scale, typically given by the event horizon on the induced worldsheet, and $\varphi(x)$ is the dynamical degree of freedom. This effective description has a natural interpretation as an Euclidean theory; however, because of the high derivative coupling, the Lorentzian description has pathologies.

The soft sector physics, described by (44), is ultimately responsible for the maximal chaos on the worldsheet. Qualitatively, this is straightforward to understand. In the two-two elastic scattering process, the four-point vertex of any semi-classical fluctuation of the string worldsheet can be resolved in terms of two interaction vertices of the fluctuation

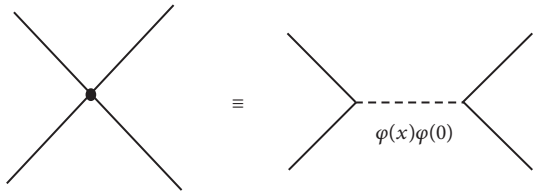

Figure 8: The four-point effective vertex contains two interaction vertices with the soft sector, along with a propagator of the same soft sector. The dashed horizontal line is the soft sector propagator, and the solid lines are external hard modes.

with the soft sector mode, and a propagator of the soft sector itself. This is pictorially demonstrated in Figure 8. This soft sector dynamics on the string worldsheet is in close resemblance with the soft sector dynamics of AdS_2 in the Jackiw-Teitelboim gravity [101]. Finally, by setting $C(t) \sim \mathcal{O}(1)$, we can determine the scrambling time. Note, further, that a direct four-point OTOC correlator yields a scrambling time $t_{sc} \sim \beta \log \sqrt{\lambda}$, where λ is the corresponding 't Hooft coupling [98]. The same result is obtained by analyzing the soft sector physics and its coupling with heavier modes in the string fluctuations [99, 100]. It can now be anticipated that, on a D-brane horizon, one would observe a similar physics, which is demonstrated explicitly in [99, 100], in which the corresponding scrambling time depends on both the rank of the gauge group, N_c, and the 't Hooft coupling.

We will end this brief section here, leaving untouched a remarkable amount of recent research in related topics. Chaotic properties of strongly coupled CFTs with or without a holographic dual are a highly evolving field of research. Moreover, the notion of chaos in quantum mechanical systems is a rich field in itself and only some explicit calculations using a particular semi-classical prescription have been made. Thus, we will leave a detailed discussion for future and, for now, shift our attention to the effective thermal description of a D-brane.

5. The Brane Worldvolume Description: A Model

Let us consider a stack of N_c D3-branes sitting at the tip of a cone, with a Sasaki-Einstein 5-manifold base, henceforth denoted by SE_5. When the $SE_5 \equiv S^5$, the 10-dimensional geometry is given by AdS_5-Schwarzschild $\times S^5$ which is dual to the $\mathcal{N} = 4$ super Yang-Mills (SYM) theory with an $SU(N_c)$ gauge group. The corresponding gravity data are given by the following: (We are using the notation used in [102].)

$$ds^2 = \frac{1}{4r^2R^2}\left(-\frac{f^2}{\widetilde{f}}dt^2 + \widetilde{f}d\vec{x}^2\right) + \frac{R^2}{r^2}dr^2 + R^2 d\Omega_5^2, \quad (45)$$

$$f = 4r^4 - b^4,$$
$$\widetilde{f} = 4r^4 + b^4, \quad (46)$$

$$F_{(5)} = (1 + \star)\,\mathrm{vol}_{S^5} = dC_{(4)} + d\widetilde{C}_{(4)}, \quad (47)$$

where $\{t, \vec{x}\}$ are the field theory space-time directions, $r \in [b, \infty)$ is the AdS-radial direction, R is the curvature of AdS, and $d\Omega_5^2$ is the metric on a unit 5-sphere. These branes source a self-dual $F_{(5)}$. Here $\star$ denotes the Hodge dual operator. The unit sphere metric can be written as

$$d\Omega_5^2 = d\theta^2 + \cos^2\theta d\Omega_3^2 + \sin^2\theta d\phi^2, \quad (48)$$

$$d\Omega_3^2 = d\psi^2 + \cos^2\psi d\beta^2 + \sin^2\psi d\gamma^2. \quad (49)$$

The corresponding black hole temperature is given by

$$T = \frac{b}{\pi R^2}. \quad (50)$$

The AdS curvature sets the 't Hooft coupling for the dual field theory *via* $R^4 = \alpha'^2 g_{YM}^2 N_c$, where α' is the string tension and g_{YM} is the gauge theory coupling.

The matter content of $\mathcal{N} = 4$ SYM is the gauge field A_μ, four adjoint fermions λ, and three complex scalars Φ^a ($a = 1, 2, 3$). This theory has an $SU(4) \sim SO(6)$ R-symmetry, which corresponds to the rotational symmetry of the S^5 in the dual gravitational description. To introduce fundamental matter, one introduces open string degrees of freedom which is equivalent to introducing additional probe branes, along the lines of [76]. As mentioned earlier, of particular interest is to add N_f probe D7-branes, in the limit $N_f \ll N_c$ to suppress backreaction. These probe branes are extended along $\{t, \vec{x}\}$ and wraps the $S^3 \subset S^5$. The codimension 2 brane is described by $\{\theta(r), \phi(r)\}$. Isometry along the ϕ-direction implies $\phi(r) = 0$, without any loss of generality. Thus, the embedding is described by a single function $\theta(r)$.

In terms of the dual gauge theory side (in this part, we closely follow the discussions in [103]), we introduce an $\mathcal{N} = 2$ hypermultiplets in the background of $\mathcal{N} = 4$ SYM. The hypermultiplets consist of two Weyl fermions, denoted by ψ and $\overline{\psi}$ and two complex scalars, denoted by q and $\overline{q}$. Here, $\{\psi, q\}$ transforms under the fundamental representation of $SU(N_c)$ and $\{\overline{\psi}, \overline{q}\}$ transforms under the anti-fundamental. The dual operators corresponding to the D7-brane profile functions θ and ϕ are given by

$$\begin{aligned}\cos\theta \longleftrightarrow \mathcal{O}_m &= i\overline{\psi}\psi + \overline{q}\left(m_q + \sqrt{2}\Phi^1\right)\overline{q}^\dagger \\ &\quad + q^\dagger\left(m_q + \sqrt{2}\Phi^1\right)q + \text{h.c.},\end{aligned} \quad (51)$$

$$\phi \longleftrightarrow \mathcal{O}_\phi = \overline{\psi}\psi + i\sqrt{2}\overline{q}\Phi^1\overline{q}^\dagger + i\sqrt{2}q^\dagger\Phi^1 q + \text{h.c.}, \quad (52)$$

where Φ^1 is a complex scalar field in the $\mathcal{N} = 4$ supermultiplet and m_q is the mass of the fundamental quark.

The Lagrangian of the worldvolume theory can be written in the $\mathcal{N} = 1$ language, as follows:

$$\begin{aligned}\mathcal{L} = \mathrm{Im}\Big[\tau\int d^4\theta\left(\mathrm{tr}\left(\overline{\Phi}_I e^V \Phi_I e^{-V}\right) + Q_r^\dagger e^V Q^r\right. \\ \left. + \overline{Q}_r^\dagger e^{-V}\overline{Q}^r\right) + \tau\int d^2\theta\left(\mathrm{tr}\left(W^\alpha W_\alpha\right) + W\right) + \text{c.c.}\Big],\end{aligned} \quad (53)$$

Table 1: Degrees of freedom in the dual field theory.

Fields	Components	Spin	$SU(2)_\Phi \times SU(2)_R$	$U(1)_R$	Δ	$U(N_f)$
Φ_1, Φ_2	X^4, X^5, X^6, X^7	0	$(1/2, 1/2)$	0	1	1
	λ_1, λ_2	1/2	$(1/2, 0)$	-1	3/2	1
Φ_3, W_α	$X_V^A = (X^8, X^9)$	0	$(0, 0)$	$+2$	1	1
	λ_3, λ_4	1/2	$(0, 1/2)$	$+1$	1	1
	v_μ	1	$(0, 0)$	0	1	1
$Q, \widetilde{Q}$	$q^m = (q, \overline{q})$	0	$(0, 1/2)$	0	1	N_f
	$\psi_i = (\psi, \psi^\dagger)$	1/2	$(0, 0)$	∓ 1	3/2	N_f

where

$$W = \mathrm{tr}\left(\epsilon_{IJK}\Phi_i\Phi_j\Phi_K\right) + \widetilde{Q}_r\left(m + \Phi_3\right)Q^r. \tag{54}$$

Here W_α denotes the vector multiplet, Φ_I, with $I = 1, 2, 3$ denoting the chiral superfields. Both of these are obtained from the $\mathcal{N} = 4$ vector multiplet. On the other hand, Q^r, $\widetilde{Q}_r$, where $r = 1, \ldots, N_f$ denotes the $\mathcal{N} = 2$ matter sector. Further details are summarized in Table 1, where the $SO(4) \equiv SU(2)_\Phi \times SU(2)_R$ symmetry corresponds to the S^3 isometry, wrapped by the D7-brane. The transverse SO(2) symmetry can be explicitly broken by giving a mass to the hypers: $m_q \neq 0$, which is proportional to the separation of the D3-branes and the D7-branes.

The effective action for the probe D7-brane is given by the Dirac-Born-Infeld (DBI) Lagrangian with an Wess-Zumino term. (Here we are using the Lorentzian signature.)

$$\begin{aligned} S_{\mathrm{D7}} &= -N_f T_{\mathrm{D7}} \int d^8\xi \sqrt{-\det\left(P\left[G_{ab} + B_{ab}\right] + 2\pi\alpha' f_{ab}\right)} \\ &\quad + \left(2\pi\alpha'\right)^2 \frac{\mu_7}{2} \int f_{(2)} \wedge f_{(2)} \\ &\quad \wedge \left(P\left[C_{(4)}\right] + P\left[\widetilde{C}_{(4)}\right]\right). \end{aligned} \tag{55}$$

Here $P[G_{ab} + B_{ab}]$ denotes the pull-back of the NS-NS sector fields: G denotes the closed-string background metric and B denotes the NS-NS field; f_{ab} is the worldvolume $U(1)$ gauge field on the probe. The four-form potentials $C_{(4)}$ and $\widetilde{C}_{(4)}$ yield the self-dual five-form. Collectively, $\{\xi\}$ denotes D7-brane worldvolume coordinates, and $T_{\mathrm{D7}} = \mu_7/g_s$ denotes the D7-brane tension. Here g_s is the string coupling constant. (Note that even though we take $N_f \neq 1$, we work with an Abelian version of the effective action. This is clearly a truncation of the full non-Abelian action to an Abelian sector. We will assume such a truncation holds true.)

We intend to design a system in which energy is constantly pumped into the probe sector. This can be achieved by exciting the gauge field. (We absorb the factor of $(2\pi\alpha')$ in the field strength.)

$$A = a_1(r)\, dx^1 = \left(-Et + a(r)\right) dx^1, \tag{56}$$

This ansatz (56), which is consistent with the equations of motion, manifestly breaks the O(3) $\longrightarrow$ O(2) in the $\vec{x}$-plane. The constant electric field E is applied along the x^1-direction, to which only the probe sector couples, in the probe limit. The function $a(r)$ is governed by the equation of motion obtained from (55), using the ansatz above. The resulting effective action for the probe D7-brane is a functional of two functions $\theta(r)$ and $a(r)$. The physical meaning of these functions can be understood from the corresponding asymptotic behaviour:

$$\lim_{r\longrightarrow\infty} a(r) = 0 + \frac{J}{2r^2} + \ldots, \tag{57}$$

$$\lim_{r\longrightarrow\infty} \theta(r) = \frac{m}{r} + \frac{c}{r^3} + \ldots. \tag{58}$$

In the dual gauge theory, the corresponding source and vevs are given by (in units $b = 1$)

$$\left\langle J^1 \right\rangle = -\left(4\pi^3\alpha'\right) N_f V_{\mathbb{R}^3} T_{\mathrm{D7}} J, \tag{59}$$

$$\begin{aligned} m_q &= \frac{m}{2\pi\alpha'}, \\ \left\langle \overline{\psi}\psi \right\rangle &= -8\pi^3\alpha' V_{\mathbb{R}^3} N_f T_{\mathrm{D7}} c. \end{aligned} \tag{60}$$

Here $\langle J^1 \rangle$ is the expectation value of the current, and m_q is the mass of the hypermultiplet and $\langle \overline{\psi}\psi \rangle$. In the limit of vanishing electric field, thermal physics drives a first-order phase transition in this system; see, *e.g.*, [38, 39], as (m_q/T) is tuned. This transition separates two phases: one containing bound mesonic degrees of freedom and a plasma phase, consisting of the $\mathcal{N} = 4$ adjoint and $\mathcal{N} = 2$ hypermultiplet degrees of freedom. A similar physics exists in the global patch of AdS as well [40].

In the presence of E but not background event horizon, $b = 0$, the boundary current in (59) by demanding a reality condition of the on-shell effective action, much like [41]. This exercise yields [104]

$$\begin{aligned} J^2 &= \frac{\left(4r_*^4 - 1\right)^2 \left(4r_*^4 + 1\right)^3 \cos^6\theta\left(r_*\right)}{64 r_*^6 \left(4r_*^4 + 1\right)^2}, \\ r_*^2 &= \frac{E + \sqrt{E^2 + 1}}{2}. \end{aligned} \tag{61}$$

The gauge theory current expectation value vanishes when $E = 0$, which is expected; it also vanishes when $\theta(r_*) = 0$. The latter corresponds to a shrinking of the S^3 (which is wrapped

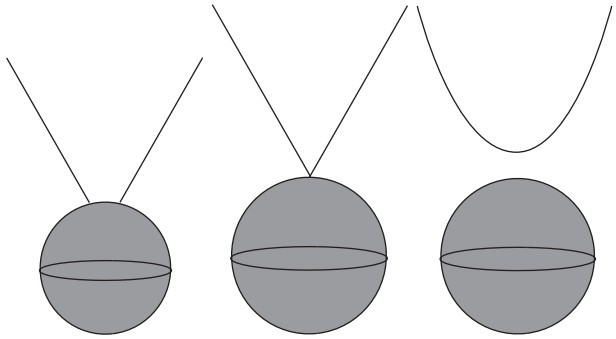

Figure 9: In the vanishing electric field limit, the D-brane (denoted by the curves above) can stay above the black hole (right-most) and fall into the black hole (left-most). These two phases are separated by a critical embedding, corresponding to the middle one.

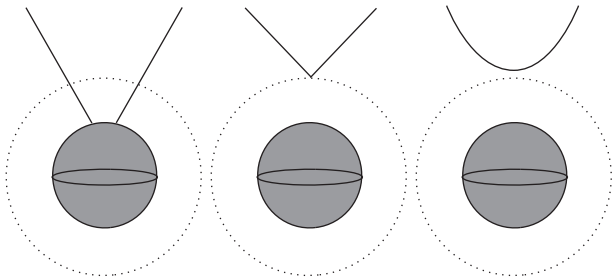

Figure 10: With a nonvanishing electric field, the new radial location r_* emerges, which is shown as the dashed circular curve above. In this case, also, the embedding functions can be divided into two categories, separated by a critical one. The critical curve is subtle to define, since the conical singularity in the critical curve of Figure 9 can occur either at the location of the background event horizon, or at r_*. Here, we will choose the latter, which will be further justified later.

by the D7-brane) before the brane can reach the radius r_*. For all our purposes, this radius r_* acts as an event horizon on the D-brane worldvolume, thereby defining a causal structure similar to a black hole in AdS. We will make this connection more precise later.

Geometrically, therefore, there is a close parallel to the purely thermal physics. When there is a black hole present in the background, the probe brane can either fall inside the black hole, or stay above it. This depends on the asymptotic separation between the D3 branes and the D7-branes. This is how a first-order phase transition separates the two phases, as the parameter (m_q/T) is tuned. This is pictorially demonstrated in Figure 9. Now, when the background black hole is absent, but a nonvanishing electric field is excited on the worldvolume, one can identify two inequivalent classes of probe brane profiles. These profiles are distinguished in terms of their boundary condition at the IR, namely:

$$\theta|_{r_{\min}} = \frac{\pi}{2}, \quad \theta'\big|_{r_{\min}} = -\infty, \quad \text{bound state}, \tag{62}$$

$$\theta|_{r_*} = \theta_0, \quad \theta'\big|_{r_*} = -\frac{1}{\widehat{r}_*}\tan\frac{\theta_0}{2}, \quad \text{plasma state}. \tag{63}$$

These boundary conditions are obtained either by regularity of the embedding function, or directly from the equations of motion. Pictorially, this is demonstrated in Figure 10. This transition is discussed in detail in [105, 106], and Figures 9 and 10 are taken from [105]. Having discussed the classical physics, we now turn to analyze the physics of fluctuations of the probe brane sector.

5.1. Fluctuations: Bosonic Sector. The D7-brane fluctuations correspond to the meson operators in the dual $\mathcal{N} = 2$ field theory. For example, the scalar meson operators are given by the following. (In reviewing this section, we follow the discussions in [107].)

$$\mathcal{O}^{A\ell}_{\text{scalar}} = \overline{\psi}_i \sigma^A_{ij} X^\ell \psi_j + \overline{q}^m X^A_V X^\ell q^m, \quad i,m = 1,2. \tag{64}$$

These operators have a conformal dimension $\Delta = 3 + \ell$. Here, $\sigma^A = (\sigma_1, \sigma_2)$ is the Pauli matrices doublet, while X^A_V, q^m, ψ_i are defined in Table 1. Also, X^ℓ denotes the symmetric traceless operator $X^{\{i_1 \cdots i_\ell\}}$ of ℓ adjoint scalars X^i, for $i = 4,5,6,7$. The mesonic operators, $\mathcal{O}^{A\ell}_{\text{scalar}}$, transform in the $(\ell/2, \ell/2)$ of the SO(4) and have +2 charge under the $\text{SO}(2) \equiv \text{U}(1)_R$.

To obtain the fluctuation action, we can expand (55) around the classical profile discussed above:

$$\begin{aligned} \theta &= \theta^{(0)} + \delta\theta, \\ \phi &= \phi^{(0)} + \delta\phi, \end{aligned} \tag{65}$$

$$f_{ab} = f^{(0)}_{ab} + \delta f_{ab}, \tag{66}$$

where all the fluctuations $\delta\theta$, $\delta\phi$, and δf_{ab} depend on all the worldvolume coordinates of the D7-brane. In general, the fluctuations can be coupled and therefore quite complicated to analyze. Substantial simplification occurs at $\theta_0(r) = 0$, which corresponds to the massless case. Also, we can consistently truncate the fluctuations oscillating only along the Minkowski-directions.

With these, the effective scalar and vector fluctuation actions are given by

$$\begin{aligned} &S_{\text{scalar}} \\ &= -T_{\text{D7}} \int d^8\xi \sqrt{-\det E^{(0)}}\, \frac{1}{2} \mathcal{S}^{ab} \left[G_{\theta\theta} \left(\partial_a \delta\theta\right) \left(\partial_b \delta\theta\right) \right], \end{aligned} \tag{67}$$

$$\begin{aligned} &S_{\text{vector}} \\ &= -T_{\text{D7}} \int d^8\xi \sqrt{-\det E^{(0)}}\, \frac{1}{4} \mathcal{S}^{aa'} \mathcal{S}^{bb'} \left(\delta f_{a'b}\right) \left(\delta f_{b'a}\right). \end{aligned} \tag{68}$$

Here the emergent metric $\mathcal{S}$ is given by

$$\mathcal{S} = \mathcal{S}_{tx^1u} \otimes \mathcal{S}_{x^2x^3} \otimes \mathcal{S}_{S^3}, \tag{69}$$

where $\mathcal{S}_{x^2x^3}$ is identical to the metric components in that plane and $\mathcal{S}_{S^3}$ is given by metric components along the S^3. The components of $\mathcal{S}$ in the $\{t, x^1 \equiv x, u\}$-plane are given by

$$\begin{aligned}
\mathcal{S}_{tt} &= G_{tt} + \frac{E^2}{G_{xx}}, \\
\mathcal{S}_{tu} &= \frac{Ea'}{G_{xx}} = \mathcal{S}_{ut}, \\
\mathcal{S}_{xx} &= \frac{E^2}{G_{tt}} + G_{xx} + \frac{a'^2}{g_{uu}}, \\
\mathcal{S}_{uu} &= g_{uu} + \frac{a'^2}{G_{xx}},
\end{aligned} \tag{70}$$

$$g_{uu} = G_{uu} + \theta'^2 G_{\theta\theta}. \tag{71}$$

This metric $\mathcal{S}$ is known as the open string metric [108], which we will elaborate on subsequently. Evidently, there is no reason that the background geometry, denoted by G, and the emergent metric $\mathcal{S}$ have the same causal structure. We will discuss some generic features of this emergent metric; however, for now, let us calculate the fermionic part of the action.

5.2. Fluctuations: Fermionic Sector. The fermionic fluctuations of the D7-brane correspond to the supersymmetric partners of the mesonic operators, discussed in the previous section. These operators are of two types. (Here also we follow the discussions in [107].)

$$\mathcal{F}^{\ell}_{\alpha} \sim \overline{q} X^{\ell} \widetilde{\psi}^{\dagger}_{\alpha} + \widetilde{\psi}_{\alpha} X^{\ell} q, \tag{72}$$

$$\mathcal{G}^{\ell}_{\alpha} \sim \overline{\psi}_i \sigma^A_{ij} \lambda_{\alpha B} X^{\ell} \psi_j + \overline{q}^m X^A_V \lambda_{\alpha B} X^{\ell} q^m, \quad A, B = 1, 2, \tag{73}$$

with conformal dimensions $\Delta = 5/2 + \ell$ and $\Delta = 9/2 + \ell$. The quadratic order fluctuation action is somewhat involved in explicit form, and therefore we will simply write down the final massaged from, obtained in [109], which is given by

$$S_{\text{spinor}} = \frac{T_{\text{D7}}}{2} \int d^8\xi \sqrt{-\det E^{(0)}} \left[\overline{\Psi}\gamma^a D_a \Psi - \mathcal{M}\overline{\Psi}\Psi\right], \tag{74}$$

$$\left\{\gamma^a, \gamma^b\right\} = 2\mathcal{S}^{ab}, \tag{75}$$

where $\mathcal{M}$ is a mass matrix which we do not specify here. The corresponding equation of motion is

$$\gamma^a D_a \Psi - \mathcal{M}\Psi = 0. \tag{76}$$

It is clear that the fluctuation equation for the fermionic sector also couples to the effective metric $\mathcal{S}$, which couples to the scalar and the vector fluctuations in the bosonic sector. These equations can be subsequently solved for the spectrum. It can already be said that the spectrum will have a quasinormal mode spectrum, analogous to a black hole geometry, when $\mathcal{S}$ contains an event horizon. It turns out that, with a nonvanishing electric field on the classical probe profile, the metric $\mathcal{S}$ indeed inherits an event horizon at r_*, which governs an effective thermal spectrum.

5.3. Open String Metric: Some Features. It is clear that the fluctuations in the D-brane, *i.e.,* the degrees of freedom living on the probe, couple to the same emergent metric. This hints towards an *open string equivalence principle* of the probe sector. Let us now discuss some generic features of the emergent open string metric, based on the examples above. The nontrivial structure exists in the $\{t, u, x\}$-subspace. Here the line-element is given by

$$\begin{aligned}
ds^2_{\text{eff}} &= \mathcal{S}_{tt}dt^2 + 2\mathcal{S}_{ut}dudt + \mathcal{S}_{uu}du^2 + \mathcal{S}_{xx}dx^2 \\
&= \mathcal{S}_{tt}d\tau^2 + \left(\mathcal{S}_{uu} - \frac{\mathcal{S}^2_{ut}}{\mathcal{S}_{tt}}\right)du^2 + \mathcal{S}_{xx}dx^2,
\end{aligned} \tag{77}$$

where we have redefined the time coordinate

$$t = \tau + h(u), \quad \text{where } h'(u) = \frac{\mathcal{S}_{ut}}{\mathcal{S}_{tt}}. \tag{78}$$

The full metric, hence, is given by

$$\begin{aligned}
ds^2_{\text{osm}} &= -\frac{u^2}{R^2}\left(f - \frac{E^2R^4}{u^4}\right)d\tau^2 + \gamma_{uu}du^2 + \gamma_{xx}dx^2 \\
&\quad + \frac{u^2}{R^2}dx^2_{\perp} + R^2\cos^2\theta d\Omega^2_3,
\end{aligned} \tag{79}$$

$$\begin{aligned}
f(u) &= 1 - \frac{u^4_H}{u^4}, \\
dx^2_{\perp} &= dx^2_2 + dx^2_3.
\end{aligned} \tag{80}$$

For brevity, we do not explicitly write down the expressions for γ_{uu}, γ_{xx}. The background in (79) is asymptotically AdS, and in the IR, it has an event horizon. This is similar to AdS-BH geometry. However, (79) has a u-dependent curvature scalar and a singularity at $u = 0$. This singularity is present event in the $u_H = 0$ limit and is solely supported by the worldvolume gauge field E.

With $\theta_0 = 0$ and $u_H = 0$, (79) takes a simpler form:

$$\begin{aligned}
ds^2_5 &= -\frac{u^2}{R^2}\left(1 - \frac{E^2R^4}{u^4}\right)d\tau^2 + \frac{R^2u^4}{u^6 - J^2R^6}du^2 \\
&\quad + \frac{u^4}{R^2}\frac{E^2R^4 - u^4}{J^2R^6 - u^6}dx^2 + \frac{u^2}{R^2}dx^2_{\perp}.
\end{aligned} \tag{81}$$

Here we have suppressed the S^3-directions. Given this geometry, we can easily check some global features, such as the status of energy conditions. For this, let us choose the null vector: $n_\mu = (n_\tau, 1, 0, 0, 0)$ with $n^2_\tau = (-g^{xx}/g^{\tau\tau})$. It can be checked that $\mathcal{E}_{\mu\nu}n^\mu n^\nu < 0$, where $\mathcal{E}_{\mu\nu}$ is the Einstein tensor corresponding to the metric (81). On physical grounds, this is not unexpected and in keeping with the idea that such an emergent geometry can not be obtained from any low energy closed string sector. Thus, this is an intrinsic open string description.

An effective temperature can be defined from the metric in (81): by Euclidean continuation of $\tau \longrightarrow i\tau_E$, periodically

compactifying the τ_E direction and demanding Euclidean regularity yield

$$T_{\text{eff}} = \sqrt{\frac{3}{2}}\frac{\sqrt{E}}{\pi R}, \quad \text{with } u_H = 0, \tag{82}$$

$$T_{\text{eff}} = \frac{1}{2\pi R}\frac{\left(6E^2 + 4(\pi TR)^4\right)^{1/2}}{\left(E^2 + (\pi TR)^4\right)^{1/4}}, \quad T = \frac{u_H}{\pi R^2}, \tag{83}$$

It is clear from the above formulae that $T_{\text{eff}} > T$. While the closed string low energy sector measures a temperature T, the corresponding open string sector measures T_{eff}. The system is, thus, inherently nonequilibrium. However, in the $N_f \ll N_c$ limit, any heat exchange is suppressed and an equilibrium-like description holds. Note that (82) and (83) correspond to the massless case: $\theta_0 = 0$. When $m_q \neq 0$, the general formula is obtained in, *e.g.,* [110].

Let us go back to (81). The similarity of the causal structure with a black hole can be established by going through a set of coordinate transformations that finally describes (81) is a Kruskal-type patch. Focussing on the near-horizon region, this can be achieved by

$$\begin{aligned} \alpha_* &= \alpha + 2M\log\left|\frac{\alpha - 2M}{2M}\right|, \\ v &= \tau' + \alpha_*, \\ u &= \tau' - \alpha_*, \\ U &= -e^{-u/4M}, \\ V &= e^{v/4M}. \end{aligned} \tag{84, 85}$$

The metric in (81), in the $\{\tau, u\}$-plane, can be written as

$$ds^2_{\text{osm}} = -\frac{32M^3}{\alpha}e^{-\alpha/2M}dUdV + ds^2_{\perp}. \tag{86}$$

For our purposes, $ds^2_{\perp}$ will play no role. Correspondingly Kruskal-Szekres time and radial coordinates can be defined as $t_K = V + U$, $x_K = V - U$. Thus, a Penrose diagram can be drawn which schematically takes the form in Figure 11. Finally, consider the $\tau' = \text{const}$ hypersurfaces in the Kruskal patch. In the following coordinate system,

$$\begin{aligned} ds^2_{\text{osm}} &= -\left(\frac{1 - M/2\beta}{1 + M/2\beta}\right)^2 d\tau'^2 + \left(1 + \frac{M}{2\beta}\right)^4 d\beta^2 \\ &\quad + ds^2_{\perp}, \\ \alpha &= \left(1 + \frac{M}{2\beta}\right)^2 \beta, \end{aligned} \tag{87}$$

the $\tau' = \text{const}$ hypersurfaces are simply $\mathbb{R}_\beta \otimes \mathbb{R}_x \otimes \mathbb{R}^2$. Nevertheless, for a given α, there are two roots of β, which are related by the symmetry: $\beta \longrightarrow M^2/4\beta$. The corresponding two regions, parametrized by the two roots of β, are connected by a constant-size Einstein-Rosen bridge. All these features are very similar to a standard black hole geometry.

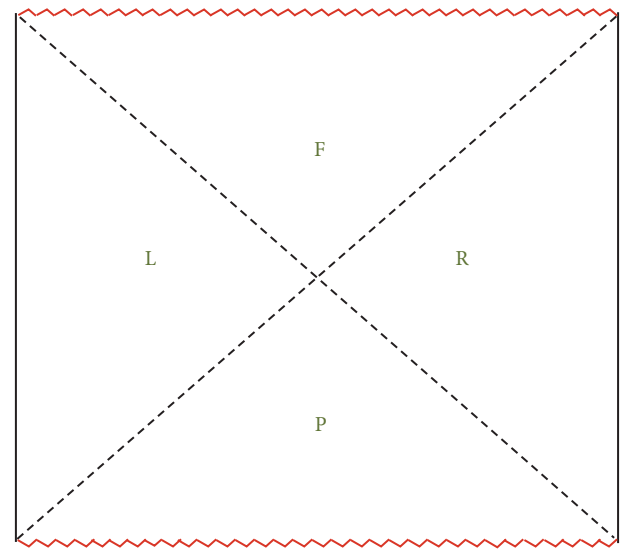

Figure 11: A qualitative picture of the Kruskal extension of the open string metric. We have drawn the Penrose diagram in a "square" form, which is not strictly correct. We will elaborate more on the Penrose diagram in later sections. This diagram is taken from [109].

6. D-Brane Description: A Different Model

It is possible to further construct explicit examples of such probe brane configurations, in a background geometry. Since such constructions can be varied in richness, we will not attempt to provide a classification; rather we will present another explicit and instructive example. In this case, we are motivated by the analytical control the model provides us with. We begin with the standard $\text{AdS}_5 \times \mathscr{M}_5$, where $\mathscr{M}_5$ is some Einstein manifold (Sasaki-Einstein, if we want to preserve, at least, $\mathcal{N} = 1$ supersymmetry). Let us choose $\mathscr{M}_5 \equiv S^5$. The probe degrees of freedom are now introduced by adding an N_f D5-branes, as shown in Table 2. In Table 2, the notation $-$ stands for a direction along the worldvolume of the brane and X represents the directions transverse to it. The directions $\{0, 1, 2, 3\}$ represent the Minkowski directions. The rest of the directions are an $\mathbb{R}^6$ transverse to the stack of D3-branes. The D3-branes are extended along the Minkowski directions, and let us split $\mathbb{R}^6 \equiv \mathbb{R}^3 \times \mathbb{R}^3$. Now, let us use $\{\rho, \Omega_2\}$ and $\{\ell, \widetilde{\Omega}_2\}$ to represent the two $\mathbb{R}^3$'s. Thus, $\{4, 5, 6\}$ corresponds to $\{\rho, \Omega_2\}$ and $\{7, 8, 9\}$ represents $\{\ell, \widetilde{\Omega}_2\}$. This configuration, which preserves eight real supercharges, was studied initially in [111, 112], from the perspective of analyzing a defect CFT system. The degrees of freedom are an adjoint vector multiplet and a hypermultiplet coming from the D3-branes in $(3 + 1)$-dimensions. The probe D5 sector yields a $(2 + 1)$-dimensional hypermultiplet in the fundamental representation.

The geometry is given by

$$ds^2 = ds^2_{\text{AdS}_5} + ds^2_{S^5}, \tag{88}$$

$$ds^2_{S^5} = R^2\left(d\psi^2 + \cos^2\psi d\Omega_2^2 + \sin^2\psi d\widetilde{\Omega}_2^2\right), \tag{89}$$

Table 2: Fundamental sector introduced in the background of N_c D3-branes.

Brane	0	1	2	3	4	5	6	7	8	9
(N_c) D3	–	–	–	–	X	X	X	X	X	X
(N_f) D5	–	–	–	X	–	–	–	X	X	X

$$\rho = u\cos\psi, \qquad \ell = u\sin\psi. \tag{90}$$

The D5-brane embedding function can be parametrized by a single function: $\psi(u)$. We assume that $P[\widetilde{\Omega}_2] = 0$, where $\widetilde{\Omega}_2$ denotes the metric components which yield the line element $d\widetilde{\Omega}_2^2$. As in the previous case, there are distinct families of embedding which correspond to different physics in the probe sector. Also, the analysis becomes simple when the fundamental sector is massless. This corresponds to setting $\psi = 0$. The induced worldvolume metric is simply an $AdS_4 \times S^2$.

To study a nontrivial dynamics of the D5-brane, we can excite a similar U(1)-flux on the worldvolume. The corresponding fluctuation analysis, by virtue of the open string equivalence principle, exhibits a similar coupling with the open string metric. (One can explicitly check this to be true. See, for example, [100, 113] for a brief discussion on this, and [100] for an explicit calculation of the same.) The metric is given by

$$ds_{\text{eff}}^2 = -\frac{u^2}{R^2}\left(f - \frac{E^2R^4}{u^4}\right)d\tau^2 + \gamma_{xx}dx^2 + \gamma_{uu}du^2 + \frac{u^2}{R^2}dy^2 + \cos^2\psi d\Omega_2^2, \tag{91}$$

$$f = 1 - \frac{u_H^4}{u^4}. \tag{92}$$

Again, we do not explicitly write down the expressions of γ_{xx} and γ_{uu}. On the embedding $\psi(u) = 0$, the open string metric in (91) yields $AdS_4 \times S^2$ when both $u_H = 0$ and $E = 0$, or asymptotically. The IR-behaviour is different from an AdS_4-BH, since the functional form of $f(u)$ is different here. Also, demanding positivity of γ_{xx} readily yields the expectation value of the current in the dual gauge theory. (In this case, one gets $j = ER^2$, independent of the background temperature $T = u_H/(\pi R^2)$.) The corresponding effective temperature is now given by

$$T_{\text{eff}} = \left(T^4 + \frac{E^2}{\pi^2R^4}\right)^{1/4}, \quad T = \frac{u_H}{\pi R^2}. \tag{93}$$

The near-horizon geometry has a similar structure as a black hole and a corresponding Penrose diagram can be drawn. Further note that, due to a substantial analytical control of this system, in [113], current-current correlation function, in the probe sector, was explicitly calculated. This correlation function turns out to possess a thermal behaviour with a temperature T_{eff}. In particular, this effective temperature appears in the fluctuation-dissipation relation. For other (scalar or fermionic) sectors, even though analytical calculations may not be feasible, because of the open string equivalence principle, a similar behaviour is expected.

Further note that this thermal imprint continues to hold beyond standard 2-point functions. In [99, 100], a four-point out-of-time order (OTOC) correlator is explicitly calculated in the same vector sector discussed in [113]. This OTOC exhibits an exponential growth with real-time and a Lyapunov exponent which satisfies the maximal chaos bound: $\lambda_L = 2\pi T_{\text{eff}}$. This bound is shown to hold for a generic system and is expected to saturate for systems with large number of degrees of freedom with a gravity dual. From a gravitational perspective, this saturation is universally described by the near-horizon dynamics of a black hole. In our case, a similar statement holds true for a geometry with a causal structure which is similar to a black hole.

Continuing on this theme, we can explicitly construct other examples where the adjoint matter sector is not described by a CFT, unlike the $\mathcal{N} = 4$ SYM. Such gauge theories can be constructed by considering the near-horizon dynamics of the Dp-branes with $p \neq 3$. We will, however, not explicitly discuss such examples, but point the reader to, *e.g.,* Sakai-Sugimoto model considered in [114, 115].

7. Branes in Spacetime: A General Description

In this section, we will discuss the essential physics, without referring to any explicit example. The basic idea is as follows: Given a low energy closed string data, in string frame, $\{G, B, \phi\}$, where G is the metric, B is the NS-NS 2-form, and ϕ is the dilaton, along with the RR sector fluxes, the geometry is essentially described by a solution of type II supergravity. In this ten-dimensional background, we imagine describing a defect D-brane, as an embedded hypersurface. This hypersurface spontaneously breaks translational symmetry of the background and the corresponding low energy sector is described by the so-called DBI action, along with Wess-Zumino terms. The latter is topological in nature and will not affect directly our discourse and therefore let us ignore such terms. The background RR-fluxes couple only to this topological sector and therefore we can ignore them for our discussions.

The essential dynamics is given by the following action, in the notation of [116]:

$$S_{\text{DBI}} = T_{\text{D}q}\int d^{q+1}\xi e^{-\phi}\sqrt{-\det\left[P\left[G+B\right] + \left(2\pi\alpha' F\right) + i\overline{\psi}\gamma\nabla\psi\right)} + \dots, \tag{94}$$

where $T_{\text{D}q}$ encodes the tension of the brane and F is the U(1)-flux on the worldvolume of the brane. The action also

contains fermionic degrees of freedom, denoted by ψ, which can be completely fixed by demanding supersymmetry of the bosonic DBI action. Here, γ denotes a gamma-matrix and ∇ is an appropriately constructed covariant derivative. For our purpose, this schematic description suffices.

Around a classical saddle of (94), there are three kinds of fluctuations modes: (i) scalar, (ii) vector, and (iii) spinor. Schematically, these fluctuations can be written as

$$X^{\mu} = X^{\mu}_{(0)} + \varphi^{i}\delta^{i}_{\mu}, \tag{95}$$

$$F_{ab} = F^{(0)}_{ab} + \mathscr{F}_{ab}, \quad \psi_{a}, \tag{96}$$

where the classical saddle is described by the data $\{X^{\mu}_{(0)}, F^{(0)}_{ab}\}$. Here μ, ν run over the entire spacetime directions, a, b run over the worldvolume directions, and i, j run over the directions transverse to the D-brane. In the scalar sector, we consider only the transverse fluctuations since longitudinal fluctuations can be gauged away by using worldvolume diffeomorphism. The Volkov-Akulov type fermionic terms are defined with gamma matrices of the following algebra:

$$\{\gamma_{a}, \gamma_{b}\} = P\left[G\right]_{ab}. \tag{97}$$

To calculate fluctuations around the saddle $\{X^{\mu}_{(0)}, F^{(0)}_{ab}\}$, one needs to invert the matrix $M = P[G + B] + (2\pi\alpha' F)$. This inversion yields [108]

$$M^{ab} = \left(\left(P\left[G+B\right] + \left(2\pi\alpha' F\right)\right)^{-1}\right)^{ab} = \mathcal{S}^{ab} + \mathscr{A}^{ab}, \tag{98}$$

where

$$\mathcal{S}^{ab} = \left(\frac{1}{P\left[G+B\right] + \left(2\pi\alpha' F^{(0)}\right)} \cdot P\left[G\right] \cdot \frac{1}{P\left[G-B\right] - \left(2\pi\alpha' F^{(0)}\right)}\right)^{ab}, \tag{99}$$

$$\mathcal{S}_{ab} = P\left[G\right]_{ab} - \left(F^{(0)} \cdot P\left[G\right]^{-1} \cdot F^{(0)}\right)_{ab}, \tag{100}$$

$$\mathscr{A}^{ab} = -\left(\frac{1}{P\left[G+B\right] + \left(2\pi\alpha' F^{(0)}\right)} \cdot F^{(0)} \cdot \frac{1}{P\left[G-B\right] - \left(2\pi\alpha' F^{(0)}\right)}\right)^{ab}. \tag{101}$$

Finally, the quadratic fluctuation Lagrangians are obtained as

$$\mathscr{L}_{\text{scalar}} = -\frac{\kappa}{2} e^{-\phi}\sqrt{-\det M}\,\mathcal{S}^{ab}\partial_{a}\varphi^{i}\partial_{b}\varphi^{i} + \ldots, \tag{102}$$

$$\mathscr{L}_{\text{vector}} = -\frac{\kappa}{4} e^{-\phi}\sqrt{-\det M}\,\mathcal{S}^{ab}\mathcal{S}^{cd}\mathscr{F}_{ac}\mathscr{F}_{bd} + \ldots, \tag{103}$$

$$\mathscr{L}_{\text{spinor}} = i\kappa e^{-\phi}\sqrt{-\det M}\,\overline{\psi}\mathcal{S}^{ab}\Gamma_{a}\nabla_{b}\psi + \ldots, \tag{104}$$

where

$$\Gamma^{a} = \left(\mathcal{S}^{ab} + \mathscr{A}^{ab}\right)\gamma_{b} \Longrightarrow \left\{\Gamma^{a}, \Gamma^{b}\right\} = 2\mathcal{S}^{ab}. \tag{105}$$

The indies above are raised and lowered with the metric G, as usual. Therefore, corresponding to two different metrics G and $\mathcal{S}$, we have two inequivalent causal structures. Note that such a possibility has already been discussed in the literature in [117, 118], irrespective of holography. We will now discuss some specific aspects of this open string metric, in more detail.

7.1. Event Horizons: Some Comments. In [116], a general formula for T_{eff} was obtained. This is the effective temperature that the probe sector measures. In general, one always observes $T_{\text{eff}} > T$; however there are known exceptions, such as [55]. Let us now consider a general case, exciting other fluxes on the worldvolume. Depending on the flux, this can correspond to turning on a chemical potential in the dual gauge theory (in the probe sector) and/or introducing a constant magnetic field. (See, *e.g.*, [105, 106, 119, 120] for a detailed discussion of such physics in the D3-D7 system and [114, 115, 121–123] for similar physics in the Sakai-Sugimoto model.)

In general, we can arrange the electric and the magnetic field to be (i) parallel or (ii) perpendicular. Assume that we have an $\mathbb{R}^{1,3}$-submanifold as the conformal boundary, where the dual gauge theory is defined. Consider, now, the case when (i) $E \parallel B$. The corresponding ansatz is

$$f = -E dt \wedge dx^{1} - a'_{x} dx^{1} \wedge du - B dx^{2} \wedge dx^{3} + a'_{t} dt \wedge du, \tag{106}$$

where $a_{x}(u)$ contains the information about the gauge theory current and $a_{t}(u)$ contains the information about the chemical potential. The open string metric can be obtained as

$$ds^{2}_{\text{eff}} = \left(\mathcal{S}_{tt} - \frac{\mathcal{S}^{2}_{tx}}{\mathcal{S}_{xx}}\right)d\tau^{2} + \left(\frac{\mathcal{S}_{tx}}{\sqrt{\mathcal{S}_{xx}}}d\tau + dX\right)^{2} + \mathcal{S}_{\perp}dx^{2}_{\perp} + \left(\frac{\mathcal{S}^{2}_{tx}\mathcal{S}_{uu} - 2\mathcal{S}_{tu}\mathcal{S}_{tx}\mathcal{S}_{ux} + \mathcal{S}_{tt}\mathcal{S}^{2}_{ux} - \mathcal{S}_{tt}\mathcal{S}_{uu}\mathcal{S}_{xx}}{\mathcal{S}^{2}_{tx} - \mathcal{S}_{tt}\mathcal{S}_{xx}}\right)du^{2}, \tag{107}$$

$$dt = d\tau - \frac{\mathcal{S}_{tx}\mathcal{S}_{ux} - \mathcal{S}_{tu}\mathcal{S}_{xx}}{\mathcal{S}^{2}_{tx} - \mathcal{S}_{tt}\mathcal{S}_{xx}}du, \tag{108}$$

$$dx^{1} = \frac{dX}{\sqrt{\mathcal{S}_{xx}}} - \frac{\mathcal{S}_{tu}\mathcal{S}_{tx} - \mathcal{S}_{tt}\mathcal{S}_{ux}}{\mathcal{S}^{2}_{tx} - \mathcal{S}_{tt}\mathcal{S}_{xx}}du, \tag{109}$$

with

$$\mathcal{S}_{\perp} = G_{xx} + \frac{B^{2}}{G_{xx}}, \qquad dx^{2}_{\perp} = \left(dx^{2}\right)^{2} + \left(dx^{3}\right)^{2}, \tag{110}$$

and

$$\begin{aligned}
\mathcal{S}_{tt} &= G_{tt} + \frac{E^2}{G_{xx}} + \frac{a_t'^2}{G_{uu}},\\
\mathcal{S}_{tx} &= \frac{a_t' a_x'}{G_{uu}},\\
\mathcal{S}_{tu} &= \frac{E a_x'}{G_{xx}},\\
\mathcal{S}_{xx} &= G_{xx} + \frac{E^2}{G_{tt}} + \frac{a_x'^2}{G_{uu}},\\
\mathcal{S}_{uu} &= G_{uu} + \frac{a_t'^2}{G_{tt}} + \frac{a_x'^2}{G_{uu}}.
\end{aligned} \tag{111, 112}$$

The location of the open string metric event-horizon is given by

$$\begin{aligned}
&\mathcal{S}_{tx}^2 - \mathcal{S}_{tt}\mathcal{S}_{xx} = 0 \Longrightarrow\\
&\widetilde{d}^2 e^{2\phi} G_{tt} + G_{xx}\left(B^2 G_{tt} + G_{tt}G_{xx}^2 + e^{2\phi} j^2\right)\Big|_{u_*} = 0 \Longrightarrow\\
&G_{tt}G_{xx} + E^2\Big|_{u_*} = 0,
\end{aligned} \tag{113}$$

with the following definitions:

$$\begin{aligned}
j &= \frac{\partial \mathcal{L}_{\mathrm{DBI}}}{\partial a_x'},\\
\widetilde{d} &= \frac{\partial \mathcal{L}_{\mathrm{DBI}}}{\partial a_t'}.
\end{aligned} \tag{114}$$

From the boundary gauge theory perspective, the fundamental sector current is proportional to j and the charge density is, up to an overall constant, given by $\widetilde{d}$. As before, the expectation value of the current can be determined by imposing regularity on the OSM metric. Note that a corresponding membrane-paradigm description, for computing transport properties of the dual gauge theory, was developed and explored in [110]. Along similar lines, one can explore the case when (ii) $E \perp B$. In this case, an additional Hall current flows, which was analyzed in, *e.g.,* [124].

7.2. Ergoplane: A Special Feature. The open string metric can also contain an "ergoplane" and therefore similar related black hole physics. This is explicitly demonstrated with the D3-D7 system in [110]. To see this, we excite a chemical potential. By setting $B = 0$ in (107), one obtains

$$\begin{aligned}
ds_{\mathrm{eff}}^2 &= \left(G_{tt}G_{xx} + E^2\right)\left[\frac{dT^2}{G_{xx}} + \frac{dX^2}{G_{xx}}\right]\\
&\quad + \frac{1}{G_{uu}}\left(a_t' dT + a_x' dX\right)^2 + \sum_{i=2}^{m} G_{xx} dx^i dx^i\\
&\quad + \left(G_{uu} + \frac{a_t'^2 G_{tt} + a_x'^2 G_{xx}}{G_{tt}G_{xx} + E^2}\right) du^2,
\end{aligned} \tag{115}$$

$$\begin{aligned}
dT &= dt + \frac{E a_x'}{G_{tt}G_{xx} + E^2} du,\\
dX &= dx - \frac{E a_t'}{G_{tt}G_{xx} + E^2} du.
\end{aligned} \tag{116}$$

The event horizon is located at $(G_{tt}G_{xx} + E^2) = 0$, and the ergoplane is located at

$$\begin{aligned}
&\frac{G_{tt}G_{xx} + E^2}{G_{xx}} + \frac{a_t'^2}{G_{uu}} = 0 \Longrightarrow\\
&\left(G_{tt}G_{xx} + E^2\right) = 0,\\
&\text{or } \left(G_{tt}G_{xx}^m + e^{2\phi} j^2\right) = 0.
\end{aligned} \tag{117}$$

This directly yields a root $u_{\mathrm{erg}} \neq u_*$. As before, j^2 is determined from a simple algebraic equation: $\widetilde{d}^2 e^{2\phi} G_{tt} + (G_{tt}G_{xx}^m + e^{2\phi} j^2) G_{xx}|_{u_*} = 0$.

Let us take a simple example, with the background if given by an AdS_{d+2}, with a vanishing dilaton. One then obtains

$$u_{\mathrm{erg}}^2 = ER^2\left(1 + \frac{\widetilde{d}^2}{E^d}\right)^{1/d} > u_*^2 = ER^2. \tag{118}$$

The event horizon and the ergoplane merge in the limit $(\widetilde{d}^2/E^d) \longrightarrow 0$ and/or $(1/d) \longrightarrow 0$. (The same statement holds for an AdS_{d+2}-BH background geometry as well.)

7.3. Exactly Solvable Toy Models: More Examples. In addition to the explicit D-brane constructions that have been discussed before, here we briefly mention some examples in which explicit analytical calculations can be performed, to arrive at the same conclusion. These are the so-called Lifshitz background of the following form:

$$ds^2 = -\frac{dt^2}{v^{2z}} + \frac{1}{v^2}\vec{dx}^2 + \frac{dv^2}{v^2}, \tag{119}$$

where $\vec{x}$ is a 2-dimensional vector and v is the radial coordinate ($v \longrightarrow 0$ corresponds to boundary and $v \longrightarrow \infty$ corresponds to the deep-IR). As before, we can consider a similar DBI-dynamics in the (119), with a worldvolume flux: $a_x = -Et + h(v)$. One readily obtains an equation of motion for the function $h(v)$, which can be solved in terms of a first

integral of motion. As before, this first integral of motion can be subsequently determined in terms of $e = (2\pi\alpha')E$.

Around this classical saddle, we consider fluctuations which yield

$$S_{\text{gauge}} = -\frac{1}{4}\int dt d^d x \sqrt{-\det(G+f)}\,\mathcal{S}^{aa'}\mathcal{S}^{bb'}\delta f_{ab}\delta f_{a'b'}, \tag{120}$$

where δf denotes gauge field fluctuations. This action results in the following equation of motion:

$$\partial_a\left[\sqrt{-\det(G+f)}\,\mathcal{S}^{aa'}\mathcal{S}^{bb'}\delta f_{a'b'}\right] = 0. \tag{121}$$

In the $\{t, v\}$-plane the corresponding OSM is given by

$$ds^2 = -\frac{g(v)}{v^{2z}}d\tau^2 + \frac{1}{g(v)}\frac{dv^2}{v^2}, \tag{122}$$

$$g(v) = 1 - e^2 v^{2z+2},$$

$$\tau = t + s(v),$$

$$\frac{ds}{dv} = -\frac{e^2 v^{1+3z}}{1 - e^2 v^{2z+2}} \tag{123}$$

With the following ansatz:

$$\delta a_\tau = \delta a_\tau(v)\, e^{-i\omega\tau},$$

$$\delta a_i = \delta a_i(v)\, e^{-i\omega\tau}, \tag{124}$$

some explicit solutions, with purely ingoing boundary condition, can be obtained as follows:

$$z = \frac{1}{2},$$

$$\delta a_x(v) = c_x\left(\frac{1-\sqrt{v}}{1+\sqrt{v}}\right)^{-i\omega/3}\left(\frac{1-\sqrt{v}+v}{1+\sqrt{v}+v}\right)^{-i\omega/6} \cdot \exp\left(\frac{i\omega}{\sqrt{3}}\arctan\left[\frac{\sqrt{3}v}{1-v}\right]\right), \tag{125}$$

$$z = 1,$$

$$\delta a_x(v) = c_x\left(\frac{1-v}{1+v}\right)^{-i\omega/4}\exp\left(\frac{i\omega}{2}\arctan(v)\right). \tag{126}$$

$$z = 2,$$

$$\delta a_x(v) = c_x\left(1-v^2\right)^{-i\omega/6}\left(1+v^2+v^4\right)^{i\omega/12} \cdot \exp\left(\frac{i\omega}{2\sqrt{3}}\arctan\left(-\frac{\sqrt{3}}{1+v^2}\right)\right). \tag{127}$$

Here c_x is a constant. Using these explicit solutions, we calculate, *e.g.,* two-point correlator, similar to [113]. As a result, we get a fluctuation-dissipation relation, with an effective temperature: $T_{\text{eff}} = ((z+1)/\pi)e^{z/(z+1)}$. While this is not surprising, it adds more explicit evidence to the theme.

7.4. The Probe Limit: Validity. Our entire discussion is based on the probe limit. Since this is a crucial ingredient in our construction, let us briefly review what this entails. At the level of the equations of motion, the Einstein tensor of a given solution must be parametrically large compared to the stress-tensor of the probe sector. Consider the decoupling limit of N_c coincident Dp-branes. These, in the string frame, are given by [75]

$$ds^2 = \left(\frac{u}{L}\right)^{(7-p)/2}\left(-dt^2 + d\vec{x}_p^{\,2}\right) + \left(\frac{L}{u}\right)^{(7-p)/2}\left(du^2 + u^2 d\Omega_{8-p}^2\right), \tag{128}$$

$$e^{\phi} = \left(\frac{u}{L}\right)^{(p-3)(7-p)/4}, \tag{129}$$

$$F_{8-p} = (7-p)\,L^{7-p}\omega_{8-p}. \tag{130}$$

Here $d\Omega_{8-p}$ denotes the line element of an $(8-p)$-sphere and ω_{8-p} denotes the corresponding volume form. For these geometries, Einstein tensor behaves as

$$E_{tt} \sim \frac{u^{5-p}}{L^{7-p}} \sim E_{xx},$$

$$E_{uu} \sim \frac{1}{u^2}, \tag{131}$$

$$E_{\alpha\beta} \sim u^0 \eta_{\alpha\beta}.$$

Here α, β run over the gauge theory directions.

Consider N_f-number of probe D$(p+4)$-branes. These span $\{t, \vec{x}_p\}$-directions and wrap three-cycle $\mathcal{X}_3 \subset S^{8-p}$. As before, we excite a U(1)-flux: $A_{x^1} = -Et + a_1(u)$. The probe energy-momentum tensor is given by

$$T_{tt} \longrightarrow \frac{u^2}{L^3} \sim T_{xx} \sim T_{x^1x^1},$$

$$T_{uu} \longrightarrow \frac{1}{u^{5-p}}, \tag{132}$$

$$T_{\alpha\beta} \longrightarrow \frac{1}{u^{3-p}}\eta_{\alpha\beta}$$

$$\text{as } u \longrightarrow \infty,$$

and

$$T_{tt} \longrightarrow (EJ)\,u^{(p-9)/2},$$

$$T_{x^1x^1} \longrightarrow \left(\frac{J}{E}\right)u^{(5-p)/2}, \tag{133}$$

$$T_{xx} \longrightarrow \left(\frac{E}{J}\right)u^{(p+3)/2},$$

$$T_{uu} \longrightarrow (EJ)\,u^{(3p-23)/2},$$

$$T_{\alpha\beta} \longrightarrow \left(\frac{E}{J}\right)u^{(3p-7)/2} \tag{134}$$

$$\text{as } u \longrightarrow 0.$$

A comparison between (131) and (132) establishes validity of the probe limit, except the case with $p = 4$. Similarly, comparing (131) with (134), we conclude that the IR will be heavily modified. In fact, this modification can only be controlled by placing an event horizon in the bulk. Further note that $T_{tt} \sim (E \cdot J)$ has an Ohmic dissipation nature, in terms of the dual gauge theory. Similar conclusions were reached in, *e.g.,* [125, 126].

7.5. Effective Thermodynamics: A Summary. The basic statement of gauge-gravity duality is an equivalence between the bulk gravitational path integral and the dual field theory path integral:

$$\begin{aligned} \mathcal{Z}_{\text{bulk}} &= \mathcal{Z}_{\text{QFT}}, \\ \mathcal{Z}_{\text{bulk}} &= e^{iS_{\text{bulk}}}, \quad S_{\text{bulk}} = S_{\text{grav}} + S_{\text{matter}}, \\ \text{subsequently } \mathcal{Z}_{\text{QFT}} &= e^{iS_{\text{QFT}}}, \\ S_{\text{QFT}} &= S_{\text{gauge}} + S_{\text{matter}}. \end{aligned} \tag{135}$$

In writing the above, we have explicitly assumed that the dual field theory is a gauge theory, with some matter content. When the matter sector consists of probe degrees of freedom, the corresponding path integral factorizes into two parts: $\mathcal{Z}_{\text{bulk}} = \mathcal{Z}_{\text{sugra}}\mathcal{Z}_{\text{sugra}}$. In the $N_c \longrightarrow \infty$ limit, a semi-classical description is viable by considering small perturbations around a classical saddle:

$$\mathcal{Z}_{\text{sugra}} = \int D\left[\delta\phi\right] D\left[\delta G\right] e^{-N_c^2(\mathcal{S}^{(0)}_{\text{sugra}} + \mathcal{S}^{(2)}_{\text{sugra}}[\delta\phi,\delta G]+\ldots)}, \tag{136}$$

where $\mathcal{S}^{(2)}_{\text{sugra}}$ is the quadratic fluctuation term. Similarly, the probe sector also has a semi-classical description. Thus, at the semi-classical level, the entire path integral factorizes into a classical piece and a quadratic fluctuation piece. Schematically, these take the following form [127]:

$$\mathcal{Z}_{\text{classical}} = e^{-N_c^2\mathcal{S}^{(0)}_{\text{sugra}} - g_sN_cN_f\mathcal{S}^{(0)}_{\text{DBI}} - g_sN_f^2\mathcal{S}^{(1)}_{\text{back-reac}}+\cdots}, \tag{137}$$

where g_s is the string coupling and $\mathcal{S}^{(1)}_{\text{back-reac}}$ denotes the backreaction of the probe sector on the classical saddle. Naively, by tuning $N_f \ll N_c$, we can safely ignore the backreaction. Note, however, that this conclusion is subtle to make, as we have already demonstrated in the previous section.

The quadratic fluctuation part can be schematically represented as

$$\begin{aligned} \mathcal{Z}_{\text{fluc}} = &\int D\left[\varphi_{\text{grav}}\right] e^{-N_c^2\mathcal{S}^{(2)}_{\text{sugra}}+\cdots} \\ &\cdot \int D\left[\varphi_{\text{brane}}\right] e^{-g_sN_cN_f\mathcal{S}^{(2)}_{\text{DBI}}+\cdots}, \end{aligned} \tag{138}$$

where φ_{grav} and φ_{brane} represent gravity and brane fluctuation modes, respectively. From this, we can already compare the relative scaling of two-point functions in the gravity and in the brane sectors, which are given by $\langle\varphi_{\text{grav}}\varphi_{\text{grav}}\rangle \sim 1/N_c^2$ and $\langle\varphi_{\text{brane}}\varphi_{\text{brane}}\rangle \sim 1/(N_cN_f)$.

Let us focus on the D-brane sector. In this sector, let us rewrite the generic form of the scalar and vector fluctuations:

$$\begin{aligned} &\mathcal{S}_{\text{scalar}} \\ &= -\frac{\kappa}{2}\int d\xi^8 \left(\frac{\det G}{\det \mathcal{S}}\right)^{1/4} \sqrt{-\det \mathcal{S}}\,\mathcal{S}^{ab}\partial_a\varphi^i\partial_b\varphi^i \\ &\quad + \ldots, \end{aligned} \tag{139}$$

$$\begin{aligned} &\mathcal{S}_{\text{vector}} \\ &= -\frac{\kappa}{4}\int d\xi^8 \left(\frac{\det G}{\det \mathcal{S}}\right)^{1/4} \sqrt{-\det \mathcal{S}}\,\mathcal{S}^{ab}\mathcal{S}^{cd}\mathcal{F}_{ac}\mathcal{F}_{bd} \\ &\quad + \ldots. \end{aligned} \tag{140}$$

Here, κ denotes an overall constant and $\ldots$ represent various interaction terms. The fields φ^i, $\mathcal{F}$ represent the scalar and vector fluctuation modes, respectively. In (139)-(140), $\mathcal{S}$ is the open string metric, which we have defined before. The kinetic term in (139) and (140) can be written in a more canonical form:

$$\begin{aligned} &\sqrt{-\det \widetilde{\mathcal{S}}}\,\widetilde{\mathcal{S}}^{ab}\left(\partial_a\varphi\right)\left(\partial_b\varphi\right), \\ &\text{and } \sqrt{-\det \widetilde{\mathcal{S}}}\,\widetilde{\mathcal{S}}^{ab}\widetilde{\mathcal{S}}^{cd}\mathcal{F}_{ac}\mathcal{F}_{bd}. \end{aligned} \tag{141}$$

The conformal factor Ω needs to be determined for each case, separately.

Before discussing the Euclidean path integral (*i.e.,* the partition function), let us briefly comment on the stress-tensor of the dual field theory. The corresponding data can be represented primarily in terms of the open string metric data, in the following form [128]:

$$\langle T^\mu_\nu\rangle \propto \int due^{\gamma\phi}\left(\frac{\det G}{\det \mathcal{S}}\right)^{1/4}\sqrt{-\det \mathcal{S}}\,\mathcal{S}^\mu_\nu, \tag{142}$$

where γ is a constant and ϕ is the dilaton field and $\mu.\nu$ are the directions along the dual field theory. In [128], several examples were discussed with explicit form of the energy-momentum tensor in the dual field theory.

In the Euclidean patch, the path integral yields a thermodynamic description in terms of a partition function. It is now expected that the probe sector thermodynamics will be simply determined in terms of the effective temperature T_{eff}. However, the entropy, which can be obtained from the partition function itself, is not given in terms of the area of the OSM event horizon. It was also argued in [129] that, in the probe limit, only free energy can be reliably calculated by computing on-shell action in the probe sector. For thermal entropy and such, the contribution coming from backreaction of the defect degrees of freedom mixes with the probe sector contribution.

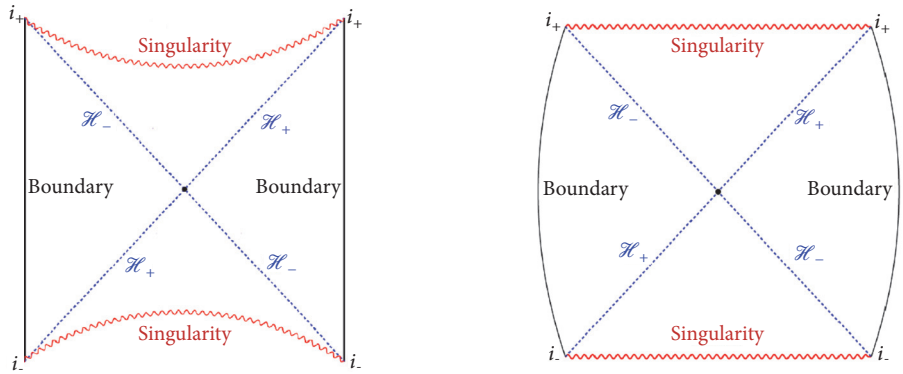

FIGURE 12: Penrose diagram corresponding to an OSM embedded in a purely AdS_3 (a) and a purely AdS_4 (b) background. The black dot at the centre corresponds to the bifurcation surface. In both these cases, there is a singularity denoted by the red curvy line.

For the case in consideration, a proposed thermodynamic free energy was discussed in [130] and subsequently generalized in [116]. The Helmholtz free energy is given by

$$\begin{aligned}\mathcal{F}_{\mathrm{H}} &= T_{\mathrm{eff}} S^{(\mathrm{E})}_{\mathrm{DBI}}\Big|_{\mathrm{on-shell}} \\ &\sim \int_0^{u_*} du d^p\xi \left(\mathcal{L}_{\mathrm{on-shell}} - j a'_x\right).\end{aligned} \tag{143}$$

Here u_* is the OSM event-horizon and $S^{(\mathrm{E})}_{\mathrm{DBI}}$ is the Euclidean DBI action. This is the only extensive quantity that we can define. The free energy, in the special case of AdS_3, contains a universal term of $(T^2_{\mathrm{eff}} - T^2)$, where T_{eff} and T are the probe and the background sector temperatures. Such a term, intuitively, captures the heat exchange across the two systems in a two-dimensional CFT.

Furthermore, the presence of the OSM event horizon and the open string data are

$$\mathcal{S} = G - \left(B \cdot G^{-1} \cdot B\right) \tag{144}$$

$$\mathcal{G}_s = \left(\frac{\det(G+B)}{\det G}\right)^{1/2}, \tag{145}$$

where G denotes the worldvolume metric and B denotes the antisymmetric two-form (with factors of α' absorbed). Here $\mathcal{G}_s$ is the open string coupling [108]. There is a natural geometric area which defines *an entropic quantity*, given by

$$s \sim \frac{1}{\mathcal{G}_s} \mathrm{Area}\,(\mathcal{S})\Big|_{\tau=\mathrm{const}, u=u_*}. \tag{146}$$

However, the physical meaning of this is unclear and it is certainly not the thermal entropy. An intriguing possibility was suggested in [51–53], in which one identifies this entropy with the entanglement entropy of the pair produced in the presence of a strong electric field. Before leaving this section, let us note that a slightly different nonequilibrium thermodynamics has been proposed and explored in [54, 56], in which the prescription is provided in the Lorentzian section of the geometry, unlike in the Euclidean section which we have discussed here.

7.6. Some Causal Features. A detailed analysis of the causal structure of such OSM geometry was discussed in [127]. We will briefly review them here. As simple examples, let us discuss cases when the background is AdS_3 and AdS_4. We imagine a space-filling D-brane (and thus a corresponding DBI-action), with the U(1) flux turned on. The explicit form of the metric is given in [127], and we will only discuss the qualitative physics here. One usually begins with a Poincaré patch description and, by going to a Kruskal extension, eventually ends up with a Penrose diagram. The resulting Penrose diagram for a purely AdS_3 and a purely AdS_4 background is shown in Figure 12. The Penrose diagrams are qualitatively similar to what one obtains by solving Einstein gravity with an AdS asymptotics. Note, however, that, in asymptotic AdS_3, the standard BTZ-type black holes do not have any singularity. For the OSM embedded in AdS_3, this is not the case and a curvature singularity exists. This singularity is visible by computing the Ricci-scalar itself.

Let us discuss some aspects of "energy conditions" for the OSM geometry. A simple way to define such conditions is to demand that the OSM geometry can be obtained by solving Einstein equations, with a suitable matter sector and translating the energy conditions on the corresponding matter sector. Thus, imagine

$$\mathcal{G}_{\mu\nu} + \Lambda g_{\mu\nu} = \mathcal{T}_{\mu\nu}, \tag{147}$$

where $\Lambda = -d(d-1)/2$ is the cosmological constant in asymptotically AdS_{d+1}-background, $\mathcal{G}_{\mu\nu}$ is the Einstein tensor of the OSM, and $\mathcal{T}_{\mu\nu}$ is the putative matter field.

Defined this way, an AdS_3-OSM yields

$$\mathcal{T}_{\mu\nu} t^\mu t^\nu \geq 0, \tag{148}$$

where t^μ is an arbitrary timelike vector; and hence Weak Energy Condition (WEC) is satisfied. Similarly, Strong Energy Condition (SEC) is also satisfied. The Null Energy Condition (NEC), on the other hand, yields $\mathcal{T}_{\mu\nu} n^\mu n^\nu < 0$, for arbitrary null vectors n^μ, and is violated. For the AdS_4-osm, with a similar choice for the timelike and the null vector, WEC yields $\mathcal{T}_{\mu\nu} t^\mu t^\nu < 0$ and is thus violated. On the other hand, the NEC evaluates to $\mathcal{T}_{\mu\nu} n^\mu n^\nu = 0$.

In view of (141), one may explore similar questions for the conformal metric $\widetilde{\mathcal{S}}$. For the conformal OSM, in asymptotic AdS_3, one obtains

$$\widetilde{\mathcal{T}}_{\mu\nu}t^\mu t^\nu < 0 \Longrightarrow \text{WEC violated}, \tag{149}$$

$$\widetilde{\mathcal{T}}_{\mu\nu}n^\mu n^\nu > 0 \Longrightarrow \text{NEC satisfied}. \tag{150}$$

For asymptotic AdS_4, the conformal factor is identity. We can also check that a conformal AdS_5-OSM violates WEC, while both NEC and SEC are satisfied. In brief, the conformal OSM always violates the WEC. Therefore there cannot be any area-increasing theorem for such event horizons.

7.7. A Dynamical Example. In a special example, discussed in [34], a dynamical OSM geometry can also be constructed. Let us begin with the following background:

$$ds^2 = -u^2 f(u)\, dV^2 + 2dVdu + u^2 dx_d^2, \tag{151}$$

where we have used Eddington-Finkelstein ingoing coordinate

$$dt = dV + h(u)\, du, \quad \text{with } h(u) = -\frac{1}{u^2 f(u)}. \tag{152}$$

The metric takes the usual black hole metric form in the $\{t, u\}$-patch. The corresponding DBI action takes the following schematic form:

$$S_{\text{DBI}} = -\tau \int d^{d+2}\xi e^{-\phi} G_{xx}^{d/2} X, \qquad X = \left[1 + G_{xx}^{-1}\left(2f_{xu}f_{xV} - f_{xu}^2 G_{tt}\right)\right]^{1/2}, \tag{153}$$

where the U(1)-flux on the worldvolume is given by $f = f_{xu}(u)dx \wedge du + f_{xV}(u)dx \wedge dV$.

A simple solution of the resulting equations of motion can be obtained for AdS_4 [34], characterized by one undetermined function: $f_{xV} = E(V)$. The corresponding OSM now takes the form:

$$ds^2_{\text{osm}} = \left(G_{tt} + \frac{E(V)^2}{G_{xx}}\right) dV^2 + 2dVdu + u^2 dx_2^2, \tag{154}$$

which has an AdS-Vaidya form, with a dynamically evolving apparent and event horizon. Choosing an appropriate function $E(V)$, an event horizon formation on the brane can be easily described. In the dual gauge theory, one subsequently obtains a time-dependent current $\langle j(t)\rangle \sim E(t)$.

8. Conclusions

In this review, we have discussed various examples in which the nonlinear dynamics can give rise to an effective causal structure. When this causal structure is similar to that of a black hole, many similarities to classical as well as quantum properties of black holes become manifest. This bears substantial resemblance to other nonlinear systems that describe gravity-like phenomena, known as *Analogue Gravity*; see, *e.g.,* [131] for a detailed review on this. For the cases considered here, this causal structure emerges from an open string equivalence principle and this is what forms the analogue to gravity.

However, our attempts have been to briefly review the essential ideas, some explicit and simple examples on which these ideas are rather manifest. We have certainly not made any attempt to review the vast literature on the physics of probes traveling through a thermal medium in a strongly coupled gauge theory. The basic ingredients used to study this are open strings in a supergravity background. In the probe limit, the corresponding string profile can develop a world-sheet event horizon, which plays a crucial role in determining energy loss, drag force, stochastic Brownian motion of the probe. For a more extensive review on these, we will refer the reader to [31]. Beyond the probe limit, the open string backreaction estimates, *e.g.,* also the radiation produced by the quark-like degree of freedom. See, *e.g.,* [132, 133] for some of the early studies including the string backreaction. In a similar time-dependent context, far less explicit examples are known with backreaction from D-branes, since, technically, this a much harder problem to tackle. See, *e.g.,* [134] for a perturbative analysis of the backreaction.

Staying in the probe limit, while there are similarities with a black hole, there are unsettled issues as well. One of the main issues is about the physical meaning of the area of the event horizon in all of the cases we have discussed above. For a black hole, this corresponds to the thermal entropy; moreover, one can prove area increasing theorems (with certain energy conditions for the matter field) in coherence with the second law of thermodynamics. This, however, is in stark contrast with what we have reviewed here. First, we can identify the Euclidean path integral as the corresponding thermal free energy and, therefore, derive the thermal entropy from this free energy. It is rather easy to see that this does not equal the area of the event horizon on the string worldsheet, or of the open string metric geometry. Secondly, as we have explicitly discussed *energy conditions* for such cases, there is no area increase theorem for such horizons.

One intriguing proposal of [52] is to view this area as a measure of *entanglement entropy*, since the open string event horizon is created due to a Schwinger pair creation on the D-brane and is therefore intimately related to entanglement. This is explicitly demonstrated by establishing that the Lorentzian section of the string worldsheet in [88] is the analytic continuation of worldsheet instantons that describe Schwinger pair production of fundamental degrees of freedom. A similar statement on D-branes is desirable; however, to the best of our knowledge no such explicit connection has been made yet.

Complexity is a well-defined notion in quantum systems, which measures the minimum number of unitary operations required to reach a certain state starting from a base-state. Based on the eternal black holes in AdS, recently it has been suggested in [135] that computational complexity in the dual CFT is measured, geometrically, by the Einstein-Rosen bridge in the eternal black hole spacetime. Since, at present, it remains unclear how to precisely define complexity in a QFT framework, we will not delve deeper into this issue. We

will, however, simply note that, from a geometric point of view, the string worldsheet or the D-brane open string metric that we have reviewed here naturally allows us to define such a quantity. Indeed, in [98], it has already been explicitly discussed. It would be very interesting to explore this issue further, since the two-dimensional worldsheet allows for an excellent analytical control over such issues.

Finally, we end by briefly commenting on one of the most interesting questions in black hole physics: the information paradox. Since the causal structure in the probe sector is closely similar to the causal structure of a black hole, in the eternal patch (*i.e.,* the thermofield double), one can address the nature of this paradox, following the proposal in [12]. In the standard thermofield double scenario, the mismatch between the gravity correlator and the unitary CFT correlation occurs at an order $e^{-c_1 S}$, where S is the entropy of the system and c_1 is an irrelevant constant. For a purely gravitational system, $S \sim 1/G_N$ and therefore the mismatch in correlators occurs at a nonperturbative order in $1/G_N$. This regime requires a highly interacting string theory, since $G_N \sim g_s^2$.

On a string worldsheet, a naíve analysis following [12] would imply that the mismatch between the geometric correlator and the CFT correlator occurs at a nonperturbative order in $e^{-c_2 S}$, where c_2 is, as before, an unimportant constant. In this case, $S \sim 1/\ell_s^2$, where ℓ_s is the string length and it does not depend on the string coupling. The Nambu-Goto theory receives no correction in ℓ_s and therefore, it may be possible to make quantitative progress in estimating such nonperturbative effects.

Finally, we end this review with the mention of the Lieb-Robinson bound, which provides an emergent upper bound on how fast information can propagate in a generic nonrelativistic quantum mechanical system, with local interactions. While this limiting velocity is system specific, it rather intriguingly suggests a *relativity-like* structure for quantum nonrelativistic systems, at least in the kinematic sense. It will be interesting to understand the physics of this better and perhaps explore a possible connection to what we have discussed in this review.

Conflicts of Interest

The author declares that there are no conflicts of interest.

Acknowledgments

We thank Sumit Das, Jacques Distler, Roberto Emparan, Willy Fischler, Vadim Kaplunovsky, Sandipan Kundu, Hong Liu, Gautam Mandal, David Mateos, Andy O'Bannon, Bala Sathiapalan, Julian Sonner, and Javier Tarrío for numerous discussions and conversations on related topics. We specially thank Tameem Albash, Avik Banerjee, Veselin Filev, Clifford Johnson, Sandipan Kundu, and Rohan Poojary on various collaborations that helped form the bulk of this review article. We also thank Mariano Chernicoff, Alberto Guijosa, and Juan Pedraza for giving the permission to use several figures from their papers. This work is supported by the Department of Atomic Energy, Govt. of India.

References

[1] R. P. Feynman and J. Vernon, "The theory of a general quantum system interacting with a linear dissipative system," *Annals of Physics*, vol. 24, pp. 118–173, 1963.

[2] J. Schwinger, "Brownian motion of a quantum oscillator," *Journal of Mathematical Physics*, vol. 2, pp. 407–432, 1961.

[3] L. Keldysh, "Diagram technique for nonequilibrium processes," *Soviet Physics—Journal of Experimental and Theoretical Physics*, vol. 47, pp. 1515–1527, 1964.

[4] K.-c. Chou, Z.-b. Su, B. L. Hao, and L. Yu, "Equilibrium and nonequilibrium formalisms made unified," *Physics Reports*, vol. 118, no. 1-2, pp. 1–131, 1985.

[5] N. P. Landsman and C. G. van Weert, "Real- and imaginary-time field theory at finite temperature and density," *Physics Reports*, vol. 145, no. 3-4, pp. 141–249, 1987.

[6] A. Kamenev and A. Levchenko, "Keldysh technique and non-linear σ-model: basic principles and applications," *Advances in Physics*, vol. 58, no. 3, pp. 197–319, 2009.

[7] F. M. Haehl, R. Loganayagam, and M. Rangamani, "Schwinger-Keldysh formalism. Part I: BRST symmetries and superspace," *Journal of High Energy Physics*, vol. 2017, no. 06, article 069, 2017.

[8] F. M. Haehl, R. Loganayagam, and M. Rangamani, "Schwinger-Keldysh formalism. Part II: thermal equivariant cohomology," *Journal of High Energy Physics*, vol. 2017, no. 06, article 070, 2017.

[9] F. M. Haehl, R. Loganayagam, p. Narayan, and M. Rangamani, "Classification of out-of-time-order correlators," *SciPost Physics*, vol. 6, no. 1, 2019.

[10] Y. Takahashi and H. Umezawa, "Thermo field dynamics," *Collective Phenomena*, vol. 2, no. 55, 1975.

[11] W. Israel, "Thermo-field dynamics of black holes," *Physics Letters A*, vol. 57, no. 2, pp. 107–110, 1976.

[12] J. Maldacena, "Eternal black holes in anti-de Sitter," *Journal of High Energy Physics*, vol. 2003, no. 04, article 021, 2003.

[13] J. Maldacena and L. Susskind, "Cool horizons for entangled black holes," *Fortschritte der Physik/Progress of Physics*, vol. 61, no. 9, pp. 781–811, 2013.

[14] K. Aamodt et al., "Elliptic flow of charged particles in Pb-Pb collisions at 2.76 TeV," *Physical Review Letters*, vol. 2010, no. 5, Article ID 252302, 2010.

[15] K. M. O'Hara, S. L. Hemmer, M. E. Gehm, S. R. Granade, and J. E. Thomas, "Observation of a strongly interacting degenerate fermi gas of atoms," *Science*, vol. 298, no. 5601, pp. 2179–2182, 2002.

[16] J. Maldacena, "The large N limit of superconformal field theories and supergravity," *Advances in Theoretical and Mathematical Physics*, vol. 38, no. 1113, 1999.

[17] S. S. Gubser, I. R. Klebanov, and A. M. Polyakov, "Gauge theory correlators from non-critical string theory," *Physics Letters B*, vol. 428, no. 1-2, pp. 105–114, 1998.

[18] E. Witten, "Anti de Sitter space and holography," *Advances in Theoretical and Mathematical Physics*, vol. 2, no. 2, pp. 253–291, 1998.

[19] O. Aharony, S. S. Gubser, J. Maldacena, H. Ooguri, and Y. Oz, "Large N field theories, string theory and gravity," *Physics Reports*, vol. 323, no. 3-4, pp. 183–386, 2000.

[20] D. T. Son and A. O. Starinets, "Minkowski-space correlators in AdS/CFT correspondence: recipe and applications," *Journal of High Energy Physics*, vol. 2002, no. 09, article 042, 2002.

[21] C. P. Herzog and D. T. Son, "Schwinger-Keldysh propagators from AdS/CFT correspondence," *Journal of High Energy Physics*, vol. 2003, no. 03, article 046, 2003.

[22] N. Iqbal and H. Liu, "Real-time response in AdS/CFT with application to spinors," *Fortschritte der Physik/Progress of Physics*, vol. 57, no. 5-7, pp. 367–384, 2009.

[23] K. Skenderis and B. C. van Rees, "Real-time gauge/gravity duality," *Physical Review Letters*, vol. 101, no. 8, Article ID 081601, 2008.

[24] K. Skenderis and B. C. van Rees, "Real-time gauge/gravity duality: prescription, renormalization and examples," *Journal of High Energy Physics*, vol. 2009, no. 05, article 085, 2009.

[25] J. Casalderrey-Solana, H. Liu, D. Mateos, K. Rajagopal, and U. A. Wiedemann, *Gauge/String Duality, Hot QCD and Heavy Ion Collisions*, Cambridge University Press, Cambridge, UK, 2014.

[26] O. DeWolfe, S. S. Gubser, C. Rosen, and D. Teaney, "Heavy ions and string theory," *Progress in Particle and Nuclear Physics*, vol. 75, pp. 86–132, 2014.

[27] S. S. Gubser and A. Karch, "From gauge-string duality to strong interactions:a pedestrian's guide," *Annual Review of Nuclear and Particle Science*, vol. 59, pp. 145–168, 2009.

[28] S. A. Hartnoll, "Lectures on holographic methods for condensed matter physics," *Classical and Quantum Gravity*, vol. 26, no. 22, Article ID 224002, 2009.

[29] S. A. Hartnoll, A. Lucas, and S. Sachdev, "Holographic quantum matter," https://arxiv.org/abs/1612.07324.

[30] S. R. Das, "Old and new scaling laws in quantum quench," *Progress of Theoretical and Experimental Physics*, vol. 2016, no. 12, Article ID 12C107, 2016.

[31] V. E. Hubeny and M. Rangamani, "A holographic view on physics out of equilibrium," *Advances in High Energy Physics*, vol. 2010, Article ID 297916, 84 pages, 2010.

[32] A. G. Green and S. L. Sondhi, "Nonlinear quantum critical transport and the schwinger mechanism for a superfluid-mott-insulator transition of bosons," *Physical Review Letters*, vol. 95, Article ID 267001, 2005.

[33] A. G. Green, J. E. Moore, S. L. Sondhi, and A. Vishwanath, "Current noise in the vicinity of the 2D superconductor-insulator quantum critical point," *Physical Review Letters*, vol. 97, no. 22, Article ID 227003, 2006.

[34] A. Karch and S. L. Sondhi, "Non-linear finite frequency quantum critical transport from AdS/CFT," *Journal of High Energy Physics*, vol. 2011, no. 01, article 149, 2011.

[35] S. Kirchner and Q. Si, "Quantum criticality out of equilibrium: steady state in a magnetic single-electron transistor," *Physical Review Letters*, vol. 103, no. 20, Article ID 206401, 2009.

[36] L. F. Cugliandolo, J. Kurchan, and L. Peliti, "Energy flow, partial equilibration, and effective temperatures in systems with slow dynamics," *Physical Review E: Statistical, Nonlinear, and Soft Matter Physics*, vol. 55, no. 4, pp. 3898–3914, 1997.

[37] J. Babington, J. Erdmenger, N. Evans, Z. Guralnik, and I. Kirsch, "Chiral symmetry breaking and pions in nonsupersymmetric gauge/gravity duals," *Physical Review D: Particles, Fields, Gravitation and Cosmology*, vol. 69, no. 6, Article ID 066007, 2004.

[38] D. Mateos, R. C. Myers, and R. M. Thomson, "Holographic phase transitions with fundamental matter," *Physical Review Letters*, vol. 97, no. 9, Article ID 091601, 2006.

[39] T. Albash, V. Filev, C. V. Johnson, and A. Kundu, "Topology-changing first order phase transition and the dynamics of flavor," *Physical Review D: Particles, Fields, Gravitation and Cosmology*, vol. 77, no. 6, Article ID 066004, 2008.

[40] A. Karch and A. O'Bannon, "Chiral transition of $N = 4$ super Yang-Mills theory with flavor on a 3-sphere," *Physical Review D: Particles, Fields, Gravitation and Cosmology*, vol. 74, no. 8, Article ID 085033, 2006.

[41] S. S. Gubser, "Drag force in AdS/CFT," *Physical Review D: Particles, Fields, Gravitation and Cosmology*, vol. 74, no. 12, Article ID 126005, 2006.

[42] C. P. Herzog, A. Karch, P. Kovtun, C. Kozcaz, and L. G. Yaffe, "Energy loss of a heavy quark moving through $N = 4$ supersymmetric Yang Mills Plasma," *Journal of High Energy Physics*, vol. 2006, no. 7, article 013, 2006.

[43] K. Peeters and M. Zamaklar, "Dissociation by acceleration," *Journal of High Energy Physics*, vol. 2008, no. 1, article 038, 2008.

[44] V. E. Hubeny and G. W. Semenoff, "String worldsheet for accelerating quark," *Journal of High Energy Physics*, vol. 2015, no. 10, article 071, 2015.

[45] J. de Boer, V. E. Hubeny, M. Rangamania, and M. Shigemori, "Brownian motion in AdS/CFT," *Journal of High Energy Physics*, vol. 2009, no. 07, article 094, 2009.

[46] D. T. Son and D. Teaney, "Thermal noise and stochastic strings in AdS/CFT," *Journal of High Energy Physics*, vol. 2009, no. 7, article 021, 2009.

[47] G. C. Giecold, E. Iancu, and A. H. Mueller, "Stochastic trailing string and Langevin dynamics from AdS/CFT," *Journal of High Energy Physics*, vol. 2009, no. 7, article 33, 2009.

[48] J. Casalderrey-Solana, K.-Y. Kim, and D. Teaney, "Stochastic string motion above and below the world sheet horizon," *Journal of High Energy Physics*, vol. 2009, no. 12, article 066, 2009.

[49] M. Chernicoff, J. A. García, A. Güijosa, and J. F. Pedraza, "Holographic lessons for quark dynamics," *Journal of Physics G: Nuclear and Particle Physics*, vol. 39, no. 5, Article ID 054002, 2012.

[50] M. Chernicoff, A. Güijosa, and J. F. Pedraza, "Holographic EPR pairs, wormholes and radiation," *Journal of High Energy Physics*, vol. 2013, no. 10, article 211, 2013.

[51] K. Jensen and A. Karch, "Holographic dual of an Einstein-Podolsky-Rosen pair has a wormhole," *Physical Review Letters*, vol. 111, no. 21, Article ID 211602, 2013.

[52] J. Sonner, "Holographic schwinger effect and the geometry of entanglement," *Physical Review Letters*, vol. 111, no. 21, Article ID 211603, 2013.

[53] K. Jensen and J. Sonner, "Wormholes and entanglement in holography," *International Journal of Modern Physics D*, vol. 23, no. 12, Article ID 1442003, 2014.

[54] S. Nakamura, "Nonequilibrium phase transitions and nonequilibrium critical point from AdS/CFT," *Physical Review Letters*, vol. 109, no. 12, Article ID 120602, 2012.

[55] S. Nakamura and H. Ooguri, "Out of equilibrium temperature from holography," *Physical Review D: Particles, Fields, Gravitation and Cosmology*, vol. 88, no. 12, Article ID 126003, 2013.

[56] H. Hoshino and S. Nakamura, "Effective temperature of nonequilibrium dense matter in holography," *Physical Review D: Particles, Fields, Gravitation and Cosmology*, vol. 91, no. 2, Article ID 026009, 2015.

[57] M. Matsumoto and S. Nakamura, "Critical exponents of nonequilibrium phase transitions in AdS/CFT correspondence," *Physical Review D: Particles, Fields, Gravitation and Cosmology*, vol. 98, no. 10, 2018.

[58] H. Hoshino and S. Nakamura, "Lorentz transformation of temperature and effective temperature," 2018, https://arxiv.org/abs/1807.10132.

[59] S. R. Das, T. Nishioka, and T. Takayanagi, "Probe branes, time-dependent couplings and thermalization in AdS/CFT," *Journal of High Energy Physics*, vol. 2010, no. 7, article 071, 2010.

[60] M. Ali-Akbari and H. Ebrahim, "Meson thermalization in various dimensions," *Journal of High Energy Physics*, vol. 2012, no. 4, article 145, 2012.

[61] M. Ali-Akbari and H. Ebrahim, "Thermalization in external magnetic field," *Journal of High Energy Physics*, vol. 2013, no. 3, article 045, 2013.

[62] https://www.physik.uni-augsburg.de/theo1/hanggi/Casas.pdf.

[63] L. F. Cugliandolo, "The effective temperature," *Journal of Physics A: Mathematical and General*, vol. 44, no. 48, Article ID 483001, 2011.

[64] S. Caron-Huot, P. M. Chesler, and D. Teaney, "Fluctuation, dissipation, and thermalization in non-equilibrium AdS 5 black hole geometries," *Physical Review D: Particles, Fields, Gravitation and Cosmology*, vol. 84, no. 2, Article ID 026012, 2011.

[65] P. Castorina, D. Kharzeev, and H. Satz, "Thermal hadronization and Hawking–Unruh radiation in QCD," *The European Physical Journal C*, vol. 52, no. 1, pp. 187–201, 2007.

[66] M. Novello, V. A. De Lorenci, J. M. Salim, and R. Klippert, "Geometrical aspects of light propagation in nonlinear electrodynamics," *Physical Review D: Particles, Fields, Gravitation and Cosmology*, vol. 61, no. 4, Article ID 045001, 2000.

[67] D. Kharzeev and K. Tuchin, "From color glass condensate to quark-gluon plasma through the event horizon," *Nuclear Physics A*, vol. 753, no. 3-4, pp. 316–334, 2005.

[68] D. Kharzeev, E. Levin, and K. Tuchin, "Multiparticle production and thermalization in high-energy QCD," *Physical Review C: Nuclear Physics*, vol. 75, Article ID 044903, 2007.

[69] P. Braun-Munzinger, K. Redlich, and J. Stachel, "Particle production in heavy ion collisions," in *Quark–Gluon Plasma*, R. C. Hwa and X.-N. Wang, Eds., pp. 491–599, 2004.

[70] J. Cleymans and H. Satz, "Thermal hadron production in high energy heavy ion collisions," *Zeitschrift für Physik C Particles and Fields*, vol. 57, no. 1, pp. 135–147, 1993.

[71] F. Becattini and U. W. Heinz, "Thermal hadron production in p p and p anti-p collisions," *Zeitschrift für Physik C Particles and Fields*, vol. 76, no. 2, pp. 269–286, 1997.

[72] G. 't Hooft, "A planar diagram theory for strong interactions," *Nuclear Physics B*, vol. 72, no. 3, pp. 461–473, 1974.

[73] G. 't Hooft, "Dimensional reduction in quantum gravity," *Classical and Quantum Gravity*, vol. 284, Article ID 930308, 1993.

[74] L. Susskind, "The world as a hologram," *Journal of Mathematical Physics*, vol. 36, no. 11, article 6377, 1995.

[75] N. Itzhaki, J. M. Maldacena, J. Sonnenschein, and S. Yankielowicz, "Supergravity and the large N limit of theories with sixteen supercharges," *Physical Review D: Particles, Fields, Gravitation and Cosmology*, vol. 58, no. 4, 046004, 11 pages, 1998.

[76] A. Karch and E. Katz, "Adding flavor to AdS/CFT," *Journal of High Energy Physics*, vol. 2002, no. 6, article 43, 2002.

[77] M. Chernicoff and A. Paredes, "Accelerated detectors and worldsheet horizons in AdS/CFT," *Journal of High Energy Physics*, vol. 2011, no. 3, article 063, 2011.

[78] E. Caceres, M. Chernicoff, A. Guijosa, and J. F. Pedraza, "Quantum fluctuations and the Unruh effect in strongly-coupled conformal field theories," *Journal of High Energy Physics*, vol. 2010, no. 6, article 078, 2010.

[79] C. Fefferman and C. R. Graham, "Conformal invariants," *Élie Cartan et les Mathématiques d'Aujourd'hui*, vol. 95, 1985.

[80] S. de Haro, K. Skenderis, and S. N. Solodukhin, "Holographic reconstruction of spacetime and renormalization in the AdS/CFT correspondence," *Communications in Mathematical Physics*, vol. 217, no. 3, pp. 595–622, 2001.

[81] K. Skenderis, "Asymptotically anti-de Sitter spacetimes and their stress energy tensor," *International Journal of Modern Physics A - World Scientific*, vol. 16, no. 5, pp. 740–749, 2001.

[82] K. Skenderis, "Lecture notes on holographic renormalization," *Classical and Quantum Gravity*, vol. 19, no. 22, pp. 5849–5876, 2002.

[83] A. Mikhailov, "Nonlinear waves in AdS/CFT correspondence," https://arxiv.org/abs/hep-th/0305196.

[84] M. Chernicoff and A. Güijosa, "Acceleration, energy loss and screening in strongly-coupled gauge theories," *Journal of High Energy Physics*, vol. 2008, no. 06, article 005, 2008.

[85] M. Chernicoff, J. A. Garcia, and A. Guijosa, "Generalized Lorentz-Dirac equation for a strongly coupled gauge theory," *Physical Review Letters*, vol. 102, no. 24, Article ID 241601, 2009.

[86] M. Chernicoff, J. A. Garcia, and A. Guijosa, "A tail of a quark in N=4 SYM," *Journal of High Energy Physics*, vol. 2009, no. 9, article 080, 2009.

[87] J. Penedones, "TASI Lectures on AdS/CFT," *World Scientific*, pp. 75–136, 2017.

[88] B. W. Xiao, "On the exact solution of the accelerating string in AdS(5) space," *Physics Letters B*, vol. 665, no. 4, pp. 173–177, 2008.

[89] C. Athanasiou, P. M. Chesler, H. Liu, D. Nickel, and K. Rajagopal, "Synchrotron radiation in strongly coupled conformal field theories," *Physical Review D*, vol. 84, Article ID 126001, 2010.

[90] P. C. Davies, T. Dray, and C. A. Manogue, "Detecting the rotating quantum vacuum," *Physical Review D: Particles, Fields, Gravitation and Cosmology*, vol. 53, no. 8, pp. 4382–4387, 1996.

[91] Y. Sekino and L. Susskind, "Fast scramblers," *Journal of High Energy Physics*, vol. 2008, no. 10, article 065, 2008.

[92] R. Bhattacharya, D. P. Jatkar, and A. Kundu, "Chaotic correlation functions with complex fermions," https://arxiv.org/abs/1810.13217.

[93] J. Maldacena, S. H. Shenker, and D. Stanford, "A bound on chaos," *Journal of High Energy Physics*, vol. 2016, no. 08, article 106, 2016.

[94] S. H. Shenker and D. Stanford, "Black holes and the butterfly effect," *Journal of High Energy Physics*, vol. 2014, no. 03, article 067, 2014.

[95] S. H. Shenker and D. Stanford, "Multiple shocks," *Journal of High Energy Physics*, vol. 2014, no. 12, article 046, 2014.

[96] S. H. Shenker and D. Stanford, "Stringy effects in scrambling," *Journal of High Energy Physics*, vol. 2015, no. 05, article 132, 2015.

[97] K. Murata, "Fast scrambling in holographic Einstein-Podolsky-Rosen pair," *Journal of High Energy Physics*, vol. 2017, no. 11, article 049, 2017.

[98] J. de Boer, E. Llabrés, J. F. Pedraza, and D. Vegh, "Chaotic strings in AdS/CFT," *Physical Review Letters*, vol. 120, no. 20, Article ID 201604, 2018.

[99] A. Banerjee, A. Kundu, and R. R. Poojary, "Strings, Branes, Schwarzian Action and Maximal Chaos," 2018, https://arxiv.org/abs/1809.02090.

[100] A. Banerjee, A. Kundu, and R. Poojary, "Maximal Chaos from Strings, Branes And Schwarzian Action," https://arxiv.org/abs/1811.04977.

[101] J. Maldacena, D. Stanford, and Z. Yang, "Conformal symmetry and its breaking in two-dimensional nearly anti-de Sitter space," *PTEP. Progress of Theoretical and Experimental Physics*, vol. 2016, no. 12, Article ID 12C104, 2016.

[102] T. Albash, V. Filev, C. V. Johnson, and A. Kundu, "Quarks in an external electric field in finite temperature large N gauge theory," *Journal of High Energy Physics*, vol. 2008, no. 8, article 092, 2008.

[103] R. C. Myers, A. O. Starinets, and R. M. Thomson, "Holographic spectral functions and diffusion constants for fundamental matter," *Journal of High Energy Physics. A SISSA Journal*, vol. 2007, no. 11, article 091, 2007.

[104] A. Karch and A. O'Bannon, "Metallic AdS/CFT," *Journal of High Energy Physics*, vol. 2007, no. 9, article 024, 2007.

[105] T. Albash, V. Filev, C. V. Johnson, and A. Kundu, "Finite temperature large N gauge theory with quarks in an external magnetic field," *Journal of High Energy Physics*, vol. 2008, no. 7, article 080, 2008.

[106] J. Erdmenger, R. Meyer, and J. P. Shock, "AdS/CFT with flavour in electric and magnetic Kalb-Ramond fields," *Journal of High Energy Physics. A SISSA Journal*, vol. 2007, no. 12, article 091, 2007.

[107] I. Kirsch, "Spectroscopy of fermionic operators in AdS/CFT," *Journal of High Energy Physics*, vol. 2006, no. 09, article 052, 2006.

[108] N. Seiberg and E. Witten, "String theory and noncommutative geometry," *Journal of High Energy Physics*, vol. 1999, no. 09, article 032, 1999.

[109] A. Kundu, "Effective temperature in steady-state dynamics from holography," *Journal of High Energy Physics*, vol. 2015, no. 9, article 042, 2015.

[110] K.-Y. Kim, J. P. Shock, and J. Tarrio, "The open string membrane paradigm with external electromagnetic fields," *Journal of High Energy Physics*, vol. 2011, no. 6, article 017, 2011.

[111] O. DeWolfe, D. Z. Freedman, and H. Ooguri, "Holography and defect conformal field theories," *Physical Review D: Particles, Fields, Gravitation and Cosmology*, vol. 66, no. 2, Article ID 025009, 2002.

[112] V. G. Filev, "Hot defect superconformal field theory in an external magnetic field," *Journal of High Energy Physics*, vol. 2009, no. 11, article 123, 2009.

[113] J. Sonner and A. G. Green, "Hawking radiation and nonequilibrium quantum critical current noise," *Physical Review Letters*, vol. 109, Article ID 091601, 2012.

[114] O. Bergman, G. Lifschytz, and M. Lippert, "Response of holographic QCD to electric and magnetic fields," *Journal of High Energy Physics*, vol. 2008, no. 05, article 007, 2008.

[115] C. V. Johnson and A. Kundu, "External fields and chiral symmetry breaking in the Sakai-SUGimoto model," *Journal of High Energy Physics*, vol. 2008, no. 12, article 053, 2008.

[116] A. Kundu and S. Kundu, "Steady-state physics, effective temperature dynamics in holography," *Physical Review D*, vol. 91, no. 4, Article ID 046004, 2015.

[117] G. W. Gibbons, "Aspects of born-infeld theory and string/M theory," *Revista Mexicana de Física*, vol. 49S1, no. 19, 2003.

[118] G. W. Gibbons and C. A. Herdeiro, "Born-infeld theory and stringy causality," *Physical Review D: Particles, Fields, Gravitation and Cosmology*, vol. 63, Article ID 064006, 2001.

[119] D. Mateos, S. Matsuura, R. C. Myers, and R. M. Thomson, "Holographic phase transitions at finite chemical potential," *Journal of High Energy Physics*, vol. 2007, no. 11, article 085, 2007.

[120] N. Evans, A. Gebauer, and K. Kim, "E, B, μ, T phase structure of the D3/D7 holographic dual," *Journal of High Energy Physics*, vol. 2011, no. 5, article 067, 2011.

[121] C. V. Johnson and A. Kundu, "Meson spectra and magnetic fields in the Sakai-Sugimoto model," *Journal of High Energy Physics*, vol. 2009, no. 07, article 103, 2009.

[122] O. Bergman, G. Lifschytz, and M. Lippert, "Magnetic properties of dense holographic QCD," *Physical Review D: Particles, Fields, Gravitation and Cosmology*, vol. 79, Article ID 105024, 2009.

[123] E. G. Thompson and D. T. Son, "Magnetized baryonic matter in holographic QCD," *Physical Review D: Particles, Fields, Gravitation and Cosmology*, vol. 78, Article ID 066007, 2008.

[124] A. O'Bannon, "Hall conductivity of flavor fields from AdS/CFT," *Physical Review D: Particles, Fields, Gravitation and Cosmology*, vol. 76, Article ID 086007, 2007.

[125] S. A. Hartnoll, J. Polchinski, E. Silverstein, and D. Tong, "Towards strange metallic holography," *Journal of High Energy Physics*, vol. 2010, no. 4, article 120, 2010.

[126] F. Bigazzi, A. L. Cotrone, and J. Tarrío, "Charged D3-D7 plasmas: novel solutions, extremality and stability issues," *Journal of High Energy Physics*, vol. 2013, no. 7, article 074, 2013.

[127] A. Banerjee, A. Kundu, and S. Kundu, "Emergent horizons and causal structures in holography," *Journal of High Energy Physics*, vol. 2016, no. 9, article 166, 2016.

[128] A. Banerjee, A. Kundu, and S. Kundu, "Flavour fields in steady state: stress tensor and free energy," *Journal of High Energy Physics*, vol. 2016, article 102, no. 2, 2016.

[129] A. Karch, A. O'Bannon, and E. Thompson, "The stress-energy tensor of flavor fields from AdS/CFT," *Journal of High Energy Physics*, vol. 2009, no. 4, article 021, 2009.

[130] M. S. Alam, V. S. Kaplunovsky, and A. Kundu, "Chiral symmetry breaking and external fields in the Kuperstein-Sonnenschein model," *Journal of High Energy Physics*, vol. 2012, no. 4, article 111, 2012.

[131] C. Barceló, S. Liberati, and M. Visser, "Analogue gravity," *Living Reviews in Relativity*, vol. 8, no. 12, 2005.

[132] S. S. Gubser, S. S. Pufu, and A. Yarom, "Sonic booms and diffusion wakes generated by a heavy quark in thermal AdS/CFT," *Physical Review Letters*, vol. 100, Article ID 012301, 2008.

[133] S. S. Gubser, S. S. Pufu, and A. Yarom, "Shock waves from heavy-quark mesons in AdS/CFT," *Journal of High Energy Physics*, vol. 2008, no. 7, article 108, 2008.

[134] B. Sahoo and H.-U. Yee, "Electrified plasma in AdS/CFT correspondence," *Journal of High Energy Physics*, vol. 2010, no. 11, article 095, 2010.

[135] L. Susskind, "Computational complexity and black hole horizons," *Fortschritte der Physik/Progress of Physics*, vol. 64, no. 1, pp. 24–43, 2016.

Hindawi
Advances in High Energy Physics
Volume 2019, Article ID 9781620, 14 pages
https://doi.org/10.1155/2019/9781620

Research Article

Gauge from Holography and Holographic Gravitational Observables

José A. Zapata

Centro de Ciencias Matemáticas, Universidad Nacional Autónoma de México, Morelia, MICH, Mexico

Correspondence should be addressed to José A. Zapata; zapata@matmor.unam.mx

Received 12 September 2018; Revised 13 December 2018; Accepted 6 January 2019; Published 7 February 2019

Guest Editor: Esperanza Lopez

In a spacetime divided into two regions U_1 and U_2 by a hypersurface Σ, a perturbation of the field in U_1 is coupled to perturbations in U_2 by means of the holographic imprint that it leaves on Σ. The linearized gluing field equation constrains perturbations on the two sides of a dividing hypersurface, and this linear operator may have a nontrivial null space. A nontrivial perturbation of the field leaving a holographic imprint on a dividing hypersurface which does not affect perturbations on the other side should be considered physically irrelevant. This consideration, together with a locality requirement, leads to the notion of gauge equivalence in Lagrangian field theory over confined spacetime domains. Physical observables in a spacetime domain U can be calculated integrating (possibly nonlocal) gauge invariant conserved currents on hypersurfaces such that $\partial\Sigma \subset \partial U$. The set of observables of this type is sufficient to distinguish gauge inequivalent solutions. The integral of a conserved current on a hypersurface is sensitive only to its homology class $[\Sigma]$, and if U is homeomorphic to a four ball the homology class is determined by its boundary $S = \partial\Sigma$. We will see that a result of Anderson and Torre implies that for a class of theories including vacuum general relativity all local observables are holographic in the sense that they can be written as integrals of over the two-dimensional surface S. However, nonholographic observables are needed to distinguish between gauge inequivalent solutions.

1. Context

Motivated by the development of black hole thermodynamics [1, 2], more than two decades ago pioneers of modern physics put forward a holographic principle that sparked immense interest in the community [3, 4]. More recently, motivations from string theory lead to the discovery of the gauge/gravity correspondence [5] providing an avenue for defining new quantum gravity theories. Interestingly, quantum information has been found to play an important role in the gauge/gravity correspondence [6–9].

Despite its motivation, this article does not contribute by elongating the promising road towards quantum gravity emerging from the gauge/gravity correspondence, and our work is classical in substance.

A recurrent theme in this study is that a hypersurface locally splits spacetime into two regions and can be thought of as the communication channel between them.

Spacetime localized properties of the field will be of our interest. Since measuring devices live in spacetime as well, measurement will be understood as the interaction between the system of interest (a certain field) and the measuring device (a field or a detector modeled otherwise). Think for example of a beam interacting with a screen for a short period of time; a spacetime description of the situation takes place in a bounded spacetime domain U where part of its boundary is the world history of the screen. In this situation, our point of view will be that measurement did not take place inside a spacetime region U where the field lives but at a boundary where it interacts with another system. We will focus on the idea that measurement requires a division of a system into two subsystems, the system of interest, and the reference system with respect to which we measure. A division of the field into two subsystems is achieved by considering a bounded spacetime region and considering the field inside U as the system of interest and the field outside the region as the reference with respect to which we measure. The system of interest interacts with the reference system though the boundary of the region ∂U. We will exhibit observables for pure gravity defined on spacetime domains with boundary

defined by considering the field at ∂U, together with its partial derivatives, as a reference system.

From this point of view, there could be field configurations in U which are different, but which cannot be distinguished by the reference system, which for us is the field outside of U (or the field together with enough partial derivatives at ∂U).

We will also play with the idea of having the ability of separating a system into subsystems in arbitrary ways as indicated by splitting a spacetime region into subregions like $U = U_1 \#_\Sigma U_2$ (which means that the union of the subregions is U and the intersection is the hypersurface Σ). We will study the gluing conditions that the field and its perturbations satisfy at hypersurfaces Σ serving as communication channel between subsystems.

From the study of how perturbations propagate through communicating hypersurfaces a condition for gauge equivalence naturally arises. We complement it with requirements of locality and relativity of measurement to give rise to a notion of gauge vector fields which is suited to work on spacetime confined domains. This notion of gauge becomes a cornerstone for the version of Lagrangian field theory presented in this work and for the study of observables and holography given in the rest of the article.

A close relative to our proposal is the discovery of holographic behavior in gauge theories confined to bounded domains; more precisely, that the presence of boundaries in gauge theories leads to "would be gauge degrees of freedom" living at the boundary [10, 11] showing that entanglement entropy, gauge, and locality are interestingly intertwined [12, 13].

Our interest on communicating hypersurfaces Σ and on measurement makes it natural to consider observables modeled by the integration of currents on hypersurfaces. We want to consider the data at Σ as characterizing a solution (at least partially) in a neighborhood of Σ and we want the function to depend on the solution being as independent of Σ as possible. This is our reason for considering conserved currents. Additionally since our intention is to model measurement, we should consider gauge invariant conserved currents. In the paper we show that observables calculated integrating this type of currents are capable of distinguishing gauge inequivalent solutions.

In bounded spacetime domains U with the topology of a ball observables calculated integrating conserved currents do not depend on more details of the integrating hypersurface than its boundary, $S = \partial\Sigma \subset \partial U$. The hypersurface can be deformed within U keeping its boundary fixed and the evaluation of the observable would not change. On the other hand, the field inside U is completely determined by the field (together with enough of its partial derivatives) in ∂U. Generic observables in bounded spacetime domains can be thought of as complicated functionals of the field in ∂U.

It is natural to wonder about observables calculated from conserved currents which depend only on the field at the codimension two surface $S = \partial\Sigma$. We study this type of holographic observables in detail.

Before we finish setting up the context of this study, we have to give a pair of remarks. The first one regards the causal structure. General relativity is one of the theories that we intend to cover in our study, and it sets spacetime geometry as a dynamical field interacting with matter fields. Since causal structure follows from spacetime geometry, at the initial stage of our setting we consider a spacetime M without a prefixed causal structure which could let us talk about spacelike surfaces or Cauchy surfaces for example. Once we have a metric, or a class of metrics, we can refer to a causal structure. The previous remark gives us the opportunity to mention that we will consider observables which are not defined for all field configurations (or for all solutions). Important observables will need a specific physical context to be defined, and this context may only be consistent in a domain of definition consisting of a certain class of fields. A mathematical side to the same issue could be that the expressions defining a given observable may be well defined only in a certain domain.

The second remark is about the term "local". In this introductory section we already mentioned "spacetime localized" properties of the field; it refers to properties of the field inside a bounded spacetime region U. This term will not appear often and if it does its meaning should be clear. We also mentioned a principle of "locality of measurement" when we were talking about our notion of gauge equivalence. We will see later that this refers to being able to calculate a physical observable as a sum of "local contributions" where each of them is gauge invariant in the appropriate context. In the next section we will talk about "local functionals" of the field. This term will appear often and it refers to functionals depending on the field and finitely many of its partial derivatives. But the terminology needs to be more specific. A physical observable f is called "spacetime local" if it is calculated integrating a density which depends on finitely many partial derivatives of the field. A physical observable f_Σ calculated integrating a current is said to be "hypersurface local" if the current depends on finitely many partial derivatives of the field. Consider a field theory which admits a formulation in terms of initial data. Call T_Σ the map sending initial data to solutions. We can use the pullback map T_Σ^* to transform spacetime covariant functionals into functionals of initial data. Since this procedure involves integrating nonlinear equations, it is generically a nonlocal procedure which transforms spacetime local functionals into functionals which fail to be hypersurface local. There are very few hypersurface local observables apart from Noether charges. A set of observables calculated integrating currents needs to include observables which are not hypersurface local to be rich enough to describe the system.

The organization of this paper is as follows. In Section 2 we will present a version of Lagrangian field theory and pay special attention to the gluing conditions that the field and its perturbations satisfy at hypersurfaces Σ separating the system of interest into two pieces. We chose a version of field theory based in two aspects which we considered essential for our study: spacetime covariance and locality. The version of Lagrangian field theory that we describe in the next section is a spacetime covariant and local description in the sense of Oeckl's General Boundary Formulation of field theory [14]. The example of two-dimensional abelian BF theory is developed in this section with the intention of providing a

simple example which is useful for the rest of the article. General relativity is mentioned frequently in the paper, but instead of performing technical calculations for that example we give references for the results that we mention. In Section 3 we develop a notion of gauge equivalence appropriate for bounded spacetime regions. With this notion of gauge, the version of Lagrangian field theory presented here is completed. Our argument supporting the definition equivalence is a covariant and local version of Newton's principle of determinacy. In Section 4 we study the class of observables that can be calculated integrating gauge invariant conserved currents. In Section 5 we describe how results of Anderson and Torre [15, 16] imply that hypersurface local gravitational observables (in the vacuum) are holographic. In Section 6 we present families of gravitational observables which are holographic and large families of observables which are not holographic. Section 7 contains a summary of our work and gives some concluding remarks.

2. Lagrangian Classical Field Theory

In this section we give a brief review of the version of Lagrangian classical field theory that will be used in this work. It will also be useful to fix the notation for the rest of the article. Local functionals and the variational principle are elegantly treated in the jet bundle using the tools of the variational bicomplex. Vector fields in the space of solutions play an important role in our work, in particular because observables and observable currents have associated Hamiltonian vector fields. In order to correctly model those vector fields we have to step out of the geometrical formalism of the jet bundle and work at the level of sections using analytical methods. Here we will give a minimal description of the part of this formalism that is essential for presenting our results. For an excellent short introduction the variational bicomplex see [17], and for a combination of this framework with analytical methods see [18, 19]. First we will have a general review of the formalism, and we will finish the section with the example of two-dimensional abelian BF theory. We choose this example because it is very simple and it still lets us illustrate how the formalism works for field theories with gauge freedom. In the paper we will often mention general relativity, but we will not do the calculations here and just cite the relevant references.

2.1. General Framework. We will aim to have a *local description* of field theory closely related to the General Boundary formulation of field theory [14]. In our setting there is a fixed spacetime manifold M of dimension $n = 4$, and we will study the field in a region $U \subset M$ which may have a boundary and corners.

There is a bundle over spacetime $\pi : Y \longrightarrow M$ with an $m-$dimensional fiber F, and the field studied in this work is considered to be a section of the restriction of the bundle to the region of interest, $\phi : U \longrightarrow Y|_U$.

Points in the $k-$jet bundle $\pi_{k,0} : J^kY \longrightarrow Y$, $k = 1, 2, \ldots$ are equivalence classes of local sections of π that agree up to k-th order partial derivatives when evaluated at a given point $x \in M$. The evaluation of a section of the original bundle is written using a local chart as $\phi(x) = (x^1, \ldots, x^i, \ldots, x^n; u^1, \ldots, u^a, \ldots, u^m) \in Y|_U$. Accordingly, the k-jet gets the following coordinates:

$$\begin{aligned}&\left(x; u^{(k)}\right)\\ &\coloneqq \left(x^1, \ldots, x^i, \ldots, x^n; u^1, \ldots, u^a, \ldots, u^m; \ldots, u^a_I, \ldots\right),\\ &\in J^kY\Big|_U\end{aligned} \tag{1}$$

where $i = 1, \ldots, n$; $a = 1, \ldots, m$; and $I = (i_1, \ldots, i_k)$ is a *multi-index* consisting on an unordered k-tuple of coordinate indices (because this type of indices indicate a k-th order partial derivative of a section). We write $|I| \coloneqq i_1 + \cdots + i_n = 0, 1, \ldots, k, i_j \geq 0, i_j \in \mathbb{N}$ for the degree of the multi-index. (In the case $I = \emptyset$ we set $u^a_\emptyset = u^a$.)

Different jets are related by projection maps. The projection $\pi_{k+r,k} : J^{k+r}Y \longrightarrow J^kY$ is defined by erasing the coordinates that do not fit in the jet of lower order. In this structure the infinite jet $J^\infty Y$ is the jet of highest order. That is, it is a space from which there is a projection to every jet of finite order; and one can think of any jet of finite order as a truncation of the infinite jet. This idea is formalized defining the infinite jet by an inverse limit. For notational convenience we denote the infinite jet simply by JY.

Smooth functions on JY are those and only those that can be pulled back from a jet of finite order. Vector fields on JY are derivative operators on the ring of smooth functions.

Given a section $\phi : U \subset M \longrightarrow Y|_U$, its prolongation to the $k-$jet $j^k\phi : U \subset M \longrightarrow J^kY|_U$ is

$$\begin{aligned}j^k\phi(x) = \Bigg(&x^1, \ldots, x^i, \ldots, x^n; \phi^1(x), \ldots, \phi^m(x); \ldots,\\ &\frac{\partial^{|I|}\phi^a}{\partial^{i_1}x^1 \cdots \partial^{i_n}x^n}(x), \ldots\Bigg).\end{aligned} \tag{2}$$

In classical field theory the main objects are not points of Y but sections of Y. Thus, curves of sections and flows of sections will be of primary importance. It turns out that given any section $\phi \in \mathrm{Hists}_U$ the tangent space to the space of sections $T_\phi \mathrm{Hists}_U$ can be properly modeled by objects (vector fields) coming from the jet, but generic vector fields in Hists_U cannot.

A vector field in Y generates a flow of points in Y. Vector fields sending sections into sections without moving points in the base manifold are vertical vector fields

$$V = 0\frac{\partial}{\partial x^i} + V^a\frac{\partial}{\partial u^a}. \tag{3}$$

If the coefficients are allowed to depend on partial derivatives of the field up to finite order this "vector field" (called an *evolutionary vector field*) would generate a flow of sections that if seen in the jet JY would be generated by the vector field in JY

$$jV = \sum_{|I|=0}^{\infty}\left(D_IV^a\right)\frac{\partial}{\partial u^a_I}, \tag{4}$$

where D_i is the total derivative (to be defined below) and where D_I implies a successive application of the total derivative as indicated by the multi index I. The important property of evolutionary vector fields is that they send sections in JY which are prolongations of sections of Y into other sections that are prolongations. The coefficients in the expansion of a vector field in JY in terms of a basis are functions in the jet; that is, they may depend on arbitrarily many, but finite, partial derivatives of the field. When seen from the point of view natural to the infinite dimensional manifold Hists_U the vector fields obtained from vector fields in the jet belong to a very special class; they are called local vector fields. At the end of this section we will mention that at the level of solutions $\mathrm{Sols}_U \subset \mathrm{Hists}_U$ generic vector fields are not local vector fields, and including nonlocal vector fields is essential for a physically appropriate treatment of classical field theory [19, 20].

A convenient basis for differential forms in JY is generated by wedge products of the set of generators $\{dx^i, \vartheta^a_I\}$, where

$$\vartheta^a_I \coloneqq du^a_I - \sum_{j=1}^{n} u^a_{(I,j)} dx^j. \tag{5}$$

Factors of the type dx^i are called "horizontal" and factors of the type ϑ^a_I are called "vertical". The space of p-forms is a direct sum of spaces $\mathbf{\Omega}^{r,s}(JY)$ which are products of exactly r horizontal one forms and s vertical one forms. Since the differential brings up the degree of forms by one, the direct sum structure makes the differential split as a sum of operators

$$\mathsf{d} = \mathsf{d}_\mathsf{h} + \mathsf{d}_\mathsf{v}, \tag{6}$$

where $\mathsf{d}_\mathsf{h} : \mathbf{\Omega}^{r,s}(JY) \longrightarrow \mathbf{\Omega}^{r+1,s}(JY)$ and $\mathsf{d}_\mathsf{v} : \mathbf{\Omega}^{r,s}(JY) \longrightarrow \mathbf{\Omega}^{r,s+1}(JY)$ are characterized by their action on functions

$$\begin{aligned} \mathsf{d}_\mathsf{h} f &= \left(\frac{\partial f}{\partial x_i} + u^a_{(J,i)} \frac{\partial f}{\partial u^a_J} \right) dx^i = \left(D_i f\right) dx^i, \\ \mathsf{d}_\mathsf{v} f &= \frac{\partial f}{\partial u^a_I} \vartheta^a_I. \end{aligned} \tag{7}$$

The differentials of the generators are

$$\begin{aligned} \mathsf{d}_\mathsf{h} dx^i &= 0, \\ \mathsf{d}_\mathsf{v} dx^i &= 0, \\ \mathsf{d}_\mathsf{h} \vartheta^a_I &= dx^i \wedge \vartheta^a_{(I,i)}, \\ \mathsf{d}_\mathsf{v} \vartheta^a_I &= 0. \end{aligned} \tag{8}$$

The following identities are easy to verify:

$$\begin{aligned} \mathsf{d}_\mathsf{h}{}^2 &= 0, \\ \mathsf{d}_\mathsf{v} \mathsf{d}_\mathsf{h} &= -\mathsf{d}_\mathsf{h} \mathsf{d}_\mathsf{v}, \\ \mathsf{d}_\mathsf{v}{}^2 &= 0. \end{aligned} \tag{9}$$

$$\begin{aligned} \iota_X \mathsf{d}_\mathsf{h} F &= -\mathsf{d}_\mathsf{h} \iota_X F, \\ j\phi^* \mathsf{d}_\mathsf{h} G &= d j\phi^* G, \end{aligned} \tag{10}$$

where X is any evolutionary vector field, ϕ is an arbitrary section of Y, F is a differential form of horizontal degree k and vertical degree r, G is a differential form of horizontal degree k and vertical degree 0, and d stands for the de Rham differential in M. In the closely related context of the covariant phase space formulation of classical field theory [18, 21] the counterpart of d_v is the field differential (or variational differential), and d_h leads to the spacetime differential.

Let us consider Hamilton's principle of extremal action for a Lagrangian density of kth order, $L(j\phi(x)) = L(x^i, \phi^a(x), \partial_i \phi^\alpha(x), \partial_{I=(i_1,\ldots 1_k)} \phi^a(x))$. Given a history ϕ, the variation of the action induced by the evolutionary vector field V is written as

$$dS_U\left[V_\phi\right] = \int_U j\phi^* \mathscr{L}_{jV} L = \int_U j\phi^* \iota_{jV} \left(E\left(L\right) + \mathsf{d}_\mathsf{h} \Theta_L\right), \tag{11}$$

where an essential result of calculus of variations says that integration by parts lets us write any differential form of type $\mathbf{\Omega}^{n,1}(JY)$, like $\mathsf{d}_\mathsf{v} L$, uniquely as a source form plus a boundary term, $\mathsf{d}_\mathsf{v} L = I(\mathsf{d}_\mathsf{v} L) + \mathsf{d}_\mathsf{h} \Theta_L$, and we have defined $E(L) = I(\mathsf{d}_\mathsf{v} L)$. (A source form has horizontal degree n and its vertical part is proportional to the generator ϑ^a which sees the variation of the field and not the partial derivatives of the variation.) For a description of the integration by parts operator see [17].

The field equation is written as $j\phi^* E(L) = 0$. Histories solving the field equation are called solutions $\phi \in \mathrm{Sols}_U \subset \mathrm{Hists}_U$. The space Sols_U is an infinite dimensional manifold; the tangent space of a solution $T_\phi \mathrm{Sols}_U$ is generated by variations of the field induced by evolutionary vector fields V satisfying the linearization of the field equation around ϕ. Our notation will be as follows: V induces a tangent vector $v_\phi \in T_\phi \mathrm{Sols}_U$. In this language the conservation of the presymplectic current $\Omega_L = -\mathsf{d}_\mathsf{v} \Theta_L$ follows from $0 = \mathsf{d}_\mathsf{v}{}^2 L = \mathsf{d}_\mathsf{v}(E(L) + \mathsf{d}_\mathsf{h} \Theta_L)$ and is written as the vanishing of the differential form $\mathsf{d}_\mathsf{h} \iota_{jW} \iota_{jV} \Omega_L$ when restricted to points of the jet $j\phi(x)$ which are the image of a solution and when both inserted variations satisfy the linearization of the field equation around ϕ. If we integrate $\mathsf{d}_\mathsf{h} \iota_{jW} \iota_{jV} \Omega_L$ on a hypersurface Σ we obtain the functional $\int_\Sigma j^* \phi \iota_{jW} \iota_{jV} \Omega_L$ measuring the presymplectic product of the variations induced by V and W which due to the conservation law is insensitive to deformations $\Sigma' = \Sigma + \partial B$.

Vector fields in Sols_U, assignments of tangent vectors to points, are not properly modeled by objects of the jet. It turns out that for nonlinear PDEs generic vector fields in Sols_U are not local. In particular, we will see later on in the paper that for vacuum general relativity Anderson and Torre [15, 22] showed that the set of local vector fields do not generate all the nontrivial flows in Sols that are relevant to study field theory. Generic flows in Sols_U are generated by nonlocal vector fields in Sols_U.

For example, if we are interested in using two vector fields v, w in Sols_U to insert them in the presymplectic form to obtain the functional that calculates their presymplectic

product, the calculations leads to the integral of a conserved current that is nonlocal. We will change our notation to accommodate for nonlocal objects; we will write

$$\omega_{L\,\Sigma}(v,w)[\phi] = \int_{\Sigma} \widetilde{\Omega}_L(v,w)[\phi], \tag{12}$$

where the presymplectic current evaluated on tangent vectors to a given solution is the same that we defined above, but if we insert tangent vectors which do not vary locally (when the solution is modified) the result is not a differential form in the jet.

When dealing with nonlocal objects (like nonlocal vector fields or nonlocal currents) we will work at the level of sections and modify the notation as done with the functional written above. Thus, symbols with a tilde denote $n-1$ forms in M which depend on the field (possibly in a nonlocal way) and on (possibly nonlocal) vector fields. An important remark is that we do not need to define the objects with tildes separately because if a given solution is chosen with the aim of evaluating the functional, we can work with local objects using the formulas written above using the language of the jet.

According to the terminology that we declared in the introductory section, the functional $\omega_{L\,\Sigma}(v,w)$ is not hypersurface local.

2.2. Example: Two-Dimensional Abelian BF Theory. This example will take place considering that spacetime is a cylinder, $M = \mathbb{R}\times S^1$. We can consider that the region of interest is $U = [t_i, t_f]\times[\theta_i,\theta_f]$.

The fields that we will consider are a 1-form in M, which we call A, and a 0-form, which will be denoted by B. The field bundle is $Y = T^*M \oplus M\times\mathbb{R}$. We could continue calling the total field ϕ, but we choose to change to a more descriptive symbol. A history in U will be denoted by $Æ : U \longrightarrow Y|_U$. We choose a chart in U with coordinates (t,θ), and in Y we denote points using the induced local trivialization. Then the evaluation of a section may be written as $Æ(t,\theta) = (t,\theta; A_t(t,\theta), A_\theta(t,\theta), B(t,\theta))$. We may also use a more compact notation $Æ(x) = (x^i; A_i(x), B(x))$

The evaluation of the prolongation of the section in the jet is written as $jÆ(x) = (x^i; A_i(x), B(x); v_{ij} = \partial_j A_i(x), v_j^B = \partial_j B(x); \ldots)$. The curvature of A is denoted by F and in the local trivialization it is written as $F_{ij}dx^i\wedge dx^j = (1/2)(v_{ji} - v_{ij})dx^i\wedge dx^j$. When pulled back to M, the curvature yields a two form which is determined by a function specifying the proportionality factor with respect to the area form $dt\wedge d\theta$ given by the chart.

The basis for tangent vectors in the jet induced by the chart can be written as $\{\partial_i = \partial/\partial x^i, \partial^j = \partial/\partial A_j, \partial_B = \partial/\partial B; \partial^{ji} = \partial/\partial v_{ji}, \partial_B^j = \partial/\partial v_j^B; \ldots\}$. The basis of one forms adapted to the vertical horizontal decomposition is $\{dx^i, \vartheta_j = dA_j - v_{ji}dx^i, \vartheta^B = dB - v_i^B dx^i; \vartheta_{ji} = dv_{ji} - v_{jik}dx^k, \vartheta_i^B = dv_i^B - v_{ik}^B dx^k; \ldots\}$. Notice that we have simplified the natural notation in the sense that we could have decided to write ϑ_j^A instead of the simplified symbol ϑ_j and the same for all the vertical generators related to partial derivatives of the A field. Then we are using a notation in which the presence of a super index B means that it is related to the B field and the absence of a superscript means that it is related to the A field.

We live as an exercise to the reader to calculate the horizontal and vertical differentials of the coordinate functions that we chose for JY. The most relevant in the calculations below are $\mathsf{d}_{\mathsf{v}}B = \vartheta^B$, $\mathsf{d}_{\mathsf{v}}F_i j = (1/2)(\vartheta_{ji} - \vartheta_{ij})$, $\mathsf{d}_{\mathsf{h}}B = v_j^B dx^j$, $\mathsf{d}_{\mathsf{h}}\vartheta_i = dx^j\wedge\vartheta_{ij}$.

We consider the first order action

$$S_U[Æ] = \int_U jÆ^* BF. \tag{13}$$

This is the two-dimensional version of a class of field theories whose quantization was called "quantum cohomology" by Horowitz in the paper [23] where he introduces BF theories as nonabelian generalizations of this class of field theories.

We start calculating $\mathsf{d}_{\mathsf{v}}L$; we obtain

$$\mathsf{d}_{\mathsf{v}}L = \left(\vartheta^B F_{ij} + \frac{1}{2}B\left(\vartheta_{ji} - \vartheta_{ij}\right)\right)dx^i\wedge dx^j. \tag{14}$$

After integration by parts (to get rid of differential forms which see partial derivatives of the variation) we obtain

$$\mathsf{d}_{\mathsf{v}}L = \left(v_i^B\vartheta_j + F_{ij}\vartheta^B\right)\wedge dx^i\wedge dx^j + \mathsf{d}_{\mathsf{h}}\left(-B\vartheta_j\wedge dx^j\right). \tag{15}$$

From this calculation we can read the field equations (which turn out to be linear)

$$\begin{aligned} dB &= 0,\\ dA &= 0, \end{aligned} \tag{16}$$

and also the presymplectic current

$$\Theta_L = -B\vartheta_j\wedge dx^j, \tag{17}$$

$$\Omega_L = \vartheta^B\wedge\vartheta_j dx^j. \tag{18}$$

The space of solutions in this example is formed by pairs consisting of a constant function (the B field) and a closed 1-form (the A field). Notice that since the field equations are linear, perturbations of the field obey the same equations.

This example is completely different from general relativity in the sense that vector fields in the space of solutions can be modeled by local vector fields. The field equations and the linearized field equations are linear, and every class of solutions modulo gauge contains local representatives. Then if we work with only local fields and local vector fields the description continues being physically appropriate.

In the next section we will be able to comment on the space of solutions modulo gauge. Then it will be clear why is that Horowitz called the quantization of this class of theories quantum cohomology.

3. Gauge from Holography

Consider a solution of the field equations ϕ and a hypersurface Σ separating spacetime into two connected components

U_1 and U_2 that intersect along Σ. Clearly, if we restrict the solution to one of the components we get a solution in a restricted domain $\phi_i = \phi|_{U_i}$. Consider a different solution ϕ_1' over subdomain U_1 such that its restriction to Σ coincides with ϕ_1 up to its partial derivatives of order k and recall that the field equation is of order $k+1$. It is fact that we could cut and paste to replace the portion of solution over U_1 with ϕ_1' and generate a different solution $\phi' = \phi_1' \#_\Sigma \phi_2$. As far as the field over U_2 is concerned, the cut and paste operation is not physically relevant. In the case in which the field in U_1—the system of interest—is being studied through measurements at $\Sigma = \partial U_1 = U_1 \cap U_2$, the field configurations ϕ_1 and ϕ_1' are not distinguishable by any measuring device. Therefore a natural extension to Newton's principle of determinacy to this scenario requires declaring ϕ_1 and ϕ_1' as physically equivalent.

Let us study the cut and paste operation just described. Consider two domains intersecting at a hypersurface Σ in such a way that they form a composite domain $U = U_1 \cup U_2$. If the field $\phi = \phi_1 \#_\Sigma \phi_2$ is considered as smooth at each subdomain but only continuous over Σ, the variation of the action for the composite domain $dS_U[W_\phi] = (dS_{U_1} + dS_{U_2})[W_\phi]$ includes a term

$$\int_\Sigma \left(j\phi_1^* - j\phi_2^*\right) \iota_{jW} \Theta_L. \tag{19}$$

A physical field in U must be an extremum of the action for all variations vanishing at zeroth order over ∂U. That is, the allowed variations do not affect the evaluation of the field at the boundary, but they can induce changes in the partial derivatives of the field at the boundary. Given a history $\phi \in \mathrm{Hists}_U$, let us call $\mathbb{V}_\phi^{\partial U} \subset T_\phi \mathrm{Hists}_U$ the space of variations considered by Hamilton's principle of extremum action. As described in the previous section, we will model $T_\phi \mathrm{Hists}_U$ by evolutionary vector fields in the jet. We will study the conditions for extremality of the action in two steps corresponding to a decomposition of $\mathbb{V}_\phi^{\partial U}$ as a sum of two of its subspaces $\mathbb{V}_\phi^{\partial U} = \mathbb{V}_\phi^{\partial U_1, \partial U_2} + \mathbb{W}_\phi^{\partial U, U_1, U_2}$, where the first summand is the space of variations vanishing at zeroth order over ∂U_1 and ∂U_2 and the second summand is the space of variations vanishing at zeroth order over ∂U and satisfying the linearization of the field equation (possibly with source if ϕ is not a solution) in the interior of the domains U_1 and U_2. Consider an arbitrary $V \in \mathbb{V}_\phi^{\partial U}$; it generically does not belong to $\mathbb{V}_\phi^{\partial U_1, \partial U_2}$ because it may not vanish at zeroth order over $\Sigma \setminus \partial\Sigma$. However since the restriction to $\Sigma \setminus \partial\Sigma$ of the zeroth order component of elements of $\mathbb{W}_\phi^{\partial U, U_1, U_2}$ is completely unconstrained, there is a (possibly not unique) $W \in \mathbb{W}_\phi^{\partial U, U_1, U_2}$ such that $V - W \in \mathbb{V}_\phi^{\partial U_1, \partial U_2}$.

Thus, the extremality of the action is equivalent to demanding first extremality with respect to variations in $\mathbb{V}_\phi^{\partial U_1, \partial U_2}$ and later extremality with respect to variations in $\mathbb{W}_\phi^{\partial U, U_1, U_2}$. We know that the first condition is equivalent to imposing the field equation in the interior of the domains U_1 and U_2. The second condition does not impose any further restriction to the field in the interior of the domains U_1 and U_2, but it requires that (19) vanishes for every $W \in \mathbb{W}_\phi^{\partial U, U_1, U_2}$. Integration by parts is unnecessary if $\Theta_L|_\Sigma$ is already a source form, as happens with the usual definition. The resulting gluing field equation of order k demands that the V-momentum crossing Σ coming from U_1 needs to match the V-momentum crossing Σ coming from U_2.

Because of our interest in the type of relative measurements described in Section 1, we are particularly interested in the propagation of variations of the field through hypersurfaces. Consider a one parameter family of fields ϕ_t (starting at $\phi_{t=0} = \phi$ and generated by the flow of the vector field $v = v_1 \#_\Sigma v_2$) satisfying the field equation in U_1 and U_2 and solving the gluing problem over Σ for each value of the parameter. Now we are considering vector fields in Sols_U, and as we mentioned earlier, restricting to local vector fields could be physically inappropriate. Following the notation of Section 2 , we will indicate vector fields in the space of solutions by lower case letters and they will be inserted in multilinear operators denoted by letters with a tilde over them indicating that they are defined at the level of sections and they may be nonlocal. Recall that we do not need to define the objects with tildes separately because if a given solution is chosen with the aim of evaluating the functional, we can work with local objects using the formulas written in the language of the jet. Since (19) vanishes for any $W \in \mathbb{W}_\phi^{\partial U, U_1, U_2}$ when evaluated at $\phi_t = \phi + tv + O(t^2)$; then up to first order in the t parameter $(\Theta_L(j(\phi + t(v_1 - v_2)))|_\Sigma$ vanishes when restricted to $\mathbb{W}_\phi^{\partial U, U_1, U_2}$. Thus, the linearized gluing field equation for the vector field $v = v_1 \#_\Sigma v_2$ is the requirement that

$$\left(\left(\mathscr{L}_{v_1 - v_2} \widetilde{\Theta}_L\right)(w)\right)[\phi]\Big|_\Sigma = -\widetilde{\Omega}_L(v_1 - v_2, w)[\phi]\Big|_\Sigma, \tag{20}$$

vanishes for any $w \in \mathbb{W}_\phi^{\partial U, U_1, U_2}$. A more convenient statement is that for any solution ϕ and any w satisfying the linearized field equations (20) vanishes up to an exact differential linear in w. Our derivation of (20) uses $\mathscr{L}_x = \iota_x \delta + \delta \iota_x$, where δ stands for the field derivative, and the property that $(v_1 - v_2)_\phi|_\Sigma = 0$ implies that $(v_1 - v_2)_\phi$ is in the kernel of $\widetilde{\Theta}_L|_\Sigma$.

It is interesting to characterize pairs of perturbations V_1 and V_1' in U_1 that would be compatible with the same perturbation V_2 on U_2. There are two conditions: the first one is a continuity requirement along Σ, stating that the perturbations evaluated at the hypersurface agree. This condition, written in terms of their difference $x = v_1' - v_1$, is the zeroth order condition $x|_\Sigma = 0$. The second condition arising from the linearized gluing equation is that $\widetilde{\Omega}_L(x, w)[\phi]|_\Sigma$ be an exact differential for any solution ϕ and for any vector field w in Sols_U. This condition carries information about the perturbations in the bulk of U_1 because, even when it is a condition imposed at Σ, it is sensitive to directional derivatives of the perturbation in directions transversal to the hypersurface. Moreover, of the two conditions the second one is the only one capable of transmitting information about x in the bulk from U_1 to U_2 through Σ. We will call $v|_\Sigma$ the *holographic imprint* of a perturbation; the second condition compares the holographic imprint of two perturbations and it decides if they are distinguishable or not. Notice that, this

condition is linear in X and it may have a nontrivial null space. In that case, there would be some perturbations which are different in the bulk of U_1, but such that their difference $x = v_1' - v_1 \neq 0$ cannot be resolved by this condition; those aspects of bulk perturbation are filtered out by the gluing condition at Σ and do not couple to v_2.

Now let us consider a spacetime domain U without any physical division into subdomains, and study the propagation of perturbations through thought hypersurfaces arbitrarily placed inside U. A vector field x satisfying the condition $x|_\Sigma = 0$ for every hypersurface $\Sigma \subset U$ is the zero perturbation $x = 0$. On the other hand, there may be nonzero vector fields x such that

$$\widetilde{\Omega}_L(x, w)[\phi] \quad \text{is an exact differential} \tag{21}$$

for any solution ϕ and any vector field w in Sols_U. Such a vector field hits a hypersurface $\Sigma \subset U$ leaving a *null holographic imprint*, one that necessarily loses all information transversal to the hypersurface, for *any* hypersurface. The conservation law for the presymplectic current described in Section 2 implies that $\widetilde{\Omega}_L(x, w)[\phi]|_\Sigma$ is an exact differential for a given hypersurface Σ if and only if it is also an exact differential for any homologous hypersurface $\Sigma' = \Sigma + \partial B$. Notice that vector fields of this type form a vector space. If these perturbations are regarded as physically irrelevant, and the space of physical perturbations is considered to be the quotient vector space in which perturbations satisfying condition (21) are identified with zero, then we could say that physical perturbations are those capable of transmitting holographic information. This is a mild type of holographic principle which in the context of this work, where spacetime geometry has not been fixed a priori, may be thought of as the covariant ingredient needed for Newton's principle of determinism. Elevating this to a definition is described in the title of this article with the phrase *gauge from holography*. In Section 5 we will talk about local gravitational observables exhibiting holographic behavior; there our use of the term holographic is in the stronger sense meaning that the observables can be evaluated through integration over codimension two surfaces.

Relativity and locality of measurement motivate the second condition needed in our definition of gauge perturbations. The simplest way to present it is recalling that we were searching for conditions for two variations of the field v_1, v_1' on a spacetime domain U_1 to be indistinguishable to any field perturbation v_2 over the spacetime domain U_2 intersecting with U_1 at Σ. Now we will consider the situation in which we have one domain of interest $U \subset M$ with two perturbations v, v' and we look for conditions that make those two perturbations indistinguishable to any perturbation w of the field in the complement of U. Those indistinguishable perturbations will be called gauge related in U. Because perturbations in U are judged with respect to perturbations in its complement, it makes sense to demand that gauge perturbations do not disturb the reference system. Then since ∂U separates U from its complement, we should demand that a gauge vector field x act trivially in the boundary

$$\left(x_\phi\right)\Big|_{\partial U} = 0 \quad \text{for any solution.} \tag{22}$$

Now we comment on locality of measurement. Consider a situation in which spacetime M has a Cauchy surface $\widetilde{\Sigma}$ without boundary and where there is an observable of interest which is calculated as the integral of a gauge invariant current, e.g., $f_{\widetilde{\Sigma}}[\phi] = \int_{\widetilde{\Sigma}} \widetilde{F}[\phi]$. We may calculate $f_{\widetilde{\Sigma}}[\phi]$ as a sum of local contributions one of which corresponds to our spacetime domain of interest as $f_\Sigma[\phi] = \int_\Sigma \widetilde{F}[\phi]$, where $\Sigma = \widetilde{\Sigma} \cap U$. The locality condition amounts to requiring that for any gauge invariant current. (A current $\widetilde{F}$ is declared to be invariant under vector field x in the space of solutions if and only if $\mathscr{L}_x \widetilde{F}[\phi]$ is a pure divergence for any solution.) and for any hypersurface with $\partial\Sigma \subset \partial U$ integrals of the type $f_\Sigma[\phi]$ can be evaluated and are gauge invariant. The locality condition is satisfied if (22) holds. If we do not impose that gauge transformations act trivially on the boundary we would end up in a situation in which $f_{\widetilde{\Sigma}}[\phi]$ is a gauge invariant observable which may be calculated as a sum of local pieces, but in which the terms of the sum are not gauge invariant individually.

Definition 1 (Gauge vector fields in U). A vector field x in Sols_U is declared to be a gauge vector field if and only if x_ϕ is in the null space of the linearized field equation for every hypersurface and every solution ϕ, and it additionally vanishes at ∂U. More precisely, we demand that

(i) x satisfies (21);

(ii) x satisfies (22).

Isolated gravitational systems may be modeled over a spacetime domain of the type $U = \Sigma \times [0, 1]$ with the boundary $\partial\Sigma \times [0, 1]$ representing a world tube at spatial infinity (and possibly an inner boundary modeling a horizon). Our framework applies to any Lagrangian formulation of general relativity, where it is known that all generators of diffeomorphisms x induce perturbations such that $\widetilde{\Omega}_L(x, w)[\phi]$ is a pure divergence [24], which implies that x satisfies Condition (i) of the definition of gauge vector fields. However, regarding variations that do not vanish at infinity as gauge is inappropriate since they modify the reference frame needed to define energy, momentum and angular momentum. Thus, preserving a reference frame at the boundary that may be used as a reference for measurements is another motivation for Condition (ii) of the definition of gauge.

The standard definition for gauge perturbations used in Lagrangian field theory (appropriate in manifolds with no boundary) is in terms of families of symmetries of the Lagrangian depending on a parameter that may be locally varying, and through Noether's second theorem this is related to ambiguities and over determination in the field equation (see [21]). It is known that the standard definition implies our Condition (i), and there are works which have conjectured that Condition (i) may be equivalent to that definition (see for example [25]).

It can be verified that this definition of gauge perturbations leads to a Lie subalgebra of the algebra of vector fields in Sols_U and to a notion of gauge equivalence among solutions; see [26] for a proof.

Now it may be illustrative for the reader to go back to the two-dimensional abelian BF theory example. We have already calculated Ω_L for that example in (17). It is not difficult to show that condition (21) for the vector field in the space of solutions implies that it must generate transformations in the closed one form by exact forms, i.e., $A' = A + df$ for some function of the base manifold f.

Recall that in the example spacetime was a cylinder $M = \mathbb{R} \times S^1$. If the domain of interest is the whole spacetime we can ignore Condition (ii) for gauge vector fields. In this case the space of solutions modulo gauge is the two-dimensional space parametrizing constant functions (the B field) and cohomology classes of 1-forms (the A field). On the other hand, if there are boundaries in the region of interest U the space of solutions modulo gauge is larger. The usual space of solutions modulo gauge would be recovered only after gluing all the regions of our subdivision of spacetime. In the next subsection we will see that Condition (ii) allows for the existence of nontrivial observables measuring A degrees of freedom in bounded regions U of spacetime.

4. Observables from Currents

It is natural to consider functions of the field calculated integrating currents over hypersurfaces. If the currents depend locally on the field and its partial derivatives those functions may be written as $f_\Sigma[\phi] = \int_\Sigma j\phi^* F$; in the general case we use the notation

$$f_\Sigma[\phi] = \int_\Sigma \widetilde{F}[\phi]. \tag{23}$$

This functional is gauge invariant if the hypersurface is such that $\partial\Sigma \subset \partial U$ and the current is gauge invariant in the sense that for every gauge vector field x and every solution ϕ the Lie derivative of the current $\mathscr{L}_x \widetilde{F}[\phi]$ yields a pure divergence. Moreover, a current is conserved if when evaluated on any solution the function does not depend on local deformations of the hypersurface of the type $\Sigma' = \Sigma + \partial B$. In this case the resulting observable is a function of the solution ϕ defined by the current (and the homology type of the surface).

A physical observable f is spacetime local if it is calculated integrating a density which depends on finitely many partial derivatives of the field. A physical observable f_Σ calculated integrating a current is said to be hypersurface local if the current $\widetilde{F}|_\Sigma$ depends on finitely many partial derivatives of the field; for those currents we could write $\widetilde{F}[\phi]|_\Sigma = j\phi^* F|_\Sigma$ for some differential form F in the restriction of the jet to Σ. The locality of an observable current $\widetilde{F}$ can also be determined by an almost locally Hamiltonian vector field v associated with it; if v is a depends on finitely many partial derivatives of the field then the current is local and the observable is hypersurface local. Consider a field theory which admits a formulation in terms of initial data. Call T_Σ the map sending initial data to solutions. We can use the pull-back map T_Σ^* to transform spacetime covariant functionals into functionals of initial data. Since this procedure involves integrating nonlinear equations, it is generically a nonlocal procedure which transforms spacetime local functionals into functionals which fail to be hypersurface local.

There are very few hypersurface local observables, but we will see in this section that there are plenty of (possibly nonlocal) observables calculated integrating currents. One reason to suspect it is that T_Σ^* transforms every spacetime observable into an observable depending on initial data and if the resulting observable is a current (calculated with a collection of maps T_Σ^* labeled by the integrating hypersurface), it must be conserved.

Here we will consider this type of observables where the domain of definition of the current may be a proper open subset of the space of fields [27]. Consequently, we consider physical observables which may be only defined in certain open domain of the space of solutions.

Since in this work we will refer multiple times to (possibly nonlocal) gauge invariant conserved currents defined in an open domain of the space of solutions, we will use the term *observable current* to refer to a current of this type.

In order to make definitions a bit more concrete let us consider as an example two-dimensional abelian BF theory as defined in Section 2.2. The field equation for the A field is $dA = 0$; then A is a conserved current and the functional

$$hol_\Sigma[Æ] = \int_\Sigma A \tag{24}$$

is gauge invariant if $\partial\Sigma \subset \partial U$. That is, the functional hol_Σ is defined in the space of solutions modulo gauge in U, and its value is independent of deformations of the integrating surface of the form $\Sigma' = \Sigma + \partial R$ with $R \subset U$.

Notice that if Condition (ii) for gauge vector fields were not present we would not have a gauge invariant observables measuring A degrees of freedom in bounded domains. In that situation, if we glued a collection of bounded domains $\{U_I\}$ that covered spacetime $M = \mathbb{R} \times S^1$ we would discover that even when there were no observables measuring the A field in each of the domains U_I, after gluing them all together an observable measuring the holonomy of A around a noncontractible loop in the cylinder would appear. In contrast, in our setting the mentioned physical observable in M is the sum of local contributions which when considered in the bonded spacetime regions where they are defined are gauge invariant with respect to the appropriate notion of gauge (not with respect to the notion of gauge relevant when the region under study is the complete spacetime).

The resulting family of observables is a large family capable of distinguishing solutions which are not gauge related. Thus, the family of observables includes Noether charges for systems with simple Lagrangian symmetries whose generators are defined everywhere in the domain of the Lagrangian density, and it includes many more observables. Two aspects of our treatment are essential for proving separability of points in the space of solutions modulo gauge: The first one is properly modeling the space of variations of a given solution and the space of vector fields in Sols_U as discussed in Section 2. The second essential aspect is allowing observables which are not defined for all fields, but which are defined only in a certain open domain in Sols_U. This will allow a tight correspondence between the differential of

observable currents and almost locally Hamiltonian vector fields. A locally Hamiltonian vector field v in U is a vector field in Sols_U which preserves the multisymplectic form in the sense that for any solution ϕ and any two vector fields w, z in Sols_U

$$\left(\mathscr{L}_v \widetilde{\Omega}_L\right)(w,z)\,[\phi] \quad \text{is an exact differential vanishing at } \partial U. \tag{25}$$

Locally Hamiltonian vector fields in U preserve the presymplectic forms $\omega_\Sigma(w,z)[\phi] = \int_\Sigma \widetilde{\Omega}_L(w,z)[\phi]$ defined using any hypersurface with $\partial\Sigma \subset \partial U$. An *almost locally Hamiltonian* vector field is a solution of the linearized field equation satisfying a version of (25) in which the condition that the exact differential should vanish at ∂U is not imposed. Thus, almost locally Hamiltonian vector fields may not preserve the presymplectic forms due to boundary terms. The importance of this type of vector fields for us is that given a solution ϕ we can model the tangent space of the space of solutions $T_\phi \mathrm{Sols}_U$ by vertical vector fields in the jet satisfying the linearized field equation which moreover are almost locally Hamiltonian; we drop the condition over ∂U for the boundary term in (25) because it could become an obstruction to generating $T_\phi \mathrm{Sols}_U$. There is an alternative to working with almost locally Hamiltonian vector fields, if the domain of interest is of the form $U = \Sigma \times [0,1]$, it is endowed with a foliation by Cauchy surfaces Σ_t, and we are only interested in evaluating integrals on hypersurfaces belonging to the foliation. The alternative is to work with locally Hamiltonian vector fields using a version of (25) in which the exact differential is required to vanish only over $\partial\Sigma \times [0,1]$. This alternative does not make sense if the metric is not such that the leaves of the foliation are Cauchy surfaces. If the gravitational field is part of the system under study, using this alternative implies considering only some allowed fields. For a discussion see Appendix A .

The linearized field equation is a nonlinear partial differential equation, which is linear only when not studied in the whole jet, but only on $j\phi(U)$ for a fixed solution ϕ; thus when the linearized field equation is considered in the jet, its solutions may exist only in a certain open domain. Since we are interested in providing conserved currents which are linked to given solutions of the linearized field equation, it is important for us to consider conserved currents which may be defined only on a certain open domain. Given any almost locally Hamiltonian vector field v there is a (nonempty) family of observable currents which have it as their associated almost Hamiltonian vector field. That is, for any solution of the field equation ϕ there is a family of observable currents such that for any vector field w in Sols_U

$$\left(\mathscr{L}_w \widetilde{F} + \widetilde{\Omega}_L(v,w)\right)[\phi] \tag{26}$$

is an exact differential. Thus, the derivative of $f_\Sigma[\phi]$ in the direction of a perturbation w, which we will write as $\mathscr{L}_w f_\Sigma[\phi]$, is given by $-\omega_\Sigma(v,w)[\phi]$ except for a boundary term which would vanish if the integrating hypersurface has no boundary or if w_ϕ vanishes over $\partial\Sigma$.

It turns out that, in field theories with local degrees of freedom, observable currents can distinguish gauge inequivalent solutions. A local version this statement is as follows: Consider any given solution ϕ and any given curve of solutions ϕ_t starting at $\phi_0 = \phi$ and determined by a vector field w in Sols_U which is not a gauge vector field. We will see that

$$\left.\frac{d}{dt}\right|_{t=0} f_\Sigma[\phi_t] \neq 0. \tag{27}$$

Now we sketch the main part of the proof leaving out a case whose treatment requires a more detailed calculation for Appendix B.

There are two nonexclusive possibilities for w not being a generator of gauge transformations; the first one is that condition (21) fails and the second one is that condition (22) fails. Consider now the case in which condition (21) does not hold for w. Thus, there is a solution ϕ, a vector field v in Sols_U and a point p in the interior of U such that. Now we will denote points in spacetime by the letter p in order to avoid confusion with our notation for vector fields in the space of solutions.

$$\widetilde{\Omega}_L(w,v)\,[\phi]\,(p) \quad \text{is } \underline{\text{not}} \text{ an exact differential.} \tag{28}$$

At this stage, our argument needs a concrete statement for the properties assumed about field theories with local degrees of freedom. We assume that in a theory with local degrees of freedom all perturbations of the field which are not gauge generators have conjugated perturbations which are localized; more precisely, given (i) any point $p \in U$, (ii) any solution ϕ and (iii) a w satisfying the condition stated in (28), we assume that there must be a hypersurface Σ containing p (in which we chose an auxiliary volume element vol_Σ) and a choice of v vector field in Sols_U (which can be chosen to be almost locally Hamiltonian) such that (28) holds and where $(\widetilde{\Omega}_L(w,v)[\phi])|_\Sigma = \lambda \mathrm{vol}_\Sigma$ with the proportionality constant λ satisfying $\lambda(p) > 0$ and $\lambda|_{\mathscr{U}} \geq 0$ where $\mathscr{U}$ is a neighborhood of p contained in the interior of Σ such that $v|_{\Sigma\setminus\mathscr{U}} = 0$. Then

$$\left.\frac{d}{dt}\right|_{t=0} f_\Sigma[\phi_t] = \int_\Sigma \mathscr{L}_w \widetilde{F}[\phi] = -\omega_\Sigma(w,v) > 0, \tag{29}$$

which concludes the part of the proof that we give in the main body of the article.

Previous works on similar approaches to classical field theory argue that there are not many physical observables arising from integrating conserved currents besides Noether charges (see for example [18, 28–31]). The definitions on which our work is based differ from those used in the cited literature in two aspects: First, we allow for nonlocal currents. Second, the currents that we consider may be defined only in a certain open domain in Sols_U. The previous paragraph shows that the observable currents considered here are an interesting source of physical observables.

The case that was not covered in the proof given above is that relation (22) fails, which means that there is a solution ϕ and a point $p \in \partial U$ such that $w_\phi(p) \neq 0$. Since the subcase in which (21) fails was treated above, considering the case where

(22) fails and (21) holds would conclude the proof; this is the case in which W is not a gauge perturbation only because it fails to vanish over ∂U — a "would be gauge" perturbation. Since this part of the proof involves detailed expressions of the boundary terms we deal with it in Appendix B.

Before closing this section we comment on the type of measurements of the bubble chamber, which are not properly modeled integrating currents. We consider that if the field of interest ϕ couples with the measuring field ψ in such a way that gauge equivalent fields $\phi_A \sim \phi_B$ are resolved, it should be claimed that the measuring field significantly disturbs the system, and the actual field being measured is the one corresponding to the composite system. If the system is not considerably disturbed, the measurement induces a perturbation of the field satisfying the linearized field equation (which could be chosen to be almost locally Hamiltonian). In this scenario, the tools provided in this section show that an alternative equivalent description of the measurement is constructed integrating a conserved current.

5. Hypersurface Local Gravitational Observables Are Holographic

We saw that a perturbation of the field modeled by an almost locally Hamiltonian vector field v is related to a family of observable currents by (26). If we call an element of this family $\widetilde{F}_0$ all the other elements of the family differ from it by "a constant" $\widetilde{F} = \widetilde{F}_0 + K$, where an observable induced by the "constant" k_Σ is "field independent except for possible field dependence" due to boundary terms; in particular, when $\partial\Sigma = \emptyset$ the observable k_Σ is truly field independent. Another important aspect of the relation set up by (26) is that given an observable current $\widetilde{F}$ there is a whole class of almost locally Hamiltonian vector fields related to it. The difference between any two such perturbations $x = v_1 - v_2$ satisfies (21).

The results described in the previous section show that the family of observable currents and perturbations satisfying (26) is capable of distinguishing gauge inequivalent solutions. This suggests that all observable currents may satisfy that equation for a given almost locally Hamiltonian perturbation, and the intuition turns out to be a fact. For a more thorough explanation see [26].

Consider observables calculated integrating conserved currents of the type f_Σ as defined in (23) in a bounded spacetime domain with the topology of a four ball. In such a domain the homology type of a hypersurface with $\partial\Sigma \subset \partial U$ is determined by the spacetime codimension two surface $S = \partial\Sigma$. (Hypersurfaces Σ and Σ' are considered homologous if $\Sigma' = \Sigma + \partial B$ where B is dimension n manifold with boundary contained in the closed spacetime domain U.) Due to the conservation law, evaluation of this type of observables depends only on the homotopy type of Σ, and in this situation Σ's homotopy type is determined by S. Additionally, after our notion of gauge excluded perturbations which do not propagate trough hypersurfaces, the field modulo gauge in the interior is determined by $j\phi|_{\partial U}$. Thus, the evaluation of an observable of this type is determined by S and by $j\phi|_{\partial U}$. This result suggests studying an interesting subclass of these observables such that their evaluation depends on $j\phi|_S$ even if the evaluation cannot be achieved integrating a differential form on S. We will see below that in the case of general relativity hypersurface local observables of the type f_Σ can be evaluated as integrals of differential forms over $S = \partial\Sigma$.

Let us recall the terminology declared in the introductory section now that we have developed concepts and notation that let us be more explicit. A physical observable f is spacetime local if it is calculated integrating a density which depends on finitely many partial derivatives of the field. A physical observable f_Σ calculated integrating a current is said to be hypersurface local if the current $\widetilde{F}|_\Sigma$ depends on finitely many partial derivatives of the field; for those currents we could write $\widetilde{F}[\phi]|_\Sigma = j\phi^* F|_\Sigma$ for some differential form F in the restriction of the jet to Σ. The locality of an observable current $\widetilde{F}$ can also be determined by an almost locally Hamiltonian vector field v associated with it; if v depends on finitely many partial derivatives of the field, then the current is local and the observable is hypersurface local. We also mentioned in the introduction that for a field theory admitting a formulation in terms of initial data, the integration of the field equations induces a map which generically sends local spacetime covariant functionals into functionals of initial data which fail to be hypersurface local.

Consider general relativity on a spacetime domain U. The field describing the system is the spacetime metric g_{ab} and perturbations are written as $g_{ab} \longmapsto g_{ab} + h_{ab}$. A perturbation corresponding to a (possibly field dependent) diffeomorphism generator $X[g]$ has the form $h^X_{ab}[g] = \nabla_{(a}X_{b)}[g]$. It is a well-known fact that for general relativity perturbations corresponding to diffeomorphisms satisfy the linearized field equation and satisfy (21); that is, their insertion in the presymplectic current yields a pure divergence (see for example [24]). According to our definition, the gauge generators of general relativity in the given domain turn out to be vector fields generating diffeomorphisms whose restriction to ∂U is the identity.

Then the observables related to a gauge vector field x by (26) yield no information because they are field independent. However, if x satisfies (21) but does not vanish over ∂U its associated observables $f^x_\Sigma[g]$ do carry nontrivial information. Those observables may have a field dependence due to boundary terms

$$f_\Sigma[g] = \int_\Sigma \widetilde{F}^x[g] = \text{const.} + \int_{\partial\Sigma} \widetilde{\sigma}^x[g], \tag{30}$$

where $\widetilde{\sigma}^x$ is a field dependent $n-2$ differential form. Even when these observables are initially written in terms of bulk fields, they can be calculated as integrals on the boundary of the integrating hypersurface; one may say that those observables are holographic.

Anderson and Torre [15, 22] proved that the only solutions of the linearized field equation for vacuum general relativity in the absence of matter $h_{ab}(jg(x)) = h_{ab}(x, g, \partial_x g, \ldots)$ depending on an arbitrary, but finite, number of partial derivatives of the metric are

$$h_{ab} = h^X_{ab} + cg_{ab}. \tag{31}$$

Their result shows that, apart from rescaling generators, all *local* vector fields in Sols_U are gauge or "would be gauge" vector fields. Moreover, since rescaling generators are not almost locally Hamiltonian vector fields, those vector fields are not associated with gravitational observables. A corollary of Torre [16] can be read as saying that *all hypersurface local gravitational observables (in the vacuum) are holographic*.

In the next section we will exhibit a family of holographic gravitational observables and a large family of nonholographic gravitational observables.

In contrast to the case of general relativity, as discussed in Section 2.2 the example of two-dimensional abelian BF theory is so simple that local fields and local vector fields are enough for a physically reasonable model of the system. The observable currents that we exhibited in Section 4 for that field theory are local and the induced observables hol_Σ are not holographic. However if the domain of interest is not the cylinder spacetime but a domain U with the topology of a ball, the closed form A becomes exact when restricted to U, and the observables hol_Σ are indistinguishable from observables which are holographic.

Khavkine has proposed a generalized notion of spacetime local observables and exhibited a large family of gravitational observables which are spacetime local according to his definition [27]. As mentioned previously, if those observables are transformed into functionals of initial data and those functionals turn out to be integrals of currents, they would generically be nonlocal observable currents.

6. Examples of Gravitational Observables, Holographic and Not Holographic

For the sake of concreteness, in this section we will consider a spacetime domain U with the topology of a four ball.

There are many gravitational observables in our setting. According to the conventions stated in the previous paragraph, the components of the induced metric on the boundary (the pull back of the spacetime metric to the boundary) $q_{ij}^{\partial U}(p)$ evaluated any point $p \in \partial U$ are considered observables.

This fact just talks about our choice of reference system. Part of our motivation to impose (22) to gauge vector fields was to provide a reference with respect to which we could measure the system of interest, the bulk field. The observables mentioned in the previous paragraph are not of physical interest in themselves, but they will enable us to define interesting gravitational observables.

In Section 4 we described how in our framework given an almost locally Hamiltonian vector field which is not a gauge perturbation there is a family of observable currents corresponding to the given vector field. We also argued that for field theories with local degrees of freedom there are plenty of almost locally Hamiltonian vector fields which are not gauge. Since for any observable associated with a locally Hamiltonian vector field which is not gauge the second term in (26) does not vanish, those observables are not holographic.

In the previous section we asked if hypersurface nonlocal gravitational observables could be approximated by local ones implying that nonlocal gravitational observables are also holographic. With the aide of (26) we see that this question is equivalent to asking if for any given solution ϕ the tangent space to the space of solutions at ϕ can be generated by local almost locally Hamiltonian vector fields, where the term "locally Hamiltonian" refers to preserving the presymplectic form and the term "local" refers to depending on partial derivatives of the field of at most order k for some finite k. In this terminology Anderson and Torre's result cited above says that the tangent space to the space of solutions of vacuum general relativity based on any solution is not generated by the local solutions of the linearized field equation. Local perturbations generate only gauge or would be gauge directions, proving that hypersurface nonlocal gravitational observables cannot be approximated by hypersurface local ones.

A large family of observables is given by the symplectic product of physical perturbations (see [26]). There is a subfamily which is holographic and a subfamily which is not. Assume that we are given two almost locally Hamiltonian vector fields v, w. The observable referred to as the symplectic product is

$$\omega_{L\,\Sigma}(v, w)[\phi] = \int_\Sigma \widetilde{\Omega}_L(v, w)[\phi]. \tag{32}$$

It is simple to verify that this observable is associated with the Hamiltonian vector field $[v, w]$. If $[v, w]$ satisfies (21) and does not vanish in the jet over ∂U, then $\omega_{L\,\Sigma}(v, w)$ is a nontrivial holographic observable. These are not very extravagant conditions; in the case of general relativity, they would be satisfied by two diffeomorphisms generators whose commutator does not vanish over ∂U. A point that needs to be mentioned is that in general relativity the diffeomorphism generators may be field dependent and in this way observables of this type encode nontrivial information about the field. On the other hand, if $[v, w]$ does not satisfy (21) the second term of (26) does not vanish implying that $\omega_{L\,\Sigma}(v, w)$ is not a holographic observable.

Below we give another family of examples of gravitational observables that can be defined thanks to the existence of a reference at the boundary. If the reader would like to have further motivation for considering bounded spacetime domains, it could be illuminating to read Appendix A. There we use a covariant initial value formulation on a given hypersurface with boundary Σ, which may be thought of as a laboratory where enough data is retrieved at a given time as to determine a solution inside $U = D(\Sigma)$, to discuss key aspects of the formalism described earlier in this article.

When the location of individual points inside U can be determined in terms of matter fields, a wealth of options for gravitational observables opens up. Different variants of the procedure to construct observables of the system of gravity coupled to matter used at the beginning of our argument have appeared in uncountably many references. If two points $p_1, p_2 \in U$ (which are sufficiently close according to the metric field) are located using relations involving matter fields an example of an observable is the length of a geodesic $\gamma_{p_1 p_2}$

$$\text{Length}\left(\gamma_{p_1p_2}\right)[g,\phi], \tag{33}$$

where we have denoted the gravitational field by g and the matter fields collectively by ϕ. If the gauge choice is changed, the location of p_1 and p_2 in the coordinate chart will change and the coordinate expression of the metric will also change in such a way as to leave the value of the observable unchanged; this is what makes it a physical observable. Notice that the condition that the points p_1 and p_2 be sufficiently close forces us to consider observables which are only locally defined in the space of fields. This observable depends on the gravitational field and on the matter fields relative to which the points are located.

On the other hand, if the points p_1 and p_2 belong to ∂U they can also be determined by the matter fields (or even by the gravitational field) outside of U. If this is done, the family of observables $\text{Length}(\gamma_{p_1p_2})$ has the interpretation of measuring the gravitational field in U with respect to a reference frame determined by the fields outside of U; then we can proceed assuming that $\text{Length}(\gamma_{p_1p_2})$ measures the gravitational field inside U and is defined without the need of matter fields inside U. Furthermore, considering the restriction of the field to ∂U as unaffected by changes of gauge (as demanded by (22)) implies that the function $\text{Length}(\gamma_{p_1p_2})$ depending only gravitational field inside U is an observable. The interpretation of such an observable is that it measures the field inside U with respect to a reference system located at ∂U which could be thought of as determined by fields outside of U.

Similar arguments could be used to define physical observables measuring areas of minimal surfaces determined by curves fixed at ∂U, or measuring volumes enclosed by collections of such surfaces.

Are observables in these families holographic? They are not. One way to see that this might be true is to observe that the requirement for the functional to be an observable is that $\gamma_{p_1p_2}$ is a *spacetime geodesic* and when spacetime data has to be retrieved from initial data at a given hypersurface the nonlinear field equations together with any gauge condition used enable calculations which need to be solved to have the location of the spacetime geodesic determined in terms of the initial data. Torre's result [16] confirms that our suspicion that $\text{Length}(\gamma_{p_1p_2})$ is not a holographic observable is in fact correct.

7. Conclusions

We started reviewing the notion of what a gauge perturbation is in the context of Lagrangian field theories defined on confined spacetime domains. The initial assumptions included that we are working in a covariant setting in which spacetime geometry may be one of the dynamical fields, implying that there is no causal structure fixed a priori. The initial consideration to determine which perturbations are considered gauge was a covariant form of a determinism principle thoroughly explained in Section 3. The outcome was (21), and it emerged from a study of how perturbations propagate through hypersurfaces as dictated by the linearized gluing equation. Since the transmission of information through spacetime codimension one surfaces played a key role, we referred to the argument as gauge from holography, and it was admitted that the term referred to a mild type of holography as compared to the holographic behavior of hypersurface local gravitational observables described on Section 5 which is associated with spacetime codimension two surfaces.

At first glance, it may seem that both aspects of holography mentioned in the previous paragraph are disjointed, and that the term holography refers to completely are unrelated phenomena in both instances. However, the work presented in this article shows the intimate relationship between them: first of all, from our definition of gauge vector fields and our considerations of observables which are only locally defined in the space of solutions, we could give a straight forward argument proving that observables calculated integrating observable currents f_Σ (see (17)) are capable of distinguishing gauge inequivalent solutions. A key ingredient of the argument was that almost locally Hamiltonian vector fields (these are perturbations of the field which respect the presymplectic form up to boundary terms which may not vanish) defined locally in the jet generate the tangent space to the space of solutions based at any solution. Second, any almost locally Hamiltonian vector field v induces a (family of locally defined) observables f^v_Σ which are holographic if V satisfies (21) and they are nontrivial if condition (22) is not satisfied. Thus, field perturbations related to nontrivial holographic observables are exactly those which could be referred to as "would be gauge vector fields" in the sense that they are not gauge only due to the presence of a boundary. The information encoded in those observables can be nontrivial because the perturbations satisfying (21)—in the case of general relativity the diffeomorphism generators—may depend nontrivially on the field.

In Section 6 we exhibited a large family of examples of observables corresponding to the symplectic product of field perturbations, and we characterized the subfamily consisting of nontrivial holographic observables.

Observables in nonlinear theories with gauge redundancies defined in spacetime domains foliated by Cauchy surfaces with no boundary are expected to be nonlocal in the sense of depending on infinitely many derivatives of the field. A brief discussion of the reasons behind this expectation is given in Section 6. However, we saw that in the presence of boundaries nontrivial observables with holographic behavior arise.

Can every gravitational observable be approximated by local observables, inheriting their holographic behavior? This issue is addressed in Section 6, where we show that this is not the case.

Is the family of holographic observables capable of separating points in the space of solutions modulo gauge? The arguments given above tell us that this question is equivalent to asking if for any given solution the tangent space to the space of solutions based on it is generated by gauge vector fields together with would be gauge vector fields, which is clearly not the case.

Appendix

A. Working with Bounded Spacetime Domains in the Covariant Initial Value Formulation

In this appendix we motivate working with bounded spacetime domains from the point of view of a covariant initial value formulation on a given hypersurface with boundary which may be thought of as a laboratory where data is retrieved at a given time. We comment on the correspondence between this formalism and the one used in the main body of this article emphasizing interpretational issues which arise when setting up the correspondence and their relation with two key aspects of our formalism: considering locally defined observables and the notion of gauge.

For the sake of concreteness, consider the following scenario for gravitational thought measurements on earth: Earth's southern hemisphere is covered by laboratories (covering a layer from a height of 0 to 100 meters above the sea level) equipped with clocks and measuring devices for gravitational field, and all the matter fields coupling to it, and their rates of change as to have initial data at a certain time slice Σ for the system consisting of gravity and gravitating matter. From those measurements we should be able to predict (and retrodict) physical properties of the fields inside the domain of dependence of that hypersurface $D(\Sigma)$. In order to start calculations we choose a coordinate chart for a spacetime region containing $D(\Sigma)$ and also choose a gauge. Then the measurements are translated into functionals of the initial conditions for a system of partial differential equations that can be solved inside $D(\Sigma)$. In fact, one thing that can be calculated is the actual location of $D(\Sigma)$ according to the chosen coordinate chart. Let us call U the spacetime domain resulting from a truncation of $D(\Sigma)$ with a topology of the type $\Sigma \times [0,1]$ (where Σ is a three dimensional ball). The domain U is endowed with a foliation in which one of the leaves is a truncation of Σ. A truncation procedure starts with removing a tubular neighborhood T of $\partial\Sigma$ from Σ, and consider $A = D(\Sigma \setminus T)$. Then consider the subset B of $D(\Sigma)$ which is covered by leaves Σ_t with $t \in [\epsilon, 1-\epsilon]$. A truncation with the properties we seek is $U = A \cap B$. Let us assume that the system, consisting of general relativity coupled to matter, has a description in which active spacetime diffeomorphisms are a gauge symmetry. In this case, the location of $D(\Sigma)$ in the host four manifold is gauge dependent. Picturing $D(\Sigma)$ as a given portion of a four manifold implies either partially fixing the gauge or considering equivalence classes (somehow defined in terms of the fields themselves) which are the ones associated with $D(\Sigma)$ resulting in a formalism where active diffeomorphisms are no longer a gauge symmetry. The formalism described in Sections 1 and 3, in particular the definition of gauge perturbations, includes these ideas at its core; from the outset we worked on a given spacetime domain U (which may be a portion of spacetime and where gluing descriptions over such spacetime domains enjoys of interesting properties [26]). Thus, one way of picturing the spacetime domains U endowed with a foliation used in the main body of this article may be as truncated domains of dependence of a given hypersurface with boundary. However, this interpretation works only in a certain regime of fields whose induced causal structure is compatible with such an interpretation. Observables would have that interpretation only (and possibly be well defined only) for a given domain of fields. Working with locally defined observables is a crucial point of our framework.

B. Completion of the Proof of Equation (27)

In this appendix the submanifold of the jet in which the field equation $E(L) = 0$ holds will be denoted by $\mathscr{E}_L \subset JY$; the space whose elements are solutions of the linearized field equation will be denoted by $\mathfrak{F}_U$, those which are almost locally Hamiltonian by $\widehat{\mathfrak{F}}_U^{\mathrm{LH}}$, and the locally Hamiltonian ones by $\mathfrak{F}_U^{\mathrm{LH}}$. Clearly $\mathfrak{F}_U^{\mathrm{LH}} \subset \widehat{\mathfrak{F}}_U^{\mathrm{LH}} \subset \mathfrak{F}_U$.

Here we consider the case in which the curve of solutions ϕ_t with $\phi_0 = \phi$ is determined by a vector field w in Sols_U which satisfies condition (21) and does not satisfy condition (22). Thus, w satisfies the following two conditions:

(i) $(\widetilde{\Omega}_L(w,z)[\phi] = d\widetilde{\rho}^w(z))[\phi]$

for every solution ϕ and every vector field z in Sols_U, and where $\widetilde{\rho}^w$ is an operator which depends linearly on a vector field and acts as a differential operator in the field and it is valued in $n-2$ forms of M.

(ii) $w_\phi(p) \neq 0$

for some solution ϕ and some $p \in \partial U$.

Now we choose an almost locally Hamiltonian vector field v in Sols_U, which means that $\mathscr{L}_v\widetilde{\Omega}_L(y,z)[\phi] = d\widetilde{\sigma}^v(y,z)[\phi]$ for every solution ϕ and every pair of vector fields y, z in Sols_U, and where $\widetilde{\sigma}^v$ is an operator depending linearly on each of the vector fields and acting as a differential operator in the field. Condition (26) expressing the compatibility of v with a current $\widetilde{F}$ may be written as $(\mathscr{L}_z\widetilde{F} + \widetilde{\Omega}_L(v,z))[\phi] = d\widetilde{\sigma}^F(z)[\phi]$ for every solution ϕ and every vector field z in Sols_U and where the differential operator $\widetilde{\sigma}^F$ satisfies $\widetilde{\sigma}^v(y,z)[\phi] = (-\delta\widetilde{\sigma}^F + \widetilde{\lambda}^F)(y,z)[\phi]$ (with $d\widetilde{\lambda}^F(y,z)[\phi] = 0$) for every solution ϕ and every pair of vector fields y, z in Sols_U. Then

$$\begin{aligned}\mathscr{L}_w\widetilde{F}\,[\phi] &= -\widetilde{\Omega}_L\,(v,w)\,[\phi] - d\widetilde{\sigma}^F\,(w)\,[\phi] \\ &= d\left(-\widetilde{\rho}^w\,(v) - \widetilde{\sigma}^F\,(w)\right)[\phi]\,,\end{aligned} \tag{B.1}$$

where we have used (i).

The equation $(d/dt)|_{t=0} f_\Sigma[\phi_t] = \int_\Sigma \mathscr{L}_w\widetilde{F} = 0$ is one scalar condition which can be studied with v and $\widetilde{\lambda}^F$ as unknowns. Clearly for generic values of v and $\widetilde{\lambda}^F$ the above equation does not hold. In this way we arrive to the desired conclusion that also in the case considered in this appendix observables constructed integrating observable currents suffice to separate points in the curve of solutions ϕ_t in a neighborhood of $\phi_0 = \phi$.

For a more detailed presentation, see [26].

Data Availability

No data were used to support this study.

Conflicts of Interest

There are no conflicts of interest associated with the publication of this work.

Acknowledgments

I would like to thank Igor Khavkine for important clarifications on the subject of local observables. I acknowledge correspondence and discussions about the subject of the article with Jasel Berra, Homero Daz, Laurent Fridel, Alberto Molgado, Robert Oeckl, Michael Reisenberger, Charles Torre, José A. Vallejo, and Luca Vitagliano. This work was partially supported by Grants PAPIIT-UNAM IN 109415 and IN100218 and by a sabbatical grant by PASPA-UNAM.

References

[1] J. D. Bekenstein, "Black holes and entropy," *Physical Review D: Particles, Fields, Gravitation and Cosmology*, vol. 7, pp. 2333–2346, 1973.

[2] J. M. Bardeen, B. Carter, and S. W. Hawking, "The four laws of black hole mechanics," *Communications in Mathematical Physics*, vol. 31, pp. 161–170, 1973.

[3] G. Hooft, "Dimensional reduction in quantum gravity," *General Relativity and Quantum Cosmology*, 1993, https://arxiv.org/abs/gr-qc/9310026.

[4] L. Susskind, "The world as a hologram," *Journal of Mathematical Physics*, vol. 36, no. 11, pp. 6377–6396, 1995.

[5] M. Maldacena, "The large-N limit of superconformal field theories and supergravity," *International Journal of Theoretical Physics*, vol. 38, no. 4, pp. 1113–1133, 1999.

[6] S. Ryu and T. Takayanagi, "Holographic derivation of entanglement entropy from AdS/CFT," *Physical Review Letters*, vol. 96, Article ID 181602, 2006.

[7] H. Liu and S. J. Suh, "Entanglement tsunami: Universal scaling in holographic thermalization," *Physical Review Letters*, vol. 112, no. 1, Article ID 011601, 2014.

[8] S. H. Shenker and D. Stanford, "Black holes and the butterfly effect," *Journal of High Energy Physics*, vol. 03, Article ID 067, 2014.

[9] W. Donnelly and S. B. Giddings, "How is quantum information localized in gravity?" *Physical Review D: Particles, Fields, Gravitation and Cosmology*, vol. 96, no. 8, Article ID 086013, 2017.

[10] L. Freidel and A. Perez, "Quantum gravity at the corner," *Universe*, vol. 4, no. 10, 107 pages, 2018.

[11] W. Donnelly and L. Freidel, "Local subsystems in gauge theory and gravity," *Journal of High Energy Physics*, no. 9, p. 102, 2016.

[12] W. Donnelly, "Entanglement entropy and nonabelian gauge symmetry," *Classical and Quantum Gravity*, vol. 31, no. 21, Article ID 214003, 2014.

[13] W. Donnelly and S. B. Giddings, "Observables, gravitational dressing, and obstructions to locality and subsystems," *Physical Review D: Particles, Fields, Gravitation and Cosmology*, vol. 94, no. 10, Article ID 104038, 2016.

[14] R. Oeckl, "General boundary quantum field theory: foundations and probability interpretation," *Advances in Theoretical and Mathematical Physics*, vol. 12, no. 2, pp. 319–352, 2008.

[15] C. G. Torre and I. M. Anderson, "Symmetries of the Einstein equations," *Physical Review Letters*, vol. 70, no. 23, pp. 3525–3529, 1993.

[16] C. G. Torre, "Gravitational observables and local symmetries," *Physical Review D: Particles, Fields, Gravitation and Cosmology*, vol. 48, no. 6, pp. R2373–R2376, 1993.

[17] I. M. Anderson, "Introduction to the variational bicomplex," in *Mathematical Aspects of Classical Field Theory*, M. Gotay, J. Marsden, and V. Moncrief, Eds., vol. 132 of *Contemporary Mathematics*, pp. 51–73, 1992.

[18] M. Forger and S. V. Romero, "Covariant Poisson brackets in geometric field theory," *Communications in Mathematical Physics*, vol. 256, no. 2, pp. 375–410, 2005.

[19] I. Khavkine, "Covariant phase space, constraints, gauge and the Peierls formula," *International Journal of Modern Physics A*, vol. 29, no. 5, Article ID 1430009, 2014.

[20] K. Fredenhagen and K. Rejzner, "Batalin-Vilkovisky formalism in the functional approach to classical field theory," *Communications in Mathematical Physics*, vol. 314, no. 1, pp. 93–127, 2012.

[21] J. Lee and R. M. Wald, "Local symmetries and constraints," *Journal of Mathematical Physics*, vol. 31, no. 3, pp. 725–743, 1990.

[22] I. M. Anderson and C. G. Torre, "Classification of local generalized symmetries for the vacuum Einstein equations," *Communications in Mathematical Physics*, vol. 176, no. 3, pp. 479–539, 1996.

[23] G. T. Horowitz, "Exactly soluble diffeomorphism invariant theories," *Communications in Mathematical Physics*, vol. 125, no. 3, pp. 417–437, 1989.

[24] A. Ashtekar, O. Reula, and L. Bombelli, "The covariant phase space of asymptotically flat gravitational fields," Technical Report PRE-32421, 1990.

[25] E. G. Reyes, "On covariant phase space and the variational bicomplex," *International Journal of Theoretical Physics*, vol. 43, no. 5, pp. 1267–1286, 2004.

[26] H. G. Daz-Marn and J. A. Zapata, "Observable currents and a covariant Poisson algebra of physical observables," *High Energy Physics*, 2017, https://arxiv.org/abs/1704.07955.

[27] I. Khavkine, "Local and gauge invariant observables in gravity," *Classical and Quantum Gravity*, vol. 32, no. 18, Article ID 185019, 19 pages, 2015.

[28] F. Hélein and J. Kouneiher, "The notion of observable in the covariant Hamiltonian formalism for the calculus of variations with several variables," *Advances in Theoretical and Mathematical Physics*, vol. 8, no. 4, pp. 735–777, 2004.

[29] I. V. Kanatchikov, "Canonical structure of classical field theory in the polymomentum phase space," *Reports on Mathematical Physics*, vol. 41, no. 1, pp. 49–90, 1998.

[30] J. Kijowski, "A finite-dimensional canonical formalism in the classical field theory," *Communications in Mathematical Physics*, vol. 30, no. 2, pp. 99–128, 1973.

[31] H. Goldschmidt and S. Sternberg, "The Hamilton-Cartan formalism in the calculus of variations," *Annales de l'Institut Fourier*, vol. 23, no. 1, pp. 203–267, 1973.

Hindawi
Advances in High Energy Physics
Volume 2018, Article ID 3702498, 5 pages
https://doi.org/10.1155/2018/3702498

Research Article

Cosmological Constant from the Entropy Balance Condition

Merab Gogberashvili [1,2]

[1] *Javakhishvili Tbilisi State University, 3 Chavchavadze Avenue, Tbilisi 0179, Georgia*
[2] *Andronikashvili Institute of Physics, 6 Tamarashvili Street, Tbilisi 0177, Georgia*

Correspondence should be addressed to Merab Gogberashvili; gogber@gmail.com

Received 4 August 2018; Accepted 16 September 2018; Published 26 November 2018

Guest Editor: Cynthia Keeler

In the action formalism variations of metric tensors usually are limited by the Hubble horizon. On the contrary, variations of quantum fields should be extended up to the event horizon, which is the real boundary of the spacetime. As a result the entanglement energy of quantum particles across the apparent horizon is missed in the cosmological equations written for the Hubble volume. We identify this missing boundary term with the dark energy density and express it (using the zero energy assumption for the finite universe) as the critical density multiplied by the ratio of the Hubble and event horizons radii.

Many authors consider so-called emergent theories in which gravity is not a fundamental field, but like thermodynamics or hydrodynamics is defined for the matter in bulk [1–7]. One such approach is the thermodynamic model of gravity [3–15], where spacetime emerges from the properties of the "universal" ensemble of quantum particles. In this approach the entropy, rather than the energy density, plays the crucial role.

Since in General Relativity horizons are unavoidable and horizons block information, entropy and temperature can be introduced for spacetime. One such boundary is the apparent horizon with the radius (for the spatially flat universe),

$$R_H = \frac{1}{H} \approx 14.5\, Gly, \tag{1}$$

where $H \equiv \dot{a}/a$ is the Hubble parameter. For the Hubble volume,

$$V_H = \frac{4}{3}\pi R_H^3, \tag{2}$$

having the surface area

$$A_H = 4\pi R_H^2, \tag{3}$$

one can associate the temperature [16, 17],

$$T = \frac{1}{2\pi R_H}, \tag{4}$$

and an entropy [18, 19],

$$S_H = \frac{A_H}{4G}, \tag{5}$$

where G is the Newton constant.

The concept of entropy is a powerful tool in thermodynamics, information theory, and quantum physics and allows us to study different aspects of physical systems using a similar mathematical framework. In quantum mechanics a measurement is considered as the interaction of three systems: the quantum object, memory (measurement device), and observer. Then the total entropy of the ensemble of all quantum particles, which is formed by the information, statistical (thermodynamic), and quantum (entanglement) components [20, 21], can be assumed to be zero [15]. In this case the universe can always remain in pure state and only allow a unitary time-evolution, as it is suggested by von Neumann's model. Also the "universal" entropy remains zero at all stages of universe's evolution, while any subsystem (for example, the Hubble volume) has nonzero entropy.

In our previous papers it was demonstrated that "world ensemble" approach is compatible with the existing field-theoretical descriptions, as the relativistic [11, 12] and quantum [13] properties are emerging from its properties. Moreover, the model allows us to explain the hierarchy problem in particle physics by the fact that our underlying assumption

that any gravitational interaction of two particles involves interactions with all particles of the world ensemble effectively weakens the observed strength of gravity by the factor proportional to the number of particles in the ensemble [14].

As it was noted in [15], the convenient physical parameter to measure information can be an action, which in most cases is an additive quantity like entropy, also contains positive and negative components, and exhibits the unique discrete value, the action quantum $\hbar$ [22]. Then the maximum entropy principle in thermodynamics [23–25] and the least action principle in field theory lead to the same formalism. The relation of the classical action of a physical system to the thermodynamic entropy translates the condition of entropy neutrality into the zero action principle: the sum of all components of the action for a physical system (including the boundary terms) is zero. One consequence of this principle for the whole universe is the zero-energy condition,

$$\rho_U = 0, \tag{6}$$

i.e., the total density of all the forms of energy in the universe, ρ_U, at any moment of time should be zero. This mean that the universe can emerge without violation of the energy conservation, which appears to be preferable point of view in cosmology [26, 27].

In this paper we want to connect the entanglement energy of quantum particles across the apparent horizon, which is missed in the classical cosmological equations written for the Hubble volume, with the dark energy (DE), origin of which remains a mystery [28]. It is known that DE can be modelled by Einstein's cosmological constant, for which a typical fit to current observational data gives $\Lambda \approx 3 \times 10^{-122}\, sec^{-2}$. However, in quantum field theory, the natural value of Λ is of the order of unity. This discrepancy is one of the biggest challenges in modern cosmology and fundamental physics [29, 30].

Alternatives of the introduction of a cosmological constant are that DE arises from the evolution of dynamical fields of an unknown origin, or modifications of General Relativity. In order to distinguish between these hypotheses, a worldwide effort is ongoing to measure the effective equation of state and clustering properties of DE, using wide field cosmological surveys [31]. For reviews on the DE and theories, see [32–35] and references therein.

One promising approach for solving the DE puzzle is the Holographic DE model [36–39], which is based on the quantum zero-point energy predicted by an effective quantum field theory. The primary model of this kind, which as the IR cut-off uses the apparent horizon of the universe, R_H, has serious drawbacks [40–43], since for the DE density predicts the value:

$$\rho_{DE} = 2\pi\rho_c, \tag{7}$$

where

$$\rho_c = \frac{3H^2}{8\pi G} \tag{8}$$

denotes the critical density. As we see ρ_{DE} in Holographic DE model (7) is larger than observed; in fact it even exceeds ρ_c. To solve this failure physicists are considering [44] (i) interactions between the cosmos sectors, (ii) various models for entropies, and (iii) different from R_H cut-offs.

We note that, based on spacetime thermodynamics, a proper causal boundary of the classical spacetime is its apparent horizon [45, 46], meaning that the metric fluctuations are bounded by R_H and also that thermodynamics laws are satisfied on this boundary [47, 48]. Moreover, the event horizon in the context of cosmology as well as in the context of a black hole is always defined globally, as the causal structure of spacetime is a global thing (see more discussions in [39]).

From the other hand, the quantum fluctuations of matter fields should be limited not by the Hubble horizon (1), but by the event horizon,

$$R_e = \int_1^\infty \frac{da}{a^2 H(a)} \approx 16.7\, Gly, \tag{9}$$

which represents a real boundary of spacetime. Then the entanglement energy of quantum particles across the apparent horizon R_H, which is defined as disturbed vacuum energy due to the presence of a boundary [49], is missed in the cosmological equations written for the Hubble volume and can be taken into account by introduction of a boundary term. It was found that the perfect fluid of entanglement has a negative pressure [50] and can be interpreted as the origin of DE.

The terms corresponding to entanglement across R_H should disappear in the equation of state of classical fields. Indeed, for the light-like geodesics, which describe the Hubble horizon in the spatially flat universe, the Einstein equations written in the form of the first law [4–8],

$$\left(R_{\mu\nu} - \frac{1}{2} g_{\mu\nu} R\right) u^\mu u^\nu = 8\pi G T_{\mu\nu} u^\mu u^\nu, \tag{10}$$

do not contain the DE terms. This equation involves additional vector field u^ν, but contains all information content of the ordinary tensorial Einstein equations, because it is demanded that it holds for all u^ν. In addition, if one assumes that u^ν is an orthogonal to the observers horizon null vector field [5–8],

$$g_{\mu\nu} u^\mu u^\nu = 0, \tag{11}$$

in that obtained from (10) tensorial Einstein equations,

$$R_{\mu\nu} - \frac{1}{2} g_{\mu\nu} R = 8\pi G \left(T_{\mu\nu} + g_{\mu\nu}\Lambda\right), \tag{12}$$

Λ arises as an integration constant, which is not connected with the large constant vacuum energy terms in matter Lagrangians and needs to be fixed using an extra physical principle. For example, since we know that information is a physical entity [51–55], it can be identified with the amount of information accessible to an eternal observer at the horizon [8], or with the energy of collective gravitational interactions of all particles in the finite universe [9, 10].

Equation (10) has the natural interpretation as the balance of gravitational and matter heat densities, where the right

hand side represents the matter heat density, in the spirit of the first law of thermodynamics. This is obvious, for example, for the case of ideal fluid using the classical Gibbs-Duhem relation,

$$T_{\mu\nu}u^{\mu}u^{\nu} \longrightarrow \rho + p = \frac{TS_m}{V}, \tag{13}$$

where T is the temperature and S_m is the entropy of the matter in the volume V.

Connections of the cosmological constant with the boundary conditions and generalized equations of state can be demonstrated also from the cosmological equations. For a homogeneous, isotropic, and flat universe ($k = 0$) there are two independent Friedmann equations with the cosmological term Λ:

$$\begin{aligned} H^2 &= \frac{8\pi G}{3}\rho + \frac{1}{3}\Lambda \\ \dot{H} + H^2 &\equiv \frac{\ddot{a}}{a} = -\frac{4\pi G}{3}(\rho + 3p) + \frac{1}{3}\Lambda. \end{aligned} \tag{14}$$

Using the first equation of (14) the second equation can be reexpressed without Λ,

$$\dot{H} = -4\pi G(\rho + p). \tag{15}$$

From system (14) one can obtain also the matter energy-momentum conservation condition,

$$\partial_{\nu}T^{\nu\mu} = 0, \tag{16}$$

which leads to

$$\dot{\rho} = -3H(\rho + p). \tag{17}$$

Due to the presence of derivatives in (16) the cosmological constant Λ does not appear in (17) as well.

If instead of (14) one will choose (15) and (17) as the independent system of cosmological equations, Λ obtains the role of integration constant which can be fixed from an equation of state. Indeed, combining (15) with (17) and integrating over the time we have

$$H^2 = \frac{8\pi G}{3}\rho + C, \tag{18}$$

where the cosmological term reappears in the form of an arbitrary constant C, which should be chosen as

$$C = \frac{1}{3}\Lambda, \tag{19}$$

in order to obtain the first Friedmann equation in (14).

To find the value of DE density in our approach let us estimate the entropy input in a region as the sum of the entropy flux (entropy received per unit surface) transferred through the boundary and the entropy supplied by internal sources (entropy generated per unit volume). If we neglect the entropy supplied by internal sources, then according to the Second Law of Thermodynamics the time derivative of the entropy contained within the volume, S, is equal to the flux of the matter entropy, S_m, through the boundary A,

$$\frac{dS}{dt} = S_m A. \tag{20}$$

Using the relations of types (5) and (13), (20) takes the form

$$\frac{1}{4G}\frac{dA}{dt} = \frac{\rho + p}{T}A. \tag{21}$$

For the Hubble volume, taking into account (3) and (4), this equation leads to one of the cosmological equations (15). Then combined with the energy conservation equation (17) and integrating over time we find again (18), where C corresponds to some hidden amount of energy.

For the finite universe limited by the event horizon, R_e, the energy balance condition (18) should obtain the form

$$\frac{1}{R_e^2} = \frac{8\pi G}{3}\rho_U, \tag{22}$$

without the boundary term. Then the zero energy condition (6) allows us to fix C in (18) as

$$C = \frac{1}{R_e^2}. \tag{23}$$

Therefore, using (1) and (9) for the DE density, we find

$$\rho_{DE} = \rho_c\frac{C}{H^2} = \rho_c\frac{R_H^2}{R_e^2} = 0.75\rho_c, \tag{24}$$

which is very close to the observed value of the DE.

Note that the relation (24) must be valid at any time of cosmological evolution, which gives time-dependence of DE. Moreover, the parameter C in the energy balance condition (18) can change the sign in the situation when the Hubble horizon crosses the event horizon. In General Relativity, as we know, Λ is a true constant. However, an expanding universe is not expected to have a static vacuum energy density and there is the possibility that Λ is actually a time dependent quantity. In order to implement the notion of a smoothly evolving vacuum energy density is not necessary to introduce ad hoc scalar fields [56–58], as usually done in quintessence formulations. Let us mention a dynamical approach based on extending the variational principle by promoting Λ from being a parameter to a field [59–61]. In this modified variational approach the resulting history is indistinguishable from General Relativity with a constant value of Λ put in by hand at the right value at each observational time. In our model Λ also appears to be time dependent and even can be negative, positive, or zero at different stages of the universe evolution. This fact can be used to model, for example, the end of the inflation epoch.

To conclude, in this paper we estimate the DE density within the thermodynamic model of gravity using the zero energy condition: the total energy of the universe inside its event horizon is zero. We notice that in the action formalism variations of metric tensor should be limited by the Hubble horizon, which represents a causal boundary of

classical spacetime. On the contrary, variations of quantum fields are limited by the event horizon, which is the real boundary of the spacetime. Then the entanglement energy of quantum particles across the apparent horizon is missed in the cosmological equations written for the Hubble volume. We identify this entanglement density with the DE, which can be introduced as a boundary term in the cosmological equations. In our model the DE density equals the critical density reduced by the ratio of the squares of the Hubble and event horizons radii (24), having the value in good agreement with the observational data. In our approach DE density appears to be time dependent and can change the sign, what can explain transitions form accelerations to decelerations at different epoches of cosmological evolution.

Data Availability

The data used to support the findings of this study are available from the corresponding author upon request.

Conflicts of Interest

The author declares that there are no conflicts of interest.

References

[1] A. Connes and C. Rovelli, "von Neumann algebra automorphisms and time-thermodynamics relation in generally covariant quantum theories," *Classical and Quantum Gravity*, vol. 11, no. 12, article 2899, 1994.

[2] C. Rovelli and M. Smerlak, "Thermal time and Tolman–Ehrenfest effect: 'temperature as the speed of time'," *Classical and Quantum Gravity*, vol. 28, no. 7, Article ID 075007, 2012.

[3] E. P. Verlinde, "On the origin of gravity and the laws of Newton," *Journal of High Energy Physics*, vol. 2011, no. 4, article 29, 2011.

[4] T. Jacobson, "Thermodynamics of spacetime: the Einstein equation of state," *Physical Review Letters*, vol. 75, no. 7, article 1260, 1995.

[5] T. Padmanabhan, "Thermodynamical aspects of gravity: new insights," *Reports on Progress in Physics*, vol. 73, no. 4, Article ID 046901, 2010.

[6] T. Padmanabhan, "Emergent Gravity Paradigm: Recent Progress," *Modern Physics Letters A*, vol. 30, no. 03n04, Article ID 1540007, 2015.

[7] T. Padmanabhan, "Distribution function of the atoms of spacetime and the nature of gravity," *Entropy*, vol. 17, no. 11, pp. 7420–7452, 2015.

[8] M. Gogberashvili and U. Chutkerashvili, "Cosmological constant in the thermodynamic models of gravity," *Theoretical Physics*, vol. 2, no. 4, pp. 163–165, 2017.

[9] M. Gogberashvili and I. Kanatchikov, "Cosmological parameters from the thermodynamic model of gravity," *International Journal of Theoretical Physics*, vol. 53, no. 5, pp. 1779–1783, 2014.

[10] M. Gogberashvili, "On the dynamics of the ensemble of particles in the thermodynamic model of gravity," *Journal of Modern Physics*, vol. 5, pp. 1945–1957, 2014.

[11] M. Gogberashvili, "'Universal' FitzGerald contractions," *The European Physical Journal C*, vol. 63, no. 2, pp. 317–322, 2009.

[12] M. Gogberashvili and I. Kanatchikov, "Machian origin of the entropic gravity and cosmic acceleration," *International Journal of Theoretical Physics*, vol. 51, no. 3, pp. 985–997, 2012.

[13] M. Gogberashvili, "Thermodynamic gravity and the schrodinger equation," *International Journal of Theoretical Physics*, vol. 50, no. 8, pp. 2391–2402, 2011.

[14] M. Gogberashvili, "A machian solution of the hierarchy problem," *The European Physical Journal C*, vol. 54, no. 4, pp. 671–674, 2008.

[15] M. Gogberashvili, "Information-probabilistic description of the universe," *International Journal of Theoretical Physics*, vol. 55, no. 9, pp. 4185–4195, 2016.

[16] S. W. Hawking, "Particle creation by black holes," *Communications in Mathematical Physics*, vol. 43, no. 3, pp. 199–220, 1975.

[17] S. W. Hawking, "Black holes and thermodynamics," *Physical Review D: Particles, Fields, Gravitation and Cosmology*, vol. 13, no. 2, article 191, 1976.

[18] J. D. Bekenstein, "Black holes and entropy," *Physical Review D: Particles, Fields, Gravitation and Cosmology*, vol. 7, no. 8, article 2333, 1973.

[19] J. D. Bekenstein, "Generalized second law of thermodynamics in black-hole physics," *Physical Review D: Particles, Fields, Gravitation and Cosmology*, vol. 9, no. 12, article 3292, 1974.

[20] W.-Y. Hwang, "A coherent view on entropy," *Natural Science*, vol. 6, no. 7, pp. 540–544, 2014.

[21] D. Song, "Negative entropy and black hole information," *International Journal of Theoretical Physics*, vol. 53, no. 4, pp. 1369–1374, 2014.

[22] A. Annila, "All in action," *Entropy*, vol. 12, no. 11, pp. 2333–2358, 2010.

[23] E. T. Jaynes, "Information theory and statistical mechanics," *Physical Review Journals Archive*, vol. 106, no. 4, article 620, 1957.

[24] E. T. Jaynes, "Gibbs vs Boltzmann entropies," *American Journal of Physics*, vol. 33, article 391, 1965.

[25] E. T. Jaynes, *Maximum Entropy and Bayesian Methods in Inverse Problems*, C. R. Smith and W. T. Grandy Jr., Eds., Reidel, Dordrecht, Germany, 1985.

[26] R. P. Feynman, F. B. Morinigo, and G. Wagner, *Feynman Lectures on Gravitation*, Addison-Wesley, Reading, MA, USA, 1995.

[27] S. Hawking, *A Brief History of Time*, Bantam, Toronto, Canada, 1988.

[28] M. Roos, *Introduction to Cosmology*, John Wiley and Sons, UK, 2003.

[29] S. Weinberg, "The cosmological constant problem," *Reviews of Modern Physics*, vol. 61, no. 1, article 1, 1989.

[30] M. P. Hobson, G. P. Efstathiou, and A. N. Lasenby, *General Reltivity: An Introduction for Physicists*, Cambridge University Press, Cambridge, UK, 2006.

[31] K. Bamba, S. Capozziello, S. Nojiri, and S. D. Odintsov, "Dark energy cosmology: the equivalent description via different theoretical models and cosmography tests," *Astrophysics and Space Science*, vol. 342, no. 1, pp. 155–228, 2012.

[32] T. Padmanabhan, "Cosmological constant—the weight of the vacuum," *Physics Reports*, vol. 380, no. 5-6, pp. 235–320, 2003.

[33] S. Capozziello and V. Faraoni, *Beyond Einstein Gravity*, Springer, Dordrecht, The Netherlands, 2010.

[34] A. Joyce, B. Jain, J. Khoury, and M. Trodden, "Beyond the cosmological standard model," *Physics Reports*, vol. 568, pp. 1–98, 2015.

[35] S. Nojiri, S. D. Odintsov, and V. K. Oikonomou, "Modified gravity theories on a nutshell: Inflation, bounce and late-time evolution," *Physics Reports*, vol. 692, pp. 1–104, 2017.

[36] A. G. Cohen, D. B. Kaplan, and A. E. Nelson, "Effective field theory, black holes, and the cosmological constant," *Physical Review Letters*, vol. 82, no. 25, Article ID 4971, 1999.

[37] S. Thomas, "Holography stabilizes the vacuum energy," *Physical Review Letters*, vol. 89, no. 8, Article ID 081301, 2002.

[38] S. D. H. Hsu, "Entropy bounds and dark energy," *Physics Letters B*, vol. 594, no. 1-2, pp. 13–16, 2004.

[39] M. Li, "A model of holographic dark energy," *Physics Letters B*, vol. 603, no. 1-2, pp. 1–5, 2004.

[40] B. Guberina, R. Horvat, and H. Nikolić, "Non-saturated holographic dark energy," *Journal of Cosmology and Astroparticle Physics*, vol. 2007, no. 01, article 012, 2007.

[41] R. Horvat, "On the internal consistency of holographic dark energy models," *Journal of Cosmology and Astroparticle Physics*, vol. 2008, no. 10, article 022, 2008.

[42] S. Gao, "Explaining holographic dark energy," *Galaxies*, vol. 1, no. 3, pp. 180–191, 2013.

[43] S. Gao, "A conjecture on the origin of dark energy," *Chinese Physics Letters*, vol. 22, no. 3, article 783, 2005.

[44] S. Wang, Y. Wang, and M. Li, "Holographic dark energy," *Physics Reports*, vol. 696, pp. 1–57, 2017.

[45] S. A. Hayward, S. Mukhoyama, and M. C. Ashworth, "Dynamic black-hole entropy," *Physics Letters A*, vol. 256, no. 5-6, pp. 347–350, 1999.

[46] D. Bak and S.-J. Rey, "Cosmic holography," *Classical and Quantum Gravity*, vol. 17, no. 15, article 83, 2000.

[47] R. G. Cai and S. P. Kim, "First law of thermodynamics and Friedmann equations of Friedmann-Robertson-Walker universe," *Journal of High Energy Physics*, vol. 2005, no. 02, article 050, 2005.

[48] M. Akbar and R. G. Cai, "Thermodynamic behavior of the Friedmann equation at the apparent horizon of the FRW universe," *Physical Review D: Particles, Fields, Gravitation and Cosmology*, vol. 75, Article ID 084003, 2007.

[49] S. Mukohyama, M. Seriu, and H. Kodama, "Can the entanglement entropy be the origin of black-hole entropy?" *Physical Review D: Particles, Fields, Gravitation and Cosmology*, vol. 55, no. 12, Article ID 7666, 1997.

[50] J.-W. Lee, J. Lee, and H.-C. Kim, "Dark energy from vacuum entanglement," *Journal of Cosmology and Astroparticle Physics*, vol. 2007, no. 08, article 005, 2007.

[51] R. Landauer, "Irreversibility and heat generation in the computing process," *IBM Journal of Research and Development*, vol. 5, no. 3, pp. 183–191, 1961.

[52] R. Landauer, "Information is physical," in *Proceedings of the Workshop on Physics and Computation (PhysComp '92)*, IEEE Computer Society Press, Los Alamitos, Calif, USA, 1993.

[53] L. Brillouin, "The negentropy principle of information," *Journal of Applied Physics*, vol. 24, no. 9, Article ID 1152, 1953.

[54] L. Brillouin, *Science and Information Theory*, Academic, New York, NY, USA, 1962.

[55] L. Brillouin, *Scientific Uncertainty and Information*, Academic, New York, NY, USA, 1964.

[56] J. Sola, "Vacuum energy and cosmological evolution," *AIP Conference Proceedings*, vol. 1606, no. 1, article 19, 2014.

[57] J. Sola, "Cosmological constant and vacuum energy: old and new ideas," *Journal of Physics: Conference Series*, vol. 453, no. 1, Article ID 012015, 2013.

[58] J. Sola, "Cosmologies with a time dependent vacuum," *Journal of Physics: Conference Series*, vol. 283, no. 1, Article ID 012033, 2011.

[59] D. J. Shaw and J. D. Barrow, "A testable solution of the cosmological constant and coincidence problems," *Physical Review D: Particles, Fields, Gravitation and Cosmology*, vol. 83, no. 4, Article ID 043518, 2011.

[60] J. D. Barrow and D. J. Shaw, "New solution of the cosmological constant problems," *Physical Review Letters*, vol. 106, no. 10, Article ID 101302, 2011.

[61] J. D. Barrow and D. J. Shaw, "The value of the cosmological constant," *General Relativity and Quantum Cosmolog*, vol. 43, no. 10, pp. 2555–2560, 2011.

Hindawi
Advances in High Energy Physics
Volume 2018, Article ID 7801854, 9 pages
https://doi.org/10.1155/2018/7801854

Research Article

Apparent Horizon and Gravitational Thermodynamics of Universe in the Eddington-Born-Infeld Theory

Jia-Cheng Ding, Qi-Qi Fan, Cong Li, Ping Li, and Jian-Bo Deng

Institute of Theoretical Physics, Lanzhou University, Lanzhou 730000, China

Correspondence should be addressed to Jian-Bo Deng; dengjb@lzu.edu.cn

Received 6 July 2018; Revised 3 September 2018; Accepted 6 September 2018; Published 18 November 2018

Guest Editor: Esperanza Lopez

The thermodynamics of Universe in the Eddington-Born-Infeld (EBI) theory was restudied by utilizing the holographic-style gravitational equations that dominate the dynamics of the cosmical apparent horizon Υ_A and the evolution of Universe. We started in rewriting the EBI action of the Palatini approach into the Bigravity-type action with an extra metric $q_{\mu\nu}$. With the help of the holographic-style dynamical equations, we discussed the property of the cosmical apparent horizon Υ_A including timelike, spacelike, and null characters, which depends on the value of the parameter of state w_m in EBI Universe. The unified first law for the gravitational thermodynamics and the total energy differential for the open system enveloped by Υ_A in EBI Universe were obtained. Finally, applying the positive-heat-out sign convention, we derived the generalized second law of gravitational thermodynamics in EBI Universe.

1. Introduction

Gravitational thermodynamics is quite an interesting question, which has attracted much attention. Recently, many studies have covered both the first and second laws of gravitational thermodynamics for the Friedmann-Robertson-Walker (FRW) Universe with a generic spatial curvature. The inspired work is the first law of thermodynamics for Universe by Cai and Kim [1], which is a part of the effort to seek the connections between thermodynamics and gravity [2] after discovering the black-hole thermodynamics [3, 4]. In [1, 5], Akbar and Cai reversed the formulation by rewriting the Friedmann equations into the heat balance equation and the unified first law of thermodynamics at the cosmical apparent horizon, for General Relativity (GR), Gauss-Bonnet, and Lovelock gravity. The results in [5] were soon generalized to other theories of gravity, such as the scalar-tensor gravity [6], $f(R)$ gravity [7], braneworld scenarios [8–10], generic $f(R, \phi, \nabla_\mu\phi\nabla^\mu\phi)$ gravity [11], and Horava-Lifshitz gravity [12, 13], to construct the effective total energy differentials by the corresponding modified Friedmann equations.

Inspired by the gravitational thermodynamics in these gravitational theories [5–14] and characteristics of the EBI action, we focused on generalizing the results to the EBI gravity. The Eddington-Born-Infeld action (EBI) was proposed in [15], which could mimic the presence of dark energy and dark matter in the expansion of Universe [15–17] so that EBI gravity can be regarded as a candidate for nonparticulate dark matter and dark energy, and it could also modify the Newton-Poisson equation that leads to flat rotation curves for galaxies. Generally, the EBI action is a Palatini-type action where the metric $g_{\mu\nu}$ is not associated with the connection $C^\lambda_{\mu\nu}$. However, by defining an extra metric $q_{\mu\nu}$ to satisfy the condition in [15, 18], the EBI action can be rewritten as the Bigravity-type action.

In this paper, we derived the holographic-style dynamical equations and discussed the properties of the cosmical apparent horizon Υ_A in EBI Universe, which rely on the contents inside the cosmical apparent horizon including the matter and the dark energy provided by the cosmological constant Λ and the spacetime self-coupling. Furthermore, we applied the Misner-Sharp energy, the Cai-Kim temperature $\widehat{T}_A$, and the Hawking-Bekenstein entropy S_A to obtain the unified first law for the gravitational thermodynamics and the total energy differential for the open system enveloped by Υ_A

in EBI Universe. Finally, we derived the generalized second law of the nondecreasing entropy $S_{eff}^{(A)}$ enclosed by Υ_A in EBI Universe.

This paper is organized as follows. In Section 2, we reviewed the cosmical apparent horizon and derived the holographic-style dynamical equations in the EBI theory. Then we discussed the properties of the cosmical apparent horizon. In Section 3, the unified first law of gravitational thermodynamics and the Clausius equation on Υ_A for an isochoric process in EBI Universe were discussed. And we derived the total energy differential enclosed by Υ_A in EBI Universe. In Section 4, the generalized second law of gravitational thermodynamics in the EBI Universe was derived. Conclusions and discussion are given in Section 5.

2. Dynamics of the Cosmical Apparent Horizon in Eddington-Born-Infeld Gravity

2.1. Apparent Horizon. Physically, apparent horizons constitute the observable boundary which is the largest boundary of Universe in an instant. Mathematically, apparent horizons are many hypersurfaces where the outward expansion rate $\theta_{(\ell)}$ or the inward expansion rate $\theta_{(n)}$ is equal to zero. In general, the first kind of apparent horizons where $\theta_{(\ell)} = 0$ and $\theta_{(n)} \neq 0$ usually locates near the black holes, and the another kind of apparent horizon where $\theta_{(n)} = 0$ and $\theta_{(\ell)} \neq 0$ appears in the vicinity of the expanding boundary of Universe, called the cosmical apparent horizons. In this paper, we only discussed the cosmical apparent horizon via dynamic equations of Universe and thermodynamic methods.

In order to calculate the apparent horizon of the cosmology, we use the FRW metric to describe the spatially homogeneous and isotropic Universe [1, 19]

$$ds^2 = -dt^2 + \frac{a(t)^2}{1-kr^2}dr^2 + a(t)^2 r^2\left(d\theta^2 + \sin^2\theta d\varphi^2\right) \quad (1)$$

where $a(t)$ is the scale factor of the evolution of Universe and the index k denotes the normalized spatial curvature, with $k = \{+1, 0, -1\}$ corresponding to closed, flat, and open Universes, respectively. Using the spherical symmetry, the metric can be rewritten as

$$ds^2 = h_{\alpha\beta}dx^\alpha dx^\beta + \Upsilon^2\left(d\theta^2 + \sin^2\theta d\varphi^2\right) \quad (2)$$

where $h_{\alpha\beta} \coloneqq \mathrm{diag}[-1, a(t)^2/(1-kr^2)]$ represents the transverse 2-metric spanned by $(x^0 = t, x^1 = r)$ and $\Upsilon \coloneqq a(t)r$ stands for the astronomical circumference/areal radius. Based on the FRW metric, one can structure the following null tetrad adapted to the spherical symmetry and the null radial flow:

$$\begin{aligned}
\ell^\mu &= \frac{1}{\sqrt{2}}\left(1, \frac{\sqrt{1-kr^2}}{a}, 0, 0\right)\\
n^\mu &= \frac{1}{\sqrt{2}}\left(-1, \frac{\sqrt{1-kr^2}}{a}, 0, 0\right)\\
m^\mu &= \frac{1}{\sqrt{2}\Upsilon}\left(0, 0, 1, \frac{i}{\sin\theta}\right)\\
\overline{m}^\mu &= \frac{1}{\sqrt{2}\Upsilon}\left(0, 0, 1, -\frac{i}{\sin\theta}\right),
\end{aligned} \quad (3)$$

corresponding to the metric signature $(-,+,+,+)$. By calculating the Newman-Penrose spin coefficients $\rho_{NP} \coloneqq -m^\mu\overline{m}^\nu\nabla_\nu\ell_\mu$ and $\mu_{NP} \coloneqq \overline{m}^\mu m^\nu\nabla_\nu n_\mu$, the outward expansion rate $\theta_{(\ell)} = -(\rho_{NP} + \overline{\rho}_{NP})$ and the inward expansion rate $\theta_{(n)} = -(\mu_{NP} + \overline{\mu}_{NP})$ are, respectively, given by

$$\begin{aligned}
\theta_{(\ell)} &= \sqrt{2}\left[H + \Upsilon^{-1}\sqrt{1 - \frac{k\Upsilon^2}{a^2}}\right]\\
\theta_{(n)} &= \sqrt{2}\left[-H + \Upsilon^{-1}\sqrt{1 - \frac{k\Upsilon^2}{a^2}}\right],
\end{aligned} \quad (4)$$

where $H \coloneqq \dot{a}/a$ is the Hubble parameter of cosmic spatial expansion. The overdot denotes the derivative with respect to the comoving time t.

For the expanding Universe ($H > 0$), the cosmical apparent horizon is given by

$$\Upsilon_A = \frac{1}{\sqrt{H^2 + k/a^2}}, \quad (5)$$

derived from $\theta_{(n)} = 0$ and $\theta_{(\ell)} > 0$ corresponding to the unique marginally inner trapped horizon where $\partial_\mu\Upsilon$ becomes a null vector with $g^{\mu\nu}\partial_\mu\Upsilon\partial_\nu\Upsilon = 0$ [20]. Then one derives the temporal derivative of (5)

$$\dot{\Upsilon}_A = -H\Upsilon_A^3\left(\dot{H} - \frac{k}{a^2}\right) \quad (6)$$

that is a kinematic equation of the cosmical apparent horizon.

2.2. The Holographic-Style Dynamical Equations in Eddington-Born-Infeld Universe. The action of Eddington-Born-Infeld theory is given by [15–18]

$$\begin{aligned}
S_{EBI}\left(g_{\mu\nu}, C^\mu_{\nu\rho}, \mathscr{L}_m\right) = \frac{1}{16\pi G}\int d^4x\left\{\sqrt{-g}\,(R - 2\Lambda)\right.\\
\left. + \frac{2}{\alpha\ell^2}\sqrt{-\det\left(g_{\mu\nu} - \ell^2 K_{\mu\nu}(C)\right)}\right\} + \int d^4x\sqrt{-g}\mathscr{L}_m,
\end{aligned} \quad (7)$$

where R is the Ricci scalar for the metric $g_{\mu\nu}$ and g represents the determinant of $g_{\mu\nu}$. $K_{\mu\nu}$ is two-order Riemann curvature tensor dependent on the connection $C^\mu_{\nu\rho}$, provided by the Palatini approach. Λ is the cosmological constant and α is an arbitrary constant. G is the gravitational constant and $\mathscr{L}_m$ is the Lagrangian density of matter.

Applying the Bigravity method [18] to replace the connection $C^{\mu}_{\nu\rho}$ by the extra metric $q_{\mu\nu}$ in the EBI theory, the action (7) can be rewritten into the Bigravity-type action

$$S_{EBI} = \frac{1}{16\pi G}\int d^4x\left\{\sqrt{-g}\,(R-2\Lambda)+\sqrt{-q}\,(K-2\lambda) - \frac{1}{\ell^2}\sqrt{-q}\left(q^{\alpha\beta}g_{\alpha\beta}\right)\right\}+\int d^4x\sqrt{-g}\mathscr{L}_m, \tag{8}$$

where

$$q_{\mu\nu} = -\frac{1}{\alpha}\left(g_{\mu\nu}-\ell^2K_{\mu\nu}\right). \tag{9}$$

$K_{\mu\nu}$ is the Ricci tensor for the extra metric $q_{\mu\nu}$ and K is the Ricci scalar for the extra metric $q_{\mu\nu}$. λ is a constant ($\lambda \equiv \alpha/\ell^2$) corresponding to $q_{\mu\nu}$ and q is the determinant of $q_{\mu\nu}$. Here, both $g_{\mu\nu}$ and $q_{\mu\nu}$ are innate metrics of spacetime and they are mutually independent. Hence, $(1/\ell^2)\sqrt{-q}(q^{\alpha\beta}g_{\alpha\beta})$ can be regarded as the term from self-coupling of spacetime.

Varying the Bigravity-type action (8) with respect to the metric $g_{\mu\nu}$, we get the field equations [15]

$$R_{\mu\nu}-\frac{1}{2}Rg_{\mu\nu} = 8\pi GT^{(m)}_{\mu\nu}-\Lambda g_{\mu\nu} - \frac{1}{\ell^2}\frac{\sqrt{-q}}{\sqrt{-g}}g_{\mu\alpha}q^{\alpha\beta}g_{\beta\nu}, \tag{10}$$

where $-(1/\ell^2)(\sqrt{-q}/\sqrt{-g})g_{\mu\alpha}q^{\alpha\beta}g_{\beta\nu}$ is the energy-momentum tensor of the spacetime self-coupling.

The matter content of Universe is construed as the perfect fluid whose the energy-momentum tensor is

$$T^{\mu(m)}_{\nu} = \mathrm{diag}\left[-\rho_m, p_m, p_m, p_m\right] \quad with\ \frac{p_m}{\rho_m} =: w_m, \tag{11}$$

where w_m refers to the Equation-of-State (EoS) parameter of the perfect fluid. In order to study the cosmological property of the EBI Universe, we made $g_{\mu\nu}$ be the FRW metric and assumed the extra metric $q_{\mu\nu}$ [15, 21] as

$$ds_q^2 = -Udt^2+\frac{a(t)^2V}{1-kr^2}dr^2+a(t)^2Vr^2d\theta^2 + a(t)^2Vr^2\sin^2\theta d\varphi^2, \tag{12}$$

where U and V are two undetermined positive functions independent with t.

Depending on the field equation and the two metrics, we get the first Friedmann equation

$$\frac{\dot{a}^2}{a^2}+\frac{k}{a^2}-\frac{\Lambda}{3} = \frac{8\pi G\rho_m}{3}+\frac{1}{3\ell^2}\sqrt{\frac{V}{U}}V \tag{13}$$

and the second Friedmann equation

$$\frac{\dot{a}^2}{a^2}+\frac{k}{a^2}+2\frac{\ddot{a}}{a}-\Lambda = -8\pi Gp_m+\frac{1}{\ell^2}\sqrt{\frac{V}{U}}U. \tag{14}$$

Eq. (14) can be rewritten into

$$2\dot{H}+3H^2+\frac{k}{a^2}-\Lambda = -8\pi Gp_m+\frac{1}{\ell^2}\sqrt{\frac{V}{U}}U, \tag{15}$$

which is equivalent to

$$\Upsilon_A^{-3}\left(\dot{\Upsilon}_A-\frac{3}{2}H\Upsilon_A\right) = \left[4\pi Gp_m-\frac{\Lambda}{2}-\frac{1}{2\ell^2}\sqrt{\frac{V}{U}}U\right]H. \tag{16}$$

With the help of (13) and (15), we obtain

$$\dot{H}-\frac{k}{a^2} = -4\pi G\left(\rho_m+p_m\right)-\frac{1}{2\ell^2}\sqrt{\frac{V}{U}}\left(V-U\right). \tag{17}$$

Based on (5) and (13), we get

$$\Upsilon_A^{-2} = \frac{8\pi G}{3}\rho_m+\frac{\Lambda}{3}+\frac{1}{3\ell^2}\sqrt{\frac{V}{U}}V \tag{18}$$

and substituting (17) into (6), we get

$$\dot{\Upsilon}_A = H\Upsilon_A^3\left[4\pi G\left(\rho_m+p_m\right)+\frac{1}{2\ell^2}\sqrt{\frac{V}{U}}\left(V-U\right)\right]. \tag{19}$$

Eq. (16), (18), and (19) are the holographic-style dynamical equations of the cosmical apparent horizon [14], which means the evolution of Universe has a relation with the cosmical apparent horizon. If one takes $U = V = 1$ and $\Lambda = 0$, the holographic-style dynamical equations will return to the condition of the Einstein theory.

Furthermore, from (13) and (14), we can obtain the acceleration equation of the EBI Universe

$$\frac{\ddot{a}}{a} = -\frac{4\pi G}{3}\left(\rho_m+3p_m\right)+\frac{\Lambda}{3}-\frac{1}{2\ell^2}\sqrt{\frac{V}{U}}\left(\frac{1}{3}V-U\right) = -4\pi G\rho_m\left[w_m+\frac{1}{3}-\frac{\Lambda}{12\pi G\rho_m} + \frac{1}{8\pi G\rho_m\ell^2}\sqrt{\frac{V}{U}}\left(\frac{1}{3}V-U\right)\right]. \tag{20}$$

2.3. The Characters of the Cosmical Apparent Horizon. In general, the cosmical apparent horizon is not null surface, which is different from the event and particle horizon. The equation of the cosmical apparent horizon in comoving coordinates is [22]

$$\mathscr{F}(t,r) = a(t)\,r-\frac{1}{\sqrt{H^2+k/a^2}} = 0. \tag{21}$$

Its normal has components

$$N_\mu = \nabla_\mu\mathscr{F}\big|_{AH} = \left\{\left[\dot{a}r+\frac{H\left(\dot{H}-k/a^2\right)}{\left(H^2+k/a^2\right)^{3/2}}\right]\delta_{\mu0}+a\delta_{\mu1}\right\}\Bigg|_{AH} = H\Upsilon_A\left[1+\left(\dot{H}-\frac{k}{a^2}\right)\Upsilon_A^2\right]\delta_{\mu0}+a\delta_{\mu1} = H\Upsilon_A^3\frac{\ddot{a}}{a}\delta_{\mu0}+a\delta_{\mu1}. \tag{22}$$

The norm squared of the normal vector is

$$\begin{aligned} N_a N^a &= 1 - kr_A^2 - H^2\Upsilon_A^6\left(\frac{\ddot{a}}{a}\right)^2 \\ &= H^2\Upsilon_A^2\left[1 - \Upsilon_A^4\left(\frac{\ddot{a}}{a}\right)^2\right] \\ &= H^2\Upsilon_A^6\left(\Upsilon_A^{-2} - \frac{\ddot{a}}{a}\right)\left(\Upsilon_A^{-2} + \frac{\ddot{a}}{a}\right), \end{aligned} \tag{23}$$

where $r_A = \Upsilon_A/a$. Substituting (20) and (18), we get

$$\begin{aligned} N_a N^a = \mathscr{H}(w_m) = -H^2\Upsilon_A^6(4\pi G\rho_m)^2 &\left[w_m - \frac{1}{3}\right. \\ &- \frac{\Lambda}{6\pi G\rho_m} - \frac{1}{8\pi G\rho_m\ell^2}\sqrt{\frac{V}{U}}\left(\frac{1}{3}V + U\right)\Bigg]\Bigg[w_m + 1 \\ &+ \frac{1}{8\pi G\rho_m\ell^2}\sqrt{\frac{V}{U}}(V - U)\Bigg], \end{aligned} \tag{24}$$

where we consider that $N_a N^a$ is only the quadratic function $\mathscr{H}(w_m)$ representing the inner product of the normal vector of the cosmical apparent horizon. The quadratic function $\mathscr{H}(w_m)$ has two zero points, $w_m = 1/3 + \Lambda/6\pi G\rho_m + (1/8\pi G\ell^2\rho_m)\sqrt{V/U}((1/3)V + U)$ and $w_m = -[1 + (1/8\pi G\ell^2\rho_m)\sqrt{V/U}(V - U)]$.

Considering the properties of the quadratic function $\mathscr{H}(w_m)$, we get three results as follows (considering the condition that $\Lambda > -(1/\ell^2)\sqrt{V/U}V - 8\pi G\rho_m$).

(A) When $w_m = 1/3 + \Lambda/6\pi G\rho_m + (1/8\pi G\ell^2\rho_m)\sqrt{V/U}((1/3)V + U)$ or $w_m = -[1 + (1/8\pi G\ell^2\rho_m)\sqrt{V/U}(V - U)]$, $N_a N^a = 0$ that shows the normal vector N^a is a null vector and the apparent horizon Υ_A is a null surface. It coincides with the cosmological event horizon $\Upsilon_E = a\int_t^\infty a^{-1}d\hat{t}$, which is a future-pointed null causal boundary [19, 22]. And it shares the signature of isolated black-hole horizons [23].

(B) When $-[1 + (1/8\pi G\ell^2\rho_m)\sqrt{V/U}(V - U)] < w_m < [1/3 + \Lambda/6\pi G\rho_m + (1/8\pi G\ell^2\rho_m)\sqrt{V/U}((1/3)V + U)]$, $N_a N^a > 0$ that shows N^a is a spacelike vector and Υ_A is the timelike surface. Υ_A has the signature $(-, +, +)$ that shares the signature of a quasi-local timelike membrane in black-hole physics [20, 24].

(C) When $[1/3 + \Lambda/6\pi G\rho_m + (1/8\pi G\ell^2\rho_m)\sqrt{V/U}((1/3)V + U)] < w_m$ or $w_m < -[1 + (1/8\pi G\ell^2\rho_m)\sqrt{V/U}(V - U)]$, $N_a N^a < 0$ that shows N^a is a timelike vector and Υ_A is the spacelike surface. Its signature is $(+, +, +)$ that is same as the signature of the dynamical black-hole horizons [25].

As we know, the present Universe is an accelerated expanding Universe that means the matter outside the cosmical apparent horizon may enter into the cosmical apparent horizon. Hence we considered that the timelike cosmical apparent horizon is reasonable and the range of the EoS parameter $-[1 + (1/8\pi G\ell^2\rho_m)\sqrt{V/U}(V - U)] < w_m < [1/3 + \Lambda/6\pi G\rho_m + (1/8\pi G\ell^2\rho_m)\sqrt{V/U}((1/3)V + U)]$ is significative, which is similar to the range of the EoS parameter $(-1 < w < 1/3)$ in Einstein Universe [14].

3. Thermodynamics of the Holographic-Style Dynamical Equations in the Eddington-Born-Infeld Universe

Based on the holographic-style dynamical equations (18), (19), and (16) in Section 2, we continue to investigate the thermodynamics about the cosmical apparent horizon. Firstly, we define the effective energy within a sphere of radius Υ (surface area $A = 4\pi\Upsilon^2$ and volume $\widehat{V} = (4/3)\pi\Upsilon^3$): $E_{eff} = \rho_{eff}\widehat{V}$, which is the entire energy enveloped by the cosmical apparent horizon Υ_A (take $\widehat{V}$ to represent the volume in order to distinguish the function V).

3.1. Unified First Law of Thermodynamics. Applying the Misner-Sharp mass/energy $E_{MS} \coloneqq (\Upsilon/2G)(1 - h^{\alpha\beta}\partial_\alpha\Upsilon\partial_\beta\Upsilon)$ [26, 27] to be the effective energy E_{eff} and substituting $h_{\alpha\beta} = \mathrm{diag}[-1, a^2/(1 - kr^2)]$, one obtains

$$dE = -\frac{\dot{\Upsilon}_A}{G}\frac{\Upsilon^3}{\Upsilon_A^3}dt + \frac{3}{2G}\frac{\Upsilon^2}{\Upsilon_A^2}d\Upsilon \tag{25}$$

and

$$dE = -\frac{1}{G}\frac{\Upsilon^3}{\Upsilon_A^3}\left(\dot{\Upsilon}_A - \frac{3}{2}H\Upsilon_A\right)dt + \frac{3}{2G}\frac{\Upsilon^2}{\Upsilon_A^2}adr. \tag{26}$$

For the EBI Universe, substituting (16) and (18) into (25), the total energy differential in the (t, Υ) coordinates is obtained

$$\begin{aligned} dE = A&\left[\rho_m + \frac{1}{8\pi G\ell^2}\sqrt{\frac{V}{U}}V + \frac{\Lambda}{8\pi G}\right]d\Upsilon \\ &- A\left[(\rho_m + p_m) + \frac{1}{8\pi G\ell^2}\sqrt{\frac{V}{U}}(V - U)\right] \\ &\cdot H\Upsilon dt, \end{aligned} \tag{27}$$

where $A = 4\pi\Upsilon^2$. Similarly, we can obtain

$$\begin{aligned} dE = A&\left[\rho_m + \frac{1}{8\pi G\ell^2}\sqrt{\frac{V}{U}}V + \frac{\Lambda}{8\pi G}\right]adr \\ &- A\left[p_m - \frac{1}{8\pi G\ell^2}\sqrt{\frac{V}{U}}U - \frac{\Lambda}{8\pi G}\right]\cdot H\Upsilon dt, \end{aligned} \tag{28}$$

which is the total energy differential in the (t, r) coordinates. From the above two equations, we can know that the EoS parameter from spacetime self-coupling w_{ac} is negative, because of the energy density term "$(1/8\pi G\ell^2)\sqrt{V/U}V$" and the intensity of pressure "$-(1/8\pi G\ell^2)\sqrt{V/U}U$".

The unified first law of (equilibrium) thermodynamics is given by

$$dE = A\Psi + Wd\widehat{V}, \tag{29}$$

proposed by Hayward [28]. W is the work density, given by

$$W \coloneqq -\frac{1}{2}T^{\alpha\beta}_{(m)}h_{\alpha\beta}, \tag{30}$$

where $h_{\alpha\beta} = \mathrm{diag}[-1, a(t)^2/(1-kr^2)]$. $\mathbf{\Psi}$ is the energy supply covector, $\mathbf{\Psi} = \mathbf{\Psi}_\alpha dx^\alpha$, where

$$\mathbf{\Psi}_\alpha \coloneqq T^\beta_{\alpha(m)}\partial_\beta \Upsilon + W\partial_\alpha \Upsilon. \tag{31}$$

Here, W and $\mathbf{\Psi}_\alpha$ are invariant. Moreover, the definitions of W and $\mathbf{\Psi}_\alpha$ are valid for all spherically symmetric spacetimes and FRW spacetime.

In the EBI theory, the field equations can be rewritten into

$$R_{\mu\nu} - \frac{1}{2}Rg_{\mu\nu} = 8\pi G T^{(eff)}_{\mu\nu}, \tag{32}$$

where we define an effective energy-momentum tensor

$$\begin{aligned} T^{(eff)}_{\mu\nu} = T^{(m)}_{\mu\nu} - \frac{\Lambda}{8\pi G}g_{\mu\nu} - \frac{1}{8\pi G\ell^2}\sqrt{\frac{V}{U}}UV \\ \cdot g_{\mu\alpha}q^{\alpha\beta}g_{\beta\nu}. \end{aligned} \tag{33}$$

From the above equation, we can consider that the effective energy-momentum tensor includes the part of the dark energy corresponding to the terms with Λ and (U, V). Then we can generalize Hayward's unified first law of (equilibrium) thermodynamics into the EBI Universe by taking $T^{(eff)}_{\mu\nu}$ to replace $T^{(m)}_{\mu\nu}$. Imitating the definitions of W and $\mathbf{\Psi}_\alpha$ [28], we define

$$dE = A\widetilde{\mathbf{\Psi}} + \widetilde{W}d\widehat{V} \tag{34}$$

and

$$\widetilde{\mathbf{\Psi}} = \widetilde{\mathbf{\Psi}}_\alpha dx^\alpha, \tag{35}$$

where

$$\widetilde{W} \coloneqq -\frac{1}{2}T^{\alpha\beta}_{(eff)}h_{\alpha\beta} \tag{36}$$

and

$$\widetilde{\mathbf{\Psi}}_\alpha \coloneqq T^\beta_{\alpha(eff)}\partial_\beta \Upsilon + \widetilde{W}\partial_\alpha \Upsilon. \tag{37}$$

We consider that the FRW metric $g_{\mu\nu}$ is physically subsistent, which is used to raise or descend the index here, and another metric $q_{\mu\nu}$ is an extra metric provided by the primordial mechanism of Universe. Based on this, we get

$$\begin{aligned} T^\beta_{\alpha(eff)} &= g^{\mu\beta}T^{(eff)}_{\mu\alpha} \\ &= g^{\mu\beta}T^{(m)}_{\mu\alpha} - \frac{\Lambda}{8\pi G}\delta^\beta_\alpha - \frac{1}{8\pi G\ell^2}\sqrt{\frac{V}{U}}UVq^{\beta\mu}g_{\mu\alpha} \end{aligned} \tag{38}$$

and

$$\begin{aligned} T^{\alpha\beta}_{(eff)} &= g^{\mu\alpha}g^{\nu\beta}T^{(eff)}_{\mu\nu} \\ &= g^{\mu\alpha}g^{\nu\beta}T^{(m)}_{\mu\nu} - \frac{\Lambda}{8\pi G}g^{\alpha\beta} - \frac{1}{8\pi G\ell^2}\sqrt{\frac{V}{U}}UVq^{\alpha\beta}. \end{aligned} \tag{39}$$

Substituting $h_{\alpha\beta} = \mathrm{diag}[-1, a(t)^2/(1-kr^2)]$, we obtain

$$\begin{aligned} \widetilde{W} &= -\frac{1}{2}\left[T^{00}_{(eff)}h_{00} + T^{11}_{(eff)}h_{11}\right] \\ &= \frac{1}{2}(\rho_m - p_m) + \frac{\Lambda}{8\pi G} + \frac{1}{8\pi G\ell^2}\sqrt{\frac{V}{U}}\left(\frac{U+V}{2}\right); \end{aligned} \tag{40}$$

$$\widetilde{\mathbf{\Psi}}_t = -\frac{1}{2}\left[(\rho_m + p_m) + \frac{1}{8\pi G\ell^2}\sqrt{\frac{V}{U}}(V-U)\right]H\Upsilon; \tag{41}$$

$$\widetilde{\mathbf{\Psi}}_r = \frac{1}{2}\left[(\rho_m + p_m) + \frac{1}{8\pi G\ell^2}\sqrt{\frac{V}{U}}(V-U)\right]a. \tag{42}$$

Substituting $\widetilde{\mathbf{\Psi}}_t$, $\widetilde{\mathbf{\Psi}}_r$, and $\widetilde{W}$ into (34), we get

$$\begin{aligned} dE &= A\widetilde{\mathbf{\Psi}} + \widetilde{W}d\widehat{V} = A\left[\widetilde{\mathbf{\Psi}}_t dt + \widetilde{\mathbf{\Psi}}_r dr + \widetilde{W}d\Upsilon\right] \\ &= A\left[-p_m + \frac{\Lambda}{8\pi G} + \frac{1}{8\pi G\ell^2}\sqrt{\frac{V}{U}}U\right]H\Upsilon dt \\ &\quad + A\left[\rho_m + \frac{\Lambda}{8\pi G} + \frac{1}{8\pi G\ell^2}\sqrt{\frac{V}{U}}V\right]adr, \end{aligned} \tag{43}$$

which is the expression of dE in (t, r) coordinates.

Naturally, because of the invariance of $\widetilde{W}$ and $\widetilde{\mathbf{\Psi}}$, we can rewrite these in the (t, Υ) coordinates, given by

$$\begin{aligned} dE &= A\widetilde{\mathbf{\Psi}} + \widetilde{W}d\widehat{V} = A\left[\widetilde{\mathbf{\Psi}}'_t dt + \widetilde{\mathbf{\Psi}}'_\Upsilon d\Upsilon + \widetilde{W}d\Upsilon\right] \\ &= -A\left[(\rho_m + p_m) + \frac{1}{8\pi G\ell^2}\sqrt{\frac{V}{U}}(V-U)\right]H\Upsilon dt \\ &\quad + A\left[\rho_m + \frac{\Lambda}{8\pi G} + \frac{1}{8\pi G\ell^2}\sqrt{\frac{V}{U}}V\right]d\Upsilon, \end{aligned} \tag{44}$$

where

$$\widetilde{\mathbf{\Psi}}'_t = -\left[(\rho_m + p_m) + \frac{1}{8\pi G\ell^2}\sqrt{\frac{V}{U}}(V-U)\right]H\Upsilon \tag{45}$$

and

$$\widetilde{\mathbf{\Psi}}'_\Upsilon = \frac{1}{2}\left[(\rho_m + p_m) + \frac{1}{8\pi G\ell^2}\sqrt{\frac{V}{U}}(V-U)\right]. \tag{46}$$

It illustrates our hypothesis of replacing $T^{(m)}_{\mu\nu}$ by $T^{(eff)}_{\mu\nu}$ is reasonable that (43) and (44) are, respectively, identical to (28) and (27). The unified first law for gravitational thermodynamics of Universe is totally different from the first law in the black-hole thermodynamics [14]. Eq. (43) and (44) are both called "the unified first law" for the EBI Universe's gravitational thermodynamics.

3.2. Clausius Equation on the Cosmical Apparent Horizon for an Isochoric Process. Having obtained the unified first law $dE = A\widetilde{\mathbf{\Psi}} + \widetilde{W}d\widehat{V}$ in EBI Universe, we are interested in the region enclosed by the cosmical apparent horizon Υ_A.

Eq. (19) leads to

$$\frac{\dot{\Upsilon}_A}{G}dt = A_A\left[(\rho_m + p_m) + \frac{1}{8\pi G\ell^2}\sqrt{\frac{V}{U}}(V-U)\right]H\Upsilon_A \cdot dt, \tag{47}$$

where $A_A = 4\pi\Upsilon_A^2$. The left-hand side of (47) can be manipulated into [14]

$$\frac{\dot{\Upsilon}_A}{G}dt = \frac{1}{2\pi\Upsilon_A}\cdot\left(\frac{2\pi\Upsilon_A\dot{\Upsilon}_A}{G}\cdot dt\right) = \frac{1}{2\pi\Upsilon_A}d\left(\frac{\pi\Upsilon_A^2}{G}\right). \tag{48}$$

One applies the geometrically defined Hawking-Bekenstein entropy [4, 29] (in the units $\hbar = c = k[Boltzmann\ constant] = 1$)

$$S_A = \frac{\pi\Upsilon_A^2}{G} = \frac{A_A}{4G}, \tag{49}$$

and the Cai-Kim temperature [1, 30]

$$\widehat{T}_A \equiv \frac{1}{2\pi\Upsilon_A}, \tag{50}$$

at the cosmical apparent horizon to simplify (48), given by $(\dot{\Upsilon}_A/G)dt = \widehat{T}_A dS_A$ (take "$\widehat{T}$" on behalf of temperature not only the Cai-Kim temperature). With the help of (45), we get $-[(\rho_m + p_m) + (1/8\pi G\ell^2)\sqrt{V/U}(V-U)]H\Upsilon_A = \widetilde{\Psi}'_t|_{(\Upsilon=\Upsilon_A)} \equiv \widetilde{\Psi}'_{tA}$. From (44) and (47), we obtain

$$\delta Q_A = \widehat{T}_A dS_A = -A_A\widetilde{\Psi}'_{tA} = -dE_A\big|_{d\Upsilon=0}, \tag{51}$$

where dE_A is the specific condition of (44) when $\Upsilon = \Upsilon_A$. Eq. (51) is actually the Clausius equation for equilibrium and reversible thermodynamic processes as same as the situation in GR [14]. After considering the EBI theory, the Clausius equation is generalized to include dark energy from the cosmological constant Λ and the effect the self-coupling of spacetime (U, V), which may explain the problems about the cosmic expansion.

Finally, for the open system enveloped by Υ_A, we substitute the unified first law (44) and the Clausius equation (51) into the total energy differential

$$dE_A = -\widehat{T}_A dS_A + \left[\rho_m + \frac{\Lambda}{8\pi G} + \frac{1}{8\pi G\ell^2}\sqrt{\frac{V}{U}}V\right]d\widehat{V}_A, \tag{52}$$

where the "-" sign shows the positive-heat-out sign convention that means heat emitted by the open system takes positive values ($\delta Q_A = \delta Q_A^{(out)} > 0$) rather than the traditional positive-heat-in thermodynamic sign convention [14].

Comparing (52) with the total energy differential of the Einstein gravity, there are two extra terms $(\Lambda/8\pi G)d\widehat{V}_A$ and $(1/8\pi G\ell^2)\sqrt{V/U}Vd\widehat{V}_A$, which originate from dark energy of the cosmological constant and the spacetime self-coupling, respectively. It means that there are the matter's transition and the dark energy's fluxion on both sides of the cosmical apparent horizon during the expansion of Universe.

4. Generalized Second Laws of Thermodynamics in Eddington-Born-Infeld Universe

With the help of the first holographic-style dynamical equation (18), the effective energy ($E_{MS} = \Upsilon^3/2G\Upsilon_A^2$) can be rewritten into

$$E_{MS} = \rho_{eff}\left(\frac{4}{3}\pi\Upsilon^3\right) = \rho_{eff}\widehat{V}, \tag{53}$$

where $\rho_{eff} = \rho_m + \Lambda/8\pi G + (1/8\pi G\ell^2)\sqrt{V/U}V$. Then we can rewrite the Friedmann equations into

$$\frac{\dot{a}}{a} + \frac{k}{a} = \frac{8\pi G\rho_{eff}}{3} \tag{54}$$

and

$$\frac{\dot{a}}{a} + \frac{k}{a} + 2\frac{\ddot{a}}{a} = -8\pi G p_{eff}, \tag{55}$$

where we define that $p_{eff} = p_m - \Lambda/8\pi G - (1/8\pi G\ell^2)\sqrt{V/U}U$. Based on two above equations, one can obtain the continuity equation in the EBI theory

$$\dot{\rho}_{eff} + 3\frac{\dot{a}}{a}\left(\rho_{eff} + p_{eff}\right) = 0. \tag{56}$$

In many papers [31–33], the entropy S_m of the cosmic energy-matter content with temperature $\widehat{T}_m$ is always determined by the traditional Gibbs equation $dE = \widehat{T}_m dS_m - p_m d\widehat{V}$. In order to generalize to the EBI theory, we keep the same form and redefine it into the positive-heat-out sign convention for consistency with the horizon entropy S_A [14], given by

$$dE_{eff} = -\widehat{T}_{eff}dS_{eff} - p_{eff}d\widehat{V}. \tag{57}$$

From $dE_{eff} = \rho_{eff}d\widehat{V} + \widehat{V}d\rho_{eff}$, we obtain

$$\widehat{T}_{eff}dS_{eff} = -\widehat{V}d\rho_{eff} - \left(\rho_{eff} + p_{eff}\right)d\widehat{V}. \tag{58}$$

Based on the continuity equation (56), we obtain

$$d\rho_{eff} = -3H\left(\rho_{eff} + p_{eff}\right)dt. \tag{59}$$

When $\Upsilon = \Upsilon_A$, one can get

$$\widehat{T}_{eff}dS_{eff}^{(A)} = A_A\left(\rho_{eff} + p_{eff}\right)\cdot\left(H\Upsilon_A - \dot{\Upsilon}_A\right)dt, \tag{60}$$

where $A_A = 3/2G\rho_{eff}$. With the help of (19), (60) yields

$$\dot{S}^{(A)}_{eff} = -\frac{9}{4G}\cdot\frac{H\Upsilon_A}{\widehat{T}_{eff}} \cdot\frac{1}{\rho^2_{eff}}\left(\rho_{eff}+p_{eff}\right)\left(\frac{1}{3}\rho_{eff}+p_{eff}\right) \tag{61}$$

that is the evolution of the effective inner entropy enclosed by Υ_A.

In order to discuss $\dot{S}^{(A)}_{eff}$ more concretely, we assume that $\rho_{aux} \equiv \rho_m + (1/8\pi G\ell^2)\sqrt{V/U}V$ and $p_{aux} \equiv p_m - (1/8\pi G\ell^2)\sqrt{V/U}U$, which are two auxiliary parameters. Following $p_m = w_m\rho_m$, we set

$$p_{eff} = \varepsilon_{eff}\rho_{eff} \tag{62}$$

and

$$p_{aux} = \sigma_{aux}\rho_{aux}, \tag{63}$$

where ε_{eff} and σ_{aux} are the parameters of state like w_m. And (61) can be simplified as

$$\dot{S}^{(A)}_{eff} = -\frac{9}{4G}\cdot\frac{H\Upsilon_A}{\widehat{T}_{eff}}\cdot\left(\varepsilon_{eff}+1\right)\left(\varepsilon_{eff}+\frac{1}{3}\right). \tag{64}$$

Based on the above assumptions, we can obtain

$$\sigma_{aux} = w_m + \frac{\sqrt{V/U}\left(w_mV+U\right)}{8\pi G\ell^2\rho_m+\sqrt{V/U}V} \tag{65}$$

and

$$\varepsilon_{eff} = \sigma_{aux} - \left(\sigma_{aux}+1\right)\frac{\Lambda}{8\pi G\rho_{aux}+\Lambda}. \tag{66}$$

Then we obtain

$$\varepsilon_{eff} = \frac{8\pi G\ell^2\rho_m}{8\pi G\ell^2\rho_m+\sqrt{V/U}V+\Lambda\ell^2}\cdot w_m - \frac{\sqrt{V/U}U+\Lambda\ell^2}{8\pi G\ell^2\rho_m+\sqrt{V/U}V+\Lambda\ell^2}. \tag{67}$$

As a result, $\dot{S}^{(A)}_{eff}$ can be rewritten into

$$\dot{S}^{(A)}_{eff} = -\frac{9}{4G}\cdot\frac{H\Upsilon_A}{\widehat{T}_{eff}}\cdot\left(\frac{8\pi G\ell^2\rho_m}{8\pi G\ell^2\rho_m+\sqrt{V/U}V+\Lambda\ell^2}\right)^2 \cdot\left[w_m+1+\frac{\sqrt{V/U}\left(V-U\right)}{8\pi G\ell^2\rho_m}\right] \cdot\left[w_m+\frac{1}{3}+\frac{\sqrt{V/U}\left((1/3)V-U\right)}{8\pi G\ell^2\rho_m}-\frac{\Lambda}{12\pi G\rho_m}\right]. \tag{68}$$

Physically, temperature is positive ($\widehat{T}_{eff} > 0$) and the present Universe is expanding ($H > 0$).

If Λ satisfies the precondition ($\Lambda > -(1/\ell^2)\sqrt{V/U}V - 8\pi G\rho_m$) shown in Section 2, we can exactly obtain that $[1+\sqrt{V/U}(V-U)/8\pi G\ell^2\rho_m] > [1/3+\sqrt{V/U}((1/3)V-U)/8\pi G\ell^2\rho_m - \Lambda/12\pi G\rho_m]$. And (68) illustrates that

(A) when $-[1+\sqrt{V/U}(V-U)/8\pi G\ell^2\rho_m] < w_m < -[1/3+\sqrt{V/U}((1/3)V-U)/8\pi G\ell^2\rho_m - \Lambda/12\pi G\rho_m]$, $\dot{S}^{(A)}_{eff} > 0$;

(B) when $-[1+\sqrt{V/U}(V-U)/8\pi G\ell^2\rho_m] > w_m$ or $-[1/3+\sqrt{V/U}((1/3)V-U)/8\pi G\ell^2\rho_m - \Lambda/12\pi G\rho_m] < w_m$, $\dot{S}^{(A)}_{eff} < 0$;

(C) when $w_m = -[1+\sqrt{V/U}(V-U)/8\pi G\ell^2\rho_m]$ or $-[1/3+\sqrt{V/U}((1/3)V-U)/8\pi G\ell^2\rho_m - \Lambda/12\pi G\rho_m]$, $\dot{S}^{(A)}_{eff} = 0$.

On the other hand, from the acceleration equation of the EBI Universe (20), we know that when $w_m < -[1/3 - \Lambda/12\pi G\rho_m + \sqrt{V/U}((1/3)V-U)/8\pi G\ell^2\rho_m]$, the present Universe is an accelerated expanding Universe. Hence, if $V < 3U - 8\pi G\ell^2\rho_m\sqrt{U/V}$, w_m has the possibility to be a positive number to produce an accelerated expanding Universe, which is different from the result of Einstein Universe [14].

In a word, the physical effective entropy $S^{(A)}_{eff}$ inside the cosmical apparent horizon satisfies $\dot{S}^{(A)}_{eff} > 0$ for the stage of accelerated expansion ($\ddot{a} > 0$) when $-[1+\sqrt{V/U}(V-U)/8\pi G\ell^2\rho_m] < w_m < -[1/3+\sqrt{V/U}((1/3)V-U)/8\pi G\ell^2\rho_m - \Lambda/12\pi G\rho_m]$. Noteworthily, $S^{(A)}_{eff}$ is composed of the matter's entropy and the dark energy's entropy.

5. Conclusions and Discussion

In this paper, we obtained the gravitational dynamics in the EBI Universe. Firstly, we derived the holographic-style dynamical equations. Because of the present accelerated expanding Universe that means the outer matter can enter into the cosmical apparent horizon, we considered the timelike cosmical apparent horizon is reasonable and $-[1+(1/8\pi G\ell^2\rho_m)\sqrt{V/U}(V-U)] < w_m < [1/3+\Lambda/6\pi G\rho_m + (1/8\pi G\ell^2\rho_m)\sqrt{V/U}((1/3)V+U)]$ is a rational range of the matter's EoS parameter.

Secondly, based on the holographic-style dynamical equations, we obtained two forms of the total energy differential in the (t,Υ) coordinates and (t,r) coordinates. And we proved that these two forms of the total energy differential can be derived from the unified first laws of the gravitational dynamics $dE = A\widetilde{\Psi}+\widetilde{W}d\widehat{V}$ by redefining the effective energy-momentum tensor $T^{(eff)}_{\mu\nu}$ in Hayward's approach [28].

Thirdly, we derived the total energy differential for the open system enveloped by Υ_A, $dE_A = -\widehat{T}_A dS_A + [\rho_m + \Lambda/8\pi G + (1/8\pi G\ell^2)\sqrt{V/U}V]d\widehat{V}_A$, where the two extra terms $(\Lambda/8\pi G)d\widehat{V}_A$ and $(1/8\pi G\ell^2)\sqrt{V/U}Vd\widehat{V}_A$ are, respectively, corresponding to the dark energy and the spacetime self-coupling in EBI Universe. It illustrates that not only the matter's transition but also the dark energy's fluxion arises

on the cosmical apparent horizon Υ_A with the expansion of Universe.

Finally, we discussed the properties of the effective entropy $S_{eff}^{(A)}$ enclosed by the cosmical apparent horizon Υ_A in EBI Universe. The results show that when $-[1 + \sqrt{V/U}(V-U)/8\pi G\ell^2\rho_m] < w_m < -[1/3 + \sqrt{V/U}((1/3)V - U)/8\pi G\ell^2\rho_m - \Lambda/12\pi G\rho_m]$ and $\ddot{a} > 0$, the generalized second law of the nondecreasing entropy $S_{eff}^{(A)}$ is obtained. If V satisfies the condition $V < 3U - 8\pi G\ell^2\rho_m\sqrt{U/V}$, w_m can be a positive number to generate an accelerated expanding Universe, which is different from the results in Einstein Universe.

In addition to all the above we would like to point out that the method of the theories we mentioned in our paper satisfying the equilibrium thermodynamics does not mean this method fits all possible theories. Actually, nonequilibrium thermodynamics might be also a good way in finding new gravitational theories [34–36], which would be a further task for us to study.

Data Availability

No data were used to support this study.

Conflicts of Interest

The authors declare that there are no conflicts of interest regarding the publication of this paper.

Acknowledgments

We would like to thank the National Natural Science Foundation of China (Grant No. 11571342) for supporting us on this work.

References

[1] R. G. Cai and S. P. Kim, "First law of thermodynamics and Friedmann equations of Friedmann-Robertson-Walker universe," *Journal of High Energy Physics*, vol. 2005, no. 02, p. 050, 2005.

[2] T. Padmanabhan, "Thermodynamical aspects of gravity: new insights," *Reports on Progress in Physics*, vol. 73, no. 4, Article ID 046901, 2010.

[3] S. W. Hawking, "Black hole explosions?" *Nature*, vol. 248, no. 5443, pp. 30-31, 1974.

[4] J. D. Bekenstein, "Black holes and entropy," *Physical Review D*, vol. 7, pp. 2333–2346, 1973.

[5] M. Akbar and R.-G. Cai, "Thermodynamic behavior of the friedmann equation at the apparent horizon of the frw universe," *Physical Review D*, vol. 75, Article ID 084003, 2007.

[6] R.-G. Cai and L.-M. Cao, "Unified first law and the thermodynamics of the apparent horizon in the frw universe," *Physical Review D*, vol. 75, Article ID 064008, 2007.

[7] M. Akbar and R.-G. Cai, "Thermodynamic behavior of field equations for $f(R)$ gravity," *Physics Letters B*, vol. 648, no. 2, pp. 243–248, 2007.

[8] R. G. Cai and L. M. Cao, "Thermodynamics of apparent horizon in brane world scenario," *Nuclear Physics B*, vol. 785, no. 1, pp. 135–148, 2007.

[9] A. Sheykhi, B. Wang, and R.-G. Cai, "Thermodynamical properties of apparent horizon in warped DGP braneworld," *Nuclear Physics B*, vol. 779, no. 1, pp. 1–12, 2007.

[10] A. Sheykhi, B. Wang, and R.-G. Cai, "Deep connection between thermodynamics and gravity in Gauss-Bonnet braneworlds," *Physical Review D*, vol. 76, no. 2, Article ID 023515, 2007.

[11] K. Bamba, C.-Q. Geng, and S. Tsujikawa, "Equilibrium thermodynamics in modified gravitational theories," *Physics Letters B*, vol. 688, no. 1, pp. 101–109, 2010.

[12] R.-G. Cai and N. Ohta, "Horizon thermodynamics and gravitational field equations in Hŏrava-Lifshitzgravity," *Physical Review D*, vol. 81, no. 8, Article ID 084061, 2010.

[13] Q.-J. Cao, Y.-X. Chen, and K.-N. Shao, "Clausius relation and Friedmann equation in FRW universe model," *Journal of Cosmology and Astroparticle Physics*, vol. 2010, no. 5, p. 030, 2010.

[14] D. W. Tian and I. Booth, "Apparent horizon and gravitational thermodynamics of the universe: solutions to the temperature and entropy confusions and extensions to modified gravity," *Physical Review D*, vol. 92, Article ID 024001, 2015.

[15] M. Banados, "Eddington-Born-Infeld action for dark matter and dark energy," *Physical Review D*, vol. 77, Article ID 123534, 2008.

[16] A. De Felice, B. Gumjudpai, and S. Jhingan, "Cosmological constraints for an Eddington-Born-Infeld field," *Physical Review D*, vol. 86, no. 4, Article ID 043525, 2012.

[17] M. Bañados, P. G. Ferreira, and C. Skordis, "Eddington-born-infeld gravity and the large scale structure of the universe," *Physical Review D*, vol. 79, no. 6, Article ID 063511, 2009.

[18] M. Bañados, A. Gomberoff, D. C. Rodrigues, and C. Skordis, "Note on bigravity and dark matter," *Physical Review D*, vol. 79, no. 6, Article ID 063515, 2009.

[19] D. Bak and S.-J. Rey, "Cosmic holography," *Classical and Quantum Gravity*, vol. 17, no. 15, p. L83, 2000.

[20] S. A. Hayward, "General laws of black-hole dynamics," *Physical Review D*, vol. 49, pp. 6467–6474, 1994.

[21] M. Bañados and P. G. Ferreira, "Eddington's theory of gravity and its progeny," *Physical Review Letters*, vol. 105, no. 1-2, Article ID 011101, 2010.

[22] V. Faraoni, "Cosmological apparent and trapping horizons," *Physical Review D*, vol. 84, no. 2, Article ID 024003, 2011.

[23] A. Ashtekar, S. Fairhurst, and B. Krishnan, "Isolated horizons: hamiltonian evolution and the first law," *Physical Review D*, vol. 62, Article ID 104025, 2000.

[24] I. Booth, "Black-hole boundaries," *Canadian Journal of Physics*, vol. 83, no. 11, pp. 1073–1099, 2005.

[25] A. Ashtekar and B. Krishnan, "Dynamical horizons: energy, angular momentum, fluxes, and balance laws," *Physical Review Letters*, vol. 89, no. 26, 261101, 4 pages, 2002.

[26] C. W. Misner and D. H. Sharp, "Relativistic equations for adiabatic, spherically symmetric gravitational collapse," *Physical Review A*, vol. 136, no. 2, pp. B571–B576, 1964.

[27] S. A. Hayward, "Gravitational energy in spherical symmetry," *Physical Review D*, vol. 53, no. 4, pp. 1938–1949, 1996.

[28] S. A. Hayward, "Unified first law of black-hole dynamics and relativistic thermodynamics," *Classical and Quantum Gravity*, vol. 15, no. 10, pp. 3147–3162, 1998.

[29] J. M. Bardeen, B. Carter, and S. W. Hawking, "The four laws of black hole mechanics," *Communications in Mathematical Physics*, vol. 31, pp. 161–170, 1973.

[30] R.-G. Cai, L.-M. Cao, and Y.-P. Hu, "Hawking radiation of an apparent horizon in a FRW universe," *Classical and Quantum Gravity*, vol. 26, no. 15, Article ID 155018, 2009.

[31] R. Brustein, "Generalized second law in cosmology from causal boundary entropy," *Physical Review Letters*, vol. 84, no. 10, pp. 2072–2075, 2000.

[32] M. R. Setare, "Generalized second law of thermodynamics in quintom dominated universe," *Physics Letters B*, vol. 641, no. 2, pp. 130–133, 2006.

[33] A. Abdolmaleki, T. Najafi, and K. Karami, "Generalized second law of thermodynamics in scalar-tensor gravity," *Physical Review D*, vol. 89, no. 10, Article ID 104041, 2014.

[34] C. Eling, R. Guedens, and T. Jacobson, "Nonequilibrium thermodynamics of spacetime," *Physical Review Letters*, vol. 96, no. 12, Article ID 121301, 2006.

[35] G. Chirco, C. Eling, and S. Liberati, "Reversible and irreversible spacetime thermodynamics for general Brans-Dicke theories," *Physical Review D*, vol. 83, no. 2, Article ID 024032, 2011.

[36] G. Chirco and S. Liberati, "Nonequilibrium thermodynamics of spacetime: The role of gravitational dissipation," *Physical Review D: Particles, Fields, Gravitation and Cosmology*, vol. 81, no. 2, Article ID 024016, 2010.

Hindawi
Advances in High Energy Physics
Volume 2018, Article ID 9151707, 27 pages
https://doi.org/10.1155/2018/9151707

Research Article

Spread of Entanglement in Non-Relativistic Theories

Sagar F. Lokhande

Institute for Theoretical Physics, University of Amsterdam, Science Park 904, 1098 XH Amsterdam, Netherlands

Correspondence should be addressed to Sagar F. Lokhande; sagar.f.lokhande@gmail.com

Received 7 September 2018; Accepted 26 October 2018; Published 12 November 2018

Guest Editor: Sandipan Kundu

We use a simple holographic toy model to study global quantum quenches in strongly coupled, hyperscaling-violating-Lifshitz quantum field theories using entanglement entropy as a probe. Generalizing our conformal field theory results, we show that the holographic entanglement entropy of small subsystems can be written as a simple linear response relation. We use this relation to derive a time-dependent first law of entanglement entropy. In general, this law has a time-dependent term resembling relative entropy which we propose as a good order parameter to characterize out-of-equilibrium states in the post-quench evolution. We use these tools to study a broad class of quantum quenches in detail: instantaneous, power law, and periodic.

1. Introduction

1.1. Quantum Quenches and Entanglement Entropy. Studying the evolution of quantum field theories (QFTs) after generic time-dependent perturbations is an important problem. If H_0 denotes the time-independent Hamiltonian of a QFT defined on a manifold $\mathbb{R} \times \mathbb{R}^{d-1}$, one is often interested in a time-dependent perturbation

$$H(t) = H_0 + \delta H(t). \tag{1}$$

where $\delta H(t)$ could correspond to making a coupling in the Hamiltonian time-dependent [1] such as

$$H(t) = H_0 + \int d^{d-1}x J\left(t, x^i\right) O\left(t, x^i\right), \tag{2}$$

with $O(t, x^i)$ denoting a generic operator in the theory and $J(t, x^i)$ its corresponding source. A perturbation of the above kind, followed by unitary quantum evolution, is called a *Quantum Quench*. If the theory was in a pure state $|\Psi_0\rangle$ before the quench, unitarity of the post-quench evolution implies that it will remain in a pure state. However, experimental studies in ultracold atoms [2] and theoretical arguments [3–5] suggest that the end state of the evolution looks thermal to a very good approximation when studied with local, coarse-grained probes. This process is often termed *thermalization*. If a quantum quench acts uniformly at all space points such that $J(t, x^i) \equiv J(t)$, it is known as a *Global Quench*. In this paper, we will only discuss quenches of this kind.

Study of global quenches was initiated in [1] using *boundary conformal field theory* techniques of [6]. For the case of free field theories, [7] made significant progress using symmetries of the theory. Let us begin by considering a global quench to a more general conformal field theory (CFT). In this case, one-point functions are known to thermalize instantaneously [8–10], thus forcing one to look for better probes of thermalization in CFTs. Natural choices are non-local observables like two-point correlation functions, Wilson lines, and entanglement entropy. Although all of these have been studied recently [11], entanglement entropy is the most attractive of these, and for good reasons. As shown in [11], entanglement entropy equilibriates slower compared to other quantities for a finite-duration global quench, thus determining the physical rate of thermalization of the theory. It has further been used as an order parameter for phases of quantum matter [12]. The entanglement shared between regions codifies all possible correlations between them, making it very useful. For example, mutual information, a combination of entanglement entropies of two regions, gives an upper bound on all possible connected two-point functions between operators in the two regions [13]. Lastly, entanglement entropy grows in time after a quench (as we

will discuss in great detail later), thus making the quench a way to generate entanglement. This is a goal of great interest in quantum information theory [14].

Entanglement entropy of a subregion A (also called subsystem interchangeably) in the CFT is defined as the von Nuemann entropy of A

$$S_A \equiv -\operatorname{tr}\left(\rho_A \log \rho_A\right), \tag{3}$$

where $\rho_A = \operatorname{tr}_{A^c} \rho$ is the reduced density matrix on the region A. In a QFT, the entanglement entropy is generally calculated using the replica trick [15] but it is UV-divergent for any subregion A and any state ρ, due to the short-distance divergences. To obtain a finite answer, one often considers the *difference* between the entanglement entropies of A in two nearby states. The authors in [16] studied the time evolution of entanglement entropy of a general subregion in (1+1) dimensional CFT and showed that the entanglement entropy increases linearly in time and saturates after a specific time. However, technical difficulties do not allow one to generalize these calculations to higher dimensions easily (Nevertheless, recently some progress has been made on this account in the dilute gas limit in [17]).

In such cases, the AdS/CFT correspondence [18–20] has been very useful. It maps a strongly coupled *holographic* CFT to a weakly coupled theory of gravity in AdS space. Thus quantum quenches in such CFTs correspond to classical time evolution of the semi-classical theory of gravity. A general asymptotically AdS spacetime in the Feffermann-Graham gauge looks like

$$ds^2 = \frac{L^2}{z^2}\left(dz^2 + g_{\mu\nu}\left(z, x^\mu\right) dx^\mu dx^\nu\right), \tag{4}$$

where x^μ parameterizes the CFT which lives on the boundary of this spacetime $z \longrightarrow 0$. Operators in the CFT correspond to matter fields in this geometry. Then, if the CFT Hamiltonian is perturbed such as in (2), the insertion of the operators $O(t, x^i)$ in the CFT acts as sources for the matter fields in AdS and changes their boundary conditions. The full matter plus gravity system evolves in time and this evolution can be used to understand the post-quench evolution in the CFT. AdS spacetime can be thought of as a box and thus acts as a potential well for the matter fields. These then fall into the center of AdS and, after sufficient time, generically form a black hole [21–23] (However, see [24] for an interesting discussion of a class of initial conditions that do not result in black hole formation. Whether a generic perturbative initial condition leads to a collapse or not is still an open problem. See [25] and references therein for a discussion about this). Thermalization in the CFT is thus described by black hole formation in the dual semi-classical theory of gravity in AdS, as has been noted by several authors [23, 26, 27]. Consequently, collapsing solutions to semi-classical gravity in AdS are one of the most widely used tools to study quenches in holographic CFTs [11, 28–31]. Apart from weak-field analytic study in [9], they have also been studied using probe D-branes [32–34] and numerical methods [8, 35].

In 2006, Ryu and Takayanagi [36] proposed that the entanglement entropy of a subregion A in the CFT is given by the minimal area of a bulk co-dimension 2 surface homologous to A at the AdS boundary

$$S_A = \min_{\gamma_A} \frac{\operatorname{Area}\left(\gamma_A\right)}{4G_N}, \tag{5}$$

with the *homology condition* $\partial\gamma_A \approx \partial A$. Due to the simplicity of this formula, *holographic entanglement entropy* has received a lot of attention in the past decade (see [37] for a recent review). However, this formula works only for time-independent states. To calculate entanglement entropy of a subregion in a time-dependent state, one needs to use the covariant generalization of this formula, proposed in [38]. This general proposal is called HRT proposal and it states that

$$S_A = \operatorname*{ext}_{\gamma_A} \frac{\operatorname{Area}\left(\gamma_A\right)}{4G_N}, \tag{6}$$

where γ_A now denotes an extremal codimension-2 surface in the AdS bulk, i.e., one with vanishing trace of the extrinsic curvature.

Using the HRT proposal, [39] initiated the study of time-dependent holographic entanglement entropy, in the context of quenching a holographic (1+1) D CFT. They considered an abrupt (instantaneous) global quench to the CFT, such as

$$H(t) = H_0 + \Theta(t) \int d^{d-1}x O\left(t, x^i\right), \tag{7}$$

where $\Theta(t)$ is the Heaviside Theta function. As the operators $O(t, x)$ are uniformly inserted in the CFT, the dual bulk fields get sourced everywhere at the boundary of the AdS_3. If these operators have conformal dimensions much smaller than the central charge, the bulk fields are light and then the quench is described by a 3D geometry with a thin, uniform shell of infalling matter that forms a black hole. This geometry is well-studied and known as the *Vaidya Geometry* [40]

$$ds^2 = \frac{L^2}{z^2}\left(\frac{dz^2}{f(t,z)} - f(t,z)\, dt^2 + dx^2\right), \tag{8}$$

where the function $f(t, z)$ determines the horizon(s) of the black hole and is called the *Blackening Function*. The end state of the quench will be a stationary state that looks thermal locally, with a temperature fixed in terms of the blackening function of the black hole. Like the field theory calculation of [16] in the (1+1) D CFT, [39] found a linear growth of entanglement entropy with time. Reference [41] generalized this holographic calculation to the case where the initial state is not vacuum but a thermal state or a typical pure state. These works for lower-dimensional field theories using the properties of (2+1) D AdS gravity, which is special in various ways. Reference [42] instead considered the evolution of holographic entanglement entropy in (2+1) D CFT, exploring evolving geometries in AdS_4. They also observed a linear behavior for the growth of entanglement entropy, but noticed some novel phenomena, such as a discontinuity in the time derivative of entanglement entropy near the time when it is about to saturate. Motivated by these examples, [43, 44] considered the case of general dimensional CFTs. For

subsystems whose characteristic size R is much greater than the temperature scale $1/T$, they found that the time evolution of holographic entanglement entropy has a linear regime

$$\delta S_A(t) = v_E s_{\text{eq}} \mathscr{A}_\Sigma t, \tag{9}$$

where s_{eq} is the entropy density of the subsystem in the final state, $\mathscr{A}_\Sigma$ is the area of the *entangling surface* in the CFT, and v_E is a subsystem-independent constant called the *Entanglement Velocity*. Furthermore, the rate of growth in this linear regime was found to be bounded by 1 (in units $c = 1$). As envisaged by [16] using a quasi-particle description for the propagation of this entanglement, [17] showed that this bound is a consequence of the causality of the d (spacetime) dimensional CFT.

However, these works focused on the limit of large subsystem sizes. Reference [45] proposed a method to explore the entanglement entropies when the subsystem sizes are small compared to the final temperature. They observed a perturbative expansion for the area of the extremal surface and used that to study the post-quench evolution after an instantaneous quench. Reference [46] used a similar method to study the very interesting case of a global quench that is linear in time. But it was only in [47] that a comprehensive study of growth of entanglement entropy in the small subsystem regime was undertaken. Reference [47] studied a wide class of global quenches, including instantaneous, power law t^p with arbitrary p and periodic quenches. This was possible due to a novel interpretation that the growth of entanglement entropy after a quench can be understood as a linear response of the subsystem (in time) to the energy the quench injects. This interpretation allows one to rewrite the entanglement entropy (and other related information-theoretic quantities) as a convolution of two functions: a kernel that depends on the shape and size of the subsystem and a source that only depends on the energetics of the quench:

$$\delta S_A(t) = \int_{-\infty}^{\infty} \mathrm{d}t' \, \mathfrak{m}\left(t - t'\right) \mathfrak{n}\left(t'\right). \tag{10}$$

This interpretation is very useful. As described in detail in [47], it implies the existence of a *time-dependent first law of entanglement* for small subsystems. Moreover, such a law can be used to define a time-dependent quantity analogous to relative entropy that would measure the distance between out-of-equilibrium states explored during the post-quench evolution and either the initial or the final equilibrium state.

1.2. Hyperscaling-Violating-Lifshitz Theories. In this paper, we would like to study global quantum quenches when the CFT is in an excited state $|\Psi\rangle$ which partially breaks the full conformal symmetry. These states have a finite energy density and charge density $\rho(x^\mu)$. The conserved current for the charge is dual to a $U(1)$ gauge field $A_M(z, x^\mu)$ in the AdS bulk. Finite charge density then implies that this gauge field has a *non-normalizeable* mode at the boundary [48], which plays the role of a chemical potential for the charge. Since there is a *finite* energy and charge density, these generically backreact on the AdS geometry, modifying the interior [49–51]. (In the simplest case, the backreaction is known to uniquely give the AdS-Reissner-Nordstrom metric [52]. But this is known to be unstable at low temperatures [51]) We will further include fermions ψ^M in the bulk and focus on the action

$$\mathscr{S} = \int d^{d+1}x \sqrt{-g} \left(R - 2\Lambda - \frac{1}{4e^2} F_{MN} F^{MN} + \mathscr{L}_{\text{f}}\right). \tag{11}$$

where $\mathscr{L}_{\text{f}}$ denotes an ideal fluid Lagrangian at zero temperature for the fermions. Using this, [50] showed that the solutions to the equations of motion are

$$\begin{aligned} ds^2 &= \frac{L^2}{y^2}\left(dy^2 - \frac{dt^2}{y^{2(z-1)}} + dx_i^2\right), \\ A &= \frac{\sigma e}{y^{z-1}} dt, \end{aligned} \tag{12}$$

where the exponent z is fixed in terms of mass of the fermion. AdS radius L appears in the metric because the finite charge density $\rho(x^\mu)$ is smeared in an appropriate finite spatial region in the CFT. If we then zoom in near this region, that would correspond to zooming in on the interior part of the geometry. This part is not asymptotically AdS but instead has only part of AdS isometries. If we take this metric as an effective description of some field theory defined at its asymptotic boundary, this field theory will not be fully conformal. In fact, in the background given by the metric (12), time and space scale in an anisotropic way

$$\begin{aligned} t &\longrightarrow \alpha^z t, \\ x^i &\longrightarrow \alpha x^i, \\ y &\longrightarrow \alpha y. \end{aligned} \tag{13}$$

The constant z is a *Dynamical Critical Exponent* in this theory. It determines, for example, how the mass gap scales with respect to the coherence length ξ near the critical UV CFT

$$\text{Gap} \sim \frac{1}{\xi^z}. \tag{14}$$

Field theories with such properties are called *Lifshitz Field Theories*. They have the usual time and space translation generators (the Hamiltonian H and spatial momenta P_i) and the spatial rotation generators (angular momenta M_{ij}) but only an *anisotropic dilatation* D with the following commutation relations:

$$\begin{aligned} [D, P_i] &= iP_i, \\ [D, H] &= izH. \end{aligned} \tag{15}$$

As a consequence, they are also known as *non-relativistic* field theories. Such theories are known to describe general quantum critical points in condensed matter [53] and they can be constructed from $SU(N)$ Yang-Mills theories [54, 55]. Thus, in this effective limit, we would be describing *non-relativistic holography*.

The idea of investigating holography for theories without conformal symmetry is not new. See [56–61] for older work studying the holographic duals of *Schrödinger field theories*.

The asymptotically Lifshitz geometry (12) was first introduced in [62] to study *Lifshitz field theories*. They observed that this metric is nonsingular and all its curvature invariants are finite. However, it has a peculiar behavior near $y \longrightarrow \infty$ (the interior of the geometry) and in fact it is geodesically incomplete [62]. Thus to have a well-defined holography, one needs to find this metric as a solution of string theory. We thus need to embed the action (11) in some string model. There has been a lot of work in this direction [50, 59–61, 63–67], to name a few. Some works have advocated taking the asymptotically Lifshitz metric as a solution of general relativity with appropriate matter [68]. Energy conditions on this matter then decide what class of geometries are expected to have a Lifshitz field theory as a holographic dual. In particular, [69] showed that the condition $z > 1$ needs to hold for the Null Energy Condition (NEC) to be satisfied in the bulk (Although these works suggest that there may exist a Lifshitz holography, recently there has been some debate about what exactly the geometry dual to a UV Lifshitz critical point looks like. See [70]).

In this paper, we will study a class of excited states in the CFTs that is further qualified as follows. The IR geometry describing these states has an extra critical exponent, called the *Hyperscaling-Violating Parameter* and denoted by θ. As before, we will zoom in on the IR and take the asymptotics to define an effective, non-relativistic field theory. Following investigations in the holography of charged dilatonic black holes, it was realized [71, 72] that such geometries are good effective holographic descriptions for condensed-matter systems. The metric looks like

$$ds^2 = \frac{L^2}{y^{2(d-1-\theta)/(d-1)}}\left(dy^2 - \frac{dt^2}{y^{2(z-1)}} + dx_i^2\right), \tag{16}$$

where we recall that $i = 1, 2, \ldots, (d-1)$. In addition to Lifshitz symmetries, this metric transforms as

$$ds \longrightarrow \alpha^{\theta/(d-1)} ds, \tag{17}$$

under scaling. From now on, we will call this the *Hyperscaling-Violating-Lifshitz* metric and denote it by the acronym **hvLif**. Hyperscaling laws are well-known in condensed-matter physics. Traditionally, they are defined as those laws where the critical exponents depend on the dimension. In our case, the presence of θ roughly means that the asymptotic field theory effectively lives in $(d - \theta - 1)$ spatial dimensions instead of $(d - 1)$ spatial dimensions. This may be a concern for dimensional analysis, but the issue is resolved when one posits the existence of a length scale y_F that does not decouple in the IR.

Hyperscaling violating metrics can be obtained from the action [71]

$$\mathcal{S} = \int d^{d+1}x\sqrt{-g} \cdot \left(R - \frac{e^{\alpha\phi}}{4e^2}F_{MN}F^{MN} - \frac{1}{2}(\partial\phi)^2 - V_0\cosh(\eta\phi)\right), \tag{18}$$

where the parameters α and η determine the exponents z and θ. The potential $\cosh(\eta\phi)$ gives an asymptotically AdS solution in the limit $\phi \longrightarrow 0$ and an asymptotically **hvLif** solution in the limit $\phi \longrightarrow \infty$. For a range of exponents α and η, the metric can be shown to arise in a UV-complete theory like string theory [66, 72–74]. With these pieces of evidence, it is natural to study further the holography of hyperscaling-violating solutions in AdS spacetime. The Null Energy Condition (NEC) in the bulk imposes some constraints on the class of non-relativistic field theories dual to the hyperscaling-violating backgrounds, namely, that the critical exponents must satisfy [72, 75]

$$\begin{aligned}(d-1-\theta)\left((d-1)(z-1)-\theta\right) &\geq 0,\\ (z-1)(d-1-\theta+z) &\geq 0.\end{aligned} \tag{19}$$

We will study global quantum quenches in these field theories. These quenches correspond to classical evolution of the hyperscaling-violating background, possibly with some matter fields. In analogy with AdS/CFT correspondence, changing coupling constants in the field theory will correspond to turning on the non-normalizeable modes of some bulk matter fields. Owing to the natural gravitational potential well in the AdS spacetime, these matter fields will then collapse towards the center of AdS to eventually form a black hole. Formation of the black hole will correspond to thermalization in the dual field theory, which we assume will happen generically thanks to the strong coupling and chaotic dynamics. The simplest model to study this is to assume that the bulk matter is light and that it falls as a homogenous, thin, spherical shell. Its backreaction on the bulk geometry is then given by the Vaidya-like metric

$$ds^2 = \frac{L^2}{y^{2(d-1-\theta)/(d-1)}}\left(\frac{dy^2}{f(t,y)} - \frac{f(t,y)\,dt^2}{y^{2(z-1)}} + dx_i^2\right), \tag{20}$$

with $f(t, y)$ being the blackening function (Vaidya-like solutions in asymptotically Lifshitz backgrounds were first studied by [76]). We display it explicitly in equation (40). We will study the time-dependent holographic entanglement entropy in such a background and infer characteristics of the quenches in the asymptotic non-relativistic field theory. The entangling region in the boundary can have any geometry. For the case of strip geometries, this problem was also studied in [77, 78] but in a regime complementary to what we will study. They studied the evolution of entanglement entropy when $\ell T \gg 1$, where T denotes the temperature of the final state after thermalization. Thermalization of mutual information between two widely separated regions in a hyperscaling-violating field theory was studied in [79, 80]. We will instead study the complementary regime $\ell T \ll 1$. Unlike [77, 78], we will also consider more general quantum quenches: instantaneous, power-law with any power, and periodic in time.

1.3. Reader's Map. The plan of the paper is as follows. In Section 2, we discuss the perturbative expansion of the HRT area functional in the presence of a small parameter. In Section 2.1,

we make some general comments on holographic renormalization for asymptotically **hvLif** backgrounds. In Section 3, we discuss our Vaidya model of global quantum quenches in detail. In Section 3.1, we use the perturbative expansion of the area functional in the Vaidya model to calculate a simple integral expression for time-dependent holographic entanglement entropy (see equation (51)) which holds for any global quantum quench. In Section 4, we interpret this equation as a linear response relation and use it to derive a time-dependent generalization of the first law of entanglement entropy for small subsystems in Section 4.1. Such a law allows one to study a time-dependent analogue of relative entropy, which we discuss in Section 4.2. In Section 5, we start studying specific quantum quenches using the general machinery we have developed so far. Section 5.1 discusses in detail the instantaneous global quantum quench to the **hvLif** field theory. We once again study small subsystems and display explicitly various time-dependent quantities related to entanglement entropy. In Section 5.2, we study a finite-duration global quench that is a power law in time, with an arbitrary power. We discuss the method to obtain results in this general case and for convenience discuss the case of integer powers in detail. In Section 5.3, we elaborate on the case of a global quench linear in time. This is a special case of the power law quench but this is interesting in itself due to earlier work [46, 47]. We then come to Section 5.4 where we study a Floquet quench, a global quench that is periodic in time. This is a case of particular importance in condensed-matter community and we disucss thermalization of entanglement entropy for small subsystems for a Floquet quench. Finally, in Section 6, we conclude with a summary of our results and some directions for future work. There is an Appendix where we compute the stress tensor for **hvLif** backgrounds.

2. Perturbation Theory for Small Subsystems

From now on, we will work in an asymptotically **hvLif** spacetime and use that to study the quenches in the asymptotic non-relativistic field theories. Our results will be an approximation to quenching the specific class of excited states in CFTs that we have discussed in Section 1.

2.1. Holographic Renormalization. In this subsection, we will discuss holographic renormalization for asymptotically **hvLif** spacetimes. This is a very important problem, albeit outside the purview of this paper. Thus, we will be brief.

For a review of holographic renormalization in the case of CFTs, see [81]. Discussion of holographic renormalization for asymptotically Lifshitz backgrounds was initiated in [62, 68]. It was studied in more detail in [82–88], to name a few. In this subsection, we will follow the excellent article [75]. They study holographic renormalization in **hvLif** backgrounds using radial Hamilton-Jacobi method. In this method, one starts with a general action for the gravity-matter system

$$\mathcal{S} = \int d^{d+1}x\sqrt{-g}\left(R - \frac{F_1(\phi)}{4e^2}F_{MN}F^{MN} - \frac{1}{2}(\partial\phi)^2 - F_2(\phi) - F_3(\phi)A^2\right), \tag{21}$$

along with the usual Gibbons-Hawking boundary term. Then one takes an ADM-like ansatz for the metric and finds the Hamiltonian $\mathscr{H}$ as well Hamilton's Principal Function $\mathscr{W}$. These are related by the Hamilton-Jacobi equation

$$-\frac{\partial\mathscr{W}}{\partial y} = \mathscr{H}. \tag{22}$$

Solving this equation and using the definition of $\mathscr{W}$, one obtains the normalizeable and non-normalizeable modes for the fields. After an appropriate canonical transformation that diagonalizes the symplectic form on the space of these solutions, the normalizeable modes of the fields are identified as sources for some operators in the asymptotic field theory and the non-normalizeable modes are identified with the expectation values of these operators. Moreover, the asymptotic behavior of the solution of the Hamilton-Jacobi equation, including the finite terms, is useful in obtaining an analogue of Feffermann-Graham expansion for the fields on the **hvLif** backgrounds. The Feffermann-Graham expansion for the metric looks like

$$ds^2 = \frac{L^2}{y^{2d_\theta/(d-1)}}\left(dy^2 + g_{\mu\nu}(y, x^\mu; z, \theta)\,dx^\mu dx^\nu\right), \tag{23}$$

where, for economy of notation, we have defined

$$d_\theta \equiv d - 1 - \theta, \tag{24}$$

and $\mu = 0, 1, \ldots, d-1$. The metric $g_{\mu\nu}(0, x^\mu; z, \theta)$ defines the metric on the asymptotic boundary. We demand that this be given by

$$g_{\mu\nu}(0, x^\mu; z, \theta)\,dx^\mu dx^\nu = \lim_{y\to 0}\left(-\frac{dt^2}{y^{2(z-1)}} + dx_i^2\right). \tag{25}$$

We are interested in studying quantum quenches in the asymptotic field theory by calculating entanglement entropy of a subregion holographically. If we consider a subregion A in the field theory with a characteristic size ℓ, let y_* denote the turning point in the bulk up to which the extremal homologous surface goes. The authors in [72] have argued that the UV of the asymptotic field theory gets mapped to the IR of the gravity theory on the **hvLif** background. Thus if ℓ is small (compared to the temperature scale), y_* will be small (compared to the radius of the spacetime L). The bulk surface will then probe only the near-boundary region of the geometry.

When we do a global quantum quench in the field theory, this will in general change the geometry by a finite amount but because the subregion A is small, the reduced density matrices on A before and after the quench will differ by a small amount. In the bulk this implies that the area of the

HRT surface dual to A will get corrections from leading perturbations to the asymptotic **hvLif** metric, such as

$$g_{\mu\nu}\left(y, x^{\mu}; z, \theta\right) = g_{\mu\nu}\left(0, x^{\mu}; z, \theta\right) + \delta g_{\mu\nu}. \tag{26}$$

The leading term in the perturbation with the perturbation is a simple function of the expectation of the stress tensor

$$\delta g_{\mu\nu} = y^{d_\theta + z} \left\langle T_{\mu\nu} \right\rangle, \tag{27}$$

with the power of y fixed by symmetry. Higher powers of $T_{\mu\nu}$ are subleading for small y. If the quantum quench involved changing the coupling constant of some operator $O(t, x^i)$ in the field theory, the metric perturbation $\delta g_{\mu\nu}$ may also get corrections from the expectation value of $O(t, x^i)$ as well as from the source. We will assume that the (anisotropic) scaling dimension Δ of this operator is such that its contribution to the metric perturbation appears at subleading orders compared to that of $\langle T_{\mu\nu} \rangle$.

But the area of the HRT surface will be divergent, reflecting the fact that entanglement entropy of A in any state is UV-divergent. This divergence, however, is easy to remove: we subtract the entanglement entropy of A in vacuum from all our answers. There will in general be contributions to entanglement entropy from the source $J(t, x^i)$ directly. Understanding them will need a source-dependent renormalization, so we will subtract this as well. Thus we will calculate

$$\delta S_A(t) \equiv S_A(t) - S_A(0) - S_J(0), \tag{28}$$

where S_J is the contribution to the holographic entanglement entropy from the source.

2.2. Perturbative Expansion of the Area Functional. In the previous subsection, we have made precise the class of universal corrections we will aim to capture by calculating entanglement entropy holographically. In this subsection, we briefly review the results of [45] where they set up a perturbative calculation of holographic entanglement entropy of a subsystem in the presence of a small parameter (see also [89]). They considered the case of a homogeneous and instantaneous quench to the CFT ground state, while [47] generalized this to any homogenous quench. We will discuss such a calculation for the area of a bulk surface in asymptotically **hvLif** spacetime. We start with the HRT formula [36, 38]

$$S_A = \operatorname*{ext}_{\gamma_A} \frac{\text{Area}\left(\gamma_A\right)}{4G_N}, \tag{29}$$

where G_N is $(d+1)$ Newton's constant in $(d+1)$ dimensional bulk and γ_A is a $(d-1)$ dimensional bulk surface that is homologous to boundary subregion A. We will assume that the characteristic size ℓ of A is small compared to any other scale in the field theory, following [45, 47]. To be precise, the small parameter in our case will be

$$\lambda_A = \ell^z T, \tag{30}$$

with T denoting the temperature of the final state. We will discuss how to calculate it in Section 3.1. Let $\phi_A(\xi)$ denote all the embedding fields for the surface γ_A and $\mathscr{L}[\phi_A(\xi); \lambda_A]$ denote the Lagrange functional for the area of the surface γ_A

$$\mathscr{A} \equiv \text{Area}\left(\gamma_A\right) = \int d\xi \mathscr{L}\left[\phi_A(\xi); \lambda_A\right]. \tag{31}$$

Assuming the dimensionless parameter $\lambda_A \ll 1$, we can expand the embedding functions and the Lagrange function as follows:

$$\begin{aligned} \mathscr{L}\left[\phi_A(\xi); \lambda_A\right] &= \mathscr{L}^{(0)}\left[\phi_A(\xi); \lambda_A\right] \\ &\quad + \lambda_A \mathscr{L}^{(1)}\left[\phi_A(\xi); \lambda_A\right] \\ &\quad + \mathcal{O}\left(\lambda_A^2\right), \\ \phi(\xi) &= \phi^{(0)}(\xi) + \lambda_A \phi^{(1)}(\xi) + \mathcal{O}\left(\lambda_A^2\right), \end{aligned} \tag{32}$$

where the embedding functions that extremize the area at any given order in λ_A can in principle be obtained by solving Euler-Lagrange equations order by order in λ_A. However, as first noted in [45], the calculation of the area to order $\mathcal{O}(\lambda_A)$ becomes particularly simple. One gets

$$\begin{aligned} \mathscr{A}_{\text{on-shell}}[\phi_A(\xi)] &= \int d\xi\, \mathscr{L}^{(0)}[\phi_A(\xi); \lambda_A] + \\ &\quad \lambda_A \int d\xi\, \mathscr{L}^{(1)}[\phi_A(\xi); \lambda_A] + \\ &\quad \lambda_A \int d\xi \phi_A^{(1)} \left[\frac{d}{d\xi} \frac{\partial \mathscr{L}_A^{(1)}}{\partial \phi_A'(\xi)} - \frac{\partial \mathscr{L}^{(0)}}{\partial \phi_A(\xi)} \right] + \cdots, \end{aligned} \tag{33}$$

where we have used the equations of motion at zeroth order in λ_A. Hence the first-order correction to holographic entanglement entropy is given by

$$\mathscr{A}^{(1)}\left[\phi_A(\xi)\right] = \lambda_A \int d\xi \mathscr{L}^{(1)}\left[\phi_A(\xi); \lambda_A\right]. \tag{34}$$

This is the term we will calculate, and as we will see, it will be universal.

3. The Vaidya Model for Global Quenches

Let us start with the **hvLif** metric in (16)

$$ds^2 = \frac{1}{y^{2d_\theta/(d-1)}} \left(dy^2 - \frac{dt^2}{y^{2(z-1)}} + dx_i^2 \right), \tag{35}$$

where $y > 0$ is the bulk radial direction in the Schwarzschild frame, with the boundary at $y = 0$, and we have set the radius of the spacetime to 1. We will assume that the critical dynamical exponents z and θ, apart from the constraints (19), also satisfy

$$\begin{aligned} z &\geq 1, \\ \theta &\geq 0. \end{aligned} \tag{36}$$

As discussed in Section 1, the metric (20) (reproduced below) describes a simple model of a thin, homogenous shell of infalling matter to form a black hole with asymptotically **hvLif** geometry

$$ds^2 = \frac{1}{y^{2d_\theta/(d-1)}}\left(\frac{dy^2}{f(t,y)} - \frac{f(t,y)\,dt^2}{y^{2(z-1)}} + dx_i^2\right) \quad (37)$$

We will call this the **hvLif**-Vaidya geometry and use this to model our quenches holographically. In what follows, it will be useful to work in tortoise coordinates, also called Eddington-Finkelstein coordinates, defined by

$$du \equiv dy,\ dv \equiv dt - \frac{dy}{y^{(1-z)}f(t,y)}. \quad (38)$$

In these coordinates, the metric takes the form

$$ds^2 = \frac{1}{u^{2d_\theta/(d-1)}}\left(-\frac{2dudv}{u^{2(z-1)}} - \frac{f(u,v)\,dv^2}{u^{2(z-1)}} + dx_i^2\right). \quad (39)$$

The class of global quenches we study can be parameterized in terms of the blackening function

$$f(u,v) = 1 - g(v)\left(\frac{u}{u_H}\right)^{(z+d_\theta)}, \quad (40)$$

where the time-dependent function $g(v)$ corresponds to the quench in the boundary. We can always choose it to be bounded such that $0 \le g(v) \le 1$ and the leading term 1 indicates the time-independent vacuum. The constant u_H is the horizon radius and it encodes the equilibrium properties of the final state, a long time after the time-dependent perturbation. In case of pure AdS backgrounds, it precisely coincides with the horizon radius of the black hole formed as a result of perturbing the boundary CFT. Depending on the functional form of $g(v)$, we will distinguish between two kinds of global quenches:

(i) **Quenches of finite duration**

We will denote the duration of the quench by t_q, with reference to the Schwarzschild coordinate natural to a lab. For quenches with finite duration, $g(v)$ interpolates smoothly between two values at $t = 0$ and $t = t_q$. Denoting $g(v(t))$ by $g(t)$ for a moment

$$g(t=0) \longrightarrow 0,$$
$$g\left(t=t_q\right) \longrightarrow 1, \quad (41)$$

where we have normalized the value of g when the quench ends. From a geometrical viewpoint, at $t = 0$ we have the AdS-HSV geometry, and we turn on the quench and as a result at $t = t_q$ end up in a static black hole solution with AdS-HSV asymptotics [72, 90–93].

(ii) **Quenches of infinite duration**

In this case, we keep on perturbing the system indefinitely in time and as a result keep on inserting energy. One can still formally expand in a small parameter λ_A, but the expansion invariably becomes bad at sufficiently late times. We will not discuss very late time dynamics.

In this paper, we will mainly study quenches of finite duration.

3.1. Spread of Entanglement Entropy. In [47], we considered boundary subregions with spherical and strip geometry to study the time evolution of entanglement. But in this paper, we will only study subregions with a strip geometry. This is because, in a non-relativistic setting, it is very difficult to solve for the embedding functions with spherical geometry that extemize the area. The strip geometry will be defined on a time-slice so as to have $(d-1)$ coordinates (x, x_p^i) such that

$$-\frac{\ell}{2} \le x \le \frac{\ell}{2},\ 0 \le x_p^i \le \ell_p. \quad (42)$$

We will assume that ℓ is the smallest energy scale in the theory but, as we will see, will not need to assume anything about ℓ_p. The strip has translation invariance along the x_p^i directions since $\ell \ll \ell_p$. This translation invariance can be used to constrain the homologous surface in the bulk, which as a result is completely specified by one function $x \equiv x(u)$. We follow the usual procedure to calculate the area of this homologous surface in the bulk. It can be shown to be

$$\mathcal{A}[x(u), v(u)] = \int_0^{u_*} du\,\mathcal{L}[x(u), v(u)], \quad (43)$$

where u^* denotes the tip of the point in the bulk where the surface curves, i.e., the depth up to which the surface falls inside. The Lagrange function is given by

$$\mathcal{L}[x(u), v(u)] = \frac{2\ell_p^{(d-2)}}{u^{d_\theta}}\sqrt{x'^2 - \frac{2v'}{u^{(z-1)}} - \frac{v'^2 f(u,v)}{u^{2(z-1)}}}. \quad (44)$$

Before we proceed to calculate this, we remark the exact expansion parameter. As we argue in the Appendix, the blackening function can be used to define an "effective temperature"

$$T = \frac{1}{4\pi}\left|\frac{df(u,v)}{du}\right|_{u=u_H}. \quad (45)$$

Explicitly evaluating this, we see that the parameter $\ell^z T$ is dimensionless and we define it to be λ_A. It can also be written differently using the bulk distance u_* as

$$\lambda_A \equiv \frac{(d_\theta + z)}{4\pi}\left(\frac{u_*}{u_H}\right)^z. \quad (46)$$

The Lagrange function $\mathcal{L}[x(u), v(u)]$ now can be written as a function of this parameter and can be expanded around $\lambda_A = 0$. The zeroth-order Lagrange function and its first-order correction are then given by

$$\mathcal{L}^{(0)}[x(u), v(u)] = \frac{2\ell_p^{(d-2)}}{u^{d_\theta}}\sqrt{x'^2 - \frac{2v'}{u^{(z-1)}} - \frac{v'^2}{u^{2(z-1)}}}, \quad (47)$$

$$\mathcal{L}^{(1)}[x(u), v(u)] = \frac{\ell_p^{(d-2)} v'^2 u^{(2-d_\theta-2z)} g(v)}{\sqrt{x'^2 - 2v'/u^{(z-1)} - v'^2/u^{2(z-1)}}}. \quad (48)$$

The Euler-Lagrange equations from the zeroth-order function can be solved to obtain the solution for the extremal surface in the time-independent case. This solution is

$$x(u) = \frac{\sqrt{\pi}\Gamma\left[\left(d_\theta+1\right)/2d_\theta\right]u_*}{2d_\theta\Gamma\left[\left(2d_\theta+1\right)/2d_\theta\right]} - \frac{u^{(d_\theta+1)}}{\left(d_\theta+1\right)u_*^{d_\theta}}\,{}_2F_1\left[\frac{1}{2},\frac{\left(d_\theta+1\right)}{2d_\theta},\frac{\left(3d_\theta+1\right)}{2d_\theta};\left[\frac{u}{u_*}\right]^{2d_\theta}\right], \tag{49}$$

where ${}_2F_1(a,b,c;x)$ is the hypergeometric function and

$$v(u) = t - \frac{u^z}{z}. \tag{50}$$

Evaluating the first correction to the area at these solutions, the time-dependent change in the entanglement entropy becomes

$$\delta S_A(t) = \frac{\ell_p^{d-2}}{4G_N u_H^{d_\theta+z}}\int_0^{u_*} du u^z\sqrt{1-\left[\frac{u}{u_*}\right]^{2d_\theta}}\,g\left(t-\frac{u^z}{z}\right), \tag{51}$$

where the turning point u_* can be calculated from $x(u)$ to be

$$u_* = \frac{\ell d_\theta\Gamma\left[\left(2d_\theta+1\right)/2d_\theta\right]}{\sqrt{\pi}\Gamma\left[\left(d_\theta+1\right)/2d_\theta\right]}. \tag{52}$$

4. Entanglement as a Linear Response

Equation (51) for time evolution of entanglement entropy has a very interesting structure. In particular, if we define a time-like coordinate

$$t' \equiv \frac{u^z}{z}, \tag{53}$$

the time-dependent change in entanglement entropy can be written as the convolution equation

$$\delta S_A(t) = \int_{-\infty}^{\infty} dt'\mathfrak{m}\left(t-t'\right)\mathfrak{n}\left(t'\right) \equiv \mathfrak{m}(t) * \mathfrak{n}(t), \tag{54}$$

for some appropriate functions $\mathfrak{m}(t)$ and $\mathfrak{n}(t)$. In the theory of linear response, one of these functions, say $\mathfrak{m}(t)$, is called the input or *Source* function and the other one is called a *Response*. However, the roles of $\mathfrak{m}$ and $\mathfrak{n}$ are interchangeable due to the properties of the convolution operation.

As we argue in equation (A.22) in the Appendix, the energy density in hvLif-Vaidya spacetime is

$$\epsilon(t) = \frac{d_\theta g(t)}{16\pi G_N u_H^{d_\theta+z}}. \tag{55}$$

Now, without loss of generality, we identify the source with the energy density

$$\mathfrak{m}(t) \equiv \epsilon(t) = \frac{d_\theta g(t)}{16\pi G_N u_H^{d_\theta+z}}. \tag{56}$$

This is a natural choice for the source because this function depends only on the parameters in the quench. The response function $\mathfrak{n}_A(t)$ will then contain all the information about the geometry of the entangling subregion:

$$\mathfrak{n}(t) = \frac{2\pi\mathscr{A}_\Sigma(zt)^{1/z}}{d_\theta}\left[1-\left(\frac{t}{t_*}\right)^{2d_\theta/z}\right]^{1/2} \cdot\left[\Theta(t)-\Theta\left(t-t_*\right)\right], \tag{57}$$

where $\mathscr{A}_\Sigma = 2\ell_p^{d-2}$ is the area of the *entangling surface*, the boundary of the subregion A along the perpendicular directions, and t_* is defined in terms of u_*. Notice that we have unbounded limits in (54), but the actual integral for entanglement entropy (51) has bounded integration domain. To make this change, we have made the response function $\mathfrak{n}(t)$ an explicit function of these limits. The upper limit t_* also provides a natural reference for the domain of the response function.

For $t < 0$, there was no quench and as expected, the response function vanishes as well. Thus, the spread of entanglement is causal in our model. For finite quenches, the source function increases only up to $t = t_q$. In these cases, owing to the properties of the convolution integral, the entanglement growth saturates at a time

$$t_{\text{sat}} \equiv t_* + t_q. \tag{58}$$

As was noted in [47], writing the growth of entanglement entropy as a convolution has the added benefit that convolution integrals enjoy the following nice properties:

(i) **Linearity**

If a source is a linear combination of two independent sources $\mathfrak{m}(t) = c_1\mathfrak{m}_1(t) + c_2\mathfrak{m}_2(t)$, the convolution is the same linear combination of the individual convolutions

$$\delta S_A(t) = c_1\mathfrak{m}_1(t) * \mathfrak{n}(t) + c_2\mathfrak{m}_2(t) * \mathfrak{n}(t). \tag{59}$$

(ii) **Time-translation invariance**

A convolution is left invariant by translating it

$$\delta S_A\left(t+t_0\right) = \mathfrak{m}\left(t+t_0\right) * \mathfrak{n}(t) = \mathfrak{m}(t) * \mathfrak{n}\left(t+t_0\right). \tag{60}$$

(iii) **Differentiation rule**

If $\delta S_A(t) = \mathfrak{m}(t) * \mathfrak{n}(t)$, differentiation follows the simple rule

$$\frac{d\delta S_A(t)}{dt} = \frac{d\mathfrak{m}(t)}{dt} * \mathfrak{n}(t) = \mathfrak{m}(t) * \frac{d\mathfrak{n}(t)}{dt}. \tag{61}$$

(iv) **Integration rule**

If $\delta S_a(t) = \mathfrak{m}(t) * \mathfrak{n}(t)$, the integral of the convolution is the product of integrals.

$$\int dt\delta S_A(t) = \left[\int dt\mathfrak{m}(t)\right]\cdot\left[\int dt\mathfrak{n}(t)\right]. \tag{62}$$

One can use these properties and study a class of source functions $\mathfrak{m}(t)$ which are relatively simple. If the source function is complicated, but decomposable into a series of such simpler functions, these properties will prove useful in studying evolution of entanglement entropy in such a case.

4.1. Time-Dependent First Law of Entanglement. There always exists a First Law of Entanglement Entropy for small subregions. For the kind of quenches we are studying, the reduced density matrix for the subregion A after the quench can be written as $\rho_A = \rho_A^{(0)} + \lambda_A \Delta_\lambda \rho_A$ and so can the entanglement entropy:

$$\delta S_A(t) = \delta S_A^{(0)} + \lambda_A \Delta_\lambda S_A. \tag{63}$$

In fact, the change in the entanglement entropy can be shown to be

$$\Delta_\lambda S_A = \mathrm{tr}\left(\Delta_\lambda \rho_A K_A^{(0)}\right), \tag{64}$$

where the *Modular Hamiltonian* $K_A^{(0)}$ is defined as $K_A^{(0)} \equiv -\log(\rho_A^{(0)})$. Equation (64) is called the First Law of Entanglement Entropy.

In this subsection, we will show that there exists such a first law even in the time-dependent case for the small subregions. In (56), if we assume for a moment that the source is constant in time $g(t) = g_0$, then the entanglement growth (54) simplifies to

$$\delta S_A(t) = \frac{d_\theta g_0}{16\pi G_N u_H^{d_\theta+z}} \int_{-\infty}^{\infty} dt' \mathfrak{n}\left(t'\right). \tag{65}$$

Observe that we can explicitly calculate the indefinite integral of the non-trivial part of the response function (57):

$$\int dt\,(zt)^{1/z}\left[1-\left(\frac{t}{t_*}\right)^{2d_\theta/z}\right]^{1/2} = \frac{(zt)^{1+1/z}}{(z+1)}\,{}_2F_1\left[-\frac{1}{2}, \frac{z+1}{2d_\theta}, \frac{2d_\theta+z+1}{2d_\theta}; \left(\frac{t}{t_*}\right)^{2d_\theta/z}\right]. \tag{66}$$

Using this, we define the function

$$\mathfrak{B}(t) \equiv \frac{2\pi \mathscr{A}_\Sigma (zt)^{1+1/z}}{d_\theta (z+1)}\,{}_2F_1\left[-\frac{1}{2}, \frac{z+1}{2d_\theta}, \frac{2d_\theta+z+1}{2d_\theta}; \left(\frac{t}{t_*}\right)^{2d_\theta/z}\right], \tag{67}$$

which can be thought of as the indefinite integral of the full response function. Taking the limits $t \longrightarrow 0$ and $t \longrightarrow t_*$ of the function $\mathfrak{B}(t)$, we get the entanglement growth to be

$$\delta S_A\left(t \le t_*\right) = \frac{\mathscr{A}_\Sigma g_0}{8G_N u_H^{d_\theta+z}} \frac{(zt)^{1+1/z}}{(z+1)}\,{}_2F_1\left[-\frac{1}{2}, \frac{z+1}{2d_\theta}, \frac{2d_\theta+z+1}{2d_\theta}; \left(\frac{t}{t_*}\right)^{2d_\theta/z}\right], \tag{68}$$

$$\delta S_A\left(t \ge t_*\right) = \frac{\mathscr{A}_\Sigma g_0}{8G_N u_H^{d_\theta+z}} \cdot \frac{\sqrt{\pi}\,(zt_*)^{1+1/z}\,\Gamma\left[\left(2d_\theta+z+1\right)/2d_\theta\right]}{2(z+1)\,\Gamma\left[\left(3d_\theta+z+1\right)/2d_\theta\right]}. \tag{69}$$

We can rewrite the latter expression as

$$\delta S_A\left(t \ge t_*\right) = \frac{\delta E_A}{T_A}, \tag{70}$$

where by δE_A we denote the total energy inside the entangling surface:

$$\delta E_A = \frac{d_\theta g_0 V_A}{16\pi G_N u_H^{d_\theta+z}} = \frac{d_\theta g_0 \ell_p^{d-2} \ell}{16\pi G_N u_H^{d_\theta+z}}. \tag{71}$$

Using (52) for ℓ in terms of t_*, we can write the parameter T_A as

$$T_A = \frac{(z+1)\,\Gamma\left[\left(3d_\theta+z+1\right)/2d_\theta\right]\Gamma\left[\left(d_\theta+1\right)/2d_\theta\right]}{2\pi z \Gamma\left[\left(2d_\theta+z+1\right)/2d_\theta\right]\Gamma\left[\left(2D_\theta+1\right)/2d_\theta\right] t_*}. \tag{72}$$

It is called the *Entanglement Temperature* and has been extensively studied in literature [94–97]. Observe that the entanglement temperature only depends on the shape of the entangling surface (through t_*) and not on the quench. Thus, it is a characteristic of the subregion. In the relativistic limit ($z \longrightarrow 1, \theta \longrightarrow 0$), it reduces to the well-known expression [47, 94]

$$T_A^{\mathrm{CFT}} = \frac{(d+1)\,\Gamma\left[(d+1)/2\,(d-1)\right]\Gamma\left[d/2\,(d-1)\right]}{\pi t_* \Gamma\left[1/2\,(d-1)\right]\Gamma\left[d/(d-1)\right]}. \tag{73}$$

This equation is a manifestation of the standard First Law of Entanglement Entropy.

We now generalize this law to the case of adiabatic sources. In this case, the function $\mathfrak{m}(t)$ varies slowly and is approximately constant for time intervals of the order of t_*. To derive the first law, let us start by partially integrating the entanglement entropy integral (54), while using the source function (56). We get

$$\delta S_A(t) = \left[\epsilon\left(t-t'\right)\mathfrak{B}\left(t'\right)\right]_{t'=0}^{t'=t_*} - \int_0^{t_*} dt' \frac{d\epsilon\left(t-t'\right)}{dt'}\mathfrak{B}\left(t'\right), \tag{74}$$

where $\mathfrak{B}(t)$ is defined in (67). Note that one cannot cancel the integration measure dt' in the numerator and the denominator of the second term. One is supposed to think of the derivative of $\epsilon(t-t')$ as an independent function of t'.

Naively, this gives us the full expression for the time-dependent change in entanglement entropy. However, there is still a choice of the integration constant in the definition of the function $\mathfrak{B}(t)$, equation (67). For calculating the entanglement growth after a constant quench (see equation (68)), this choice did not matter because the integration constant got cancelled when one implemented the limits of the definite integral in the end. Here, the presence of the integration constant matters because it gives a non-vanishing term as $\epsilon(t)$ changes across an interval of size t_*. So, how do we fix this constant? We would like to reproduce the time-independent first law of entanglement entropy (70) when we make the source $\epsilon(t)$ time-independent. This fixes the constant to be $-V_A/T_A$. In particular, this implies the condition $\mathfrak{B}(t_*) = 0$, which is not surprising for a integral of a function with compact support. We also have $\mathfrak{B}(0) = -V_A/T_A$. Using these, we get

$$\delta S_A(t) = \frac{\delta E_A(t)}{T_A} - \int_0^{t_*} dt' \frac{d\epsilon\left(t-t'\right)}{dt'} \mathfrak{B}\left(t'\right). \tag{75}$$

This is then our generalization of the First Law of Entanglement to adiabatic time-dependent cases. We can identify the precise condition when this first law will hold. The adiabatic approximation is true if the integral in the equation above is not very large compared to the first term. One can thus show that if

$$\frac{d\epsilon(t)}{dt} \ll \frac{\epsilon(t)}{t_*}, \tag{76}$$

then the above first law holds.

4.2. An Analogue of Relative Entropy. In time-independent cases, relative entropy between two density matrices ρ and σ can be shown to be [98, 99]

$$S_{\text{rel}}(\rho \mid \sigma) = \Delta\langle K_\sigma\rangle - \Delta S, \tag{77}$$

where

$$\begin{aligned} \Delta K &\equiv -\operatorname{tr}(\rho\log\sigma) + \operatorname{tr}(\sigma\log\sigma), \\ \Delta S &= \operatorname{tr}(\rho\log\rho) - \operatorname{tr}(\sigma\log\sigma). \end{aligned} \tag{78}$$

We see that (75) is analogous to this. In particular, we can define a time-dependent analogue of relative entropy between the vacuum of non-relativistic field theories and thermal states produced by action of a global quench

$$\delta S_{\text{rel}}(t) \equiv \frac{\delta E_A(t)}{T_A} - \delta S_A(t), \tag{79}$$

where by δ we mean the term that remains after subtracting the vacuum quantity as well as source-dependent terms. This quantity has some nice properties. When there is no quench, it vanishes owing to the time-independent first law. For an adiabatic quench, it is very small, implying that the time-dependent excited state is not very far from the vacuum. For quenches of finite duration, it is non-zero only for $0 \le t \le t_{\text{sat}}$. Moreover, like the relative entropy, it is positive definite and hence must have an extremum in the interval $0 \le t \le t_{\text{sat}}$. All these properties suggest that this quantity can be thought of as an order parameter for out-of-equilibrium states. That is, this quantity tells us how far an out-of-equilibrium state is at time t compared to an equilibrium state with the same energy density $\epsilon(t)$.

We can in fact show that, for $0 \le t \le t_{\text{sat}}$, $\delta S_{\text{rel}}(t) \ge 0$. To see this, first we recall the integral expression for the relative entropy

$$\begin{aligned} \delta S_{\text{rel}}(t) &= \int_0^{t_*} dt' \frac{d\epsilon\left(t-t'\right)}{dt'} \mathfrak{B}\left(t'\right) \\ &= \int_{-\infty}^{\infty} dt' \frac{d\epsilon\left(t-t'\right)}{dt'} \mathfrak{B}\left(t'\right)\left[\Theta\left(t'\right) - \Theta\left(t'-t_*\right)\right]. \end{aligned} \tag{80}$$

Now, we observe that

$$\frac{d\epsilon\left(t-t'\right)}{dt'} = -\frac{d\epsilon\left(t-t'\right)}{dt}. \tag{81}$$

Hence we get

$$\begin{aligned} &\delta S_{\text{rel}}(t) \\ &= -\int_{-\infty}^{\infty} dt' \frac{d\epsilon\left(t-t'\right)}{dt} \mathfrak{B}\left(t'\right)\left[\Theta\left(t'\right) - \Theta\left(t'-t_*\right)\right] \\ &= -\frac{d\epsilon(t)}{dt} * \widetilde{\mathfrak{B}}(t), \end{aligned} \tag{82}$$

with $\widetilde{\mathfrak{B}}(t) \equiv \mathfrak{B}(t)[\Theta(t) - \Theta(t-t_*)]$. Now referring to the discussion above equation (75), $\mathfrak{B}(t) \le 0$ for $0 \le t \le t_*$ because of the choice of the integration constant. Also, $d\epsilon(t)/dt \ge 0$ due to the Null Energy Condition in the bulk. Hence, $\delta S_{\text{rel}} \ge 0$ for $0 \le t \le t_*$.

Apart from providing an order parameter to understand out-of-equilibrium states, the time-dependent relative entropy also helps us to organize the post-quench time evolution of the field theory. To see how this is done, let us first calculate the time derivative of the relative entropy using the differentiation rule of convolution

$$\begin{aligned} \frac{d\delta S_{\text{rel}}}{dt} &= -\frac{d\epsilon(t)}{dt} * \frac{d\widetilde{\mathfrak{B}}(t)}{dt} \\ &= \frac{d\epsilon(t)}{dt} * \frac{V_A}{T_A} - \frac{d\epsilon(t)}{dt} * \mathfrak{n}(t), \end{aligned} \tag{83}$$

where the first term is a boundary term from the boundary at $t = t_*$. We can now define the following regimes during the post-quench evolution:

(i) **Driven regime** ($0 \le t \le t_q$)

For $0 \le t \le t_q$, the system is being driven by the quench as $d\epsilon(t)/dt \ge 0$. Since $\mathfrak{n}(t) \ge 0$, the second term is negative wrt first in (83). However, both the terms contribute in general and there is a change in relative entropy as a function of time.

(ii) **Transient regime** ($t_q \le t \le t_{\text{sat}}$)

For $t_q \le t \le t_{\text{sat}}$, the quench has stopped acting and hence $d\epsilon(t)/dt = 0$. Thus, only the second term in (83) contributes. As a result, we get

$$\frac{d\delta S_{\text{rel}}}{dt} \le 0. \tag{84}$$

The distance in the Hilbert space between the vacuum and the excited state thus keeps decreasing with time in this regime.

5. Special Cases

In this section, we will study the growth of entanglement for small subsystems for some explicit quenches. As we will see, they cover a wide range of time-dependent perturbations to the field theory.

5.1. Instantaneous Quench. As a first example, we will study the instantaneous global quantum quench defined by $g(t) = \Theta(t)$. This will elucidate the use of the convolution formula (54) for entanglement entropy. Further, our discussion fills in a gap in the literature [77, 78] for entanglement growth after instantaneous quenches, which has focused more on large subsystems. From (51), the entanglement entropy in this case is

$$\delta S_A = \frac{\ell_p^{(d-2)}}{4G_N u_H^{(d_\theta+z)}} \int_0^{u_*} du u^z \sqrt{1-\left[\frac{u}{u_*}\right]^{2d_\theta}}\, \Theta\left(t-\frac{u_*^z}{z}\right). \tag{85}$$

The Heaviside Theta function can be used to naturally divide the evolution of entanglement entropy into the following three regimes:

(1) **Pre-quench regime**

When $t < 0$ the integrand vanishes for the entire integration domain. Hence

$$\delta S_A(t<0) = 0. \tag{86}$$

(2) **Post-saturation regime**

When $t > t_* = u_*^z/z$, the integrand is nonzero for the entire integration domain. Furthermore the final result then does not depend on time. Thus the growth of entanglement saturates in this regime and gives us the value δS_{eq} of entanglement entropy in the final equilibrium state. We will use this value later to normalize our plots.

$$\delta S_{eq} = \frac{\sqrt{\pi}\ell_p^{d-2} u_*^{1+z} \Gamma\left[\left(2d_\theta+z+1\right)/2d_\theta\right]}{8G_N(1+z)\, u_H^{d_\theta+z}\Gamma\left[\left(3d_\theta+z+1\right)/2d_\theta\right]}. \tag{87}$$

(3) **Time-dependent regime**

For $0 < t < t_*$, the value of $\delta S(t)$ is actually time-dependent. This is thus an out-of-equilibrium regime. To study this regime, we split off the equilibrium entanglement entropy of (87) and observe that we can define a dimensionless parameter

$$x \equiv \left(\frac{t}{t_*}\right)^{1/z}, \quad \text{with } t_* = \frac{u_*^z}{z}. \tag{88}$$

In terms of this parameter, the time evolution of the entanglement entropy is

$$\delta S_A(t) = \delta S_{eq} \mathcal{F}(x), \tag{89}$$

$$\mathcal{F}(x) \equiv \frac{\Gamma\left[\left(3d_\theta+z+1\right)/2d_\theta\right]}{\Gamma[3/2]\,\Gamma\left[\left(z+1\right)/2d_\theta\right]} \cdot \beta\left[x^{2d_\theta}, \frac{z+1}{2d_\theta}, \frac{3}{2}\right]. \tag{90}$$

where $\beta(z,a,b)$ is the Incomplete Beta Function.

Having described the regimes, we now observe that the problem of studying the evolution of entanglement entropy simplifies to the problem of studying the behavior of $\mathcal{F}(x)$ for different time scales. Before we study this in detail, we depict in Figure 1 the evolution of entanglement entropy for instantaneous global quenches.

5.1.1. Nature of Entanglement Growth. We now study in detail the time-dependent regime. To organize our study, we observe that the time-dependent regime can be further classified into three different subregimes. The existence of these subregimes can also be seen from Figure 1, where, as a function of time, the entanglement growth has three different functional forms. We now describe each of these subregimes in detail.

(1) **Early Time Growth.** The first subregime is the one where time is very close to zero, $t \approx 0$. This implies that the dimensionless parameter $x \approx 0$. This motivates us to expand $\mathcal{F}(x)$, given by (90), near $x = 0$. We expect that this simplifies the expression for the entanglement growth near $t \approx 0$. The expansion of $\mathcal{F}(x)$ near $x = 0$ is

$$\mathcal{F}(x) = \frac{2d_\theta \Gamma\left[\left(3d_\theta+z+1\right)/2d_\theta\right] x^{z+1}}{(z+1)\,\Gamma[3/2]\,\Gamma\left[\left(z+1\right)/2d_\theta\right]} \left(1 - \frac{z+1}{2\left(2d_\theta+z+1\right)} x^{2d_\theta} + \mathcal{O}\left(x^{4d_\theta}\right)\right), \tag{91}$$

where we have assumed $z \ge 1$ and $d_\theta \ge 0$ following [62]. Thus the time growth of entanglement entropy $\delta S(t)$ near $t \approx 0$ becomes

$$\delta S_A(t) = \frac{\ell_p^{d-2}(zt)^{1+1/z}}{4G_N(z+1)\, u_H^{d_\theta+z}} \left(1 - \frac{z+1}{2\left(2d_\theta+z+1\right)} \left[\frac{t}{t_*}\right]^{2d_\theta/z}\right). \tag{92}$$

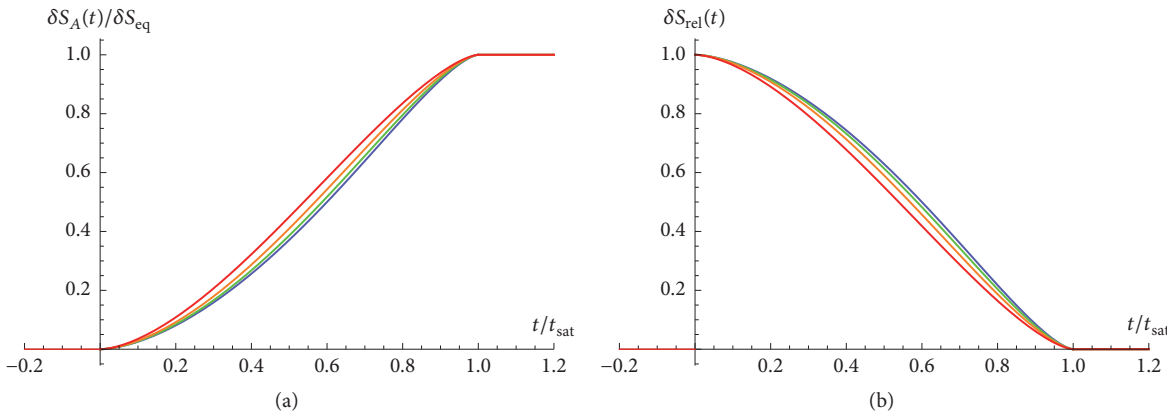

FIGURE 1: Entanglement entropy (a) and relative entropy (b) after an instantaneous quench in $d = \{2, 3, 4, 5\}$ dimensions, depicted in red, orange, green, and blue, respectively. We have set $z = 1.5$, $\theta = 0.1$, and $t_q + t_* = 1$ to obtain the plots.

If we take the limit $z \longrightarrow 1$, we recover the Vaidya solution with an asymptotically AdS background. In this limit, the above equation reproduces the well-known results for early time growth of entanglement [45], in particular the quadratic function of time. It was also argued that this time dependence is universal irrespective of the size of the subsystem [43–45]. The argument is that it is the UV part of the CFT which largely determines the early time growth and hence depends only on the symmetries [45]. We expect the same to be true of the early time entanglement growth for non-relativistic field theories under investigation here.

(2) ***Quasilinear Growth.*** The time dependence of entanglement entropy is not universal for intermediate time scales

$$0 \ll t \ll \frac{u_*^z}{z}. \tag{93}$$

It was shown in [43, 44, 77, 78] that there is a linear regime for large subsystems. But as was argued in [45, 47], there is no such regime for small subsystems. These results were for CFTs, but even in the case of non-relativistic field theories, we observe similar features. In particular, Figure 1 suggests that we can model the growth of entanglement as quasilinear. Then to study such a regime, [43–45, 47, 78] identified a parameter called *Entanglement Velocity*. For CFTs, it was defined as [43, 44]

$$\mathfrak{R}_{CFT} \equiv \frac{V}{\delta S_{eq} \mathscr{A}_\Sigma} \frac{d\delta S_A(t)}{dt}. \tag{94}$$

Following [78], we define entanglement velocity for the case of non-relativistic theories to be

$$\mathfrak{R}_{HSV}(t) = \frac{V}{\mathscr{A}_\Sigma} \frac{d\mathscr{F}(x(t))}{dt}. \tag{95}$$

Recall that from (52) we have

$$\frac{V}{\mathscr{A}_\Sigma} = \frac{\Gamma[3/2]\,\Gamma[(d-\theta)/2d_\theta]\,u_*}{d_\theta \Gamma[(d_\theta+1)/2d_\theta]}. \tag{96}$$

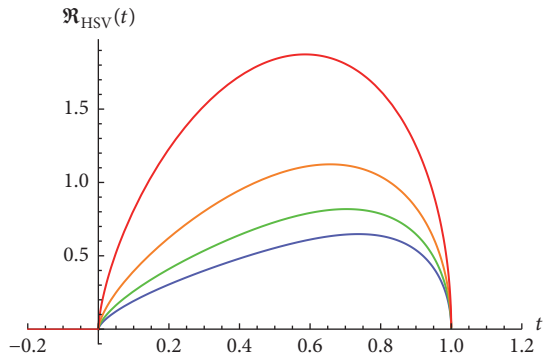

FIGURE 2: Entanglement velocity as a function of time for different values of d. The colors blue, green, red, and orange represent $d = \{5, 4, 3, 2\}$, respectively. We have set $\theta = 0.1$, $z = 1.5$, and $t_* = 1$.

A simple calculation then shows that the entanglement velocity is equal to

$$\mathfrak{R}_{HSV}(t) = \frac{2\Gamma[(3d_\theta + z + 1)/2d_\theta]\,\Gamma[(d-\theta)/2d_\theta]}{z t_* \Gamma[(z+1)/2d_\theta]\,\Gamma[(2d_\theta+1)/d_\theta]} (zt)^{1/z} \cdot \sqrt{1 - \left[\frac{t}{t_*}\right]^{2d_\theta/z}}. \tag{97}$$

As we can see, this is not independent of the subsystem. A similar feature was observed in [45, 47], contrary to the large subsystem limit, where the entanglement velocity is universal [43, 44]. In Figure 2, we plot the entanglement velocity as a function of time for different dimensions.

To understand this instantaneous velocity better, we study it in some limits. First we set $z = 1.5$ but keep θ arbitrary. This is the limit of relativistic but non-conformal field theories or the purely hyperscaling-violating theories. The time dependence of the velocity then is shown in part (a) of Figure 3. In part (b) of the same figure, we keep $\theta = 0.1$ and plot the time dependence of the velocity for different values of

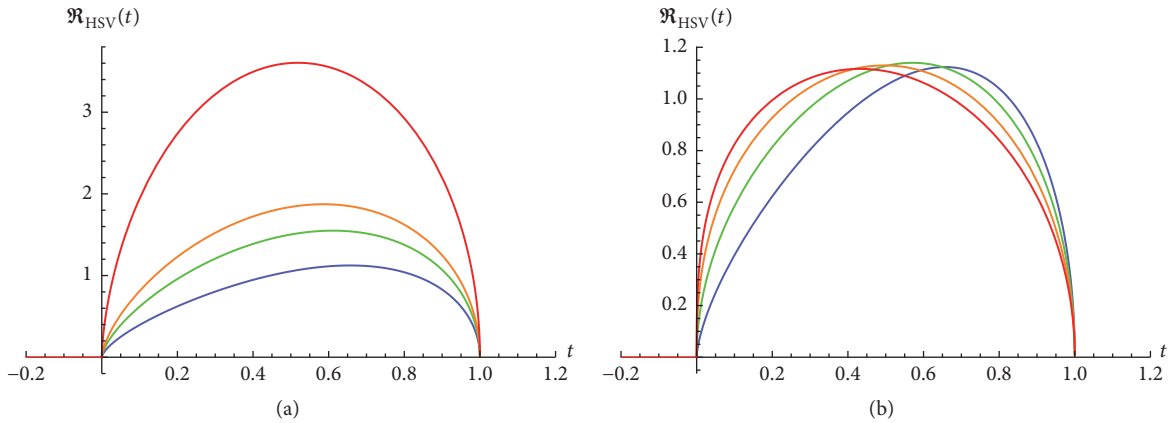

FIGURE 3: Time dependence of entanglement velocity for different values of θ and z. The colors blue, green, red, and orange represent $\theta = \{0.1, 0.8, 1.1, 1.7\}$ in part (a) and $z = \{1.5, 2, 2.5, 3\}$ in part (b), respectively. Common parameters are $d = 3$, $t_* = 1$.

z. For large subsystems, the entanglement velocity was found to be connected to the velocity of quasiparticles produced during the quench [16]. It was argued later that the spread of entanglement is causal and that this velocity is bounded by 1 in units of c [17, 43, 44]. However, the instantaneous velocity does not satisfy this bound [45, 47, 100, 101], although the time average of the velocity is bounded. This suggests that there is no quasi-particle picture for the production and propagation of entanglement for small subsystems. In the case of non-relativistic theories, the situation becomes more muddled. We will comment on these issues by studying the maximum and average velocity.

The maximum entanglement velocity in our case can be found using

$$\frac{d\mathfrak{R}_{\mathrm{HSV}(t)}}{dt} = 0 \Longrightarrow \; t_{\max} = t_* \left(d-\theta\right)^{-1/2d_\theta}, \tag{98}$$

where we have assumed that $z \geq 1$ and $\theta > 0$. This has the value

$$\mathfrak{R}_{\mathrm{HSV}}\left(t_{\max}\right) = \frac{2\Gamma\left[\left(3d_\theta + z + 1\right)/2d_\theta\right]\Gamma\left[\left(d-\theta\right)/2d_\theta\right]}{\Gamma\left[\left(z+1\right)/2d_\theta\right]\Gamma\left[\left(2d_\theta+1\right)/d_\theta\right]}\left[\frac{d_\theta}{d-\theta}\right]^{1/2} \cdot \left(d-\theta\right)^{-1/2d_\theta}\left(zt_*\right)^{(1-z)/z}, \tag{99}$$

In the AdS limit $\theta \longrightarrow 0$, $z \longrightarrow 1$, we reproduce the known result [45]

$$\mathfrak{R}_{\mathrm{CFT}}\left(t_{\max}\right) = \frac{4\Gamma\left[3/2 - 1/\left(d-1\right)\right]\Gamma\left[d/2\left(d-1\right)\right]\left(d-1\right)^{3/2}}{\Gamma\left[1/2\left(d-1\right)\right]\Gamma\left[1/\left(d-1\right)\right]d^{d/2(d-1)}}, \tag{100}$$

which gives, for example, a maximum velocity of $3/2$ for $d = 2$. In part (a) of Figure 4 we plot the maximum as a function of dimension.

It is also interesting to consider the maximum entanglement velocity as a function of z. This problem was studied numerically in [102, 103] recently. They found that the entanglement entropy for small subsystems is a linear function of z. We observe the same linear behavior, above $z = 1$, as we show in part (a) of Figure 5. Now we turn to the average entanglement velocity. It is given by

$$\mathfrak{R}_{\mathrm{avg}} \equiv \frac{1}{t_*}\int_0^{t_*} \mathfrak{R}_{\mathrm{HSV}}\left(t\right) dt. \tag{101}$$

Using (97), this can be shown to be

$$\mathfrak{R}_{\mathrm{avg}} = \frac{\sqrt{\pi}\Gamma\left[\left(d-\theta\right)/2d_\theta\right]\left(zt_*\right)^{1/z}}{t_*\Gamma\left[1/2d_\theta\right]}. \tag{102}$$

As expected, it reduces to the known expression [45, 47] in the limit of AdS-Vaidya

$$\mathfrak{R}^{\mathrm{avg}}_{\mathrm{CFT}} = \frac{\sqrt{\pi}\Gamma\left[d/2\left(d-1\right)\right]}{\Gamma\left[1/2\left(d-1\right)\right]}. \tag{103}$$

In part (b) of Figure 4 we show the average velocity as a function of the dimension. And we display the average velocity as a function of z in part (b) of Figure 5. We observe that both the maximum and the average entanglement velocities violate the bound. However, the bound was derived from relativistic considerations. The states that we work with are actually excited states that break conformal invariance. As a result, like a wave traveling in a matter that is refracting with respect to vacuum, the velocities are greater than 1.

*(3) **Near-Saturation Regime.*** We now study the last subregime of the growth of entanglement after the instantaneous quench. This is defined to be when the time t is close to the saturation time, $t \approx t_*$. Recall that $t_q = 0$ for instantaneous quenches and hence $t_{\mathrm{sat}} = t_*$. Thus, we would like to expand $\mathscr{F}(x)$ as defined in (90) around $x = 1$, approaching from below. The expansion is given by

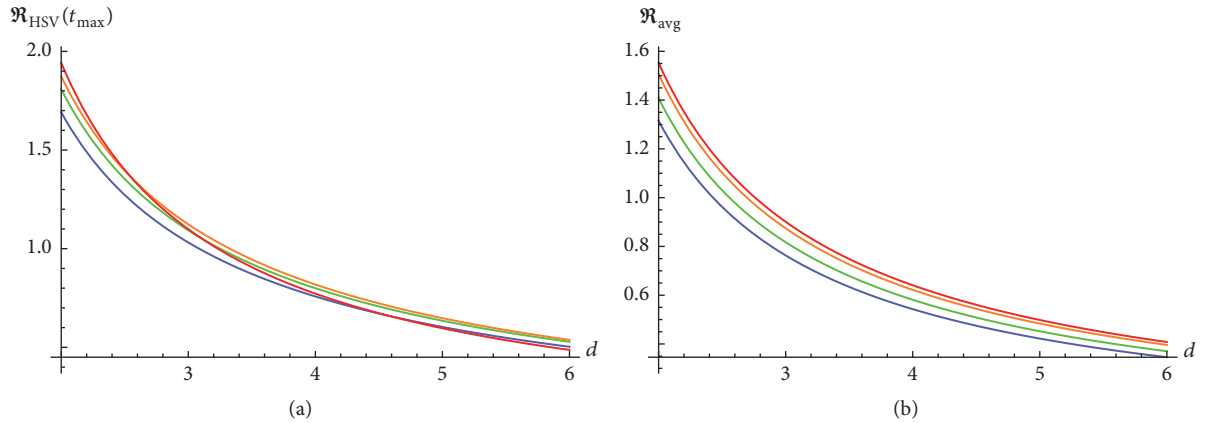

FIGURE 4: (a) Maximum and (b) average entanglement velocities as a function of d. The colors blue, green, orange, and red correspond to $z = \{1.3, 1.5, 1.9, 2.7\}$, respectively, and we have set $\theta = 0.1$, $t_* = 1$.

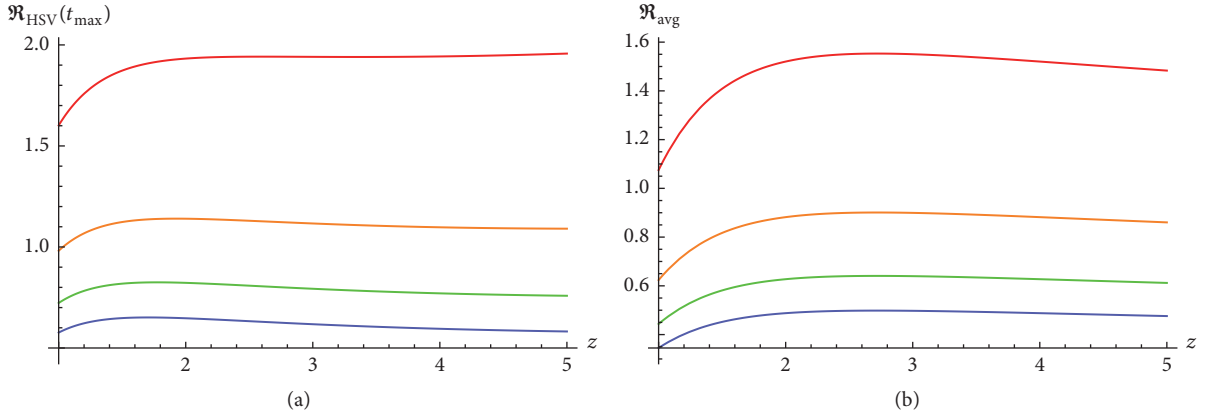

FIGURE 5: (a) Maximum and (b) average entanglement velocities as a function of z. The colors blue, green, orange, and red correspond to $d = \{5, 4, 3, 2\}$, respectively, and we have set $\theta = 0.1$, $t_* = 1$.

$$\mathscr{F}(x) = \begin{cases} 1 - \dfrac{2^{5/2} d_\theta^{3/2} \Gamma\left[\left(3d_\theta + z + 1\right)/2d_\theta\right]}{3\Gamma\left[3/2\right]\Gamma\left[\left(z+1\right)/2d_\theta\right]} (1-x)^{3/2}, & x^{2d} < x^{2(1+\theta)}, \\ 1 + \dfrac{2^{5/2} d_\theta^{3/2} \Gamma\left[\left(3d_\theta + z + 1\right)/2d_\theta\right]}{3\Gamma\left[3/2\right]\Gamma\left[\left(z+1\right)/2d_\theta\right]} (1-x)^{3/2}, & x^{2d} > x^{2(1+\theta)}. \end{cases} \tag{104}$$

This is consistent with the known results in the AdS-Vaidya limit [45, 47].

5.2. Power Law Quench. We now consider global quench that is a power law with respect to time. We will denote the power by p and keep it arbitrary. Once we have obtained the evolution of entanglement entropy in this general case, we could study the evolution of entanglement entropy for any *smooth* quench, by using, for example, Remez algorithm to rewrite the quench in a basis of polynomials. The perturbation we will consider is

$$g(t) = \sigma t^p \left[\Theta(t) - \Theta\left(t - t_q\right)\right] + \epsilon_0 \Theta\left(t - t_q\right), \tag{105}$$

where $p \in \mathbb{Z}$ and $\epsilon_0 = \sigma t_q^p$ is the final energy density when the quench stops at $t = t_q$. This perturbation defines the source function $\mathfrak{m}(t)$ in the convolution equation (54). Using the kernel (57), we get the entanglement growth to be given by the integral

$$\begin{aligned} \delta S_A(t) = {} & \frac{\sigma \mathscr{A}_\Sigma z^{1/z}}{8 G_N u_H^{d_\theta + z}} \int_{-\infty}^{\infty} d\tau \\ & \cdot \tau^{1/z} \sqrt{1 - \left[\tau/t_*\right]^{2d_\theta/z}} \left[\Theta(\tau) - \Theta(\tau - t_*)\right] \\ & \times \left[(t-\tau)^p \left[\Theta(t-\tau) - \Theta\left(t - t_q - \tau\right)\right]\right. \\ & \left. + t_q^p \Theta\left(t - t_q - \tau\right)\right]. \end{aligned} \tag{106}$$

We naturally encounter two cases: (1) $t_q < t_*$ and (2) $t_q > t_*$. In both these cases, the evolution of entanglement entropy is very similar; namely, the system is driven by the quench up to some time resulting in entanglement growth, followed by a transient regime which finally leads to saturation to an equilibrium value. In both the scenarios, the saturation time is given by $t_{\rm sat} = t_q + t_*$ and the evolution can be split and analyzed in various intervals as follows:

Regime :	Pre-quench	Initial	Intermediate	Final	Post-saturation
Case I : $t_q < t_*$	$t < 0$	$0 < t < t_q$	$t_q < t < t_*$	$t_* < t < t_{\rm sat}$	$t > t_{\rm sat}$
Case II : $t_* < t_q$	$t < 0$	$0 < t < t_*$	$t_* < t < t_q$	$t_q < t < t_{\rm sat}$	$t > t_{\rm sat}$

In Figure 6, we show schematically (this figure is a modification of a code written by Gerben W. J. Oling. I am thankful to them) the use of convolution integrals (54) to calculate the entanglement entropy in each of these regimes.

The pre-quench and post-saturation regimes are in equilibrium. In particular

$$\delta S_A(t) = 0 \quad \text{for } t < 0, \tag{107}$$

$$\delta S_A(t) = \frac{\epsilon_0 V_A}{T_A} \quad \text{for } t > t_{\rm sat}. \tag{108}$$

as expected, with T_A being given by (72). Due to equilibrium, the time-dependent relative entropy vanishes in both cases, $\delta S_{\rm rel}(t) = 0$. The initial, intermediate, and final regimes are generally time-dependent.

We now derive analytic expressions for entanglement growth. To write them succinctly, we define the following indefinite integral that depends on the subsystem:

$$\mathcal{I}^{(p)}(t,\tau) \equiv \frac{\mathcal{A}_\Sigma}{8G_N u_H^{d_\theta+z}} \int d\tau\,(t-\tau)^p\,(z\tau)^{1/z}\sqrt{1-\left[\frac{\tau}{t_*}\right]^{2d_\theta/z}}, \tag{109}$$

The entanglement growth in different regimes will be given by this integral evaluated at appropriate limits.

Now, using the binomial series

$$(t-\tau)^p = \sum_{k=0}^{\infty}\binom{p}{k} t^{p-k}(-\tau)^k, \tag{110}$$

where p is a real number, we can do the integral explicitly to obtain

$$\mathcal{I}^{(p)}(t,\tau) = \frac{\mathcal{A}_\Sigma}{8G_N u_H^{d_\theta+z}} \sum_{k=0}^{\infty}(pk)\,t^{p-k}\frac{(z\tau)^{1+1/z}(-\tau)^k}{(z+1+kz)} \times {}_2F_1\left[-\frac{1}{2}, \frac{z+1+kz}{2d_\theta}, \frac{2d_\theta+z+1+kz}{2d_\theta}; \left[\frac{\tau}{t_*}\right]^{2d_\theta/z}\right]. \tag{111}$$

This can be evaluated for any given p. For $p \in \mathbb{R}$, we get an infinite series but when p is a non-negative integer, the series is finite and gives a closed-form expression. In terms of this integral, the entanglement growth for different regimes can be written as follows:

$$\delta S_A^{(\rm I)}(t) = \begin{cases} 0, & t < 0, \\ \sigma\mathcal{I}^{(p)}(t,\tau)\big|_0^t, & 0 < t < t_q, \\ \epsilon_0\mathcal{I}^{(0)}(t,\tau)\big|_0^{t-t_q} + \sigma\mathcal{I}^{(p)}\left(t,t'\right)\big|_{t-t_q}^{t}, & t_q < t < t_*, \\ \epsilon_0\mathcal{I}^{(0)}(t,\tau)\big|_0^{t-t_q} + \sigma\mathcal{I}^{(p)}\left(t,t'\right)\big|_{t-t_q}^{t_*}, & t_* < t < t_{\rm sat}, \\ \epsilon_0\mathcal{I}^{(0)}(t,\tau)\big|_0^{t_*}, & t > t_{\rm sat}, \end{cases} \tag{112}$$

for case I and

$$\delta S_A^{(\rm II)}(t) = \begin{cases} 0, & t < 0, \\ \sigma\mathcal{I}^{(p)}(t,\tau)\big|_0^t, & 0 < t < t_*, \\ \sigma\mathcal{I}^{(p)}(t,\tau)\big|_0^{t_*}, & t_* < t < t_q, \\ \epsilon_0\mathcal{I}^{(0)}(t,\tau)\big|_0^{t-t_q} + \sigma\mathcal{I}^{(p)}(t,\tau)\big|_{t-t_q}^{t_*}, & t_q < t < t_{\rm sat}, \\ \epsilon_0\mathcal{I}^{(0)}(t,\tau)\big|_0^{t_*}, & t > t_{\rm sat}, \end{cases} \tag{113}$$

for case II, respectively, where all the evaluations are for the integration variable τ. Note that $\mathcal{I}^{(0)}(t,\tau)$ is particularly simple and has the closed-form expression

$$\mathcal{I}^{(0)}(t,\tau) = \frac{\mathcal{A}_\Sigma\,(z\tau)^{1/z}}{8G_N u_H^{d_\theta+z}(z+1)}\,{}_2F_1\left[-\frac{1}{2}, \frac{z+1}{2d_\theta}, \frac{2d_\theta+z+1}{2d_\theta}; \left[\frac{\tau}{t_*}\right]^{2d_\theta/z}\right]. \tag{114}$$

These expressions can be easily understood graphically. In the first row of Figure 7, we plot the time-dependent entanglement entropy after a power-law quench for different powers. Different regimes of entanglement growth can be identified from these plots. Nonetheless, they can be made manifest by plotting the relative entropy as a function of time, as shown in the second row of Figure 7. The figure shows a conspicuous cusp, which denotes the end of the driven regime. However, there is no singular behavior at the location of the cusp, as can be verified by studying the instantaneous rate of entanglement growth. We show this in the third row

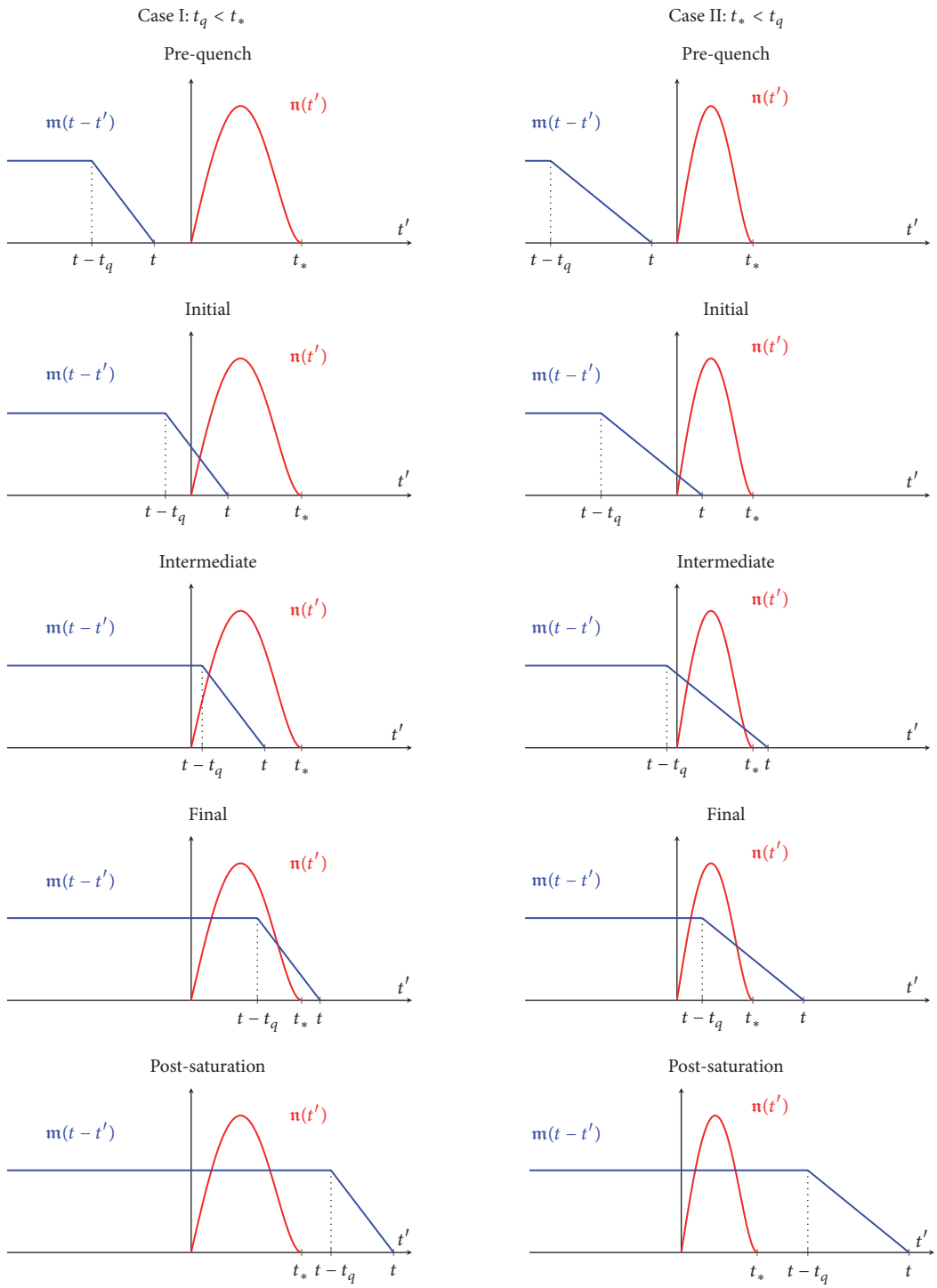

FIGURE 6: Schematic representation of the convolution integral for a power-law quench with $p = 1$. The right and left columns show the two possible cases I: $t_q < t_*$ and II: $t_* < t_q$, respectively. In the pre-quench and post-saturation regimes the integral is a constant. In the initial, intermediate, and final growth regimes the integral is time-dependent and can be performed by splitting it in various intervals, as shown in (112) and (113).

of Figure 7. As in the case of the instantaneous quench, we observe that the instantaneous entanglement velocity need not be bounded by 1.

It is interesting to ask how does the entanglement grow in different dimensions. As shown in Figure 8, we see that for different dimensions the time dependence of entanglement

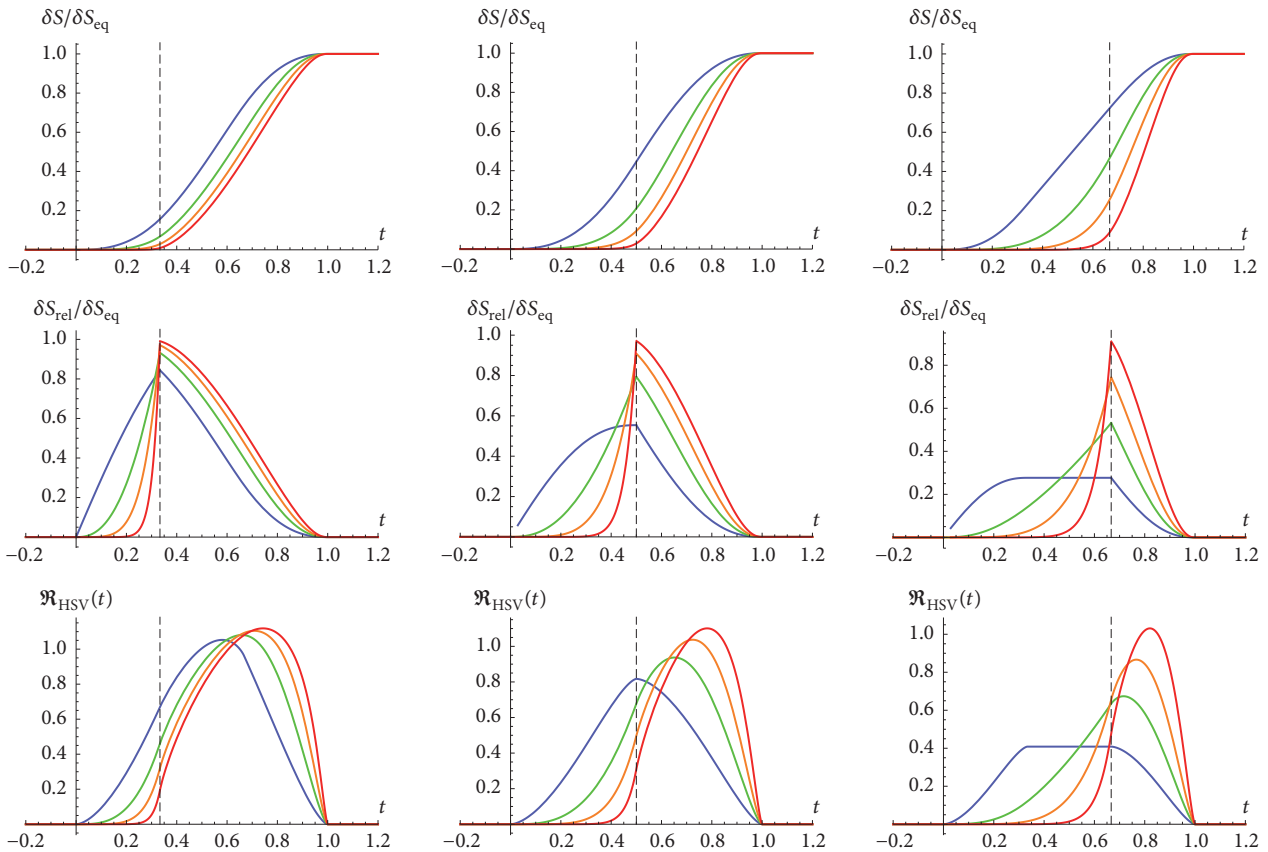

FIGURE 7: Entanglement entropy, relative entropy, and entanglement velocity for different powers after a power-law quench. Colors blue, green, orange, and red represent $p = \{1, 2.5, 5, 11.5\}$, respectively. Plots from left to right have $t_q/t_* = \{0.5, 1, 2\}$. In all plots, the dashed vertical line denotes the end of the driven phase $t = t_q$. We have set $d = 3$, $\theta = 0.1$, and $z = 1.5$.

entropy, relative entropy, and entanglement velocity is qualitatively uniform.

Finally, in Figures 9 and 10, we plot the dependence of entanglement entropy, relative entropy, and entanglement velocity as a function of z and θ, respectively. We see a qualitatively similar growth.

5.3. Linear Pump. In this subsection we will comment on the case of a linear quench $g(t) \sim t$. We call this the linear pump. For a CFT, it was studied in detail in [46, 47]. Reference [46] in particular proposed a First Law of Entanglement Rates for small subsystems given by

$$\frac{d\delta S_A(t)}{dt} = \frac{d\epsilon(t)}{dt}\frac{V_A}{T_A}, \tag{115}$$

where T_A is the entanglement temperature for a CFT calculated by the CFT limit of equation (72). This law can be interpreted as a derivative form of our general time-dependent first law of entanglement entropy (75) in the CFT limit. We now use our detailed discussion of the general power law quench from Section 5.2 to discuss the spread of entanglement entropy after a linear pump. In fact the cases $p = 1, 2$ can be solved completely analytically. The exact integrals for the linear quench can be derived from the general equations (112) and (113). Here we only discuss the plots in brief. In the first row of Figure 8, we can see the growth of entanglement entropy after a linear pump. The dashed black line indicates the end of the driven phase of entanglement growth. The four different colors indicate different dimensions. In the second row of the same figure, we have relative entropy as a function of time for different dimensions. It first increases and then decreases, unlike the case of the instantaneous quench. This behavior can be understood by observing that, until time t_q, the system is forced. As a result of this, it keeps going farther away from equilibrium. Keeping in line with our philosophy that the relative entropy measures how far the system is from equilibrium, it makes sense that it increases initially. The initial and the final states are both equilibrium states; hence the relative entropy is zero in these states. If it increases initially, it must decrease later to account for this fact.

5.4. Floquet Quench. Time periodic forces are commonly used in laboratory situations. The study of differential equations with a periodic function in the differential operator is called Floquet Theory. Adopting this name, we refer to a quench that is periodic in time as Floquet quench. Thus, the

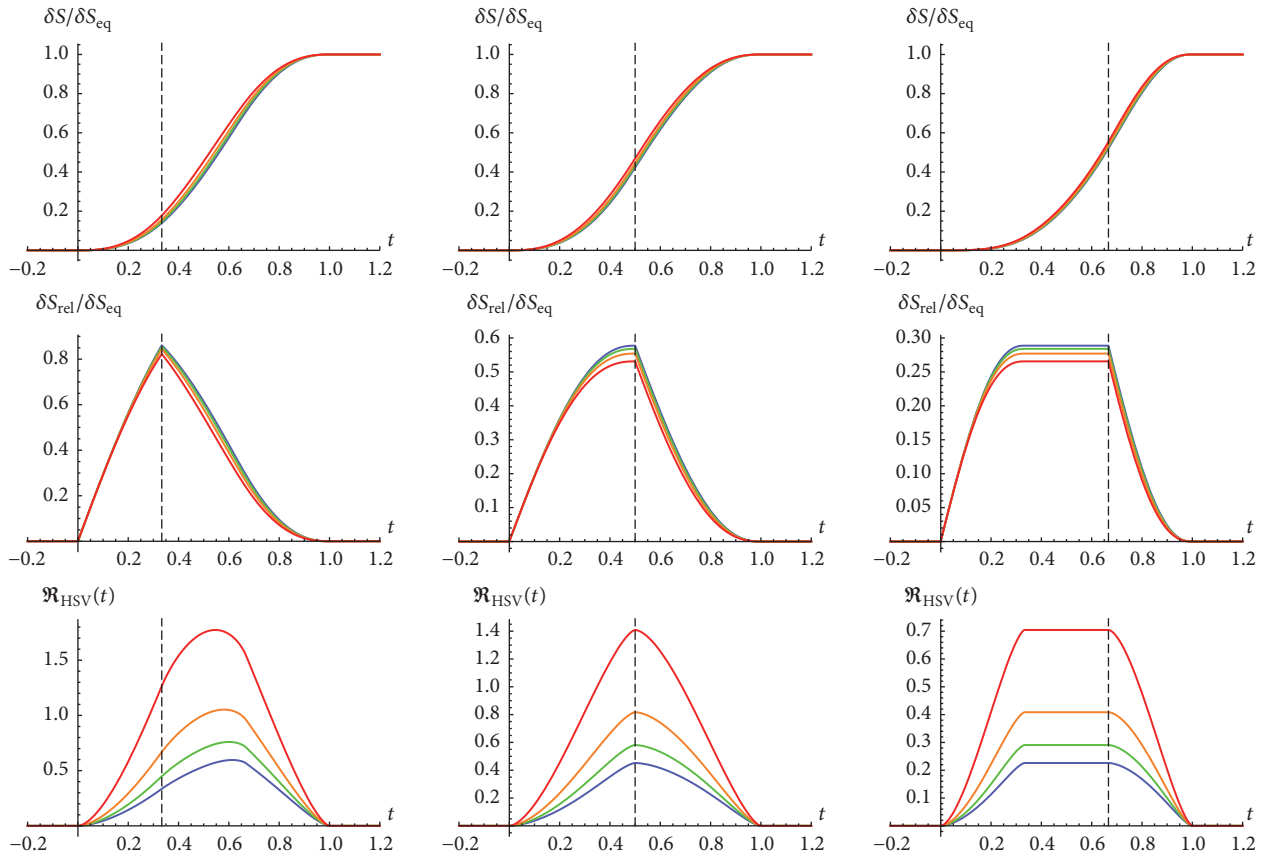

FIGURE 8: Entanglement entropy, relative entropy, and entanglement velocity for different dimensions. Colors blue, green, orange, and red represent $d = \{5, 4, 3, 2\}$, respectively. Plots from left to right have $t_q/t_* = \{0.5, 1, 2\}$. In all plots, the dashed vertical line denotes the end of the driven phase $t = t_q$. We have set $p = 1$, $\theta = 0.1$, and $z = 1.5$.

time-dependent function $g(t)$ in the source function $\mathfrak{m}(t)$ (see (56)) looks like

$$g(t) = \sin(\Omega t)\,\Theta(t), \tag{116}$$

where Ω is frequency of the external source and we have set the amplitude of the source to 1. Also observe that the quench does not have a finite duration ($t_q \longrightarrow \infty$). This case is more interesting because a Floquet quench that acts for finite duration can be very-well approximated by a finite combination of power-law quenches, whose exact description we know.

From the convolution equation (54), at late times we expect the entanglement growth to also be periodic in time. In particular, there is no saturation of entanglement. This is because the parameter t only appears in the source function, and there it is periodic with a trigonometric expression. Thus, we expect the entanglement growth to have the form

$$\delta S(t) = P(t) + \Psi \sin(\Omega t + \Phi), \tag{117}$$

where $P(t)$ is some smooth polynomial in t that interpolates to the sin function around $t = t_*$. The function $P(t)$, the amplitude Ψ, and the phase Φ are all functions of the parameters d, θ, z, Ω and the subsystem size ℓ. In fact, we can argue for the the existence of $P(t)$ on general grounds. The entanglement entropy is zero for $t < 0$ and then it starts growing at $t = 0$. However, the initial growth of entanglement is dictated solely by the symmetries of the theory to be t^{1+z}. Since, at late times, the entanglement growth is entirely driven by the periodic source, there must exist a polynomial $P(t)$ such that it interpolates smoothly between the early and the late time growth.

Expanding the sin function in a Taylor series, the exact expression for the growth of entanglement entropy becomes

$$\delta S(t) = \sum_{p=0}^{\infty} \frac{-(-1)^{(p+1)^2}\,\mathscr{A}_\Sigma \Omega^{2p+1}}{8 G_N u_H^{d_\theta+z}\,(2p+1)!} \int_0^{t_*} d\tau\,(t-\tau)^{2p+1} \cdot (z\tau)^{1/z} \sqrt{1-\left[\frac{\tau}{t_*}\right]^{2d_\theta/z}}. \tag{118}$$

Referring to the indefinite integral (109), we can write this as

$$\delta S(t) = \sum_{p=0}^{\infty} \frac{-(-1)^{(p+1)^2}\,\Omega^{2p+1}}{(2p+1)!} \mathscr{F}^{(2p+1)}(t,\tau)\Big|_{\tau=0}^{\tau=t_*} \tag{119}$$

where the exact expression for $\mathscr{F}^{(p)}(t,\tau)$ is given in (111). This gives us the entanglement growth as an infinite series of hypergeometric functions. This description of the growth is

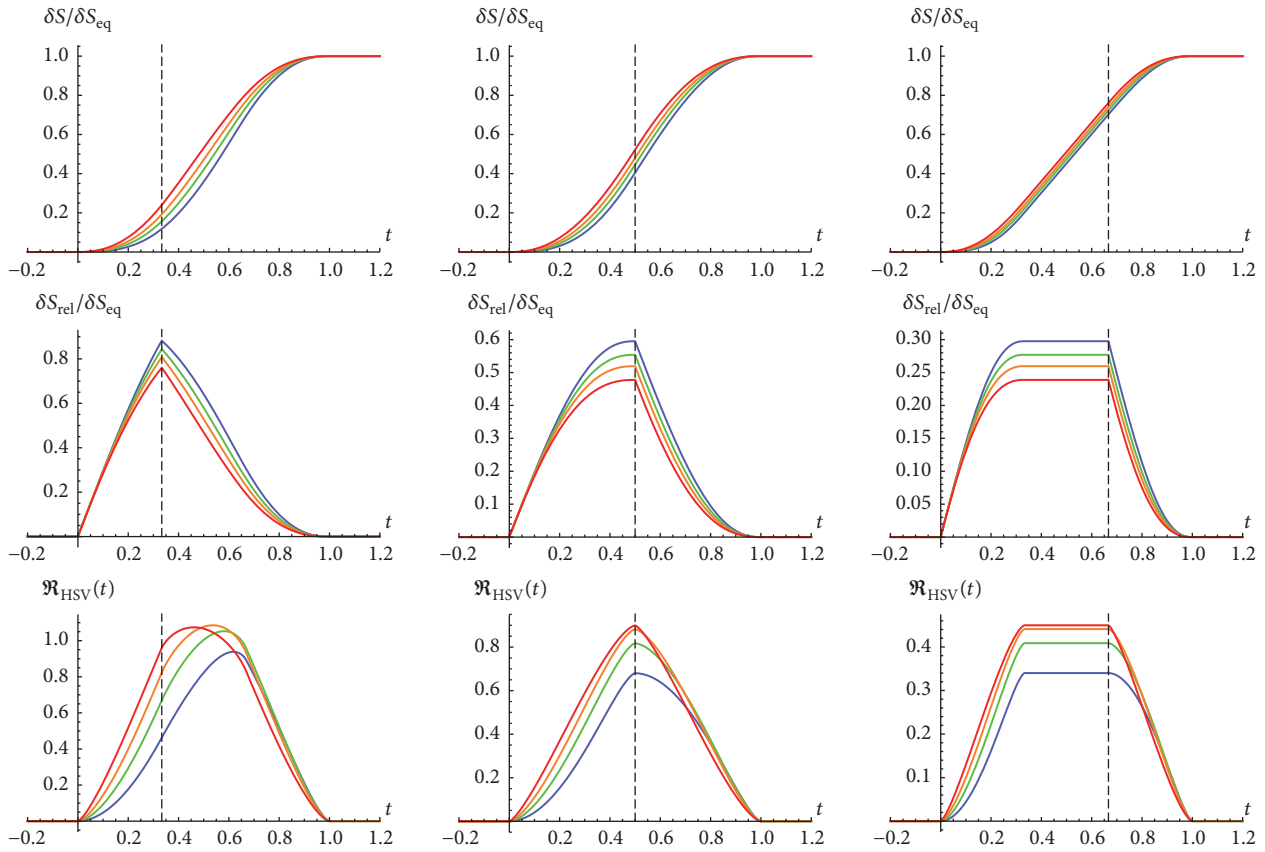

FIGURE 9: Entanglement entropy, relative entropy, and entanglement velocity for different values of z. Colors blue, green, orange, and red represent $z = \{1.1, 1.5, 2, 3\}$, respectively. Plots from left to right have $t_q/t_* = \{0.5, 1, 2\}$. In all plots, the dashed vertical line denotes the end of the driven phase $t = t_q$. We have set $d = 3$, $p = 1$, and $\theta = 0.1$.

most useful when the driving frequency Ω is small compared to 1. Then, it is possible to get a good approximation to the entanglement growth by truncating the above series at some appropriate power of Ω. In the cases when the driving frequency is not small, it is not possible to get a closed-form analytic expression for the entanglement growth with the usual methods. Thus, we will study the general case numerically instead. This interesting problem was also studied numerically in [104], without a discussion of the underlying analytic form of entanglement entropy. For the limit of small subsystems as defined in this paper, our expression for entanglement entropy as a convolution provides an explanation and the underlying analytics for their numerical results.

In Figure 11, we verify our expectation that the entanglement grows with time according to (117). In fact, after a time t_* it grows as a sin function of the same frequency as the source $g(t)$. One can also observe the relative amplitude and phase between the entanglement entropy and the energy density. The entanglement entropy has a smaller amplitude, which can be understood from the fact that, to leading order, it is the convolution of a sin function and $\tau^{1/z}$, both smaller than 1 (since t_* is effectively 1). The plots moreover show that the entanglement growth at early times interpolates to the sin growth at late time smoothly. It is possible to model this smooth interpolation using spline theory. But we will not do so in this paper.

As the dashed red line in Figure 11 indicates, the energy density oscillates. This is not physical because if the Null Energy Condition (NEC) is satisfied in the bulk, energy density should not decrease. There are two ways one can rectify this situation. The Floquet quench involves continuously driving the system externally and if NEC is applied to the whole system of the external apparatus plus **hvLif** theory together, we expect the NEC to be satisfied. Secondly, one could modify the quench by adding a linear pump to the Floquet quench. In this case, we have verified that the NEC is satisfied.

In Figure 12, we show how the entanglement growth changes as we change the number of dimensions and also its dependence on the frequency of the source.

We see that, at higher dimensions, the amplitude of the entanglement entropy is higher but it decreases as the frequency increases.

In Figure 13, we plot the dependence of entanglement entropy on the non-relativistic parameters θ and z. We see an increase in the amplitude upon increasing z but a decrease as θ is increased. Figures 11, 12, and 13 are indicative of how the amplitude of the entanglement entropy depends on various parameters but it is not very clear what is happening to the

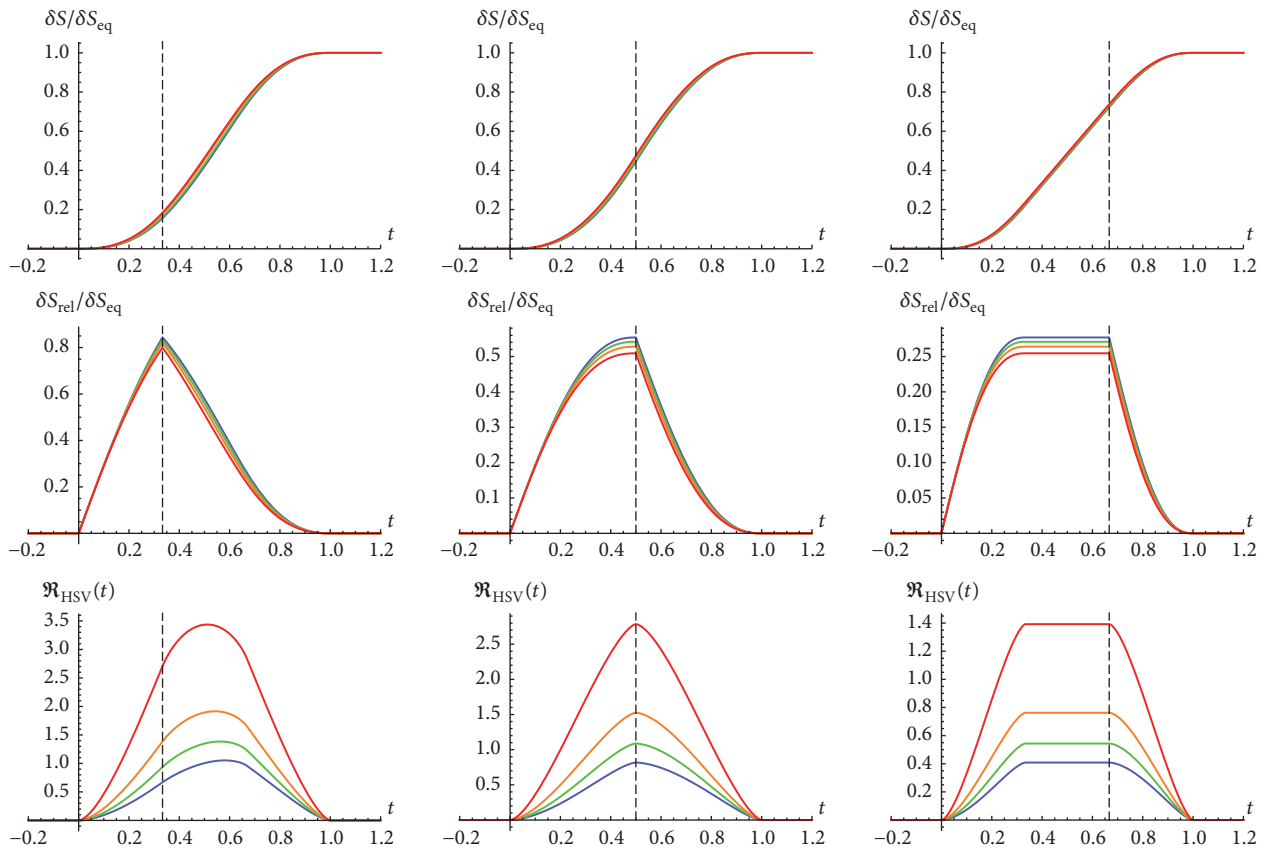

FIGURE 10: Entanglement entropy, relative entropy, and entanglement velocity for different values of θ. Colors blue, green, orange, and red represent $\theta = \{0.1, 0.7, 1.2, 1.7\}$, respectively. Plots from left to right have $t_q/t_* = \{0.5, 1, 2\}$. In all plots, the dashed vertical line denotes the end of the driven phase $t = t_q$. We have set $d = 3$, $p = 1$, and $z = 1.5$.

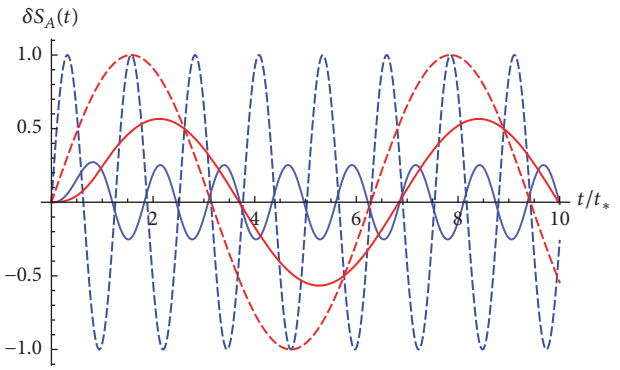

FIGURE 11: Entanglement entropy (solid line) as a function of time after a Floquet quench, plotted against the periodic source (dashed line). The colors blue and red denote frequencies $\Omega = \{5, 1\}$, respectively. We have set $d = 3$, $\theta = 0.1$, and $z = 1.5$.

phase. Hence, we can now discuss both the amplitude and the phase in some more detail. In Figure 14, we plot the amplitude of entanglement entropy as a function of dimension, z and θ. Observe that the amplitude vanishes for $\theta > d-1$ because the Vaidya solution is defined only for these values.

In Figure 15, we plot the phase of the entanglement entropy relative to the energy density as a function of dimension, z and θ. With this we conclude our discussion of Floquet quench.

6. Summary and Outlook

In this paper, we studied global quantum quenches to holographic hyperscaling-violating-Lifshitz (**hvLif**) field theories, using entanglement entropy of a subregion as a probe to study thermalization. In Section 1, we argued that such theories appear in the IR description of finite energy and finite charge density excited states in the CFT. Thus, our results describe thermalization in such states approximately.

In Section 2.1, we specialized our discussion to small subregions ($\ell^z \ll 1/T$) and precisely defined the universal corrections we calculate. Using $\ell^z T$ as a perturbative parameter, we argued in Section 2.2 that the holographic entanglement entropy becomes simple. In Section 3, we proposed the **hvLif**-Vaidya geometry

$$ds^2 = \frac{1}{u^{2d_\theta/(d-1)}}\left(-\frac{2dudv}{u^{2(z-1)}} - \frac{f(u,v)\,dv^2}{u^{2(z-1)}} + dx_i^2\right), \qquad f(u,v) = 1 - g(v)\left(\frac{u}{u_H}\right)^{z+d_\theta}. \tag{120}$$

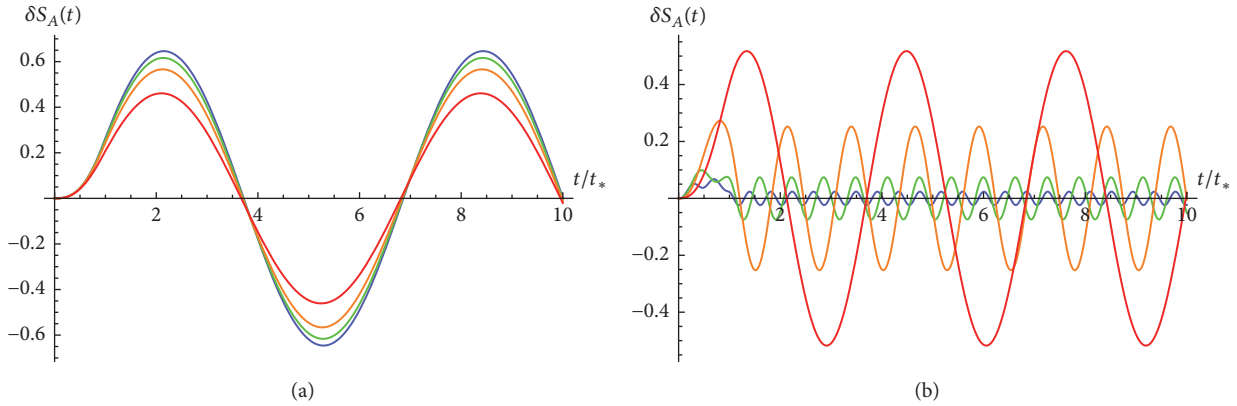

FIGURE 12: Entanglement entropy after a Floquet quench as a function of (a) dimension and (b) frequency. The colors blue, green, orange, and red denote $d = \{5, 4, 3, 2\}$ in part (a) and $\Omega = \{15, 10, 5, 2\}$ in part (b), respectively. We have set $\theta = 0.1$, $z = 1.5$.

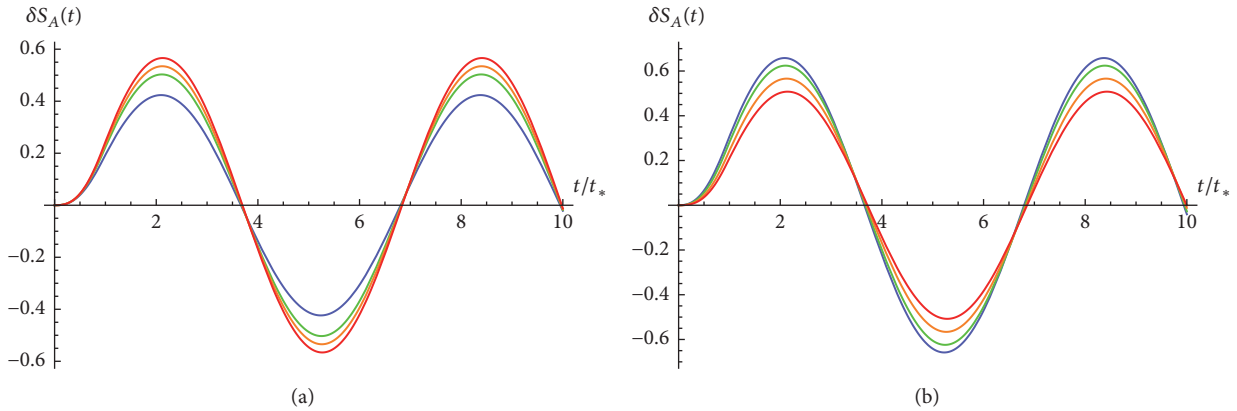

FIGURE 13: Entanglement entropy after a Floquet quench as a function of (a) θ and (b) z. The colors blue, green, orange, and red denote $\theta = \{1.3, 0.8, 0.5, 0.1\}$ in part (a) and $z = \{2.1, 1.8, 1.5, 1.3\}$ in part (b), respectively. We have set $d = 3$, $\Omega = 1$.

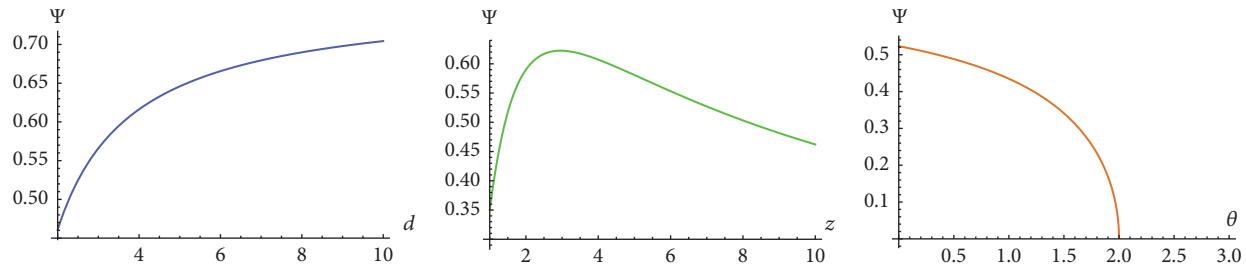

FIGURE 14: Amplitude Ψ of entanglement entropy as a function of (a) dimension, (b) z, and (c) θ. In (a), we have $\{z = 1.5, \theta = 0.1\}$. In (b), we have $\{d = 3, \theta = 0.1\}$ and in (c), $\{d = 3, z = 1.5\}$. We have set $\Omega = 1$ everywhere.

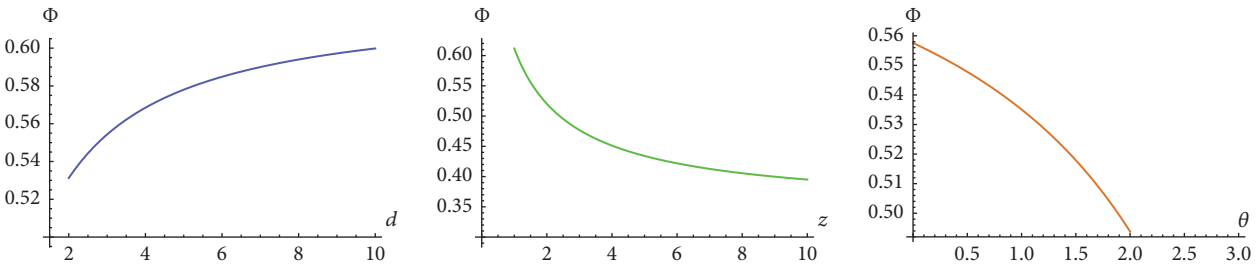

FIGURE 15: Relative phase Φ of entanglement entropy as a function of (a) dimension, (b) z, and (c) θ. In (a), we have $\{z = 1.5, \theta = 0.1\}$. In (b), we have $\{d = 3, \theta = 0.1\}$ and in (c), $\{d = 3, z = 1.5\}$. We have set $\Omega = 1$ everywhere.

as a simple holographic toy model to study the time evolution of entanglement entropy.

Using the perturbative expansion in **hvLif**-Vaidya geometry, we calculated the holographic entanglement entropy of a small subsystem A in Section 3.1 to be

$$\delta S(t) = \frac{\ell_p^{d-2}}{4G_N u_H^{d_\theta+z}} \int_0^{u_*} du u^z \sqrt{1-\left[\frac{u}{u_*}\right]^{2d_\theta}}\, g\left(t-\frac{u^z}{z}\right), \tag{121}$$

for a general quench parameterized by the function $g(v)$. Motivated by the simplicity of this equation, we interpreted this equation in Section 4 as a *Linear Response*

$$\delta S(t) = \int_{-\infty}^{\infty} dt'\, \mathfrak{m}\left(t-t'\right) \mathfrak{n}\left(t'\right) \tag{122}$$

with the *Source* function $\mathfrak{m}(t)$ given by the energy density of the quench

$$\mathfrak{m}(t) \equiv \epsilon(t) = \frac{d_\theta g(t)}{16\pi G_N u_H^{d_\theta+z}}. \tag{123}$$

and the *Kernel* function $\mathfrak{n}(t)$ given in terms of the shape and the size of the subregion

$$\mathfrak{n}(t) = \frac{2\pi \mathscr{A}_\Sigma (zt)^{1/z}}{d_\theta}\left[1-\left(\frac{t}{t_*}\right)^{2d_\theta/z}\right]^{1/2} \cdot \left[\Theta(t)-\Theta\left(t-t_*\right)\right], \tag{124}$$

This interpretation allowed us to define an adiabatic time-dependent first law of entanglement entropy for small subsystems in Section 4.1

$$\delta S_A(t) = \frac{\delta E_A(t)}{T_A} - \int_0^{t_*} dt' \frac{d\epsilon\left(t-t'\right)}{dt'} \mathfrak{B}\left(t'\right). \tag{125}$$

where the function $\mathfrak{B}(t)$ can be thought of as the *anti-derivative* of the *kernel* function

$$\mathfrak{B}(t) \equiv \frac{2\pi \mathscr{A}_\Sigma (zt)^{1+1/z}}{d_\theta (z+1)}\, {}_2F_1\left[-\frac{1}{2}, \frac{z+1}{2d_\theta}, \frac{2d_\theta+z+1}{2d_\theta}; \left(\frac{t}{t_*}\right)^{2d_\theta/z}\right] - \frac{V_A}{T_A}. \tag{126}$$

Here, $-V_A/T_A$ denotes an integration constant that is chosen to reproduce the time-independent first law of entanglement entropy (70). See the discussion above (75) for details. Moreover, in Section 4.2, we used the linear response to study a time-dependent analogue of relative entropy

$$\delta S_{\text{rel}}(t) \equiv \frac{\delta E_A(t)}{T_A} - \delta S_A(t), \tag{127}$$

which we argued is a good parameter to characterize out-of-equilibrium states at a time t compared to an equilibrium state with the energy density $\epsilon(t)$.

In Section 5, we started studying special examples of global quenches, in particular

$$g(t) = \Theta(t), \quad g(t) = \sigma t^p \left[\Theta(t) - \Theta\left(t-t_q\right)\right] + \epsilon_0 \Theta\left(t-t_q\right), \quad g(t) = \sin(\Omega t)\,\Theta(t). \tag{128}$$

In Section 5.1, we studied the first of these cases, i.e., the instantaneous quench $g(t) = \Theta(t)$, and showed that the entanglement entropy is

$$\delta S(t) = \delta S_{eq} \mathscr{F}(x), \quad \mathscr{F}(x) \equiv \frac{\Gamma\left[\left(3d_\theta+z+1\right)/2d_\theta\right]}{\Gamma[3/2]\,\Gamma\left[(z+1)/2d_\theta\right]} \cdot \beta\left[x^{2d_\theta}, \frac{z+1}{2d_\theta}, \frac{3}{2}\right], \quad \delta S_{eq} = \frac{\sqrt{\pi}\ell_p^{d-2} u_*^{1+z}\Gamma\left[\left(2d_\theta+z+1\right)/2d_\theta\right]}{8G_N(1+z)\,u_H^{d_\theta+z}\Gamma\left[\left(3d_\theta+z+1\right)/2d_\theta\right]}. \tag{129}$$

We then studied this example in great detail: deriving the early time universal growth given in equation (92), the quasilinear growth with a slope (the *entanglement velocity*) given by equation (97) and the near-saturation regime of the evolution characterized using equation (104).

For the case of the power law quench, we studied the entanglement entropy in detail in Section 5.2. For arbitrary real power $p \in \mathbb{R}$, we obtained a formal expression for the entanglement entropy as an infinite series using the explicit function

$$\mathscr{I}^{(p)}(t,\tau) = \frac{\mathscr{A}_\Sigma}{8G_N u_H^{d_\theta+z}} \sum_{k=0}^{\infty} \binom{p}{k} t^{p-k} \frac{(z\tau)^{1+1/z}(-\tau)^k}{(z+1+kz)} \times {}_2F_1\left[-\frac{1}{2}, \frac{z+1+kz}{2d_\theta}, \frac{2d_\theta+z+1+kz}{2d_\theta}; \left[\frac{\tau}{t_*}\right]^{2d_\theta/z}\right]. \tag{130}$$

For an integral power $p \in \mathbb{Z}$, we derived an explicit closed form expression for the entanglement entropy in (112) and (113). We plotted the evolution of (normalized) entanglement entropy $\delta S(t)/\delta S_{\text{eq}}$, relative entropy $\delta S_{\text{rel}}(t)/\delta S_{\text{eq}}$, and entanglement velocity $\mathfrak{R}_{\text{HSV}}(t)$ in Figures 7, 8, 9, and 10. In Section 5.3, we made some comments about the interesting particular case of the linear in time quench.

Finally, in Section 5.4, we studied a quench that is periodic in time, also called Floquet quench. We derived a formal expression for entanglement entropy in equation (119) as an infinite series. This expression is not illuminating, so we plotted entanglement entropy in Figure 11 as a function of time and in Figure 12 as a function of dimension and frequency. Figures 14 and 15 show the amplitude and the phase of the entanglement entropy as a function of d, θ, and z.

In this paper, we could not study the problem of holographic renormalization in detail. That is an obvious direction to extend our work in. Further, notwithstanding the expectation that our simple holographic toy model captures gross universal features of thermalization, it is not very realistic. It would be interesting to have a more realistic holographic model for studying quenches in **hvLif** field theories. We wish to come back to these issues in the future.

Appendix

Stress Tensor for hvLif Theories

In this appendix, we use the so-called Minimal Approach to find the stress-energy tensor for an asymptotically **hvLif** black hole in general dimensions. This method is essentially an application of the first law of thermodynamics. Let us consider the following metric of a static black hole in a **hvLif** background [72, 90–93]

$$ds^2 = \frac{1}{u^{2d_\theta/(d-1)}}\left(\frac{du^2}{f(u)} - \frac{f(u)}{u^{2(z-1)}}dt^2 + dx_i^2\right), \tag{A.1}$$

where the blackening function is

$$f(u) = 1 - \left(\frac{u}{u_H}\right)^{(d_\theta+z)}, \tag{A.2}$$

and u_H is as usual the horizon radius. The entropy of this black hole will be given by the area of the horizon in units of the $(d+1)$ dimensional Planck area $4G_N$. Using the above metric we get

$$S_{BH} = \frac{1}{4G_N}\left(\frac{1}{u_H^{2d_\theta/(d-1)}}\right)^{(d-1)/2} \times \text{Volume}. \tag{A.3}$$

Hence the entropy density becomes

$$s_{BH} = \frac{1}{4G_N}\frac{1}{u_H^{d_\theta}}. \tag{A.4}$$

Now let us calculate the temperature of this black hole. First we Eulideanize the metric as follows:

$$ds_E^2 = \frac{1}{u^{2d_\theta/(d-1)}}\left(\frac{f(u)}{u^{2(z-1)}}d\tau^2 + \frac{du^2}{f(u)} + dx_i^2\right). \tag{A.5}$$

Then, we evaluate the blackening function near the horizon.

$$f(u) \sim \frac{(u_H - u)(d_\theta + z)}{u_H}. \tag{A.6}$$

Taking into account the function multiplying the paranthesis, the x^i directions form a conformal orthogonal sphere and decouple. So we focus only on the (τ, r) direction. Then the near-horizon metric becomes

$$ds_E^2 = \Omega^2(u) \cdot\left(\frac{(u_H - u)(d_\theta + z)}{u_H u_H^{2(z-1)}}d\tau^2 + \frac{u_H du^2}{(u_H - u)(d_\theta + z)}\right), \tag{A.7}$$

where the conformal pre-factor

$$\Omega^2(u) = u^{-2d_\theta/(d-1)} \tag{A.8}$$

plays no role in defining the black hole temperature. We also note that we have evaluated the denominator of $d\tau^2$ at the horizon radius u_H, being consistent with the fact that we are evaluating the metric near the horizon. We want to find the periodicity of the coordinate τ. To do this, let us define the following coordinates:

$$\begin{aligned}\rho^2 &\equiv (u_H - u),\\ \tilde{\tau} &\equiv \frac{(d_\theta + z)}{u_H^z}\tau.\end{aligned} \tag{A.9}$$

In terms of these new coordinates the metric becomes

$$ds_E^2 = \Omega^2(u)\left(\frac{\rho^2 u_H d\tilde{\tau}^2}{(d_\theta + z)} + \frac{4u_H\rho^2 d\rho^2}{\rho^2(d_\theta + z)}\right). \tag{A.10}$$

Absorbing the factor $4u_H/(d_\theta + z)$ into $\Omega^2(u)$, we get

$$ds_E^2 = \Omega'^2(u)\left(\frac{\rho^2 d\tilde{\tau}^2}{4} + d\rho^2\right). \tag{A.11}$$

Here the coordinate $\tilde{\tau}/2$ has periodicity 2π. Thus, denoting the periodicity of the coordinate τ by β, we obtain

$$\beta = 4\pi\left(\frac{d_\theta + z}{u_H^z}\right)^{-1} \Longrightarrow\ T = \frac{(d_\theta + z)}{4\pi u_H^z}. \tag{A.12}$$

As one can check, we get the same expression for the temperature if we define it using the equation

$$T = \frac{1}{4\pi}\left|\frac{df(u)}{du}\right|_{u_H}. \tag{A.13}$$

Now we can proceed to obtain an expression for energy density using the first law

$$d\epsilon = Tds_{BH}. \tag{A.14}$$

The differential of the entropy density is

$$ds_{BH} = \frac{1}{4G_N}\frac{-d_\theta}{u_H^{(d-2-\theta)}}. \tag{A.15}$$

Therefore the energy density is given by

$$\begin{aligned}d\epsilon &= \frac{(d_\theta + z)}{4\pi u_H^z}\frac{1}{4G_N}\frac{-d_\theta}{u_H^{(d-2-\theta)}},\\ &= -\frac{d_\theta}{16\pi G_N}\frac{(d_\theta + z)}{u_H^{d-2-\theta+z}}.\end{aligned} \tag{A.16}$$

Integrating and setting the integration constant to zero, this becomes

$$\epsilon = \frac{d_\theta}{16\pi G_N}\frac{1}{u_H^{d_\theta+z}}. \tag{A.17}$$

In the case of small subsystems, the black hole entropy becomes the final entanglement entropy after the perturbation.

We could now consider making the bulk solution time-dependent in an adiabatic way, such that the blackening function is given by

$$f(t,u) = 1 - g(t)\left(\frac{u}{u_H}\right)^{d_\theta+z} \tag{A.18}$$

with $g(t)$ being an adiabatic function in time. This property implies that thermodynamics can still be defined as before and we can repeat the above derivation to obtain an energy density

$$\epsilon(t) = \frac{d_\theta}{16\pi G_N}\frac{g(t)}{u_H^{d_\theta+z}}. \tag{A.19}$$

This remains mostly constant as $g(t)$ varies slowly with time.

We may now consider a time-dependent bulk geometry that is not a small perturbation of (A.1). For example, consider the scenario where the blackening function changes abruptly at time $t = 0$

$$f(t,u) = 1 - \Theta(t)\left(\frac{u}{u_H}\right)^{d_\theta+z}. \tag{A.20}$$

In this case, thermodynamics is well-defined before and after time $t = 0$ and the respective bulk geometries are in fact static. If we repeat our derivation, we will see that there is no hindrance and now temperature will be given by (A.12) times $\Theta(t)$. Hence the energy density for these time-dependent bulk solutions will be

$$\epsilon(t) = \frac{d_\theta}{16\pi G_N}\frac{\Theta(t)}{u_H^{d_\theta+z}}. \tag{A.21}$$

Thus for adiabatic time-dependent bulk geometries or for the ones with abrupt changes, the expression for the energy density is the same. This suggests that, for general time dependence in the blackening function, the energy density may be given by the same expression. In particular, we expect the energy density to be

$$\epsilon(t) = \frac{d_\theta}{16\pi G_N}\frac{g(t)}{u_H^{d_\theta+z}}, \tag{A.22}$$

where $g(t)$ is now a general time-dependent function that characterizes the time-dependent bulk geometry.

Data Availability

The data used to support the findings of this study are included within the article.

Conflicts of Interest

The author declares that they have no conflicts of interest.

Acknowledgments

I would like to thank Juan F. Pedraza for several useful discussions. I am grateful to Juan F. Pedraza, Jay Armas, Rik van Bruekelen, and Gerben W.J. Oling, for suggestions to improve the draft. This work is supported by the Netherlands Organisation for Scientific Research (NWO-I), which is funded by the Dutch Ministry of Education, Culture and Science (OCW).

References

[1] P. Calabrese and J. Cardy, "Quantum quenches in extended systems," *Journal of Statistical Mechanics: Theory and Experiment*, no. 6, P06008, 33 pages, 2007.

[2] M. Greiner, O. Mandel, T. Esslinger, T. W. Hänsch, and I. Bloch, "Quantum phase transition from a superfluid to a Mott insulator in a gas of ultracold atoms," *Nature*, vol. 415, no. 6867, pp. 39–44, 2002.

[3] M. Rigol, V. Dunjko, and M. Olshanii, "Thermalization and its mechanism for generic isolated quantum systems," *Nature*, vol. 452, no. 7189, pp. 854–858, 2008.

[4] M. V. Berry, "Regular and irregular semiclassical wavefunctions," *Journal of Physics A: Mathematical and General*, vol. 10, no. 12, pp. 2083–2091, 1977.

[5] M. Srednicki, "Chaos and quantum thermalization," *Physical Review E: Statistical, Nonlinear, and Soft Matter Physics*, vol. 50, no. 2, pp. 888–901, 1994.

[6] H. W. Diehl, "The theory Of boundary critical phenomena," *International Journal of Modern Physics B*, vol. 11, no. 30, pp. 3503–3523, 1997.

[7] S. R. Das, D. A. Galante, and R. C. Myers, "Universality in fast quantum quenches," *Journal of High Energy Physics*, no. 2, 167, front matter+68 pages, 2015.

[8] P. M. Chesler and L. G. Yaffe, "Horizon formation and far-from-equilibrium isotropization in a supersymmetric Yang-Mills plasma," *Physical Review Letters*, vol. 102, no. 21, Article ID 211601, 2009.

[9] S. Bhattacharyya and S. Minwalla, "Weak field black hole formation in asymptotically AdS spacetimes," *Journal of High Energy Physics*, vol. 2009, no. 9, article 034, 2009.

[10] E. Caceres, A. Kundu, J. F. Pedraza, and D.-L. Yang, "Weak field collapse in AdS: introducing a charge density," *Journal of High Energy Physics*, no. 6, 111, front matter+41 pages, 2015.

[11] V. Balasubramanian, A. Bernamonti, and J. de Boer, "Holographic thermalization," *Physical Review D: Particles, Fields, Gravitation and Cosmology*, vol. 84, no. 2, Article ID 026010, 2011.

[12] I. R. Klebanov, D. Kutasov, and A. Murugan, "Entanglement as a probe of confinement," *Nuclear Physics, B*, vol. 796, no. 1-2, pp. 274–293, 2008.

[13] M. M. Wolf, F. Verstraete, M. . Hastings, and J. I. Cirac, "Area laws in quantum systems: mutual information and correlations," *Physical Review Letters*, vol. 100, no. 7, 070502, 4 pages, 2008.

[14] J. Schachenmayer, B. P. Lanyon, C. F. Roos, and A. J. Daley, "Entanglement growth in quench dynamics with variable range interactions," *Physical Review X*, vol. 3, no. 3, 2013.

[15] P. Calabrese and J. Cardy, "Entanglement entropy and quantum field theory," *Journal of Statistical Mechanics: Theory and Experiment*, no. 6, 002, 27 pages, 2004.

[16] P. Calabrese and J. Cardy, "Evolution of entanglement entropy in one-dimensional systems," *Journal of Statistical Mechanics: Theory and Experiment*, no. 4, P04010, 24 pages, 2005.

[17] H. Casini, H. Liu, and M. Mezei, "Spread of entanglement and causality," *Journal of High Energy Physics*, no. 7, 077, front matter+61 pages, 2016.

[18] M. Maldacena, "The large-N limit of superconformal field theories and supergravity," *International Journal of Theoretical Physics*, vol. 38, no. 4, pp. 1113–1133, 1999.

[19] S. S. Gubser, I. R. Klebanov, and A. M. Polyakov, "Gauge theory correlators from non-critical string theory," *Physics Letters B*, vol. 428, no. 1-2, pp. 105–114, 1998.

[20] E. Witten, "Anti de Sitter space and holography," *Advances in Theoretical and Mathematical Physics*, vol. 2, no. 2, pp. 253–291, 1998.

[21] P. Bizoń and A. Rostworowski, "Weakly turbulent instability of anti–de sitter spacetime," *Physical Review Letters*, vol. 107, no. 3, 2011.

[22] T. Banks, M. R. Douglas, G. T. Horowitz, and E. J. Martinec, *AdS Dynamics from Conformal Field Theory*, 1998.

[23] U. H. Danielsson, E. Keski-Vakkuri, and M. Kruczenski, "Black hole formation in AdS and thermalization on the boundary," *Journal of High Energy Physics*, no. 2, Paper 39, 21 pages, 2000.

[24] V. Balasubramanian, A. Buchel, S. R. Green, L. Lehner, and S. L. Liebling, "Holographic thermalization, stability of anti–de sitter space, and the fermi-pasta-ulam paradox," *Physical Review Letters*, vol. 113, no. 7, 2014.

[25] F. V. Dimitrakopoulos, B. Freivogel, M. Lippert, and I.-S. Yang, "Position space analysis of the AdS (in)stability problem," *Journal of High Energy Physics*, no. 8, 077, front matter+35 pages, 2015.

[26] E. Witten, "Anti-de Sitter space, thermal phase transition, and confinement in gauge theories," *Advances in Theoretical and Mathematical Physics*, vol. 2, no. 3, pp. 505–532, 1998.

[27] G. T. Horowitz and V. E. Hubeny, "Quasinormal modes of AdS black holes and the approach to thermal equilibrium," *Physical Review D: Particles, Fields, Gravitation and Cosmology*, vol. 62, no. 2, Article ID 024027, 11 pages, 2000.

[28] H. Ebrahim and M. Headrick, *Instantaneous Thermalization in Holographic Plasmas*, 2010.

[29] D. Galante and M. Schvellinger, "Thermalization with a chemical potential from AdS spaces," *Journal of High Energy Physics*, vol. 2012, no. 7, article no. 096, 2012.

[30] E. Caceres and A. Kundu, "Holographic thermalization with chemical potential," *Journal of High Energy Physics*, vol. 2012, article 55, 2012.

[31] V. Balasubramanian, A. Bernamonti, J. de Boer et al., "Inhomogeneous holographic thermalization," *Journal of High Energy Physics*, vol. 2013, no. 10, 2013.

[32] S. R. Das, T. Nishioka, and T. Takayanagi, "Probe branes, time-dependent couplings and thermalization in AdS/CFT," *Journal of High Energy Physics*, no. 7, 071, 42 pages, 2010.

[33] P. Basu, D. Das, S. R. Das, and K. Sengupta, "Quantum quench and double trace couplings," *Journal of High Energy Physics*, vol. 2013, no. 12, 2013.

[34] T. Ugajin, *Two Dimensional Quantum Quenches and Holography*, 2013, Two dimensional quantum quenches and holography.

[35] A. Buchel, R. C. Myers, and A. van Niekerk, "Nonlocal probes of thermalization in holographic quenches with spectral methods," *Journal of High Energy Physics*, no. 2, 017, front matter+64 pages, 2015.

[36] S. Ryu and T. Takayanagi, "Aspects of holographic entanglement entropy," *Journal of High Energy Physics*, vol. 2006, no. 8, artcile 045, 2006.

[37] M. Rangamani and T. Takayanagi, *Holographic Entanglement Entropy*, vol. 931 of *Lecture Notes in Physics*, Springer, Cham, 2017.

[38] V. E. Hubeny, M. Rangamani, and T. Takayanagi, "A covariant holographic entanglement entropy proposal," *Journal of High Energy Physics*, vol. 2007, no. 7, article 62, 2007.

[39] J. Abajo-Arrastia, J. Aparício, and E. López, "Holographic evolution of entanglement entropy," *Journal of High Energy Physics*, vol. 2010, no. 11, 2010.

[40] P. C. Vaidya, "Nonstatic solutions of Einstein's field equations for spheres of fluids radiating energy," *Physical Review*, vol. 83, pp. 10–17, 1951.

[41] T. Hartman and J. Maldacena, "Time evolution of entanglement entropy from black hole interiors," *Journal of High Energy Physics*, no. 5, 014, front matter+27 pages, 2013.

[42] T. Albash and C. V. Johnson, "Evolution of holographic entanglement entropy after thermal and electromagnetic quenches," *New Journal of Physics*, vol. 13, no. 4, p. 045017, 2011.

[43] H. Liu and S. J. Suh, "Entanglement tsunami: Universal scaling in holographic thermalization," *Physical Review Letters*, vol. 112, no. 1, Article ID 011601, 2014.

[44] H. Liu and S. J. Suh, "Entanglement growth during thermalization in holographic systems," *Physical Review D: Particles, Fields, Gravitation and Cosmology*, vol. 89, no. 6, 2014.

[45] S. Kundu and J. F. Pedraza, "Spread of entanglement for small subsystems in holographic CFTs," *Physical Review D: Particles, Fields, Gravitation and Cosmology*, vol. 95, no. 8, 086008, 26 pages, 2017.

[46] A. O'Bannon, J. Probst, R. Rodgers, and C. F. Uhlemann, "First law of entanglement rates from holography," *Physical Review D: Particles, Fields, Gravitation and Cosmology*, vol. 96, no. 6, 2017.

[47] S. F. Lokhande, G. W. J. Oling, and J. F. Pedraza, "Linear response of entanglement entropy from holography," *Journal of High Energy Physics*, no. 10, 104, front matter+39 pages, 2017.

[48] S. A. Hartnoll, "Lectures on holographic methods for condensed matter physics," *Classical and Quantum Gravity*, vol. 26, no. 22, 224002, 61 pages, 2009.

[49] S. S. Gubser and A. Nellore, "Ground states of holographic superconductors," *Physical Review D: Particles, Fields, Gravitation and Cosmology*, vol. 80, no. 10, 2009.

[50] S. A. Hartnoll, J. Polchinski, E. Silverstein, and D. Tong, "Towards strange metallic holography," *Journal of High Energy Physics*, vol. 2010, no. 4, 2010.

[51] S. A. Hartnoll and A. Tavanfar, "Electron stars for holographic metallic criticality," *Physical Review D: Particles, Fields, Gravitation and Cosmology*, vol. 83, no. 4, 2011.

[52] D. T. Son and A. O. Starinets, "Hydrodynamics of R-charged black holes," *Journal of High Energy Physics*, vol. 2006, article 052, 2006.

[53] E. Ardonne, P. Fendley, and E. Fradkin, "Topological order and conformal quantum critical points," *Annals of Physics*, vol. 310, no. 2, pp. 493–551, 2004.

[54] M. Freedman, C. Nayak, and K. Shtengel, "Line of critical points in 2+1 dimensions: Quantum critical loop gases and non-abelian gauge theory," *Physical Review Letters*, vol. 94, no. 14, 2005.

[55] P. Hořava, "Quantum criticality and Yang-Mills gauge theory," *Physics Letters B*, vol. 694, no. 2, pp. 172–176, 2011.

[56] D. T. Son, "Toward an AdS/cold atoms correspondence: a geometric realization of the Schrödinger symmetry," *Physical Review D: Particles, Fields, Gravitation and Cosmology*, vol. 78, no. 4, Article ID 046003, 2008.

[57] K. Balasubramanian and J. McGreevy, "Gravity duals for non-relativistic conformal field theories," *Physical Review Letters*, vol. 101, no. 6, Article ID 061601, 2008.

[58] W. D. Goldberger, "AdS/CFT duality for non-relativistic field theory," *Journal of High Energy Physics. A SISSA Journal*, no. 3, 069, 18 pages, 2009.

[59] A. Adams, K. Balasubramanian, and J. McGreevy, "Hot spacetimes for cold atoms," *Journal of High Energy Physics*, vol. 2008, no. 11, pp. 059-059, 2008.

[60] C. P. Herzog, M. Rangamani, and S. . Ross, "Heating up Galilean holography," *Journal of High Energy Physics. A SISSA Journal*, no. 11, 080, 27 pages, 2008.

[61] J. Maldacena, D. Martelli, and Y. Tachikawa, "Comments on string theory backgrounds with non-relativistic conformal symmetry," *Journal of High Energy Physics*, vol. 10, Article ID 072, 39 pages, 2008.

[62] S. Kachru, X. Liu, and M. Mulligan, "Gravity duals of Lifshitz-like fixed points," *Physical Review D: Particles, Fields, Gravitation and Cosmology*, vol. 78, no. 10, Article ID 106005, 8 pages, 2008.

[63] S. A. Hartnoll and K. Yoshida, "Families of IIB duals for nonrelativistic CFTs," *Journal of High Energy Physics. A SISSA Journal*, no. 12, Article ID 071, 22 pages, 2008.

[64] A. Adams, A. Maloney, A. Sinha, and S. E. Vazquez, "1/N effects in non-relativistic gauge-gravity duality," *Journal of High Energy Physics. A SISSA Journal*, no. 3, 097, 24 pages, 2009.

[65] T. Azeyanagi, W. Li, and T. Takayanagi, "On string theory duals of Lifshitz-like fixed points," *Journal of High Energy Physics*, vol. 6, Article ID 084, 2009.

[66] K. Narayan, "Lifshitz scaling and hyperscaling violation in string theory," *Physical Review D: Particles, Fields, Gravitation and Cosmology*, vol. 85, no. 10, Article ID 106006, 2012.

[67] P. Dey and S. Roy, "Lifshitz metric with hyperscaling violation from NS5-Dp states in string theory," *Physics Letters. B. Particle Physics, Nuclear Physics and Cosmology*, vol. 720, no. 4-5, pp. 419–423, 2013.

[68] M. Taylor, *Non-Relativistic Holography*, 2008, https://arxiv.org/https://arxiv.org/.

[69] C. Hoyos and P. Koroteev, "On the Null energy condition and causality in lifshitz holography," *Physical Review*, vol. 82, pp. 245-246, 2010, [Erratum: Phys. Rev.D82,109905(2010)].

[70] M. H. Christensen, J. Hartong, N. A. Obers, and B. Rollier, "Boundary stress-energy tensor and Newton-Cartan geometry in Lifshitz holography," *Journal of High Energy Physics*, no. 1, 057, front matter+69 pages, 2014.

[71] C. Charmousis, B. Gouteraux, B. S. Kim, E. Kiritsis, and R. Meyer, "Effective holographic theories for low-temperature condensed matter systems," *Journal of High Energy Physics*, vol. 2010, no. 11, article 151, 2010.

[72] X. Dong, S. Harrison, S. Kachru, G. Torroba, and H. Wang, "Aspects of holography for theories with hyperscaling violation," *Journal of High Energy Physics*, vol. 2012, article 41, 2012.

[73] E. Perlmutter, "Hyperscaling violation from supergravity," *Journal of High Energy Physics*, vol. 2012, no. 6, 2012.

[74] P. Dey and S. Roy, "From AdS to Schrödinger/Lifshitz dual space-times without or with hyperscaling violation," *Journal of High Energy Physics*, vol. 11, p. 113, 2013.

[75] W. Chemissany and I. Papadimitriou, "Lifshitz holography: the whole shebang," *Journal of High Energy Physics*, vol. 2015, no. 1, 2015.

[76] V. Keränen, E. Keski-Vakkuri, and L. Thorlacius, "Thermalization and entanglement following a nonrelativistic holographic quench," *Physical Review D: Particles, Fields, Gravitation and Cosmology*, vol. 85, no. 2, 2012.

[77] M. Alishahiha, A. Faraji Astaneh, and M. R. Mohammadi Mozaffar, "Thermalization in backgrounds with hyperscaling violating factor," *Physical Review D: Particles, Fields, Gravitation and Cosmology*, vol. 90, no. 4, 2014.

[78] P. Fonda, L. Franti, V. Keranen, E. Keski-Vakkuri, L. Thorlacius, and E. Tonni, "Holographic thermalization with Lifshitz scaling and hyperscaling violation," *Journal of High Energy Physics*, vol. 08, p. 051, 2014.

[79] W. Fischler, A. Kundu, and S. Kundu, "Holographic mutual information at finite temperature," *Physical Review D: Particles, Fields, Gravitation and Cosmology*, vol. 87, no. 12, 2013.

[80] M. R. Tanhayi, "Thermalization of mutual information in hyperscaling violating backgrounds," *Journal of High Energy Physics*, no. 3, 202, front matter+27 pages, 2016.

[81] K. Skenderis, "Lecture notes on holographic renormalization," *Classical and Quantum Gravity*, vol. 19, no. 22, pp. 5849–5876, 2002.

[82] S. F. Ross and O. Saremi, "Holographic stress tensor for non-relativistic theories," *Journal of High Energy Physics*, vol. 2009, article 009, 2009.

[83] S. F. Ross, "Holography for asymptotically locally Lifshitz spacetimes," *Classical and Quantum Gravity*, vol. 28, no. 21, 215019, 26 pages, 2011.

[84] M. Baggio, J. de Boer, and K. Holsheimer, "Hamilton-Jacobi renormalization for Lifshitz spacetime," *Journal of High Energy Physics*, no. 1, 058, 24 pages, 2012.

[85] R. B. Mann and R. McNees, "Holographic renormalization for asymptotically Lifshitz spacetimes," *Journal of High Energy Physics*, no. 10, 129, 35 pages, 2011.

[86] C. Keeler, "Scalar boundary conditions in Lifshitz spacetimes," *Journal of High Energy Physics*, no. 1, 067, front matter+17 pages, 2014.

[87] T. Andrade and S. F. Ross, "Boundary conditions for scalars in Lifshitz," *Classical and Quantum Gravity*, vol. 30, no. 6, 065009, 16 pages, 2013.

[88] T. Andrade and S. F. Ross, "Boundary conditions for metric fluctuations in Lifshitz," *Classical and Quantum Gravity*, vol. 30, no. 19, 195017, 29 pages, 2013.

[89] W. Fischler and S. Kundu, "Strongly coupled gauge theories: high and low temperature behavior of non-local observables," *Journal of High Energy Physics*, no. 5, 098, front matter+37 pages, 2013.

[90] B. Gouteraux and E. Kiritsis, "Generalized holographic quantum criticality at finite density," *Journal of High Energy Physics*, vol. 12, Article ID 36, 2011.

[91] L. Huijse, S. Sachdev, and B. Swingle, "Hidden Fermi surfaces in compressible states of gauge-gravity duality," *Physical Review B: Condensed Matter and Materials Physics*, vol. 85, Article ID 035121, 2012.

[92] M. Alishahiha, E. O'Colgain, and H. Yavartanoo, "Charged Black Branes with Hyperscaling Violating Factor," *Journal of High Energy Physics*, vol. 2012, article 137, 2012.

[93] J. F. Pedraza, W. Sybesma, and M. R. Visser, *Hyperscaling Violating Black Holes with Spherical and Hyperbolic Horizons*, 2018.

[94] J. Bhattacharya, M. Nozaki, T. Takayanagi, and T. Ugajin, "Thermodynamical property of entanglement entropy for excited states," *Physical Review Letters*, vol. 110, no. 9, 2013.

[95] M. Alishahiha, D. Allahbakhshi, and A. Naseh, "Entanglement thermodynamics," *Journal of High Energy Physics*, no. 8, 102, front matter+16 pages, 2013.

[96] G. Wong, I. Klich, L. A. Pando Zayas, and D. Vaman, "Entanglement temperature and entanglement entropy of excited states," *Journal of High Energy Physics*, vol. 2013, no. 12, 2013.

[97] D. Roychowdhury, "Entanglement rules for holographic Fermi surfaces," *Nuclear Physics. B. Theoretical, Phenomenological, and Experimental High Energy Physics. Quantum Field Theory and Statistical Systems*, vol. 909, pp. 336–344, 2016.

[98] D. D. Blanco, H. Casini, L.-Y. Hung, and R. C. Myers, "Relative entropy and holography," *Journal of High Energy Physics*, no. 8, 060, front matter+64 pages, 2013.

[99] N. Lashkari, "Relative entropies in conformal field theory," *Physical Review Letters*, vol. 113, no. 5, 2014.

[100] H. Ghaffarnejad, M. Farsam, and E. Yaraie, *Holographic Entanglement Entropy for Small Subregions and Thermalization of Born-Infeld AdS Black Holes*, 2018.

[101] H. Ghaffarnejad, E. Yaraie, and M. Farsam, *Holographic Thermalization in AdS-Gauss-Bonnet Gravity for Small Entangled Regions*, 2018.

[102] T. He, J. Magan, and S. Vandoren, "Entanglement entropy in lifshitz theories," *SciPost Physics*, vol. 3, no. 5, 2017.

[103] M. R. M. Mozaffar and A. Mollabashi, "Entanglement in Lifshitz-type quantum field theories," *Journal of High Energy Physics*, no. 7, 120, front matter+23 pages, 2017.

[104] M. Rangamani, M. Rozali, and A. Wong, "Driven holographic CFTs," *Journal of High Energy Physics*, no. 4, 093, front matter+39 pages, 2015.